STUDY OF THE IMMUNE CORRELATES OF PROTECTION IN RHESUS MACAQUES VACCINATED AGAINST SIMIAN IMMUNODEFICIENCY VIRUS

Giacomo Gorini

Girton College

Laboratory of Viral Zoonotics

Department of Veterinary Medicine

School of Biological Sciences

University of Cambridge

This dissertation is submitted for the degree of Doctor of Philosophy

September 2018

Study of the Immune Correlates of Protection in Rhesus Macaques Vaccinated against Simian Immunodeficiency Virus

After more than thirty years since the Human Immunodeficiency Virus (HIV) was identified, only the RV144 phase III vaccine clinical trial provided evidence of protection from virus infection, with 31.2% of the patients protected at three years since the end of the immunisation phase. Statistical analyses support serum IgG antibody recognition of the V2 region of viral gp120 as a mechanism of protection from acquisition. One hypothesis is that antibodies to this region might block the interaction with the integrin $\alpha4\beta7$, which protrudes from the surface of mucosal $CD4^+$ T cells and is thought to capture the virus and facilitate infection. However, that $\alpha4\beta7$ blocking might be a protective mechanism of RV144 vaccination has yet to be definitively demonstrated.

In this thesis, I aimed to describe at the molecular level the immune mechanisms of protection in a rhesus macaque (*Macaca mulatta*) vaccinated in an RV144-like schedule and protected from Simian Immunodeficiency Virus (SIV) infection, with a particular focus on the humoral immune response of the animal. More specifically, vaccine-induced monoclonal antibodies (mAbs) directed against the V2 region of SIV were isolated and characterised. One of them, NCI09, has been identified as a potent inhibitor of SIV gp120 interaction with human $\alpha4\beta7$. Notably, NCI09 antigen recognition is negatively affected by the presence of ITS41, a mAb targeting a distant epitope on V2.

Moreover, to experimentally prove this mechanism I performed the passive immunoprophylaxis of rhesus macaques using the anti-V2 mAb ITS09. Unfortunately, this mAb proved ineffective in providing protection both alone and in combination.

Finally, a vaccination protocol based on the immunisation regimen of RV144, but modified to elicit stronger immune responses was tested. Surprisingly, the protocol failed to afford protection. However, in a parallel group immunised with the standard RV144 regimen, protection was observed and correlated with the intensity of the innate immune responses.

These results provide insights into possible mechanisms of protection of RV144 vaccination against HIV. Furthermore, these findings suggest that there may be a degree of structural plasticity of the V2 region that may impact its interaction with $\alpha4\beta7$ and evasion mechanisms from a potentially protective humoral immune response.

Declaration

This dissertation is the result of my own work and includes nothing which is the outcome of work done in collaboration except as declared in the Preface and specified in the text.

I further state that this dissertation is not substantially the same as any that I have submitted or is being concurrently submitted for a degree or diploma or other qualification at the University of Cambridge or any other University or similar institution. I further state that no substantial part of my dissertation has already been submitted, or is being concurrently submitted for any such degree, diploma or other qualification at the University of Cambridge or any other University or similar institution.

This thesis does not exceed the prescribed limit of 60,000 words and 150 figures.

Giacomo Gorini, September 2018

Acknowledgements

I write this section with the intent of being more thorough than concise. First and foremost, as etiquette rightly dictates, I would like to thank my PhD supervisor Prof. Jonathan Heeney for his guidance throughout these years, his encouragement to let me explore my own ideas and trust that I would make the experiments eventually work even in times when they were actually not. You cared that I would feel like a part of your group since the very beginning and always cared that I would make the most of my Cambridge experience, a thing that greatly contributed to my happiness.

Very, very special thanks to Dr. Genoveffa Franchini, referred in this thesis as a collaborator but whom is to me much more. As a supervisor, finding the right balance between guidance and freedom is not easy, but you were a master at it. You trusted me into your laboratory as a young MSc graduate and greatly cared about my professional as well as personal development. Starting to work at the NIH represented for me the end of a path of dreaming and the start of one of realisation.

I would also like to thank Dr. Mario Roederer, for opening to me the doors of his lab and his office and allowing me to learn cutting-edge techniques in the best work environment. For encouraging me to pursue my own projects, fuelling my creativity and treating me like one of his team.

To Dr. James Arthos and Dr. Claudia Cicala, with whom I shared interest and excitement on this field of HIV vaccine research. Jim, I have missed our brainstorming sessions in your office. Claudia, thank you very much for remaining a mentor and a friend.

A very large share of gratitude also extends to Dr. Rosemarie Mason, Rosie. You started as a tutor, became a friend and eventually family. You were my go-to person for any difficulty, because you always supported me in my search for happiness. My words can hardly express how thankful I am for having had the opportunity to meet you.

To all of my mates at the Animal Models and Retroviral Vaccines Section, NCI, NIH, in particular Monica, Melvin, Dallas, Maria, Isabela, Robyn and Massimiliano. Veronica, you were much more than a lab mate. Thank you so much for always being there for me, even after Max joined the lab.

I would also like to thank my mates at the Laboratory of Viral Zoonotics, Department of Veterinary Medicine, University of Cambridge. In particular, Sam (more below), Chinedu, Constanza, Chiara, Osama, Rebecca, Paul, Sarah and Arden. I could not wait for my last year of PhD to come, so that I could join your team once and for all without having to leave. You created the perfect work environment that I knew I would find on my return from the States. I am going to miss greatly our chats, our coffees and our pints!

I would like to extend my gratitude to the mates of the Vaccine Research Center. You guys were the perfect group to work and have fun with. Starting to collaborate at the VRC is one of the best things that happened to me while I was in the US.

Special thanks to those who mentored me since the very early stages of my professional life: Dr. Antonello Bonci, Prof. Roberto Burioni, Prof. Gianni Garotta and Dr. Margaret McCluskey. Each one of you helped creating a vision of my future self and making it come true. Thank you very much for dedicating some of your time into shaping the vague desires of a young student into specific objectives to chase. What I obtained was beyond my expectations and I thank you all for your support. There is very little that I can give back to you directly, but I will follow the example that you have set so highly when, one day, I will give back to the next generation.

I would also like to express my gratitude to the teachers who helped shape my person before my career: Mrs. Montanari, Mrs. Renzi, Mr. Lotti and Mr. Picciano. Also, thanks to one of the best teachers I ever had: my dad Stefano who improvised himself as English and History lecturer when I was failing in school. Thank you for pushing me outside of Rimini when I was a teenager: visiting Oxford at age 16 was the first episode of a chain of events that is now resulting in this thesis.

A big “thank you” to Dr. Giuseppe Sautto who helped me take my first steps in the world of experimental science. In one year of MSc internship, you taught be how to build very solid technical skills and together we built the most solid friendship.

Special thanks to my extended family, my US siblings Jeremy, Randi, Sam Supnick and Hugh. You guys contributed greatly to my happiness and personal growth when I was far from home, and were always there to inspire me by example. I am very glad that we have kept in touch and I have no doubts we will keep at it.

Thanks also to my UK siblings: Sam Stubbs, who was always there to support me like a brother through my personal tribulations and professional ambitions; to Darcie for being the greatest, sassiest listener; to George, Graham and Michal. It was great to goof around, have your opinion on my (mis)adventures and witness you all pursuing your happiness each one of you in his own way.

A special mention to the kids I adopted in college, the (Certified) Swirles Lads. Thank you for accepting me as one of yours despite my old age. This was an incredible year. Although we laughed profusely and shared plenty of moments of happiness, we were always there to support each other in our difficulties during this past year. We were a great team, and I am looking forward to keeping the bonds strong and visiting each other wherever you guys are. You are a set of brilliant minds and I wish you all the greatest success in life.

Also special thanks to Girton College, where I found a family. Thanks to the beloved staff, to my fellow postgrads and to the undergrads. I treasure that feeling of excitement when, sitting at formal dinner, I would find myself surrounded by friendly faces and bright minds. Good luck to all of you.

Thank you Silvia, Elisabetta and Mattia. I find it inspirational that we all followed our own dreams independently and life decided to bring us back together. It felt like we never separated at all.

I would like to thank my Italian brothers: Federico, Luca, Nicolò and Lidia. When I announced that I would leave for Washington, DC, I was afraid that I would lose you and that the diverging

lifestyles would lead to diverging friendships. However, we were always there for each other (at least, you were for me when I needed) and I know that it will be like that for a long time.

Very special thanks to all of those whom I forgot to mention but are not going to take it personally.

Having so far thanked many fine people, I would like to dedicate a few thoughts to the macaques that allowed for the generation of the data presented in this thesis, in particular P770, “George”, from whom the NCI mAbs were cloned. These animals were always treated with the utmost care by well-trained veterinarians following rigorous guidelines approved by the Ethical Committee of the relevant institutes. The data obtained from these monkeys fuelled significant scientific advancement in the research on human as well as veterinarian lentiviral diseases. Without the sacrifice of these and other animals, modern medicine would have not been able to save or improve the standard of so many human and animal lives.

I would also like to extend my gratitude to the United States Government for welcoming me in their team and to the United States in general, for being the place where so many adventures started. DC gave me so much. Sometimes it also took a little, but it was always to teach me a lesson. In any case, I can say that I am satisfied with the end result.

To conclude, I would like to thank my family, in particular my mom Monica, my aforementioned dad Stefano and sister Giulia. Each one of you has contributed to my growth in your own way, providing the perfect balance as a result. My gratitude also extends to my beloved nonna Mimma, nonna Alma and the more recently acquired Dr. Nando. My thanks also to my brand-new brother(-in-law) Jacopo who always understood and encouraged me to keep chasing my dreams. Finally, although she contributed very little to this thesis (not because of any intentional shortcoming of hers), I can’t help but extend a sweet thought to my soon-to-be-welcomed niece whom I look very much forward to meeting.

Table of Contents

List of abbreviations and acronyms (continues on next page)

ABL - Advanced BioScience Laboratories
Ad5 - adenovirus type 5
ADCC - antibody-dependent cellular cytotoxicity
ADCP - Antibody-dependent phagocytosis
agm - African green monkey
AH - aluminium hydroxide
AID - activation-induced cytidine deaminase
AIDS - acquired immunodeficiency syndrome
AP - aluminium phosphate
ART - antiretroviral therapy
ASC - antibody secreting cell
BAMA - binding antibody multiplex assay
BCL-6 - B cell lymphoma 6
BCR - B cell receptor
BER - base excision repair
bnAb - broadly neutralising antibody
C - constant region
CCR5 - C-C chemokine receptor type 5
CD - cluster of differentiation
CDC - complement-dependent cytotoxicity
CDRs - complementarity determining region
cGMP - current good manufacturing practices
CHO - Chinese hamster ovary
cpz - chimpanzee
CRF - circulating recombinant form
CSR - class switch recombination
CTL - cytotoxic T lymphocyte
cV2 - cyclic V2
CXCR4 - C-X-C chemokine receptor type 4
D - diversity region
DC - dendritic cell
DSB - double strand break
ELISA - enzyme-linked immunosorbent assay
Env - envelope
FcR - Fc Receptor
FCRL4 - Fc receptor-like protein 4
FDC - follicular dendritic cell
Fr-MuLV - Friend-murine leukemia virus
FWR - framework region
GALT - gut-associated lymphoid tissue
GC - germinal centre
gor - gorila
HEK - human embryo kidney
HIV - human immunodeficiency virus
HPLC - high pressure liquid chromatography
HPTN - HIV Prevention Trials Network
HVTN - HIV Vaccine Trials Network
IDU - injection drug user
IFN - interferon
Ig - immunoglobulin
IgA - immunoglobulin A
IgD - immunoglobulin D
IgG - immunoglobulin G
IgH - Immunoglobulin Heavy
IgL - Immunoglobulin Light
IgM - immunoglobulin M
IgV - Immunoglobulin Variable
INSTI - integrase strand transfer inhibitor
ITIM - immunoreceptor tyrosine-based inhibitory motif
ITS - immunotechnology section
JH - joining heavy
KA - constant of association
KD - constant of dissociation
LBP - LPS binding protein
LPS - lipopolysaccharide
M - main
mAb - monoclonal antibody
mac - macaque
MAC - Membrane attack complex
MFI - mean fluorescent intensity
MHC - major histocompatibility complex
MHRP - military HIV research program

MIDAS - metal ion-dependent adhesion site

MMR - mismatch repair

MSM - men who have sex with men

MVA - modified vaccinia Ankara

N - non-M, non-O

nAb - neutralising antibody

NCI - National Cancer Institute

NIAID - National Institute of Allergy and Infectious Diseases

NIH - National Institute of Health

NNRTI - non-nucleoside reverse transcriptase inhibitor

NRTI - nucleoside reverse transcriptase inhibitor

NYVAC - New York Vaccinia

O - outlier

OD - optical density

PB - plasmablast

PFU - plaque forming unit

PI - protease inhibitor

PNG - protein N-glycosylation

pre - precursor

pro - progenitor

RA - retinoic acid

RLD - repeated low dose

RLU - relative luminescence unit

rpm - repeats per minute

RSS - recombination signal sequence

S - switch

SAP - SLAM-associated protein

SHIV - simian-human chimeric immunodeficiency virus

SHM - somatic hypermutation

SIV - simian immunodeficiency virus

sm - sooty mangabey

STIC - salt-tolerant interaction chromatography

SU - surface subunit o HIV/SIV Env

SUB - single-use bioreactor

TCID50 - 50% tissue culture infectious dose

TCR - T cell receptor

Tdt - terminal deoxynucleotidyl transferase

Tfh - T follicular helper cell

Th - helper T cell

Th17 - T-helper 17

TM - transmembrane

TMB - tetramethylbenzidine

TNF - tumor necrosis factor

Treg - regulatory T cell

USAID - United States Agency for International Development

V – variable domain

VE - vaccine efficacy

VH - variable heavy

VRC - vaccine research center

List of figures

List of tables

Other introductory material

Cluster of Differentiation (CD) Numbers

CD numbers are assigned to cell surface molecules and are used in this work to immunophenotype cells. Their function and tissue distribution are as below:

Marker	Function	Distribution
CD3	Part of the TCR complex	T cells
CD4	TCR co-receptor	T helper cells
CD8	TCR co-receptor	cytotoxic T cells
CD14	Receptor for LPS/LBP complex	monocytes
CD16	Medium-affinity IgG receptor	monocytes, NK cells
CD19	Part of the BCR complex	B cells
CD20	Promotes B cell maturation	B cells
CD21	Part of the BCR complex	B cells
CD38	Cell adhesion, signal transduction	T, B, NK cells, monocytes
CD39	ADP/ATP hydrolysis	T, B, NK cells, monocytes
CD45	Promotes cell activation	T cells, monocytes, NK cells
CD56	Cell adhesion	T cells, NK cells
CD95	Induces apoptosis	T, B, NK cells, monocytes
CD107a	Marker of degranulation/cytotoxicity	T, NK cells
CD183 (CXCR3)	Chemotaxis, adhesion	T, NK cells
CD184 (CXCR4)	Cell migration	T, B cells, monocytes
CD185	Homing, cell movement	T, B, NK cells, monocytes
CD192	Monocyte chemotaxis	T, B cells, monocytes
CD195 (CCR5)	Lymphocyte chemotaxis	T cells, monocytes
CD196 (CCR6)	Antigen-driven B cell differentiation	T, B cells
CD335 (NKp46)	Cytotoxicity-activating receptor	NK cells
CD336 (NKp44)	Cytotoxicity-activating receptor	NK cells

HIV

Throughout this thesis, Type 1 Human Immunodeficiency Virus is referred to as “HIV-1” or, for brevity, “HIV”. Type 2 Human Immunodeficiency Virus is *always* referred to as “HIV-2”.

List of collaborators

Collaborators who contributed to the experiments are listed below in no particular order. Direct experimental contributions are indicated at the start of every subsection within the sections titled “Materials and Methods”, and summarised in a table located at the end of said section. Principal investigators are underlined. I would like to take the opportunity to thank each one of the listed collaborators for their support.

NIH
Genoveffa Franchini
Mario Roederer
James Arthos
Peter Kwong
Rosemarie Mason
Claudia Cicala
Jason Gorman
Matthew Liu
Donald Van Ryk
Shari Gordon
Luca Schifanella
Namal Liyanage
Dallas Brown
Monica Vaccari
David Venzon
Elizabeth Scheideman
Abasha Williams
Stephanie Golub
Daniel Ragheb
Nga Tran
Lena Wang

ABL
Ranajit Pal
Hye Chung
Irene Kalisz

Harvard Medical School
Sampa Santra

Duke University School of Medicine
Georgia Tomaras

MHRP
Mangala Rao
Kristina Peachman

Initial remarks

My PhD studies were based on a collaboration that I established with Prof. Heeney's Laboratory of Viral Zoonotics at the Department of Veterinary Medicine at the University of Cambridge from Dr. Genoveffa Franchini's Animal Models and Retroviral Vaccines Section at the National Institutes of Health in Bethesda, Maryland, where I worked from May 2014 to September 2017. This collaboration, which formally started with my PhD program in Michaelmas 2014, aimed to define the immune mechanisms of protection in P770, a rhesus macaque (*Macaca mulatta*) which was vaccinated and thereby protected from Simian Immunodeficiency Virus infection, with a particular focus on the humoral immune response of the animal. For this purpose, I cloned and characterised monoclonal antibodies directed against a region of the virus, namely V2, located at the apex of the surface glycoprotein gp120.
In addition, a vaccination protocol based on that of the human clinical trial was modified to elicit stronger immune responses and evaluated on rhesus macaques.
Finally, I tested the efficacy of an anti-V2 mAb in providing protection from SIV infection to rhesus macaques.

In the introduction, I review the key concepts of vaccine-mediated immunity and of the development of a protective humoral immune response. I then review how the HIV epidemic originated and the current state. Finally, I summarise the results and mechanistic clues obtained from RV144, the only phase III clinical trial to ever demonstrate protection from HIV acquisition, and address the possible mechanisms behind this partial protection.

"I am not happy that I am sick. I am not happy that I have AIDS. But if that is helping others, I can at least know that my own misfortune has had some positive worth."

Rock Hudson

"I am working with people with AIDS on a daily basis. To hear that there is a possible vaccine that could come out in two or three years is no good news for these people. Most of the people we're working with now will be dead by that time"

Bob Scheckey, HIV-infected patient, April 1984

CHAPTER 1: Introduction

An introduction to vaccines

Vaccines are an important tool in Public Health for the prevention of both bacterial and viral infections and are estimated to avert 2 to 3 million deaths every year; furthermore, they have the potential of saving additional 1.5 million lives if vaccination programs are improved worldwide[1]. So far, tens of vaccines protecting both against viral and bacterial infections are approved for clinical use. In addition, vaccines for the treatment of cancer and autoimmune diseases are being developed. However, for the purpose of this thesis, the immunological mechanisms of protection against viral infections will be illustrated.

Types of Vaccines

A key difference that distinguishes types of vaccines is the form in which the antigen is delivered. Different forms are combined with different non-antigenic ingredients to guarantee the delivery of the safest, most cost-effective preparation that can efficiently activate the immune system against and provide protection from a given circulating pathogen.

Preparation of the antigen

Historically, there have been two main types of vaccines that have been used to prevent infectious diseases[2].

(I) *Attenuated* vaccines induce protection by exposing patients to debilitated forms of live virus. These are generally obtained by allowing the virus to undergo several cycles of replication in tissues or cell cultures and are now commonly used to prevent infection of rubella, mumps, measles or chickenpox.

(II) *Inactivated* vaccines are formulated with viruses that are first grown in culture and then made unable to replicate through heat or chemical treatment, most commonly with formaldehyde[3]. Although these vaccines are considered safer than their attenuated counterparts because of lower likelihood to revert to their normal virulence, their activation of the immune system is weaker as it induces a shorter-

lasting immunological memory, and thus require multiple administrations over time to maintain protection. The Salk polio and tri- and tetravalent influenza vaccines are examples of inactivated vaccines.

Although attenuation and inactivation are the traditional means my which vaccines are made, more recently other methods have been developed to specifically deliver antigens for the induction of protection.

These include subunit, synthetic and nucleic acid vaccines[4].

(III) *Subunit* vaccines (with the most widely used inducing protection against Hepatitis B) are based on the administration of a single protein of the virus, either purified from whole pathogens grown in laboratory conditions or synthetically produced starting from DNA synthesized for the gene of interest.

(IV) *Synthetic* vaccines, that have not been approved for clinical study yet, aim to induce an immune response directed exclusively against certain areas of the protein of interest.

(V) Finally, *nucleic acid* vaccines[5] (both DNA- and RNA-based) are currently being developed in preclinical and clinical settings. Instead of administering the antigen directly, these vaccines aim to deliver nucleic acids that lead to the expression of viral antigens in transduced patient cells, thus inducing an immune response. These vaccines have the advantage that nucleic acids are not costly to produce, and stable to transport. Although viral vector-delivered and synthetic DNA vaccines have been evaluated in human clinical trials and been shown to be safe and immunogenic, none has yet been licensed for human use. Two main categories of mRNA vaccines are also being evaluated: self-amplifying and non-amplifying. However, although very promising, mRNA vaccines are still relatively far from being licensed for commercial distribution.

In addition to the antigenic component, vaccines contain other ingredients: adjuvants, preservatives, stabilisers and residues of manufacture[3]. Although for the purpose of this thesis

adjuvants are particularly of interest, other ingredients will be briefly summarised for completion.

Adjuvants

Adjuvants have the goal of increasing the intensity and influencing the type of immune response against the administered antigen[6]. These are particularly necessary in cases in which the administered antigen does not induce a response strong enough to result in protection[7]. While attenuated vaccines are generally protective without the inclusion of an adjuvant in the preparation, administration of only parts of the pathogen generally elicit weaker immune responses. For this reason, adjuvants are most commonly included in inactivated and subunit vaccines.

Alum, a formulation of aluminium salts which came into clinical practice in the 1920s, is the adjuvant most commonly used and at the moment included in vaccines against Hepatitis A and B, plus other bacterial vaccines[7]. The aluminium salts included in vaccines are aluminium hydroxide (AH) or alhydrogel (a chemically crystalline form of aluminium hydroxide), as well as aluminium phosphate (AP)[8,9].However, the identification of the exact mechanism of efficacy of alum in inducing potent immune responses remains elusive[10]. *In vitro* and *in vivo* studies have resulted in three main hypotheses: (i) depot formation, (ii) antigen targeting, (iii) induction of inflammation.

(I) *Depot formation*. Upon studies on guinea pigs vaccinated against Diphtheria Toxoid, Glenny, Buttle and Stevens hypothesised that the slow elimination of alum-precipitated antigens over a long period of time from a single infection time could stimulate both primary and secondary immune responses thus resulting in increased antibody titres[11]. This theory might be justified by the fact that alum is identified as a strong antigen binder, thus it is plausible to hypothesise that the slow release of the antigen in the administration site could result in enhanced immune responses [10]. Moreover, upon interaction with aluminium salts, protein antigens are demonstrated to switch to a particulate form which, as compared to soluble antigens, better

interacts with Antigen Presenting Cells (APCs) resulting in enhanced phagocytosis[10,12,13] .

(II) *Antigen targeting*. The formation of particulates as an enhancer of APC recruitment was a "linker theory" that paved the way to develop further antigen-targeting hypotheses. A study on rabbits demonstrated the uptake of both antigen and AP by macrophages recruited to the injection site at 7 days post-vaccination[14]. Antigen targeting was defined in three phases, with the first one involving the recruitment of immune cells at the site of injection, the second the induction and maturation signals by APCs, and the third the migration of antigen-loaded APCs to the closest draining lymph node.

(III) Inflammation. It is commonly agreed that some degree of inflammation in the injection site is essential in developing an effective immune response[15], recognised as the "Danger Theory" proposed by Matzinger in 1994[16]. According to the danger theory, activation of the immune response is not dependent upon recognition of the invading viral or bacterial antigen, but rather on the elicitation of tissue damage. The signals released at the site of damage would then result in inflammation and lead to an adaptive immune response. This would be in line with the observation that administration of alum in vaccines results in the release of danger signals in the site of infection. The vaccines containing alum lead to a short-term inflammation in a normal environment, and long-term inflammation in a pathological environment at the site of injection[17,18]: indeed, alum induces uric acid or monosodium urate crystal as danger signals[18], as well as heat shock protein 70[19] and DNA[20,21]. The release of these molecules results in the activation of an immune response.

The humoral immune response

Vaccine-elicited protection is mainly attributed to the induction of antigen-specific antibodies[22]. The mechanisms behind B-cell maturation and the development of antigen-specific B cell responses, which are of particular interest in this thesis, will be reviewed more in detail below.

An overview of these responses and their role in relation to the T-cell arm of the adaptive immune response will be provided in the following paragraphs.

While antigen-specific antibody titres increase dramatically in the days/weeks following antigen encounter (**Figure 1.1**), more than a peak of antigen-specific antibodies is necessary for vaccination-mediated protection: affinity, avidity, neutralisation potential and Fc-mediated functions may all in fact play a role in providing protection from viral acquisition. These features of antibody responses are dependent on the nature of the antigen and the local immune response. Antibody affinity maturation and isotype switching are dependent on the co-stimulatory responses of T-helper cells, specifically T helper follicular cells. Similarly, Fc receptor functions are acquired by post-transcriptional modifications and are often developed in local tissues where B cell responses expand. Besides antibody-related features per se, a key function of vaccines is to induce long-term protection through the induction of long-lived plasma cells and memory B cells. While long-lived plasma cells are responsible for a steady, baseline level of antigen-specific antibody titres in plasma after the vaccine antigen is cleared, memory B cells are responsible for an antigen-reactive humoral immune response. Long-term protection is thus achieved when the steady memory is maintained at levels above protective threshold and memory B cells are able to steadily react to further interactions with the antigens and rapidly boost the titres of antigen-specific blood antibodies[23,24].

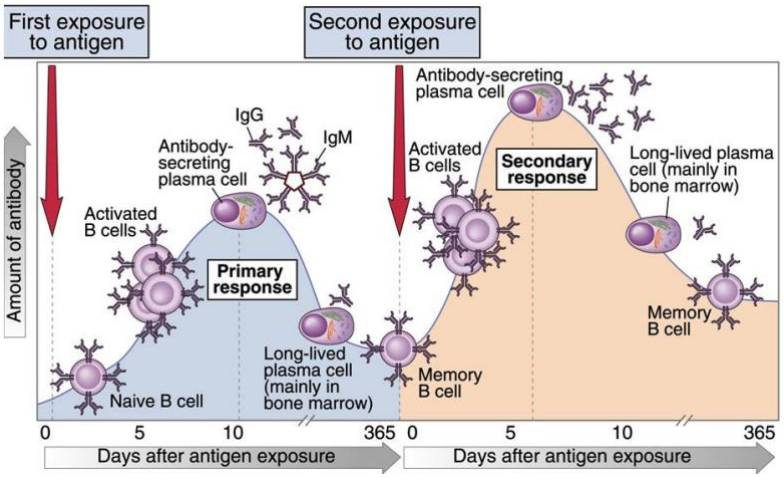

Figure 1. 1: Kinetic of primary and secondary antibody response. The primary B cell response (blue curve) leads to the generation of antigen-specific IgM- and IgG-secreting cells as well as memory B cells. Upon re-exposure, a secondary response (maroon curve) follows after which antigen-specific B cells responses are more rapidly generated, higher affinity IgG-secreting plasma cells are produced and higher antigen-specific IgG titres are achieved. (From reference [25]).

If on the one hand, however, plasma cell-secreted antigen-specific antibodies are immediate effectors of protection, T cells are essential in the induction of high-affinity antibodies and immunological memory[24].

The critical interaction between T and B cells

While antibodies act by opsonising, neutralising and possibly through Fc-mediated functions, T cells are also essential in limiting the spread of the infection or by sustaining the production of useful antibodies[23].

Cytotoxic $CD8^+$ T lymphocytes are able to limit the spread of infection by identifying and killing infected cells or through the secretion of antiviral cytokines. Antigen-specific $CD8^+$ lymphocytes have been found to be strongly induced by live, attenuated vaccines or vectored vaccines[23].

On the other hand, CD4+ T helper (Th) cells sustain the continuous production, maturation and maintenance of antigen-specific B- and $CD8^+$ T-cells responses[26]. These cells also contribute to macrophage activation[23].

Originally divided in two subsets, namely Th1 and Th2, T helper cells were then discovered to include many subsets with different functions and homing features[27]. Particularly relevant in the production of high affinity antibodies are follicular T-helper (Tfh) cells, which are located in the lymph node to sustain B-cell activation and differentiation into antibody-secreting cells (ASCs)[28]. Because Tfh cells play a major role in providing "help" to B cells for the development of high-affinity, antigen-specific antibodies, the main mechanisms and molecular players of this interaction will be reviewed more in detail in the subsections below.

However, T-helper 17 (Th17) cells will first be briefly reviewed because of their importance in the early stages of HIV infection. These cells, positive both for CCR5 and CD4, are mostly located in the skin and mucosa, where they induce neutrophil recruitment and promote local inflammation through the secretion of IL-17 (hence their name)[29,30]. These cells protect from bacteria that colonise the skin and mucosa, and a balance is maintained by the suppression exerted by regulatory T cells (Tregs) on Th17[31]. Soon after infection through the sexual route, HIV undergoes local replication at the site of infection, and is then transported by Dendritic Cells (DCs) to the lymph node, where it further replicates when exposed to resident CD4+ T cells[32]. As through most

of the infection HIV mostly displays preference for the coreceptor CCR5 rather than CXCR4, the intestinal mucosa, where large numbers of CCR5+ CD4+ Th17 cells are present, represents a rich substrate where HIV undergoes early rounds of rapid viral replication, resulting in the peak of viral load typical of acute HIV infection and depletion of the Th17 mucosal reservoir[32–34]. However, recent findings suggest that the integrin $\alpha4\beta7$ may play a fundamental role in the establishment of HIV infection in the gut tissue. The observations leading to this theory are reviewed more in detail in the last section of this chapter.

While antigen-specific serum antibodies are able to opsonise viral pathogens that enter the blood stream, their presence in the mucosa is essential to prevent pathogen replication at the first site of infection[22]. Peripheral antibodies have been demonstrated to be fundamental in preventing pathogen replication in infected wounds in the case of tetanus, in the throat in the case of diphtheria or the mucosal surface in the case of polio[35]. However, to reduce viral binding or adhesion to the tissue in the periphery, very high antibody levels need to be reached in the blood stream to allow for antibody exudation in the mucosa. The neutralisation of viruses at the mucosal level is thus mainly achieved upon vaccination through the transudation of immunoglobulin G (IgG) antibodies rather than immunoglobulin A (IgA)[23,35].

In most of the cases, inactivated vaccines do not induce antibodies responses of sufficiently high titres to prevent infection in the mucosal surface. Only after breaching through the mucosal tissue will a pathogen encounter serum IgG and be subject to the mechanisms of suppression[23]. If it is therefore to be taken into consideration that the first step towards the establishment of sustained HIV infection in humans is local replication that follows breach of the mucosal tissue. An effective HIV vaccine will therefore induce serum IgG levels that are high enough to exudate through the mucosal tissue and will bind to the virus before a local infection is established.

Mechanisms of the interaction between T and B cells

Tfh cells do not provide help to B cells through a single process or cellular product. Rather, they exert their activity through seven main distinct functions[28] as shown in **Figure 1.2**: proliferation, survival, plasma cell differentiations, somatic hypermutation, class-switch recombination, adhesion and attraction.

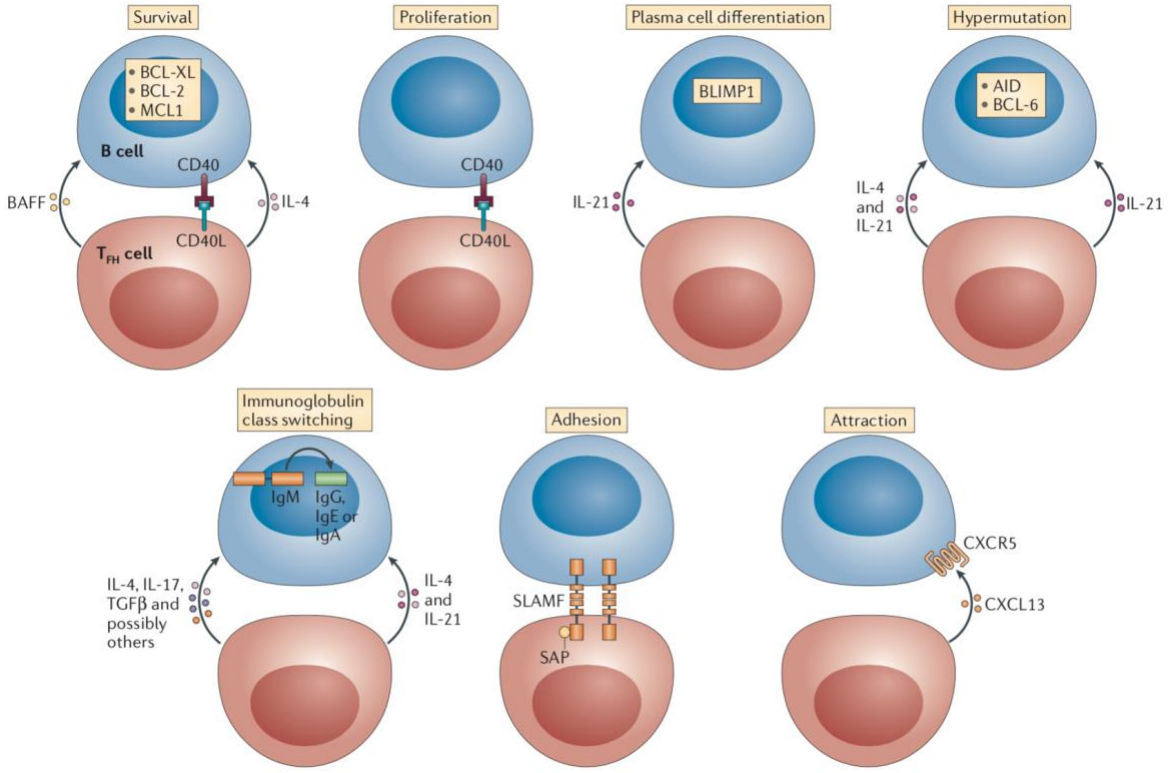

Figure 1. 2: T cell help is provided in several, different forms with different consequences. The seven main forms of this help are essential for a healthy B cell response. For synthesis, only the main factors involved in T cell help are shown, although many more molecules have been demonstrated to be involved in the regulation of these processes. Because some molecules display functional redundancies, combinatorial possibilities tightly regulate the help processes. BAFF, B cell-activating factor; BCL, B cell lymphoma; BLIMP1, B lymphocyte-induced maturation protein 1; CD40L, CD40 ligand; CXCL13, CXC-chemokine ligand 13; CXCR5, CXC-chemokine receptor 5; IL, interleukin; MCL1, myeloid cell leukaemia 1; SAP, SLAM-associated protein; SLAMF, signalling lymphocytic activation molecule F; TGFβ, transforming growth factor-β. From reference[28].

These seven different forms of help all contribute to the interactions between Tfh and B cells, with each process consisting of multiple pathways[25].

One of the main effects that Tfh cells have on B cells is the induction of proliferation, of which CD40 ligand (CD40L) is the most prominent Tfh cell player: the discovery of the interaction between B cell membrane CD40 and Tfh cell membrane CD40L created interest in the help that occurs via direct interaction between the two cell types, in addition to the secretion of and binding to cytokines[36].

Survival signals from Tfh cells are also crucial, since B cells located in the germinal centre (GC) are intrinsically pro-apoptotic[37]. The secretion of IL-4 by Tfh cells triggers pro-survival signals that

result in the transmission of survival signals within the B cells mediated by the IL-4 receptor complex[38].

As summarised more in detail in the following section, somatic hypermutation (SHM), an essential mechanism responsible for B cell affinity maturation within the GC, is mediated by the enzyme Activation-Induced Cytidine Deaminase (AID)[39–41]. It is however essential that B-cell lymphoma 6 protein (BCL-6) is co-expressed with AID by the GC B cell to repress the apoptosis programme that would otherwise result in self-destruction of the cell upon DNA damage[42]. Although the signals that induce AID and BCL-6 expression by B cells have not been defined in detail, it has been found that CD40L, IL-4 and IL-21 contribute to these mechanisms[43]. As a matter of fact, it seems that different ratios of CD40L engagement together with extracellular IL-4 and IL-21 are the primary regulators of cell proliferation, SHM and differentiation[28].

Class Switch Recombination (CSR), which is responsible for the switch from IgM secretion to other immunoglobulin subtypes (discussed more in detail below) can also be induced following instructions from Tfh cells to B cells: AID is a prime mediator of CSR, but the specific targeting of heavy chain constant region depends on additional factors that are selectively activated by cytokines which are mostly secreted by $CD4^+$ T cells[28]. For instance, human IgM to IgG CSR is most efficiently induced by IL-21, while IgE recombination is triggered at low levels of IL-21 in presence of high levels of IL-4[44,45].

Because help received by B cells extensively depends on direct contact with T cells, adhesion molecules expressed both by Tfh and B cells are fundamental players of this interaction. For instance, SLAM-associated protein (SAP) binds to the intracellular domains of surface receptors belonging to the SLAM family, which are involved in cell-to-cell adhesion[28]. Deletion of the SAP-encoding gene *Sh2d1a* results in severely impaired GCs and B cell memory[46–49], because unstable B cell-T cell adhesion does not allow Tfh cells to provide sufficient help signals to B cells.

Finally, chemoattraction is a main component of the T cell help to B cells: CXC-chemokine ligand 13 (CXCL13), the ligand for CXCR5, is constitutively secreted by human GC Tfh cells, which probably acts by recruiting B cells thus allowing Tfh-B cell colocalization and GC confinement[50,51].

T cell help is thus demonstrated to consist in a complex interplay of many factors and processes, with many inhibitory and stimulatory signals exchanged between Tfh cells and GC B cells over many rounds of B cell division, mutation and selection. Although a sufficient level of understanding of each of these processes has been reached, how these interactions are integrated to develop an efficient B cell responses is still poorly understood.

In the sections below, I will review the functional mechanisms and GC interactions that lead to the development of high-affinity plasma and memory B cell responses.

Development of antigen-specific B cell responses.

The development of antigen-specific B cell responses is a finely tuned phenomenon that occurs in GCs, which are specialised areas within the lymph node where B cells are assisted in developing effective antibody responses by T cell help and other stimulatory signals[41]. In the following sections, the molecular mechanisms of antibody diversification, the stages of development of mature GCs and the processes behind the selection of high-affinity B cell clones will be overviewed.

B Cell Receptor Diversity

The B cell receptor (BCR) serves as a receptor for antigens and is located on the surface of the B cells[52]. This receptor is made up by two immunoglobulin heavy (IgH) and two immunoglobulin light (IgL) chains encoded by the *IgH* and *IgL* loci, respectively (**Figure 1.3**). The IgL loci comprise the IgK or IgL loci. The three Ig loci are located on different chromosomes in humans and mice. The diversification strategies are largely conserved between the two species. The N-terminal ends of the heavy and light chains have a highly variable amino acid sequence, termed Variable (V) region, and are responsible for BCR-antigen interaction. On the other hand, the C-terminal ends only display a few variations in sequence and are called Constant (C) regions.

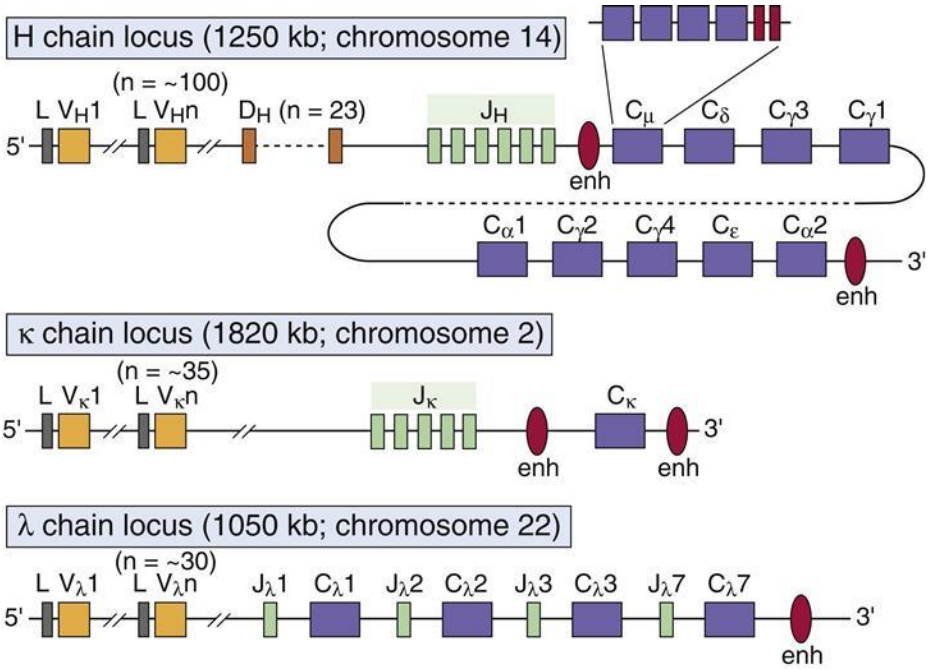

Figure 1. 3: Germ-line organization of human immunoglobulin (Ig) loci. Functional genes of the human heavy chain, κ-light chain, and λ-light chain loci are shown. Exons and introns are not drawn to scale. Each CH gene is shown as a single box but is composed of several exons, as illustrated for CH. *L*, leader (signal sequence); *V*, variable; *D*, diversity; *J*, joining; *C*, constant; *enh*, enhancer. (From reference [25]).

The generation of a broad population of B cells able to react to an enormous variety of antigens is essential to generate a humoral adaptive immune response[53]. However, IgH and IgL variable regions are not present in the germline, but assembled during early B cell development in the bone marrow or foetal liver before the cell is exposed to antigen[54]. The process, named V(D)J recombination generates a variable IgH $V_H(D)J_H$ exon through the different combination of one of the numerous IgH variable (VH), diversity (D) and joining (JH) segments located within 1 to 3 Mb from the 5' end of the IgH locus. In the IgL locus, where a diversity segment is not present, combinations of VL and JL exons are assembled[54].

The V(D)J recombination (**Figure 1.4**) is initiated by lymphocyte-specific endonucleases RAG1 and RAG2 (collectively named "RAG") which recognise recombination signal sequences (RSS) flanking the segments V, D and J[55]. RAG cleaves between the RSSs of two encoding segments, generating two double strand breaks that are then joined by the non-homologous end-joining double strand repair pathway[55–57]. Of note, before the ends are joined, random nucleotides are added de novo in the joining segments by the terminal deoxynucleotidyl transferase (Tdt), contributing to

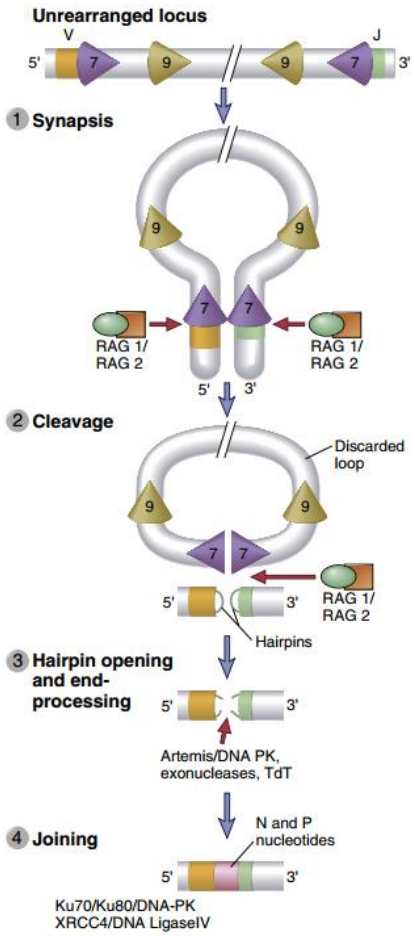

Figure 1. 4: Stages of the V(D)J recombination mechanism of the Ig loci. RAG endonucleases RAG1 and RAG2 mediate the formation of a synapsis (a loop-structure) in the unrearranged locus. When the synapsis is formed, RAG mediates cleavage between the RSSs of two encoding segments (coloured, numbered cones), thus generating double-strand breaks that are then repaired by mediators of the non-homologous end-joining double strand pathways. From reference [25]

increasing the diversity generated in the process, with the generation of an enormous repertoire of primary variable region exons[58,59]. In the final, recombined primary V region, three hypervariability regions, responsible for antigen interaction and thus named complementarity-determining regions (CDRs), are separated by more conserved framework regions (FWRs). While CDR1 and CDR2 both lie within the V segment, CDR3 is made up by part of the V and D and J segments, and thus more variable than the others[60,61].

Fully assembled IgH and IgL chain transcripts are synthesised starting from the V segment promoter in the V(D)J exon and proceeds through the exons that encode for the C regions, located downstream within 200 kb[62]. The mouse IgH locus contains eight groups of exons, each one encoding for different C_H regions (also named C_H genes) in the following order: 5' VDJ-Cμ-

Cδ-Cγ3-Cγ1-Cγ2b-Cγ2a-Cε-Cα 3'[63].The class of the BCR/antibody molecule will be determined by the exons that are expressed linked to the V region. At first, IgH variable region is transcribed together with the Cμ exons immediately downstream, or together with Cδ exons as well in some cells. Alternative splicing events will determine if the molecule is to be expressed with Cm, Cd and as a membrane-bound BCR or secreted antibody[64].However, before antigenic stimulation, B cell exclusively express membrane-bound μ or ð BCR[53].

It is important to point out that during B cell development, V(D)J recombination occurs first at the IgH locus in progenitor (pro) B cells[54,57]: these cells generate first D to JH rearrangements in both of the two IgH alleles, and only later they proceed with linking the Vh segment to the arranged DJh segments in one allele[65]. If the resulting VDJ segment is in frame, and productive, the Ig μ heavy chain protein generates a signal that prevents V – DJ recombination to occur in the second allele and directs the cell towards the precursor (pre) B cell stage. Pre B cells have thus a productive V(D)J IgH allele and an intermediate DJ allele[53]. If the TdT-induced diversification is out of frame and the resulting IgH chain non-productive, the cell will proceed and recombine the second allele which, if in frame, will push the cell to the pre B cell stage. The resulting cells will have a non-productive, out of frame and a productive VDJ allele. Generally, circa 65% of the V-DJ rearrangements are non-productive, and some 40% of normal B cells display two VDJ rearrangements. This mechanism of "allelic exclusion" has probably been developed to allow for mono-specificity of the single cells[66]. Pre B cells will then proceed and rearrange their genes for a productive IgL chain, which will pair with the μ heavy chain to yield a complete BCR μ molecule[54,57]. The resulting naïve B cells will then be able to migrate to the periphery to patrol the secondary lymphoid organs (lymph nodes, spleen and Peyer's patches) in search of their cognate antigen[53].

Somatic Hypermutation and Class Switch Recombination

Naïve B Cell activation results in the generation of B cells that secrete their BCR as an antibody. In addition, this process results in two somatic processes of genetic rearrangement that enhance antibody affinity and change antibody function. The first process, SHM, diversifies the antigen-binding region of the BCR, while CSR switches the CH exon resulting in a change of the function

of the antibody, that is the means by which the antigen is eliminated[60,67]. While SH occurs in the GCs, CSR can occur both inside and outside of the GCs[37,68,69]. Both SHM and CSR are mediated by the enzyme AID[70,71], which modifies ssDNA resulting in the deamination of cytidine residues[60]. However, the deamination is not casual and is mostly oriented in the context of preferred sequences[60] (**Figure 1.5**) Because the target of AID is ssDNA, transcription of the modified enzyme needs to be active. Both SHM and CSR rely on the normal mismatch repair processes of Base Excision Repair (BER) and mismatch repair (MMR) to convert AID-induced lesions to mutations or double strand breaks (DSB)[53].

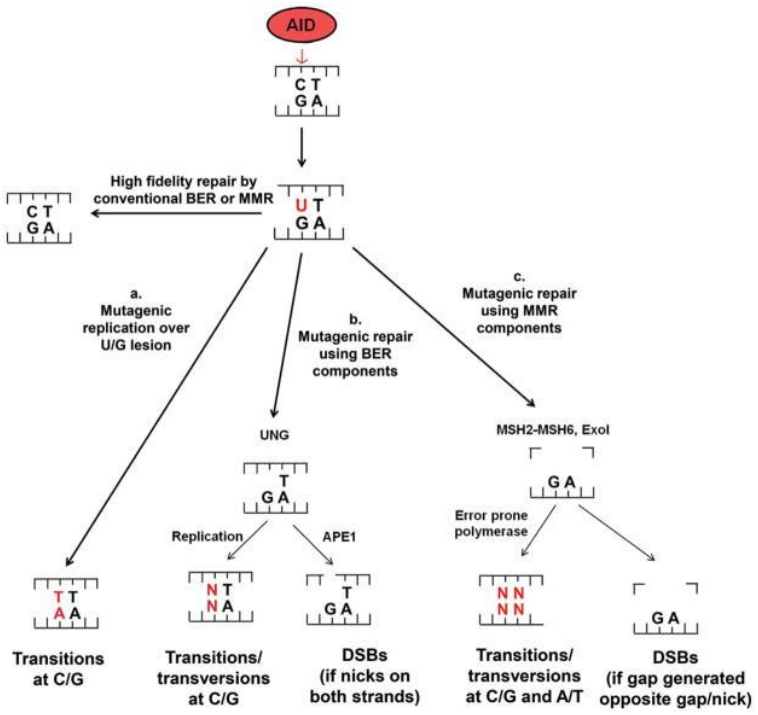

Figure 1. 5: Mechanisms of AID cytidine deamination in SHM and CSR. The deamination of cytosine residues in IgH and IgL V(D)J exons results in the reprocessing of the modified cytosines through cellular repair pathways Base Excision Repair (BER) and mismatch repair (MMR), which generally convert AID-induce lesions to point mutations or, less likely, to double-strand breaks. From reference [53].

During SHM, AID mediates the deamination of cytosine residues in IgH and IgL V(D)J exons, and the products are processed through cellular repair pathways that mostly result in point mutations (with 2/3 of substitutions being transitions) although insertions and deletions might be induced too[60,72–74]. The mutation frequency is approximately one mutation per thousand base pair per generation, with the highest concentration of mutations being localised in the CDRs[60,75,76]. The

mechanisms by which cells with mutations that increase affinity for the target antigen are selected are discussed more in detail below.

CSR, on the other hand, is mediated by the AID deamination of cytosine residues in noncoding switch (S) regions that are located upstream of each set of CH exons (with the exception for Cð exons) and are from 1 to 10 kb in length[67,77]. CSR is then finalised by the joining of two S regions where AID-initiated DSBs were generated[63,77]. As a result, a switch occurs in secretion from IgM to different IgG classes, when Cμ exons are replaced with one of the sets of CH exons located downstream[53]. The functions of each class of Ig are summarised in **Table 1.1** and discussed more in detail below.

In this way, CSR alters the effector functions of an antibody to one that may work best to eliminate the given pathogen, while maintaining the same antibody-binding specificity[53].

	Immunoglobulin								
	IgG1	IgG2	IgG3	IgG4	IgM	IgA1	IgA2	IgD	IgE
Heavy chain	γ_1	γ_2	γ_3	γ_4	μ	α_1	α_2	δ	ε
Molecular weight (kDa)	146	146	165	146	970	160	160	184	188
Serum level (mean adult mg ml^{-1})	9	3	1	0.5	1.5	3.0	0.5	0.03	5×10^{-5}
Half-life in serum (days)	21	20	7	21	10	6	6	3	2
Classical pathway of complement activation	++	+	+++	−	+++	−	−	−	−
Alternative pathway of complement activation	−	−	−	−	−	+	−	−	−
Placental transfer	+++	+	++	−/+	−	−	−	−	−
Binding to macrophages and other phagocytes	+	−	+	−/+	−	+	+	−	+
High-affinity binding to mast cells and basophils	−	−	−	−	−	−	−	−	+++
Reactivity with staphylococcal Protein A	+	+	−/+	+	−	−	−	−	−

Table 1. 1: Properties of the human immunoglobulin isotypes. While IgG1 and IgG3 display stronger activation of the classical pathway of the complement, as well as ability to trigger ADCC and ADCP, IgG2 and IgG4 have weaker Fc-related functions. IgM displays strong ability to activate the complement through the classical pathway, while IgAs can recruit macrophages and phagocytes for ADCP. Finally, IgE mostly mediates reactions to parasites such as helminths or allergy reactions through recruitment of mast cells and basophils. From reference [78].

Immunoglobulin loci in the rhesus macaque

The rhesus macaque is a critically important animal model in SIV/HIV research. However, Indian-origin rhesus macaque Ig loci have been assembled at high-coverage only recently[79]. The authors described sequence diversity in ten Indian-origin rhesus macaques of the genes encoding for the heavy chain (IGHV, IGHD, IGHJ, IGHC), the kappa light chain (IGKV, IGKJ, IGKC) and the lambda light chain (IGLV, IGLJ, IGLC). Below, I will briefly summarise the main differences and similarities between these genes in human and rhesus macaque. The information reported in this section is obtained from the work of Ramesh and collaborators[79].

Heavy Chain Genes

Humans typically carry 123-129 total IGVH genes in the IGH locus per haploid genome, of which 38-46 are functional and classified into seven families[80]. Overall, macaques have a similar number of genes, with the macaque IGHV3 family larger as compared to humans. Interestingly, the ten macaques studied by Ramesh and collaborators displayed a degree of allelic diversity comparable to that of the whole human IGHV genes in the total IMGT database. Regarding IGHD, humans typically have 23 functional genes that belong to seven families, and additional 14 open reading frames (ORFs)[80]. As the authors identified 39 genes with 49 alleles distributed in six families, macaques have a substantially expanded IGHD repertoire. Similarly, nine macaques IGHJ genes were identified, while only six have been found in human.

Finally, humans have 57 IGHC alleles representing a total of 12 IGHC genes (of which two IGHA, one IGHD, one IGHE, two IGHEP, four IGHG, one IGHGP and IGHM, where "P" indicates pseudogenes), while macaques appear to only have eight IGHC genes, lacking IGHGP, one of the two IGHEP and one IGHA. However, greater IGHC allele numbers are present in macaque than in humans. Notably, macaque and human share 80% IGHC exon pairwise identity.

Kappa Light Chain Genes

41 functional IGKV genes have been identified in humans, with a total of 67 alleles belonging to 6 families. These genes are organised in three alternating blocks in the IGKV locus. With the exception of the IGKV2 family, humans and macaques were found to have a generally similar

number of genes, although macaques display six alternating blocks of IGKV genes. Macaque IGKV genes are also more polymorphic than the human IGKV genes and, unlike humans, carry functional genes in the IGKV7 family. Similarly to humans, macaques have functional IGKV genes both in the forward and reverse orientation.

As per IGKJ genes, humans have five functional genes, and all of the macaque genes were found to have distinct human orthologs.

Both humans and macaques have only one IGKC gene. However, while five alleles were described in humans, the authors found six alleles in ten macaques, indicating that IGKC is highly diverse in macaques, in comparison to humans. Notably, the pairwise identity between human and macaque IGKC is 91.6%.

Lambda Light Chain Genes

In humans, 33 functional IGLV genes represented by 71 alleles in 10 families, with additional seven ORFs with 11 alleles identified. In macaque, most IGLV families are larger and more diverse than in human. As per IGLJ, five functional genes and two non-functional genes have been found in humans, while five functional genes have been identified in the macaque. Similarly, humans have five functional, two non-functional IGLC genes per haploid locus, with the same organisation found in macaques.

In summary, relative to humans several V gene families in all of the three Ig loci were expanded in macaques. In addition, macaque Ig V gene diversity was found to be several times higher than that in humans. These results are particularly of interest having considered that the diversity of only ten macaques examined by the authors was compared with that of the Ig loci of all humans studied to date and reported in the ImMunoGeneTics database.

Having summarised the genetic and molecular features of the B cell antibody repertoire, the Fc-related antibody effector functions will be reviewed below before proceeding to summarise the cellular mechanisms driving development of an affinity-matured, class-switched antibody response.

Antibody Effector Functions

Antibodies act by a number of mechanisms which engage other arms of the immune system[25]. Besides blocking interactions or functions of molecules through their antigen-binding region (described more in detail below in the context of HIV neutralisation), antibodies can activate the classical complement pathway (complement-dependent cytotoxicity, CDC) by interacting with C1q on the C1 complex when clustered, or coordinate the antibody-mediated and cell-mediated immune response through the engagement of Fc receptors (**Figure 1.6**)[81]. Which effector functions the antibody will initiate depends on its isotype or subclass.

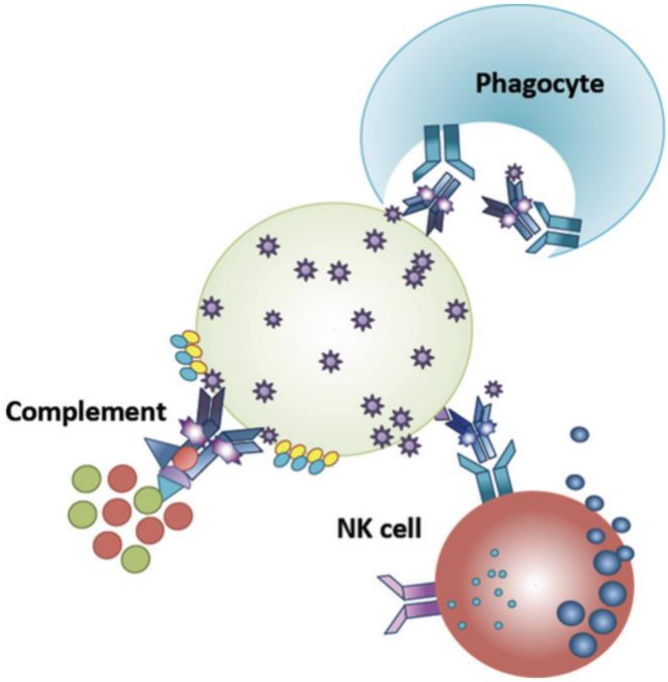

Figure 1. 6: Antiviral properties of non-neutralising antibodies. HIV-specific antibodies act by attracting the innate immune cells or complement to eliminate the infected cells through different mechanisms, such as ADCC, ADCP, and complement activation. From reference [81].

Fc Receptor-dependent functions

Fc receptors (FcRs) are immune regulatory receptors with selective, class-specific antibody binding properties: FcγR binds to IgG , FcεRI to IgE, FcαRI to IgA, FcμR to IgM and FcδR to IgD[82]. Three classes of IgG-binding receptors have been identified on leukocytes: CD64 (FcγRI), CD32 (FcγRIIa, FcγRIIb and FcγRIIc) and CD16 (FcγRIIIa and FcγRIIIb)[83]. FcγRI is identified as the highest affinity receptor, while FcγRII and FcγRIII demonstrate low to intermediate affinity[84]. The expression of FcγRs on any given cell type may change according to location, cytokine milieu and

activation state[81]. The formation of a bridge between an antigen-expressing target cell and an FcγR-bearing effector cell aims to result in target cell death either by antibody-dependent cellular cytotoxicity (ADCC) or antibody-dependent cellular phagocytosis (ADCP)[81]:

i. In the context of ADCC, which is a mechanism quite central in **Chapter 3**, FcγRs on the surface of innate effector cells (NK cells, macrophages, monocytes and eosinophils) bind to the Fc region of an IgG pre-bound to a target cell[81]. Upon binding, a signalling pathway is activated which leads to the secretion of lytic enzymes, perforin, granzymes and tumour necrosis factor, with the final killing of the target cell[85]. The level of ADCC effector function varies for different IgG subtypes, with higher ADCC effector function being mediated by IgG1 and IgG3, and lower by IgG2 and IgG4[25]. In the macaque model, vaccine-induced ADCC activity has been found to correlate with infection outcomes[86–89]. However, no study to date has directly demonstrate that ADCC-mediating antibodies are alone responsible for preventing HIV/SIV infection, as observed in a study where animals infused with nonfucosylated mAb IgG1 b12, modified to increased NK cell-mediated ADCC, were not significantly more protected that those administered with unmodified mAb[81].
ii. ADCP is a mechanism by which antibody-opsonised target cells activate the FcγR on the surface of macrophages, monocytes and dendritic cells thus inducing phagocytosis[85]. By this mechanisms, the target infected cell is degraded through acidification in the phagosome[90]. Like ADCC-inducing antibodies, it is likely that phagocytosis of HIV immune complexes increases the antiviral activity of non-neutralising or neutralising antibodies[85].

Despite the proven inability of non-neutralising, functional antibodies to protect from HIV/SIV infection[86,91–93], the biologic activity behind the protection mediated by neutralising and non-neutralising antibodies is likely different: unlike neutralising antibodies, non-neutralising antibodies must form avid immune complexes that are capable of recruiting low-affinity receptors or complement components necessary for their function[83]. Since HIV exposes a limited amount of Env products on its envelope[94], non-neutralising antibodies may only marginally impact the virus itself. However, since HIV assembles in lipid rafts[95], the higher concentration of viral products on the survace of infected cells may result in clustering of non-neutralising

antibodies and recruitment of FcRs[81]. Therefore, polyclonal non-neutralising antibodies simultaneously targeting several epitopes on a single envelope may have a better opportunity to form large immune complexes than non-neutralising monoclonal preparations[81]. It is therefore possible that cocktails of high-affinity, Fc-enhanced non-neutralising antibodies could simultaneously opsonise the surface of HIV envelope and mediate sterilising protection from infection[81].

Fc Receptor-independent functions

While ADCC and ADCP are antibody functions that depend on FcR binding, the effector function of an antibody can also be carried out independently of FcRs through the activation of the complement system[96]. CDC (**Figure 1.7**) is a function that, when lacking, can result in severely impaired antibody responses both in animals and humans[97,98].

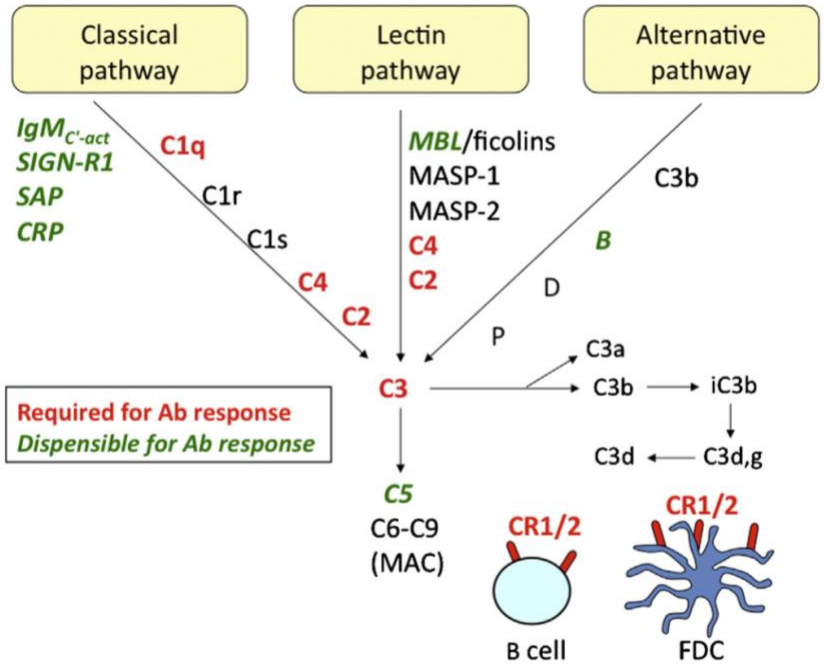

Figure 1. 7: The complement system in the antibody response. Antibody responses in animals that lack the factors and receptors shown in red are severely impaired, whereas lack of factors in green results in largely normal phenotype. The classical pathway is activated upon antibody opsonisation of target cells or organisms, the alternative pathway in response to bacterial endotoxin and the lectin pathway in response to pathogens containing cell walls rich in mannose. The final result of an effective complement response is target opsonisation and lysis through the membrane attack complex (MAC). From reference[99].

The complement system is a set of over 20 proteins that, when activated, lead to a cascade of reactions on the surface of the pathogens that ultimately kill the threat thus eliminating infection[25]. The complement system can be activated independently from the adaptive immune response through the alternative pathway, in response to presence of bacterial endotoxin, or the lectin pathway, in response to the invasion of pathogens containing mannose-rich cellular walls[96]. However, as more related to the subject discussed in this thesis, only the classical, antibody-dependent pathway of activation will be discussed in detail.

Classical complement activation occurs in a specific immune response when IgG or IgM bind to antigens located on the surface of a cell, and the Fc recruits the first complement protein, C1[96].

A cascade of events follows, with the generation of small proteins and peptides upon proteolysis of larger, inactivated complement components[96]. For instance, complement factor C3 is cleaved into C3b and C3a upon activation: while C3b remains bound to the complex on the surface of the target, acting as opsonin, the peptide C3a is released and diffuses acting as a chemotactic agent to cause inflammation[25]. A similar mechanism is observed with C5, where C5a is released and C5b acts as an opsonin[25].

Ultimately, the complement results in the activation of proteins C6, C7 and C8 which bind to the accumulating complement complex on the surface of the target, with the final recruitment of C9 proteins[100]. These C9 monomers are of elongated shape and form a structure called membrane attack complex (MAC), which takes the shape of a cylinder with a hole in the centre that pierces the membrane of the cell[101]. MAC thus initiates cell lysis or apoptosis[102].

Germinal Centres - Overview

The GCs are structures formed within lymph nodes in response to T-cell dependent antigens[103]. It is within GCs that antigen-specific B cells proliferate and differentiate into antibody-secreting cells (ASCs or plasma cells) and memory B cells that are responsible for the humoral immunity against invading pathogens. Several different cell types drive the differentiation of B cells from the GC reaction. Within the GCs, B cells proliferate at extremely high rates, and the immunoglobulin variable region (IgV) genes undergo SHM that results in increased affinity towards the target antigen[104,105]. This process, defined as affinity maturation, results in B cells

and plasma cells with potent binding affinities towards a defined antigen. It is through several rounds of positive selection and T cell help that the clones with highest affinity are selected out of a pool of randomly hypermutated cells. As a results, inferior antibody mutants are negatively selected[41].

Antigen-specific memory and plasma cells can be detected at 1 week after encounter with the antigen[106], and are possible thanks to the creation of specialised microenvironments inside of the GCs that have the purpose of confining areas of mutation and areas of selection[37].

The GC reaction upon antigen encounter

The lymph node is rich in follicles mainly comprised of naïve B cells with IgM+IgD+ phenotype, surrounded by areas rich in T cells and separated by interfollicular regions. GCs form roughly at the centre of these follicles where a network of follicular dendritic cells (FDCs), stromal cells that have long dendrites and with the ability to carry intact antigens on their surface, is present.

When an antigen is presented within the follicle, naïve B cells activate and migrate to the border of the T cell zone or to the interfollicular region, where they undergo proliferation and activate upon interaction with antigen-specific T cells[107–109]. It is important to notice that not all of the antigen-activated B cells will enter the GC reaction, as some will differentiate into short-lived plasma blasts and migrate to the medullary chords, which are specialised areas of the lymph node. The function of short-lived plasmablasts, able to secrete low-affinity antibodies, will be illustrated below.

However, of those B cells that have high affinity for the antigen, most differentiate into plasmablasts, rather than memory B cells.

One day after invasion by a pathogen or immunisation, antigen-specific B cells and T cells are interacting within the interfollicular region of the lymph node[110,111]. After interaction with dendritic cells, the T cells at this stage are already committed to differentiating into Tfh cells[110,112,113]. BCL-6, which is considered a fundamental regulator of the Tfh and GC B cell differentiation, is found upregulated in Tfh cells as early as at this stage, while B cells start expressing low levels of BCL-6 only at two days after immunisation[110,113]. Among the other

functions, this transcriptional repressor turns off genes that are involved in B cell activation and differentiation into memory B cells and plasma cells. At day 2, most of the T cells have acquired T_{FH} phenotypes (CXCR5+, PD1+, GL7+) and, at day 3, have migrated into the follicle, while it is only at day 4 that B cells migrate there.

GC formation and maturation

At day 4 early GCs within follicles can be observed. At this stage, B cells differentiate into B cell blasts, proliferate very rapidly and monopolise the network of FDCs in the centre of the follicle[103]. Of note, B cell blasts displace IgM+ IgD+ B cells, with the resulting formation of a "mantle zone" of naïve B cells around the GC. In the following two days, the GC expands rapidly because of the quick proliferation of the B cell blasts until day 7. At this stage, the GC has completely matured, and can be seen as divided into two microenvironments, namely the dark and the light zone[37,103]. The dark zone, named after its appearance in tissue samples, consists of densely packed, highly proliferating blasts and a network of cells similar in morphology to the FDCs of the light zone. The light zone is populated by lower numbers of B cells and is characterised by the concurrent presence of T_{FH} cells, FDCs and macrophages[37].

Functional aspects of the GC reaction

SHM is the intracellular molecular mechanism that drives affinity maturation of B cells in the GC. When a cell has undergone a round of SHM, it moves to the light zone and, if expressing a high-affinity BCR, is positively selected. Every high-affinity B cell is the result of several rounds of mutation and selection, favoured by the circular transit between the dark and the light zone. In the matter of a few days, memory B and plasma cells exit the GC, with every ASC releasing thousands of monoclonal antibodies per second specific for the target antigen[114]. Several mechanisms contribute to the selection of high affinity B cells:

i Cellular migration between GC zones. B cells are able to move rapidly between the dark and the light zone as a result of cell-intrinsic molecular programmes[41,115,116]. It seems that the spatial separation between the light and the dark zone is essential for

efficient rounds of affinity maturation, and is evolutionarily conserved across vertebrates[117].

ii Tfh cells. In the light zone, high-affinity B cells must be selected over low-affinity clones before they undergo further rounds of SHM in the dark zone. While it was originally believed that the selection of B cells was driven by a direct competition for the antigen taken up from FDCs[103], it is now hypothesised that competition for T help is the key factor determining the selection of high-affinity B cell clones[37]: it seems in truth that the higher affinity a B cell displays for an antigen, the more the antigen is internalised upon binding with the BCR and the more is presented on MHC complexes to Tfh cells[118]. It is this direct correlation between BCR affinity and density of peptide-Major Histocompatibility Complex (MHC) on the cell surface that results in higher T cell help and thus a selective advantage of high affinity clone: T_{FH} cells form the largest, longest contacts with B cells that present the highest concentration of antigen-MHC complexes[119]. It is fundamental to mention that the BCR in the GC is mostly dedicated to the task of antigen capture and internalisation rather than intracellular signalling[120]. The B cells that receive the greatest help are induced to divide the greatest number of times when re-entering the dark zone[121], and this in turn results in higher rates of SHM as this process induces a nucleotide exchange per 1,000 bases into the IgV genes at every round of division within the GC[60]. Of the new mutants which re-enter the light zone, those with mutations that induce higher affinity are again sent back to the dark zone for further proliferation and SHM. As a result, just a few days following immunisation, the GC reaction is dominated by the population with the highest affinity for the antigen[41].

iii Antigen masking. The role of early-originated low-affinity short-lived plasma cells is to provide a further mechanism of selection of high affinity clones: only those B cells with BCRs of higher affinity than the antibodies secreted by short-lived plasma cells will be able to compete for antigen binding and will thus proliferate and undergo SHM[122]. As antibodies with higher affinities are produced over time, the stringency of this selection mechanism increases.

Interestingly, antibody secretion as a selection mechanism is also fundamental in inter-GC communication[122], as antibodies secreted by short-lived plasma cells are able to infiltrate neighbouring GCs. However, this is not the only mechanism by which GCs communicate: Tfh cells are able to transit to and invade more than one GC and newly activated B cells can infiltrate pre-existing GCs[123,124]. This means that, while GCs have been evolved to separate sites of B cell maturation so that a variate immune response is present, not dominated by only a few clones and antigens can be targeted from different angles, coordination between different GCs is still achieved[41]. The final goal is that of producing as many antibodies with the highest affinity towards the highest number of epitopes of a given antigen. Targeting a pathogen from different angles is particularly helpful in the case of invasion from pathogens that are capable of rapidly escaping the immune responsible through antigenic variation[41].

B cell memory

The neutralising antibody response has been historically recognised of main importance in providing protection to the host from invading pathogens. If the pathogen returns a second time after a first infection or vaccination, the humoral response responds with two features, that have been described by Kurosaki et al. as “constitutive humoral memory” and “reactive immune memory”[24].

The *constitutive humoral memory* is that provided that pre-existing antibodies that were already circulating in the blood stream of the patient, secreted by specialised antibody secreting cells, that is long-lived plasma cells. Upon re-infection, these antibodies bind to and neutralise the pathogen[24].

However, a *reactive immune memory* is also activated in the case of re-infection, and results not only in an increase of antigen-binding antibodies in the blood stream, but also in the rapid development of antibodies with new binding properties. Compared with the primary antibody response, the reactive humoral memory response is generally faster, results in greater magnitude and in antibodies with greater affinity and switched isotype[24,125].

The greater magnitude of the memory as compared to the primary response is mainly caused by the survival of memory B cells generated by the primary immune response.

It is worth mentioning that recent studies demonstrated the existence of different subsets of memory B cells: (i) germinal centre-independent memory B cells[24,126,127] and (ii) unswitched IgM+ memory B cells[128–130] in addition to (iii) the widely studied germinal centre-dependent switched memory B cells. These cell types will be illustrated in the following sections, after the mechanisms by which they originate are elucidated.

Generation of T cell-dependent memory B cells

In T cell-dependent B cell responses (**Figure 1.8**), antigen-activated B cells proliferate and differentiate into any of three cell types: (i) germinal centre-independent memory B cells, (ii) germinal centre-dependent memory B cells or (ii) extrafollicular short-lived plasma cells (already illustrated above)[131]. At this stage, isotype switching occurs, while SHM is not yet initiated.

(i) Germinal centre-independent memory B cells

While high-affinity cells present more peptide-MHC to cognate Tfh cells at the B cell-T cell border in the spleen or lymph node, receive more T cell help and are directed towards the germinal centre, those with lower affinity receive less T cell help and are therefore more likely to take a germinal centre-independent destiny. Because somatic hypermutation has not yet occurred at this stage, germinal centre-independent memory B cells reflect the specificities of the naïve B cell pool that initially responded. The maintenance of a low-affinity memory has the goal to enable the maintenance of cells with a potentially broad range of antigen specificity, thus providing protection to pathogens that bear antigens similar, but not identical, to those previously encountered.

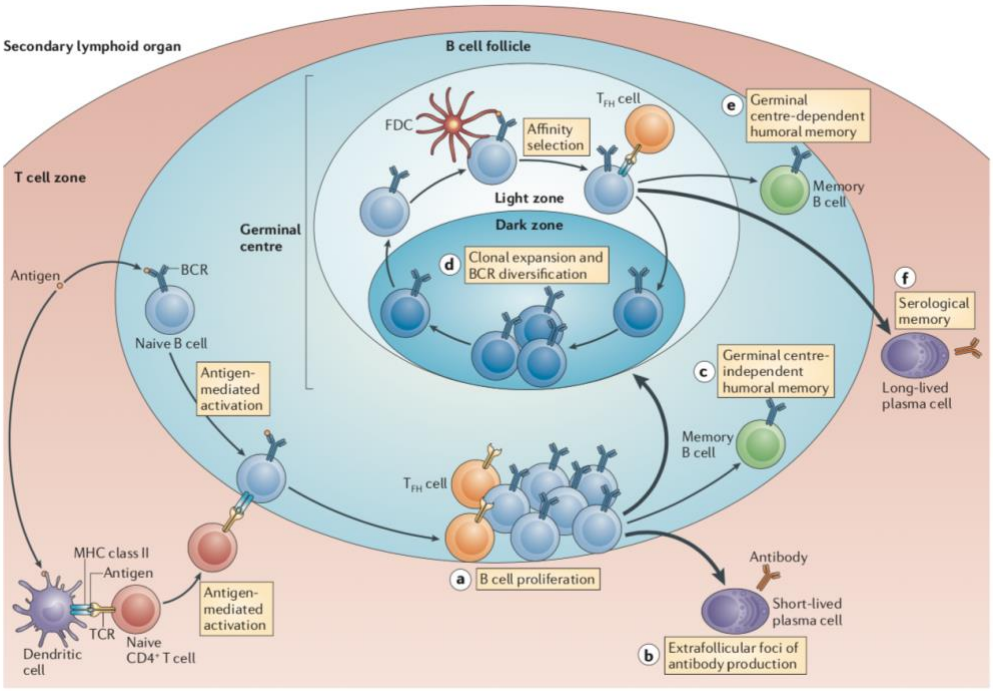

Figure 1. 8: Generation of T cell-dependent B cell memory. Antigen-activated B and T cells migrate to the borders of the B cell follicles and the T cell zones in the secondary lymphoid organs, respectively. This leads to the establishment of a stable B-T-cell interaction and enables B cells to receive help signals from CD4+ T cells. Activated B and T cells then migrate to the outer follicles, where B cells undergo proliferation (a). Some of the proliferating B cells differentiate into short-lived plasma cells (b), and others develop into germinal centre-independent memory B cells (c). Alternatively, activated B cells can return to the follicle and undergo rapid proliferation to form the germinal centre (d). In the dark zone of the germinal centre, clonal expansion of antigen-specific B cells takes place together with BCR diversification through SHM. B cells exiting the cell cycle relocate to the light zone, where they are selected on the basis of affinity for the antigen through the interaction with FDCs and Tfh cells that are coated with immune complexes. Affinity-matured germinal centre B cells can re-enter the germinal centre cycle or exit the germinal centre, either as memory B cells (e) or as long-lived plasma cells (f) that contribute to B cell memory. The strength of signals received by a B cell determine its fate: stronger signals (bold arrows) favour plasma cell or germinal centre B cell development, while weaker signals (narrow arrows) determine memory B cell differentiation. TCR: T cell receptor. (From reference [24]).

(ii) Germinal centre-dependent memory B cells

The precise mechanisms by which some of the germinal centre B cells are directed towards a memory phenotype are still unclear, as not a single master regulator of gene transcription has been identified to drive gene expression towards this differentiation. It is thus hypothesised that memory B cells differentiate randomly from germinal centre B cells into a memory phenotype.

Generation of T cell-independent memory B cells

While the major, conventional B cell population in humans and mice, B2 cells, which arise from bone marrow precursor cells have been known for a long time to generate B cell memory responses, it was found that B1 cells are also able to generate memory B cells via immune responses independent from T cell help[132–134]. B1 cells are a self-renewing subset of mature B cells that are found in abundance in the pleural and peritoneal cavities. They recognise self-components, bacterial antigens and are responsible for the production of baseline serum IgMs. These cells are also detectable, although at low frequency, in the spleen[135]. B1 cells seem responsible for providing antigen-specific B cell memory with binding features similar to those of the naïve cells from which they originated[132–136]. T-cell independent memory seems to be mostly responsible for broad specificity rather than high-affinity responses, and it is yet to be determined what selective advantage T cell-independent memory B cells have over naïve B cell counterparts, that is if they respond more rapidly and/or more robustly to a returning pathogen, as observed in the T cell-dependent B cell memory.

Memory B Cell Diversity

Several types of memory B cells are produced upon primary contact with an antigen, each one of them seen to have different functions[137]. It has been traditionally believed that there are two types of memory B cells, that is IgM+ and IgG+ cells, which are activated and take care of different tasks upon antigen reencounter[138]:

(i) IgM+ memory B cells

This hypothesis has been corroborated by recent works[129,130] where it was seen that upon antigen reencounter IgM+ memory B cells undergo proliferation and re-enter the germinal centre reaction.

(ii) IgG+ memory B cells

While IgM+ cells are more prone to re-enter the germinal centre reaction, IgG+ memory B cells are more likely to differentiate into plasmablasts (PBs). However, it is not excluded that some IgM+ clones might differentiate into PBs, or some IgG+ clones re-enter the germinal centre reaction.

(iii) IgE+ memory B cells

While IgE-mediated hypersensitivity is a key component of the pathogenesis of allergic diseases[139], IgE memory B cells have not been detected in vivo in physiological conditions. However, it is possible that IgE memory responses of high affinity can be generated through class switching of IgG1+ memory B cells which already underwent affinity maturation[140].

This is particularly significant as an apparent lack of IgE+ memory B cells, but the possible observation of IgE memory responses requires us to reconsider the concept that memory B cells of a subtype are responsible for the memory response of that particular class exclusively[24].

Properties of memory B cells

The main feature of the memory B cell response is its response to secondary antigen encounter after extended periods of time from the first response and its rapidity and intensity upon antigen re-exposure. These features are what makes vaccines successful.

Let us look into these features more in details:

(i) Stemness

Haematopoiesis is a system that relies on the maintenance of a pool of somatic stem cells together with more differentiated progenitor cells[141]. The stem cells are not only responsible for the replacement of the progenitor cells as they differentiate, but also for the renewal of the stem pool. Some hypothesise[24] that a similar mechanism might be used by the humoral memory system, which needs to efficiently produce effector cells upon antigen re-encounter but also to continue to maintain the memory pool. As it seems that the IgG+ memory B cell pool has a greater propensity to differentiate towards plasma cells than IgM+ memory cells, it is possible that while the IgG+ memory pool is more progenitor cell-like, with a propensity to differentiate towards an effective function, IgM+ clones might be responsible to replenish and maintain the memory pool.

(ii) Longevity

IgG+ memory B cells can survive independently in the absence of T cells , although it has been demonstrated in mice that the maintenance of the IgG+ memory B cell pool requires the

presence of FCDs[142]. In mouse models where the FDC activity had been impaired, the primary antibody response was unaffected, while the secondary was dramatically impaired with a decreased frequency of memory B cells specific for the antigen of challenge. These results were interpreted such that FDCs promote IgG+ memory B cell survival, by functioning as a reservoir for complexes of antigen-antibody-complement, although the specific role of antigen persistence in the memory responses is debated: if on the one hand the need for BCR signalling in the maintenance of IgG1+ memory B cell survival has been shown[143], on the other hand genetic studies have demonstrated that presence of the antigen was not required to generate IgG+ memory B cells, implicating that only the presence of a tonic BCR signal is necessary to maintain the IgG+ memory pool[144].

As in terms of the different persistence of IgM+ versus IgG+ memory B cells, a mouse study by Pape and collaborators found that IgM+ memory B cells persisted for about 500 days after antigen priming, while IgG+ memory B cells declined over this time by many factors[130]. This could be explained as a difference in the self-renewal potential of the two B cell memory subtypes or by the existence of different cell survival mechanisms.

However, in humans it seems that IgG+ memory B cells are more long-lived, and more stable over time. A famous example is that of IgG+ memory B cells specific for the 1918 pandemic strain of influenza virus that were found circulating in the blood of survivors as many as 90 years after primary exposure to the virus[145].

(iii) Responsiveness

In T cell-dependent primary B cell responses, the production of high-affinity class-switched antibodies demands for the presence of both Tfh cells and FDCs. It is thus necessary to consider both intrinsic and extrinsic B cell mechanisms.

The goal of vaccination is to induce memory B cells that differentiate very rapidly into plasmablasts which produce class-switched antibodies which have the ability to clear the infection more quickly than naïve B cells.

To explain this difference in the speed of response, two models, non-mutually exclusive, have been postulated: (i) the BCR-intrinsic model hypothesises that the cytoplasmic domain of

membrane IgG1, with highly conserved 28 aa (as opposed to the 3 of IgM), is responsible for this; (ii) the BCR-extrinsic model hypothesises that other changes, e.g. alterations in the levels of expressed transcription factors can take place during priming and are responsible for this difference. Studies of nuclear transfer in mice[146] have shown the importance of stimulation history (BCR-extrinsic model) for the responsiveness of IgG+ memory B cells, but do not exclude a role for the cytoplasmic domain of membrane IgG1, which on the other hand has been shown to dramatically enhance survival of B cells at the plasmablast stage[147].

(iv) Dependence on other cell types

On the one hand, virus-specific memory B cells can be activated in the absence of T cells[148], while on the other T cell help is necessary to reactivate memory B cells that identify monomeric protein antigens[148,149]. This is of particular interest considering that the vaccination approaches presented in this thesis include multiple administrations of monomeric Simian Immunodeficiency Virus surface protein (SU) gp120 monomeric antigens adjuvanted in alum. There exists evidence that in this kind of response, memory T cells in the secondary lymphoid tissue or in the peripheral blood help B cell activation[112,150–155]. These memory Tfh cells, in the spleen or lymph node, are found in the T cell zone as well as the B- T- cell border and in the B cell follicles[152,155]. The fundamental role of Tfh memory cells was demonstrated in a study by Ise and collaborators, where loss of memory Tfh cells abolished the reactivation of memory B cells and differentiation into plasma cells[155]. These results demonstrate how fundamental is the Tfh memory in inducing potent secondary antibody responses. The interaction between Tfh cells and B cells is due to the B cells presenting antigen via the MHC class II molecules on memory B cells[149,156]. Therefore, it seems that activation of memory Tfh cells by cognate memory B cells which are located next to each other in the secondary lymphoid tissue is a crucial determinant for the rapid activation of the humoral memory response.

FDCs also contribute to the maintenance of the memory B cell and recall response[142]. It has historically been hypothesised that FDCs are capable of retaining antigens for long periods of time, although the role of antigen persistence in the memory response is debated, and the exact role of FDCs in memory B cell maintenance is unclear[24]. One possibility is that FDCs absorb

immune complexes in non-degrading endosomal compartments, where the antigen is protected from degradation, thus retaining its availability for B cells for long periods of time[157]. It is also possible that in a secondary response, FDCs contribute by presenting antigens very quickly, as exogenous protein molecules and invading pathogens are transported to FDCs rapidly, and this transport is accelerated by their binding to pre-existing antibodies secreted during the primary response, and the subsequent complement activation. Because $IgG1^+$ memory B cells are located near to the contracted germinal centre, rich in FDCs, memory B cells are likely to capture the secondary antigen presented by FDCs very promptly[149].

(v) Re-diversification

So far, we have mostly focused on the properties of IgG+ memory B cells. IgM^+ memory B cells, on their part, can reinitiate germinal centre reaction upon antigen re-encounter[158]. These cells have increased ability to re-enter the germinal centre reaction where they undergo class switching and somatic hypermutation, thus having a role in the generation of higher-affinity IgG1 antibodies[129]. To summarise, if on the on hand $IgG1^+$ memory B cells are responsible of rapidly re-expanding the plasma cell response with antibody binding features similar to those of the primary exposure, IgM^+ memory B cells are responsible for re-entry into the germinal centre and generation of new clones, with different binding properties to guarantee a multi-layered humoral immune response[24].

Memory B Cell Exhaustion

It is worth mentioning that an imbalance of the memory B cell response occurs in the case of chronic viral infection, where there is a prolonged, high antigen load. Of this condition, HIV infection is a typical example. In chronic HIV infection, memory B cells are found to express several inhibitory receptors (e.g. immunoreceptor tyrosine-based inhibitory motif (ITIM)-containing inhibitory receptor Fc receptor-like protein 4 (FCRL4), to be unable to differentiate into antibody-secreting cells, and to have impaired proliferation[24,159]. It seems then that memory B cells in chronic HIV infection are in an exhausted state.

HIV Epidemiology

AIDS was identified as a new disease in 1981, when increasing numbers of homosexual men started to display uncommon opportunistic infections and rare malignancies[160,161]. The cause of the disease was later identified as HIV-1, a lentivirus of the family *Retroviridae* which was found to spread mainly by the sexual route, although percutaneous and perinatal routes are also possible[162–166].

As of today, HIV has infected more than 70 million people and caused as many as 35 million deaths, with the highest impact in developing countries especially in sub-Saharan Africa. Globally, 36.7 million people were living with HIV at the end of 2016[167]. If on the one hand ART has greatly reduced the toll of AIDS-related deaths, treatment requires administration of one pill a day and its access is not universal, especially in some parts of the world. That is why the development of an effective HIV vaccine is of importance to contain the increasing number of infections and HIV-related deaths.

From SIV to HIV

Since its discovery, the sudden origin of HIV has been object of deep study. In 1986, a similar virus, although with antigenic differences, was identified as causative of AIDS in individuals in west Africa[168]. The virus, named HIV-2, was found to be only distantly related to HIV-1, but shared more genetic identity to a simian virus that resulted in immunodeficiency in macaques[169,170]. Soon other viruses indicated as SIVs were found in several primates in sub-Saharan Africa, such as African green monkeys, sooty mangabeys, mandrills, chimpanzees and others[171]. A suffix is added to SIV to indicate the primate species of origin (e.g. SIVcpz indicates SIV endemic in chimpanzee populations).

Interestingly, these viruses were found to be largely non-pathogenic in the primate species they naturally infected.

It was then identified that very close simian relatives of HIV-1 were found in the chimpanzee, and relatives of HIV-2 in the sooty mangabey monkey[172,173]. These genetic relations were considered as first evidence that AIDS resulted from zoonotic transmissions of SIV from primates to humans[171]. Later studies suggested that AIDS in macaques was as well due to the cross-species

transmission of SIVsm (sooty mangabey) from African to Asian macaques. The cross-species transmission resulted in the generation of SIVmac, by the inoculation in US research centres of various species of macaques with biological samples derived from infected sooty mangabeys[174,175]. The origin of HIV-2 was instead identified as monkey-to-human transmission of SIVs from African primates[176] and remained regional, while the global human pathogen HIV-1 was acquired from chimpanzee-to-human transmission.

So far, SIV infections have only been identified in African monkeys and apes, so it seems likely that they originated in Africa only after the split of Asian and African lineage of Old World monkeys, estimated to have occurred from 6 to 10 million years ago[177]. However, it is virtually possible that SIVs that infect Asian or New World (Central, South American and Mexican Monkeys) monkeys exist but have not been identified so far, so one must be cautious in concluding that SIVs are exclusively restricted to African primates[171]. The fact that the majority of monkey and ape species are generally infected by a largely species-specific strain of SIV indicates that most transmission occur among members of the same primate species, although natural cross-species transmission has been identified. For instance, SIVgor in gorillas seems to have originated from the transmission of SIVcpz to its great ape cousin, gorillas, some 100-200 years ago[178]. Importantly, HIV-1 has likely originated from SIVcpz[171] in chimpanzees. Evidence indicates that the subspecies of chimpanzees *P. t. troglodytes* acquired and evolved a chimeric form of two different SIVs from monkeys, presumably by hunting and eating different kinds of SIV-infected preys[179].

Insights into host-to-virus adaptation

Notably, lentivirus infection in chimpanzees is characterised by lack of $CD4^+$ T cell loss, as well as the absence of generalised immune activation, in concert with the preservation of secondary lymphoid structure, especially considering MHCII APCs in infected lymph nodes[180,181]. Also, no anergy or marked loss of IL-2-producing CD4+ T cells after infection is detected[182,183]. These observations highlight the importance of maintaining normal levels of APC-CD4+ T cell interaction, which are the first symptoms of early immune disruption in AIDS-susceptible species[181].

It is to be mentioned that CD8+ CTLs in chimpanzees are able to bind to highly conserved HIV-1 Gag epitopes, which overlap with the epitopes that are bound and presented by HLA-B*57 and HLA-B*27 alleles in patients which slowly progress or do not progress to AIDS[184]. Phylogeny analysis of MHC class I alleles reveals a decrease of HLA-A, HLA-B and HLA-C lineages in chimpanzees as compared to humans. These findings are corroborated by the identification of a marked reduction in the MHC class I repertoire, especially in the HLA-B locus, by comparative analysis of intron 2 sequences[185]. These findings imply that chimpanzees might have experienced a selective bottleneck, possibly exerted by past lentiviral pandemics comparable to the present HIV-1 pandemic in humans[179]. One could hypothesise that, in the absence of antiretroviral therapy and prevention strategies, a positive selection for HLA-B alleles beneficial for long-term survival might results in humans[186].

It is however by now established that infected chimpanzees are relatively resistant to AIDS, not because they control viral replication[187], but because many have the ability to avoid the immunopathological events that disrupt lymphoid tissue function in infected humans and Asian macaques[181,183]: while chimpanzee CD4+ T cells are susceptible to SIVcpz or HIV-1 infection and cytopathology, unlike humans or macaques, most infected chimpanzees maintain their ability to replace and sustain sufficient numbers of $CD4^+$ T cells that preserve immunological integrity[180].

HIV lineages

It is important to mention that HIV-1 comprises four lineages, named groups, M, N, O and P, each one originated from separate zoonotic transmission of SIVcpz from infected chimpanzees to humans[179]. Group M (Main) was the first one to be identified, and is the most widely spread form of HIV-1: its infection of millions of people worldwide resulted in the current pandemic and has now been found in virtually every country in the World[171]; group O (Outlier) was identified in 1990 and it represents less than 1% of global HIV-1 infections, being largely restricted to Cameroon, Gabon and neighbouring countries[188–191]. Group N (Non-M, Non-O), identified by Simon and collaborators in 1998, has been documented to have caused only 13 cases in Cameroon so far[192,193]. Finally, Group P, discovered in 2009 by Plantier *et al*., has so far been

described in only two patients, namely a Cameroonian woman living in France and another person from Cameroon[171,194].

Because all four HIV-1 groups, as well as SIVgor cluster with SIVcpz from central *Pan troglodytes troglodytes* chimpanzees, this subspecies was identified as the reservoir of human and gorilla infections **Figure 1.9**. The exact means by which SIV was transmitted to humans originating HIV-1 are still unknown. However, based on the transmission mechanisms of these viruses, it is safe to hypothesise that transmission occurred through cutaneous or mucous membrane exposure to infected ape biological samples, such as blood or bodily fluids[171], most likely in episodes of bushmeat hunting[195] in the early 20th century (groups M and O) or later (groups N and P)[196–198].

These estimations are made using molecular clock methods: HIV-1 evolves at rates that are approximately one million times faster than human DNA[199,200] because the reverse transcriptase responsible of synthesizing DNA for insertion in the human genome from viral genome RNA templates is error prone, and new generations of viruses are produced quickly during replication[201,202]. Phylogenetic and statistical analyses have dated the last ancestor of HIV-1 M to 1910-1930[171,196], with the early diversification of group M occurring most likely in the area around Kinshasa, the capital of Congo (then called Leopoldville, capital of former Zaire)[171,203].

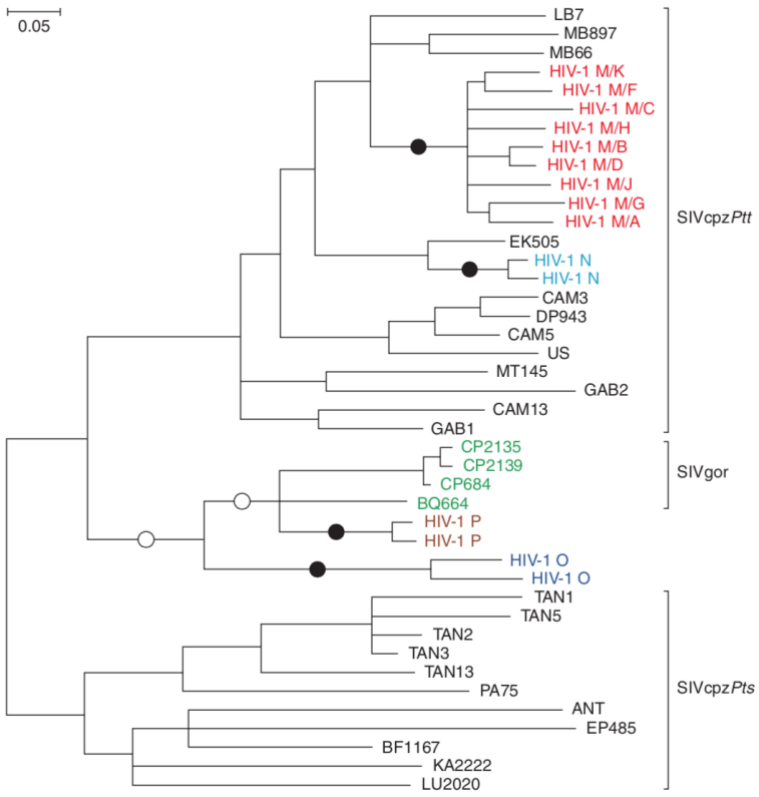

Figure 1. 9: HIV-1 origins and phylogenetic relationships of representative SIVcpz, HIV-1, and SIVgor strains. Relationships shown for a region of the viral pol gene. SIVcpz and SIVgor sequences are shown in black and green, respectively, while the four groups of HIV-1 (each of which originated from an independent cross-species transmission) are shown in different colors. White circles designate two possible alternative branches on which transmission occurred from chimpanzee to gorilla. Black circles denote the four branches where cross-species transmission to humans has occurred. Brackets at the right denote SIVcpz from *P. t. troglodytes* (SIVcpzPtt) and *P. t. schweinfurthii* (SIVcpzPts), respectively. The scale bar represents 0.05 nucleotide substitutions per site (from reference [171]).

The M Group: A Global Epidemic

As HIV-1 M spread, its dissemination was characterised by a number of founder events which led to the formation of different lineages (subtypes) that are now disseminated in different geographic areas. HIV M is categorised into nine subtypes (A-D, F-H, J, K) as well as more than forty circulating recombinant forms (CRFs) which originated by the superinfection of multiple subtypes of the same population[204].

Subtypes A and D, although originated in central Africa, are now mostly established in eastern Africa, while subtype C predominates in southern Africa and subsequently disseminated in India and other Asian countries; subtype B, which accounts for the majority of infections in Europe and

Northern and Southern America, seems to have originated from a single African strain that firstly spread in Haiti in the 1960s and then to the United States and other western countries thereafter[205].

CRF01, which is mostly spread in Thailand where it was identified in the late 1980s while causing a local heterosexual epidemic, probably originated from a single recombination event that took place in Central Africa. In the same period, the country was facing a subtype B epidemic in intravenous drug users[204]. CRF01 is now the dominant AIDS epidemic in southeast Asia[171].

The world distribution of the HIV M subtypes is reported in **Figure 1.10**, while the 2017 prevalence of HIV amongst adults (age 15-49) is reported in **Figure 1.11**.

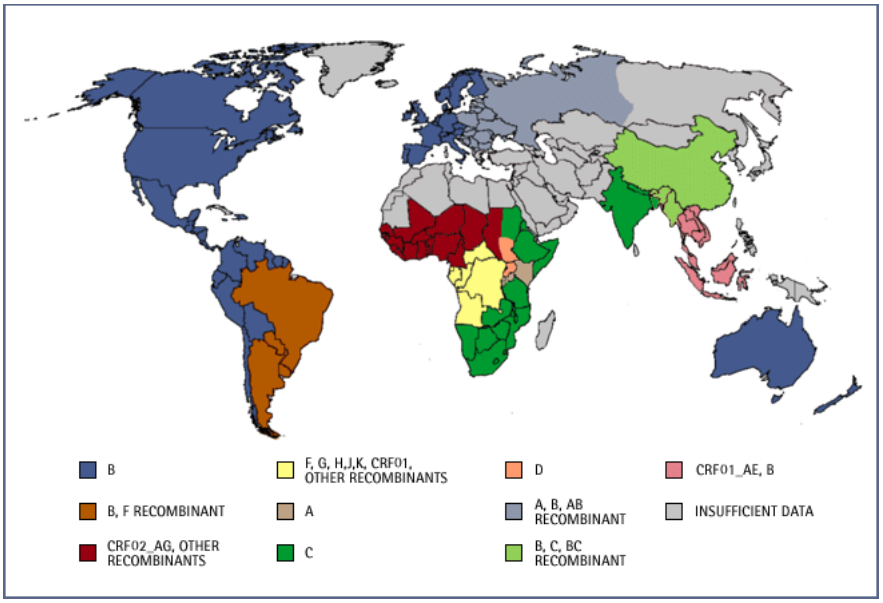

Figure 1. 10: Global distribution of HIV-1 major subtypes and recombinant forms as published in 2003 by the International AIDS Vaccine Initiative[206]. Notably, Northern America, Europe and Australia record distribution of mainly B subtype, while the C and CRF02 subtypes are mainly distributed in the African continent. South-East Asia registers a distribution of largely C, B and CRF01 subtypes.

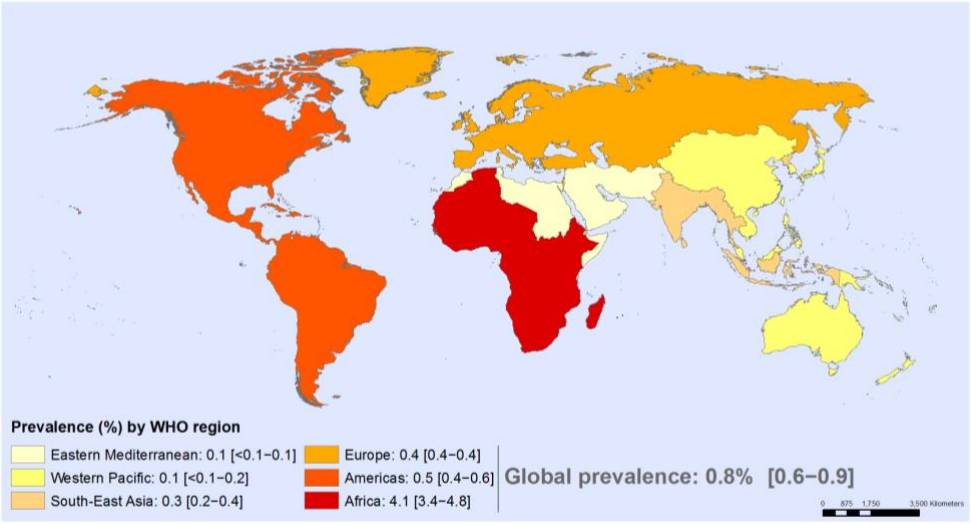

Figure 1. 11: Global HIV-1 infection situation and trends: since the beginning of the HIV M epidemic, more than 70 million people have been infected with HIV and circa 35 million have died because of HIV-related complications. Globally, an estimate of 36.9 million people were living with HIV at the end of 2017. An estimated 0.8% of adults from age 15 to 49 are living with HIV worldwide. The African region remains the most severely affected, with 4.1% of adults (nearly 1 every 25) living with HIV and accounting for nearly two-thirds of the HIV-infected people worldwide. From reference[207].

Treatment of HIV infection

Since the identification of HIV-1 as the cause of AIDS in 1983, significant progress has been made in the management of HIV infection. Combination ART was introduced as the standard treatment of HIV infection in the mid-1990s, and more than 30 agents have since been approved for the treatment of HIV-positive individuals.

As of today, five main classes of combination ART drugs are approved[208] (**Table 1.2**): One class contains drugs that interfere with viral entry into the cell (entry inhibitors) by binding to viral envelope proteins thus preventing attachment and entry into target cells; a second class contains agents that inhibit viral replication inducing chain termination after being incorporated into growing DNA strands (nucleoside reverse transcriptase inhibitors, NRTIs). A third class inhibits replication by binding directly to the reverse transcriptase (non-nucleoside reverse transcriptase inhibitors, NNRTIs). A fourth class contains agents that inhibit viral DNA integration into the target cell genome (integrase strand transfer inhibitors, INSTIs). Finally, the class of protease inhibitors

Protease inhibitors
Tipranavir/TPV (Aptivus)
Darunavir + cobicistat (Prezcobix)
Indinavir/IDV (Crixivan)
Atazanavir/ATV (Reyataz)
Atazanavir + Cobicistat (Evotaz)
Darunavir/DRV (Prezzista)
Saquinavir/SQV (Invirase)
Nelfinavir/NFV (Viracept)
Ritonavir/RTV (Norvir)
Lopinavir + Norvir (Kaltera)
Fosamprenavir/FPV (Lexiva)
Integrase inhibitors
Raltegrivir/RAL (Isentress)
Doultegravir/DTG (Tivicay)
Elvitegravir/EVG (Vitekta)
Bictegravir/BIC
Fusion/entry inhibitors
Enfuviritide/ENF (Fuzeon)
Maraviroc/MVC (Selxentry)
Multiclass single-tablet drug combination
Efavirenz + emtricitabine + tenofovir disoproxil fumarate, EFV/FTC/TDF (Atripla)
Emtricitabine + rilpivirine + tenofovir disoproxil fumarate, FTC/RPV/TDF (Complera)
Elvitegravir + cobicistat + emtricitabine + tenofovir disoproxil fumarate, EVG/COBI/FTC/TDF (Stribild)
Rilpivirine + tenofovir alafenamide fumarate + emtricitabine, RPV/TAF/FTC (Odefsey)
Elvitegravir + cobicistat + emtricitabine + tenofovir alafenamide fumarate, EVG/COBI/FTC/TAF (Genvoya)
Bictegravir + emtricitabine + tenofovir alafenamide fumarate, BIC/FTC/TAF (Biktarvy)
Abacavir + dolutegravir + lamivudine, ABC/DTG/3TC (Triumeq)
Dolutegravi + rilpivirine, DTG/RPV (Juluca)
Dolutegravir + emtricitabine + tenofovir alafenamide fumarate, DTG/FTC/TAF
Nucleoside/nucleotide analogs (NRTIs)
Lamivudine + zidovudine, 3TC/ZDV (Combivir)
Abacavir/ABC (Ziagen)
Emtricitabine/FTC (Emtriva)
Tenofovir disoproxil fumarate/TDF (Viread)
Emtricitabine + tenofovir disoproxil fumarate, FTC/TDF (Truvada)
Tenofovir alafenamide fumarate/TAF (Vemlidy)
Lamivudine/3TC (Epivir)
Abacavir sulfate + Lamivudine, ABC/3TC (Epzicom)
Abacavir sulfate + Lamivudine + Zidovudine, ABC/3TC/ZDV (Trizivir)
Stavudine/d4T (Zerit)
Didanosine/DDI (Videx, Videx EC)
Zidovudine/AZT/ZDV (Retrovir)
Non-nucleosides (NNRTIs)
Rilpivirine/RPV (Edurant)
Etravirine/ETV (Intlence)
Delavirdine/DLV (Rescriptor)
Efavirenz/EFV (Sustiva)
Nevirapine/NVP (Viramune)
Pharmacoenhancer
Ritonavir/RTV (Norvir)
Cobicistat/COBI (Tybost)

Table 1. 2: Available antiretroviral agents approved for use, reported as generic names/abbreviations (trade names). NRTI: nucleoside reverse transcription inhibitor; NNRTI, non-nucleoside reverse transcription inhibitor. From reference[208].

(PIs) contains agents that inhibit the viral protease, leading to the formation of immature viral particles.

Despite the many agents available to target diverse stages of the HIV cycle, current national and international guidelines now recommend regimens mostly based on the INSTI drug class in combination with reverse transcription inhibitors[208,209]. Administration of ART in this combination successfully and durably suppresses plasma HIV RNA levels, restores immunologic functions and reduces HIV-associated morbidity prolonging the duration and quality of survival, while also preventing HIV transmission[208]. However, different types of combinations can be recommended in particular cases, with drugs being sometimes combined into one pill[210].

Because of the marked improvements in ART potency, generally tolerable side effect profiles and relative simplicity of use[211], ART has led to increased survival in people living with HIV[212]. Moreover, results from the HIV Prevention Trials Network (HPTN) 052 study have also clearly proven the efficacy of ART for prevention of transmission[213], while TEMPRANO and START studies have shown that early ART initiation diminishes the risk of AIDS development and death[214,215].

Limits of HIV-1 infection treatment and need for vaccine

While the development of AIDS after HIV infection can be now contained by treatment, ART has some limits:

(i) *Not a cure*. As compared to when the epidemic was first identified, when HIV-1 infection came with a death sentence on the patient, ART has greatly improved the life expectancy of HIV-infected individuals. Combination treatments can allow the infected person to lead a healthy life as long as they are under treatment, with blood viral loads suppressed to undetectable levels and CD4 counts maintained to healthy levels. However, as soon as the treatment is interrupted, viral load soon is restored to high levels thus allowing the patient to transmit the virus again[216].

(ii) *Adherence*. It is necessary that the patient adheres to the ART regimen. While the regimens used to be much more complicated than they are now, it is a great progress that nowadays ART treatment requires the patient to only ingest one pill a day.

However, this solution is still far from ideal and some groups of patients may find it difficult to adhere[216].

(iii) *Distribution*. Distribution of ART in certain parts of the world is difficult, especially when considering that the current regimen requiring the administration of one pill a day demands the constant distribution of large quantities of drug, with related transportation costs and difficulties to access remote areas. Distribution of ART is thus more difficult in developing countries[217].

(iv) *Selected group lifespan gap*. Some studies have identified a small but persistent gap in the lifespan of HIV-positive versus HIV-negative individuals belonging to key populations[218,219]. For instance, NA-ACCORD study data show that 20-year-old HIV-positive adults in ART in USA or Canada have a life expectancy that approaches that of the HIV-negative population, although this benefit is not shared by individuals who are not white, have history of drug use, or began ART with low CD4 counts[220].

(v) *Ageing*. Because HIV-infected patients have an expected life span that is only slightly shorter if compared to that of uninfected individuals[211], the effects of ageing on HIV-positive people are now beginning to become evident since the introduction of ART in the mid-1990s[221,222]. Several disorders that typically affect the elderly population appear in relatively young HIV-positive individuals who can develop different pathologies including neurocognitive disorders, metabolic syndrome, cardiovascular diseases, bone abnormalities and non-HIV associated cancers[223,224]. Most of these age-associated diseases are caused, at least in part, by the chronic state of inflammation and immune activation that is observed typically in the elderlies[225], often referred to as "inflammageing"[226,227] or, in the case of the final phase of HIV infection, "inflammAIDS"[224]. This relatively new condition is extremely complex, and involves organs and systems other than those directly responsible for the state of constant immune activation[224]. Beside the behavioural risk factors, toxicity of anti-retroviral treatments and the above-mentioned chronic inflammation have been identified as important factors promoting the development of such conditions, leading to a functional decline and a vulnerability to injuries or pathologies[228].

In a scenario in which the elaboration of a definitive cure is proving extremely elusive, the development of a preventive vaccine to contain the HIV epidemic is of utmost importance. In the next chapters, I will summarise the progress made and challenges that persist in the development of an effective HIV vaccine.

The HIV Envelope Glycoprotein

The HIV Envelope glycoprotein (Env) is the single virally-encoded structure that is present on the surface of the viral envelope[229]. Functional Env is present as a non-covalently linked trimer of heterodimers, each one composed by the surface (SU) subunit gp120 and the transmembrane (TM) subunit gp41 (**Figure 1.12**)[229].

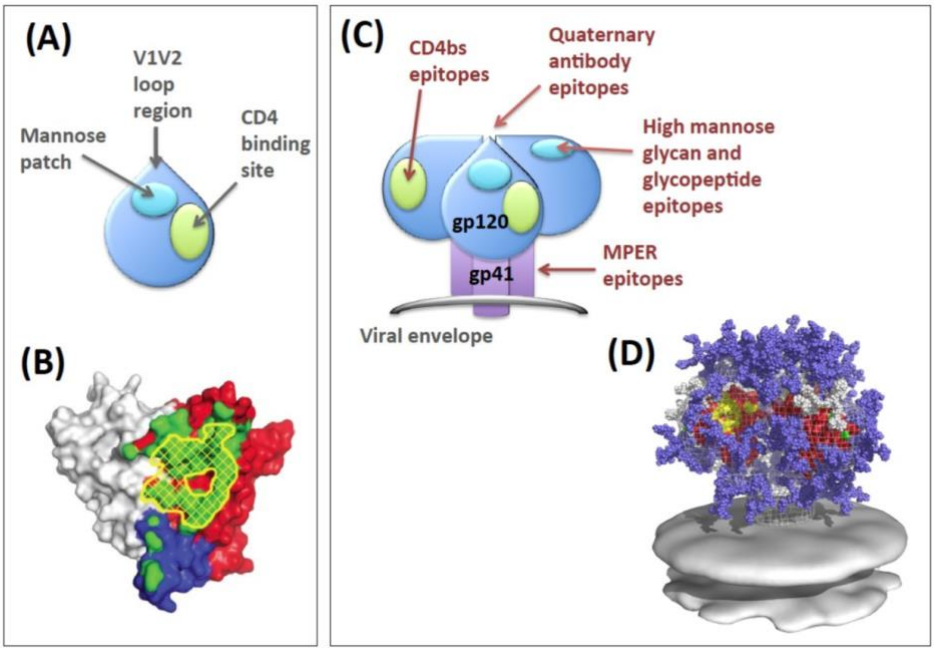

Figure 1. 12: Schematic representation of the HIV-1 Env. **A**) Representation of the major features of gp120 with the exclusion of the V1V2 loop; **B**) Model of gp120 with the inner domain represented in grey, the outer domain in red and the bridging sheet in blue. The CD4 binding site upon receptor engagement is represented in yellow cross-hatching. The epitope of anti-CD4bs mAb VRC01 is in green. **C**) Cartoon of the Env trimer with indication of the main epitopes recognised by broadly neutralising antibodies. **D**) Molecular model of the Env trimer with glycans, where red represents the surface of gp120, yellow the CD4bs, purple the glycans and the epitope of anti-glycan broadly neutralising mAb 2G12 in grey. From reference[229].

The Env gp120 and gp41 subunits: mediators of viral entry

The Env gp120 subunit is the component that engages receptor and coreceptors and initiates the entry process. Gp120 is composed of three domains: the inner and outer domains and the

bridging sheet (**Figure 1.12B**)[230]. Gp120 first establishes contact with the receptor CD4 and, subsequently, with either one of the coreceptors CCD5 or CXCR4[229]. However, optional engagement of integrin $\alpha4\beta7$ through the V1V2 domain prior to receptor binding has also been described[231] (discussed more in detail in the last section of this chapter).

The CD4 binding site (CD4bs) on gp120 is accessible to CD4, but undergoes continuous conformational changes to escape the immune response of the host[232]. Upon CD4 engagement, gp120 is stabilised in a conformation that triggers structural rearrangements which ultimately reveal the coreceptor binding site (CRbs)[229].

Following coreceptor engagement by gp120, further conformational rearrangement within Env triggers gp41 activation leading to its refolding. It is currently accepted that gp41 penetrates the target cell membrane through the formation of a coiled-coil structure that brings the viral and cellular membranes into close proximity, leading to their fusion and finally entry of the viral core into the cell[233,234].

Env-specific antibodies as mediators of viral neutralisation

Antibody-mediated viral neutralisation is a mechanism by which antibodies binding to a virus prevent it from establishing or carrying on infection by interfering with the biological function of the target antigen[235]. Because HIV Env products are the effectors of the processes of entry and fusion, neutralising antibodies targeting HIV elicit their effect by hindering the processes of target cell recognition and binding (in case of gp120-specific antibodies), or by hindering the fusion process (in case of gp41-specific antibodies)[236].

Neutralising antibodies are considered important for optimal protection against HIV since they are generally associated with protection against most viral infections[237–239], and because they provide protection against AIDS virus infection in nonhuman primates[240–242]. However, the development of effectively neutralising antibody responses against HIV through vaccination is hindered by viral escape mechanisms from the humoral immune response that are described more in detail in the section below.

Broadly neutralising antibodies (bnAbs) can be detected in approximately 25% of patients with untreated HIV infection[243], as an immune response to continuous viral replication, with the

generation of high numbers of viral variants and exposure to continuously mutating antigens[244]. However, although these bnAbs exert some pressure as they develop, the viral burden is generally not reduced, with no significant improvement on the health of the patient and no delayed progression to AIDS[245].

Continuous research on neutralising antibody responses has led to the identification of multiple areas on HIV Env that can be targeted by bnAbs (summarised in **Figure 1.13**). However, four main areas are to date generally considered to be the main targets of broadly neutralising humoral responses[229]: (i) the CD4 binding site, (ii) quaternary epitopes, (iii) the glycan-coated V1V2 and V3 viral loops and (iv) the membrane-proximal external region (MPER). bnAbs targeting these areas reduce SIV replication in nonhuman primates[246] and HIV-1 in humans[247], and can prevent SHIV infection in nonhuman primates[242,248]. However, the infection is never cleared through bnAb treatment and bnAb monotherapy always results in viral rebound from outgrowth of low-frequency resistant viral variants[242,247] .

Mechanisms of HIV Evasion from the Humoral Immune Response

The defence mechanisms employed by HIV-1/SIV to escape the humoral immune response of the host have been widely studied. A number of structural features have been evolved by the virus to reduce antibody recognition of functional, conserved regions on gp120[250].

Integration

Like all retroviruses, HIV/SIV replication goes through a proviral DNA intermediate which is integrated into the genome of the host[251]. Although the conversion of the viral single-stranded RNA into linear double stranded DNA may help stabilise the viral genome[252], the integration of the viral DNA into the host genome permits HIV/SIV to persist for many years also in absence of viral replication and shielded from the cellular and humoral immune response[253]. In addition, integration into long-lived cells and the maintenance of a quiescent state allows viral persistence in spite of effective ART[254].

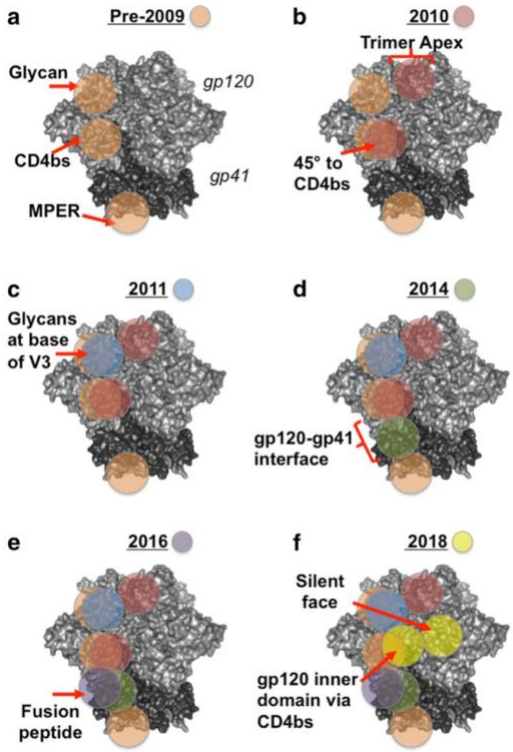

Figure 1. 13: Advances in the identification of bnAb epitopes on HIV Env over time. Each panel depicts a key advance in the discovery or refinement of neutralising epitopes. This Env figure was adapted from the BG505 SOSIP.664 trimer (PDB: 5cez), with gp120 coloured in light grey, and gp41 in dark grey. Epitope locations are indicated by red arrows, line and circles and are color-coded for each year as shown in each panel heading. Epitopes are highlighted only once in each protomer. A) By 2009, the knowledge on neutralising epitopes on Env was gained mainly by studies on bnAbs b12, 2G21, 2F5 and 4E10. B) By 2010, the trimer apex had been described following identification of bnAbs PG9 and PG16 in 2009, and the importance of the angle of approach to the CD4bs was highlighted by the discovery of VRC01 in 2010. C) The glycan patch epitope was then identified as a site of vulnerability by isolation of bnAbs PGT121 and PGT128 in 2011. D) From 2014, the discovery of PGT151, 35O22 and 8ANC195 revealed a neutralising area spanning the interface between gp120 and gp41. E) In 2016, bnAbs VRC34 and ACS202 were found to bind the gp41 fusion peptide. F) In 2018, bnAbs binding the highly glycosylated "silent" face of gp120 were described to target the CD4bs via novel contacts with the gp120 inner domain. From reference[249].

Amino Acid Sequence Variability

The continuous remodelling of the gp120 and gp41 structure and function is necessary to escape the neutralising antibodies that are developed by the host. To do this, HIV-1/SIV carries an error-prone reverse transcriptase which results in the insertion of mutations at every round of viral replication, which will in turn lead to sequence or structural modification of epitopes recognised by neutralising antibodies[250].

Variable Regions

Variable Regions on gp120 may have roles in engaging receptor or co-receptor, as well as providing means of escape from the humoral immune response.

On the one hand, V3 is necessary for virus infectivity through co-receptor engagement, and deletion of this region completely abrogates viral replication[255]. This region is also able to escape the humoral immune response through the induction of high variability in its amino acid sequence, which is however restricted to about 20% of the positions. Notably, the length of the V3 loop is poorly variable, generally constant at around 34-35 amino acids[256–262].

In contrast, V2 is not essential for virus infectivity[255], but its deletion results in loss of viral fitness, possibly because it participates in shielding the gp120 from antibodies targeting neutralising epitopes outside of V2 located in the V3 loop or the CD4 binding site[263–266].

Glycan Shields

HIV/SIV can also use glycans to occlude epitopes on gp120, as about 50% of the molecule is shielded by carbohydrates that make the protein surface inaccessible to antibodies. This glycan shield has been dubbed "the gp120 silent face"[267]. Notably, the repositioning of glycans may affect local protein folding and indirectly affect binding of neutralising antibodies to distant epitopes; similarly, the repositioning of glycans may compensate for structural changes in the envelope glycoprotein caused by changes in the primary sequence induced to escape from neutralising antibodies[250].

Antibody Interference

A viral escape mechanism by which non-protective antibodies would negatively affect the binding of antibodies to protective epitopes was initially proposed by Dulbecco *et al.* in 1956 on studies on western equine encephalitis virus and poliomyelitis virus[268]. This mechanism, named antibody interference, has since been investigated for SARS Coronavirus, Influenza Viruses and Hepatitis C Virus[269–272]. In the studies on these viruses, antibody interference has been hypothesised to be exerted by two possible molecular mechanisms: (i) steric hindrance, i.e. the physical covering of

the protective epitope by the Fc or Fab regions of the interfering antibody not directly interacting with the protective epitope or (ii) conformational changes, i.e. the induction of alterations in the three dimensional structure of the antigen that are propagated to a distant epitope that can thus not be recognized by protective antibodies. While the existence of antibody interference in the HIV-1 or SIV model has been proposed upon *in vitro* studies involving anti-HIV fusion glycoprotein gp41 mAbs[273], to our knowledge the findings reported in this thesis are the first that identify this mechanism on viral envelope gp120.

HIV vaccine clinical trials to date

HIV presents an extreme ability to evade the host immunity, so much that the plausibility of developing an HIV vaccine has been questioned repeatedly since the start of the pandemic. Increasing evidence suggests that the early stages of transmission are those that are potentially vulnerable to a vaccine-primed immune response[274]. While animal and human studies have shown that envelope-specific antibodies correlate with reduced infection risk, cytotoxic T-lymphocytes (CTLs) also have an important role in controlling viral load levels during natural infection, and therefore priming these responses with a vaccine could be useful[275,276]. It is hypothesised that an effective HIV vaccine will need to stimulate both B- and T-cell protective responses[276]. Although much progress is yet to be made to finally obtain an effective HIV vaccine, lessons can be learned from the partial or null protection observed in the large scale clinical trials performed so far. In the next sections, I will summarise the three vaccine concepts that have been tested for efficacy in humans: a gp120 Env protein to elicit cross-binding antibodies, an adenovirus vector eliciting CTLs, and a combined canarypox vector and gp120 protein eliciting both cellular and humoral immune responses. For the purpose of this thesis, particular attention will be dedicated to the latter.

VAX003/VAX004

The first phase III efficacy trials, of which the results were published in 2005 and 2006, tested the efficacy of bivalent gp120 protein in preventing HIV infection in men who have sex with men (MSM)[277] and injection drug users (IDUs)[278], respectively. No vaccine efficacy was recorded in

vaccinated as compared to placebo groups, although HIV incidence was lower in those individuals who developed stronger antibody responses[276,279]. Following analyses were unable to demonstrate that broadly neutralising antibodies, presumed a requirement for preventing infection in NHP, were elicited[240,242,248,280,281].

STEP Study

The interest for the development of CTL-inducing vaccines was due to the fact that these responses have the potential to reduce viral load or delay disease progression. DNA plasmid and viral vectors have generally been observed as able to elicit T-cell responses[276]. An adenovirus type 5 vaccine (Ad5) inducing strong CTL responses (MrkAd5 by Merck) was studied in phase 2b to detect for vaccine efficacy in preventing infection. Merck and the HIV Vaccine Trials Network (HVTN) directed studies in North and South America and in South Africa[282,283]. However, these studies were stopped early in late 2007 when they were found to meet futility thresholds. Later, an increment in virus incidence was found in recipients who were uncircumcised and had prior immunity to the vector[276,282]. Although the study was unable to reduce acquisition or post-infection viral loads, a sieve analysis on biological samples obtained from the study found that viruses infecting vaccine recipients were more likely to be antigenically different from the Env epitopes encoded by the vaccine[284]. This result suggests that T cell immunity plays a bottleneck on certain virus strains, allowing only for those antigenically distant from the immunisation strains to infect the patient. These data were the first evidence to suggest that a T cell vaccine is capable of exerting immune pressure on HIV[276].

HVTN 505

In 2009, the clinical trial HVTN 505 started to test a vaccine regimen developed by the Vaccine Research Center (VRC) and the National Institutes of Allergy and Infectious Diseases (NIAID), which consisted of a DNA prime encoding for clade B gag, pol, nef and multiclade env genes followed by administration of recombinant Ad5 boost with gag, pol and env inserts of sequence matching those of the DNA prime[285]. It is to be noted that the VRC Ad5 vector was different from that employed in the Step study. However, lessons from the Step study were learned and uncircumcised individuals or patients with pre-existing anti-Ad5 neutralising antibodies were

excluded. HVTN 505 was opened to evaluate the VRC regimen in men and transgender women who have sex with men[285], with a total of 2,504 participants. In 2013, HVTN 505 was discontinued because interim analyses indicated that the regimen was not efficacious[276].

RV144

RV144 is the only phase III HIV vaccine clinical trial where some degree of protection from infection was ever demonstrated[286]. The study started in 2003, took place in Thailand and enrolled a total of 16,402 individuals, divided in a vaccine-receiving and a placebo group. The study was possible thanks to a large collaboration, being conducted by the Thai Ministry of Public Health, sponsored by the US Army Surgeon General, and managed by the US Military HIV Research Program (MHRP) together with Thai scientists, supported by the Thai and US governments, private companies and non-profit organisations. The immunisation approach used in this trial was designed to elicit immune responses against clades B and E, which circulate in Thailand. RV144 was designed to assess the ability of the vaccine to prevent HIV infection, as well as to reduce the level of viral RNA in the blood of infected vaccinees[286,287].

The effort of setting up RV144 in Thailand

Thailand is among the first developing countries that was able to reduce the rates of HIV infection thanks to the intervention of the government, which focussed its efforts on promoting national and international collaborative research to develop and evaluate novel HIV/AIDS vaccines[287].
Despite this, AIDS is still a major cause of death in the 63 million people country, with more than one in 100 adults in the country infected by HIV[288]. After the first case of AIDS was detected in the country in 1984[289], the virus spread rapidly especially amongst MSM, sex workers, IDUs and tourists, until its containment became a national priority in 1991[287]. However, as nowadays more than a half of new cases are transmitted between spouses, a vaccine should be designed to target both high- and low-risk groups. RV144 was the first trial designed to vaccinate a cross-section of risk groups in the country[287]. Volunteers were recruited from the provinces of Chon Buri and Rayong in the south-eastern region of Thailand. Both provinces were chosen for their high HIV incidence, good infrastructures and other favourable characteristics[287,290]. The statistical

assumption of the study required it to be performed on 16,000 subjects. Of the 16,402 finally enrolled, 61% were males and 39% were females, all between 18 and 30 years of age and randomised according to their sex, age and behavioural risks[286]. With 7 subjects excluded because of positivity to HIV on the day of the first vaccination, the remaining group was split in 8197 vaccinated and 8198 placebo in a double-blind manner; the vaccines were administered through many health centres and facilities. 12,542 volunteers completed all the visits with negativity to HIV during the vaccination period[286].

HIV Clades in Thailand

The vaccine regimen of RV144 was developed to match the clades circulating in Thailand, two of which are more present in the region: B and recombinant E/A strains. As previously mentioned, Clade B is predominant in Europe and America, although the increasing globalisation has caused a surge in non-B African and Asian variants[287]. In Thailand, historically, the epidemic initially was mostly caused by subtype B in IDUs[291,292]. A second epidemic of sexually-transmitted HIV followed, with the recombinant form CRF01-AE eventually becoming the dominant subtype (90% of the circulating HIV strains in this country belong to this subtype)[287].

Vaccination regimen

The goal of the vaccine tested in RV144 was to induce HIV-specific CTL responses as well as cross-binding, possibly neutralising antibodies to clades B and A/E. Two different immunogens were chosen to be used in combination, ALVAC-HIV and AIDSVAX B/E, to be used as prime and boost, respectively.

(i) ALVAC-HIV

ALVAC-HIV (virus recombinant Canarypox vCP1521) is a viral vectored vaccine able to elicit T-cell immunity[287,293]. ALVAC-HIV, used for priming, was developed by Virogenetics Corporation (NY, USA) and manufactured by Sanofi Pasteur. The Canarypox virus is an agent of disease in birds, demonstrated to be host-range restricted and safe because shown to effectively infect human cells but not to productively yield new generations of virus[294–297]. However, despite its abortive infection in mammalian cells, ALVAC can express and present foreign proteins[298] that are

processed by MHC-I and MHC-II thus stimulating both cytotoxic (CD8) and helper (CD4) T cell responses[299,300]. As opposed to other poxvirus-based vectors such as modified vaccinia Ankara (MVA) virus and New York Vaccinia (NYVAC) vaccines, canarypox is not affected by pre-existing, vaccinia virus-specific immunity[301,302] that was elicited by vaccination against smallpox in individuals born before 1977[287].

ALVAC-HIV used in RV144 was engineered to induce the expression, in transfected cells, of HIV-1 Gag and Protease from the first HIV isolated, LAI (IIIB/BRU)[162] and HIV-1 gp120 protein from clade E. Only subtype B gag was included in the immunogen because the gag gene is fairly conserved amongst HIV subtypes as compared to env[303]. The env gene, on the other hand, carried the same sequence of that identified in 92Th023, a recombinant form of clades A and E. In the ALVAC vCP1521 construct, gp120 protein from clade E gp120 was linked to the transmembrane (TM) portion of the gp41 from LAI (subtype B): gp120 TM. This region was added to anchor the gp120 to the cell surface. ALVAC-induced co-expression of Gag, Env and protease results in the formation of virus-like particles that are released from the cell membrane[304]. The vector was propagated in chicken embryo fibroblasts and administered at a dose of 1 million 50% tissue culture infectious dose ($TCID_{50}$). The preparation was then lyophilised and reconstituted with sterile 0.4% NaCl.

(ii) AIDSVAX B/E

AIDSVAX B/E was used as a booster in RV144, and consisted of the recombinant envelope glycoprotein gp120-subunit vaccine. This vaccine was developed by Genentech and manufactured by VaxGene. The preparation contains a mixture of purified recombinant proteins expressed in Chinese Hamster Ovary (CHO) cells, that is the HIV-1 MN gp120 (subtype B) and the HIV-1 A244 gp120 (subtype E). AIDSVAX B/E was tested alone in a phase III clinical trial in 1998-1999, but was demonstrated unable to prevent HIV-1 infection[278,287].

RV144 study design

A total of six immunisations in the course of 6 months were scheduled (**Figure 1.14**): of which four with greater than 1 million TCID50 ALVAC-HIV in 1 ml intramuscularly in the left deltoid at weeks 0 (baseline), 4, 12 and 24 and two immunisations with 600 µg (50:50 of each antigen) in 1

ml AIDSVAX B/E in the right deltoid at weeks 12 and 24, at the same time of the final two ALVAC-HIV administrations. In the placebo group, participants received ALVAC Placebo, a mixture of virus stabilisers and freEze-drying medium by Sanofi Pasteur and AIDSVAX Placebo, consisting of 600 µg of alum adjuvant by VaxGen Inc. at the same time with the same route. All the volunteers were called for follow-up visits every six months for 3.5 years, with counselling for HIV prevention provided at each visit.

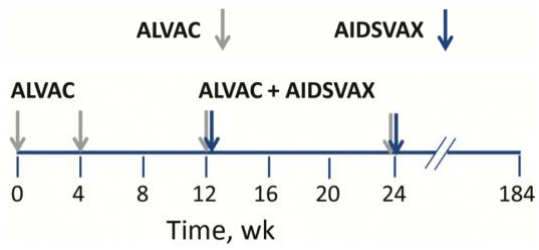

Figure 1. 14: Immunisation regimen of the RV144 study, treated group. Patients underwent four administration of the viral vector ALVAC encoding for HIV-1 Gag and Protease from the first HIV isolated, LAI (IIIB/BRU)[162] and HIV-1 gp120 protein from clade E at week 0 (baseline), 4, 12 and 24. In the last two administrations also AIDSVAX was included, containing 600 µg each of two Env antigens from subtype B and subtype E isolates. ALVAC: ALVAC-HIV; AIDSVAX: AIDSVAX B/E; wk: weeks (Adapted from reference[305]).

RV144 Protection Results

Of the 16,402 subjects enrolled, 56 out of 8200 vaccinated and 76 of 8202 placebo were found positive for HIV RNA in blood[286] which resulted in a small, but significant 31.2 vaccine efficacy ($p = 0.04$) with a 95% confidence interval[286] (**Figure 1.15**). However, a more incisive difference of 50-60% efficacy was identified between the groups at one year after immunisation, which suggested that the vaccine elicited protection which decreased over time.

Notably, there was no effect on virus level or $CD4^+$ T cell counts in the patients that were vaccinated and acquired the virus, which came as a surprise as viral control had been observed in rhesus macaques vaccinated and infected with SIV[306,307].

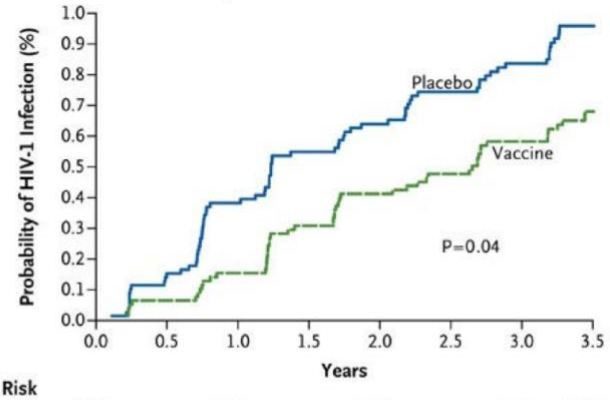

No. at Risk					
Placebo	8198	7775	7643	7441	7325
Vaccine	8197	7797	7665	7471	7347
Cumulative No. of Infections					
Placebo		30	50	65	74
Vaccine		12	32	45	51

Figure 1. 15: Kaplan-Meier cumulative rates of infection in RV144. Data reported are of the modified intention-to-treat analysis. In this group, involving 16,395 subjects (excluding 7 subjects who were found to testing positive to HIV infection at baseline), the vaccine efficacy was 31.2% with a confidence interval of 95%, P=0.04). From reference [286].

Correlates of Protection

RV144 effectively elicited binding antibodies against HIV-1 Env immunogens and p24 Gag, $CD4^+$ proliferative responses (63%) as well as $CD8^+$ T cell responses (24%), neutralising antibodies against subtype B and CRF01_AE viruses (96% and 71%, respectively) and antibody-dependent cell-mediated cytotoxicity[308].

The definition of the correlates of protection was limited by the limited sample availability, with those at peak immunogenicity, two weeks after the end of the vaccination process, being of course the most sought after. The analysis of 41 HIV-infected, vaccinated cases and 205 uninfected, vaccinated controls to identify correlates of protection identified two immune responses: (i) serum IgA binding to 14 HIV-1 envelopes negatively correlated with protection; (ii) IgG binding to a gp70 V1V2 Case A (subtype B) scaffold positively correlated with protection[309,310]. Of note, IgA levels were not found to enhance infection, but rather to undo the positive effects of vaccination. On the other hand, IgG avidity, antibody-dependent cellular cytotoxicity (ADCC), neutralising antibodies (nAbs) and cytotoxic responses were not found to correlate with the rate of HIV-1 infection. In the setting of low anti-Env IgA, increased correlation with protection was also observed for ADCC and nAbs[311,312].

V1V2 gp70, a subtype B V1V2 region attached to the murine leukaemia virus gp70 protein[310], was chosen as a reagent to be tested because preliminary data of serum antibody binding to linear overlapping peptides encompassing the whole sequence of HIV-1 *Env* demonstrated binding to the V2 region[308]. In addition, in the $\alpha4\beta7$ integrin binding site data showing that mAbs recognising conformational epitopes within V2 would block RV144 sera binding to gp120[313].

In addition, viruses isolated from HIV-1 positive individuals in vaccine and placebo groups were analysed to define if an association could be found between particular viral types and the receipt of vaccine (sieve analysis)[279,284,314–316]: viral strains that matched the vaccine sequence, which contained a lysine at position 169 (K169) within V2 were found to be blocked by vaccination, as viruses mismatched with position 181. These findings strengthened the hypothesis that antibodies directed to V2 correlate with protection from viral infection. In addition, the mAbs CH58 and CH59 cloned from vaccine recipients were found to bind within V2, in a region that partially overlaps the binding site of bnAbs CH01 and PG9, although these two mAbs were only weak virus neutralisers; both mAbs CH58 and CH59 were found to bind to position 169, and, although non-neutralisers, were found to mediate ADCC[308].

The interplay between V2 and $\alpha4\beta7$: an underlying mechanism of protection?

As previous studies have demonstrated that the C-terminal region of the V2 domain of gp120 interacts with the integrin $\alpha4\beta7$[231,317,318], in this section I will summarise the role of this integrin in HIV infection. In addition, structure and function of $\alpha4\beta7$ and the V1V2 domain on gp120 will be reviewed. Finally, I will summarise the current knowledge on the interactions between $\alpha4\beta7$ and the HIV/SIV Env.

The gut tropism of HIV

A significant feature of acute HIV infection is substantial viral replication in the gut-associated lymphoid tissue (GALT), with high-level depletion of gut CD4+ T cells[319]. This gut-directed tropism of HIV is accepted to play a fundamental role in the late development of immune deficiency. In addition, rapid CD4+ T cell loss is accompanied by significant damage to the structural integrity of the gut, which has been identified as a cause of chronic systemic immune activation[320,321].

While ART significantly extends the life of individuals infected with HIV, treatment does not fully reverse the early damage to the structural integrity of the gut, nor does it allow full replenishment of the CD4+ T cell reservoir in GALT[322]. However, in addition to replicating in GALT, HIV also replicates in the peripheral lymph nodes, the spleen and other tissues and organs[323].

α4β7 and immune cell gut tropism

Immune cells migrate to and from the GALT through the regulation of receptors that control cell trafficking. α4β7, a prime mediator of gut homing, is comprised of a 180-kDa α chain (α4) and a 130-kDa β chain (β7). α4β7 is expressed on the cell surface of subsets of B cells, CD4+ and CD8+ T cells, NK cells and macrophages. While both α4 and β7 can pair with other integrin chains, α4β7 is central in promoting lymphocyte trafficking to the GALT through the interaction with mucosal addressin cell adhesion molecule (MAdCAM). This molecule is expressed on the surface of high endothelial venules of gut inductive sites, as well as in the gut lamina propria. In addition, α4β7 is also found on the surface of FDCs in mesenteric lymph nodes[324]. However, because most of the naïve and a subset of memory CD4+ T cells express α4β7 while circulating in the peripheral lymphoid tissue, it is the tissue-specific expression of MAdCAM in the gut that defines α4β7 as a gut homing receptor[323].

Upon ligation, α4β7 delivers intracellular signals that results in the extravasation of the cell through the venules and into the gut tissue[323,325].

α4β7 and viral gut tropism

A growing number of viruses have been shown to directly interact with integrins, including foot-and-mouth disease virus, Kaposi's sarcoma-associated herpesvirus, herpes simplex virus-2, adenovirus, human papillomarivur-16, reovirus, and others[326]. Certain rotaviruses as well as HIV and SIV engage α4β7[231,327–329]. For HIV and SIV, this interaction is mediated by gp120[323]. The identification of an interaction between HIV and α4β7 provided new insights into the gut-tropic nature of HIV and SIV[231]. However, this integrin is not fundamental for entry into target cells and its exact role in HIV pathogenesis remains to be fully elucidated[323].

HIV gp120 is covered by a variable number of N-linked glycosylation sites, which are found to be lower in number in viruses isolated in the first months after infection[265]. It seems, thus, that in the early stages of infection selection is exerted against heavily glycosylated quasispecies[323]. In addition, glycan removal enhances binding of gp120 to α4β7, allowing for the hypothesis that α4β7^{high} memory CD4+ T cells are early targets of infection in the immediate period following mucosal transmission[330]. Studies in the macaque model have shown that α4β7^{high} memory CD4+ T cells are quickly depleted upon mucosal transmission of the virus[323]. Amongst the cells bearing this phenotype, Th-17 cells have been implicated as early targets of infection[323]. Notably, Sivro *et al.* reported that α4β7^{high} memory CD4^{+} T cells are preferentially depleted in the first two weeks following infection in HIV-infected women[331]. In addition, both in human and in the macaque model α4β7^{high} memory CD4^{+} T cells in blood and in the cervical tissues is associated with increased susceptibility to acquisition[332,333]. It seems therefore α4β7 plays a central role in the early stages of infection.

Anti-α4β7 mAbs in HIV/SIV treatment and prevention

The first observation that demonstrated that anti-α4β7 mAb treatment could result in controlled viral infection were provided by Ansari *et al*., when macaques treated with anti-α4β7 mAb 3 days prior and 3 weeks following intravenous SIVmac239 infection exhibited delayed peak SIV RNA and lower plasma SIV RNA level in the chronic phase as compared to untreated control macaques[334]. In addition, the authors found that treatment reduced the amount of virus in the GALT and preservation of peripheral CD4^{+} CCR5^{+} T cells. Notably, while control animals developed

AIDS 60-80 weeks after infection, in treated animals symptom onset occurred 5 years after infection[323]. Finally, CD4+ T cells in colorectal biopsies recovered to almost pre-infection levels at more than 60 months post infection after an initial loss during the acute phase of infection[335]. Therefore, treatment with anti-$\alpha4\beta7$ mAb resulted in durable effects that were able to limit damage to gut tissues and preserve CD4+ T cells for an extended period of time. In addition, the authors concluded that early virus replication in GALT and consequent inflammation and damage of gut tissue plays a role in the course of the disease throughout the years following infection.

$\alpha4\beta7^{high}$ memory CD4+ T cells co-express multiple HIV susceptibility markers, with CCR5 expression being directly correlated with the levels of $\alpha4\beta7$ on these cells[336]. These features, which make of these cells favourable targets of infection, suggest that sexually transmitted HIV/SIV may infect $\alpha4\beta7^{high}$ memory $CD4^+$ T cells in the rectal mucosa, and that these infected cells proceed to migrate to the GALT[323]. Alternatively, it is possible that after a local bout of replication in the rectal mucosa, the virus envelope incorporates cell $\alpha4\beta7$ during budding, and virus-associated $\alpha4\beta7$ mediates virus adhesion to ligand MAdCAM on high endothelial venules.
To determine if interfering with $\alpha4\beta7$-mediated infection spread would reduce the efficiency of mucosal transmission of SIV, Byrareddy *et al*. tested the effect of an anti-$\alpha4\beta7$ mAb in preventing intravaginal SIVmac251 infection in macaques[327]. Briefly, animals were pre-treated with anti-$\alpha4\beta7$ mAb at 50 mg/kg or control IgG mAb, then challenged weekly until 10 out of 12 control animals were determined to be infected. After six challenges, 10/12 controls resulted infected, while 6/12 treated macaques remained uninfected (**Figure 1.16**). While the specific mechanisms underlying protection are to be elucidated, anti-$\alpha4\beta7$ mAb treatment did not alter the number of CD4+ T cells in the vaginal compartment, although it did mask >99% of $\alpha4\beta7$ in the compartment.

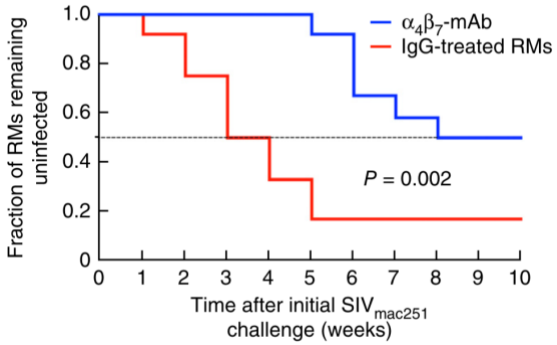

Figure 1. 16: Kaplan-Meier curves of infection in groups (n=12) of macaques treated with vedolizumab (blue line) or with a polyclonal rhesus macaque IgG preparation (red line, negative control). The treated group revealed delayed acquisition after SIVmac251 challenge as compared to the control group. From reference[327].

The authors proposed three mechanisms which might have contributed to reduced infection in the treated group. Anti-α4β7 mAb might have interfered with (i) infected T cell trafficking by blocking of α4β7 binding to MadCAM, (ii) SIV Env interactions with α4β7 and/or (iii) α4β7-mediated signalling on $CD4^+$ T cells, by MAdCAM or V2. α4β7 signalling through V2 or MAdCAM binding is in fact responsible for LFA-1 activation, an integrin which plays a central role in the establishment of virological synapses[231].

It is however not understood if α4β7+ cells contribute to the establishment of long-term viral reservoirs, and if treatment with α4β7 antagonists can play a role in reducing the size or durability of those reservoirs[323].

Anti-α4β7 mAb has also been tested as an adjunctive therapy to ART. Current ART is highly effective in allowing viremia control for an extended period of time, but since the viral reservoir persists during ART, the vast majority of HIV-infected individuals remain on therapy indefinitely to prevent blood viral load rebound. In addition, ART does not fully resolve the state of chronic immune activation which is associated with HIV infection. Given the previously discussed capacity of anti-α4β7 treatment to control viremia in SIV-infected macaques in the absence of ART[327,334], the anti-α4β7 mAb was used as an adjunctive therapy to ART. Fifteen rhesus macaques were placed on ART at 5 weeks post SIVmac239 infection[337]. Four weeks later, eight animals underwent the first out of eight anti-α4β7 mAb infusions, while seven control animals received irrelevant IgG. After nine weeks, ART was terminated.

The seven animals that received ART and control IgG showed significant plasma viral rebound, while all of the eight ART- and anti-α4β7 mAb- treated animals controlled plasma viremia to low or undetectable levels. This control persisted for more than three years, with intermittent blips of viremia in some of the animals, while blood $CD4^+$ T cell counts were restored to near pre-infection levels, with a significant recovery of gut $CD4^+$ T cells.

PET/CT image analyses determined that the addition of anti-α4β7 mAb reduced the number of infected cells in gut tissue as compared to ART alone during the dual therapy period[335]. However, because ART alone is already able to suppress plasma viremia, the mechanisms by which anti-α4β7 mAb reduced the number of gut infected cells beyond the levels achieved by ART is still unclear. Notably, upon interruption of ART and anti-α4β7 mAb the reduction of infected cells in the gut persisted. In addition, an increase in NKp44+ cells was observed[335,337,338]. In terms of adaptive immune response, no significant difference of CD8+ T cell activity was found in the two groups, and none of the animals generated neutralising antibodies. Finally, all eight of the anti-α4β7 mAb-treated animals developed measurable anti-V2 antibody responses, while only 3/7 controls developed antibodies with similar specificity. These antibodies were found to block SIVgp120 binding to α4β7[323].

Despite this wealth of results, defining a clear picture of the mechanisms ultimately responsible of control in ART-, anti-α4β7-treated macaques remains a challenging task.

α4β7 as a ligand of gp120

Arthos, collaborators and others have demonstrated that both HIV and SIV recombinant envelope proteins are able to engage the gut homing receptor integrin α4β7[231,317,318,339], suggesting that there could be a causal link between the gut-tropic characteristic of HIV/SIV infection and the physical interaction between SU and the integrin. However, the specific role of this interaction in HIV/SIV entry is not completely understood. It is established that α4β7 is not an entry receptor, as it is not required for cell infection[340,341]. Possibly, α4β7 functions as an attachment factor[342], that is as a lightning rod that, protruding from the cell surface three times in length of CD4, takes viral particles closer to cell surface to initiate receptor and coreceptor

engagement. It has been reported that gp120 binding to α4β7 also transduces signals to $CD4^+$ T cells that might favour infection in vivo[231,340].

α4β7 is present on the cell surface of naïve as well as memory CD4+ T cells[343] and, as mentioned above, it is a heterodimer built up by an α4 and a β7 chain[344,345]. Notably, α4β7 is structurally dynamic and can adopt as many as three conformation states, controlled intracellularly, of which two are extended and able to mediate adhesion of the lymphocytes[346,347]. Besides MadCAM, α4β7 is able to bind to VCAM, which is also present in the vascular endothelium[348].

V2 structure in the interaction with α4β7

A number of studies have demonstrated that the C-terminal region of V2/gp120 interacts with α4β7[231,317,318]. Arthos and collaborators demonstrated that site-directed mutagenesis of HIV gp120 in the tripeptide motif $L^{179}D^{180}V/I^{181}$ (DLV in SIV) plays a fundamental role in the interaction[231]. Notably, the motif is similar to binding epitopes in MAdCAM (LTD), VCAM (IDS) and the fragment IIICS of fibronectin (LDV). The common feature of each motif is a core Asp flanked by an aliphatic residue. Of note, in each of the natural ligands the Asp coordinates with a Mg++ ion that is located in the metal ion-dependent adhesion site (MIDAS) of β7. The presence of an Mg++ ion is required for ligand binding[346,349]. Cardozo and collaborators identified amino acids QRV (170-172) in the V1V2 domain to also influence the V2-α4β7 interaction, thus proving that the binding site in V2 is not limited to the LDV/I tripeptide exclusively[318]. Notably, the two regions of V2 are flanked by N-linked glycosylation sites (PNGs), and removal of the glycans through enzymatic digestion can increase binding of recombinant gp120 to α4β7[350], possibly allowing better access of the integrin to the integrin-binding site, or by driving the conformation of V2 into a more accessible structure.

Because the conformation of the V2 domain is structurally dynamic, this portion was deleted from the recombinant proteins used to generate the initial high-resolution structures of gp120 cocrysallised with mAb[230,267]. Both protein scaffolds and linear peptides were used to determine the conformation of V2, and showed that the domain was prone to adopt a β-strand conformation in the former, and an α-helix conformation in the latter setting.

β-strand Evidence

Cryo-election microscopy and X-ray diffraction analyses indicate that the V2 domains at the apex of the trimeric envelope spike appear in a β-strand, in the context of a β-barrel, in accordance with the structures derived from monomeric gp120 subunits and scaffolded constructs in complex with conformation-dependent mAbs[351–357]. The first V2 structure obtained presented V1V2 on a scaffold named 1FD6 in complex with PG9, a broadly neutralising, glycan-dependent mAb[355] (**Figure 1.17**). It is in this setting that V2 first appeared in the context of a Greek key motif, also comprising the V1 loop. It became clear that, structurally, V1 and V2 were both building up a region termed the V1V2 domain. Another study where the 1FD6-V1V2 domain in complex with mAb 830A provided more detail and revealed V2 in a similar beta barrel conformation[354]. However, high-resolution crystal structures allocate the LDV/I tripeptide in a buried region that would seem inaccessible to the integrin[355], and it would be reasonable to conclude that the context in which α4β7 and V2 are engaged must involve a rearrangement of the structures, with an alternative presentation of V2.

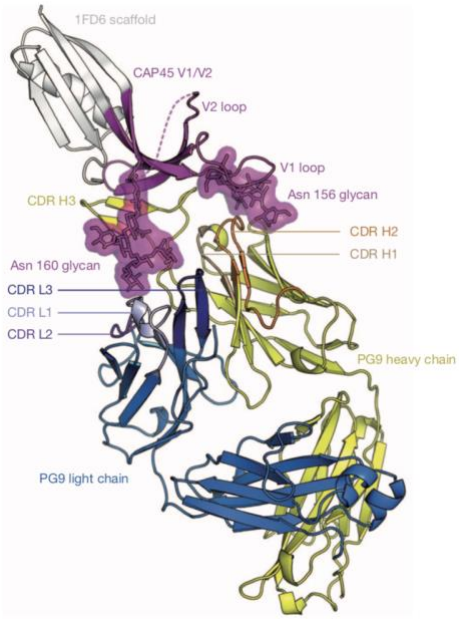

Figure 1. 17: Overall structure of the 1FD6-scaffolded V1V2 domain of HIV-1 gp120 in complex with mAb PG9. V1V2 from the CAP45 strain of HIV-1 is shown in magenta ribbons, in complex with the Fab of the antibody PG9, with the heavy and light chains shown as yellow and blue ribbons, respectively, with CDRs in different shades. Although the rest of HIV-gp120 has been replaced by the 1FD6 scaffold (white ribbons), the positions of V1V2, PG9 and the scaffold are consistent with the proposal that the viral spike is positioned towards the top of the page. The disordered region in the V2 loop is represented by a dashed line. From reference[355].

α-helix evidence

When a linear V2 peptide is left unconstrained from a scaffold or protein context, it is capable of adopting α-helical and coiled structures[358]. This was observed with two mAbs isolated from a patient enrolled in RV144 that remained uninfected. The two mAbs, namely CH58 and CH59, were analysed in complex with a linear V2 peptide derived from the gp120 of HIV isolate 92TH023[359]. Notably, the two mAbs displayed only weakly neutralising properties and were found to recognise a helix (CH58) and coiled (CH59) structure[359] (**Figure 1.18**). Notably, the CH mAbs recognise epitopes that are overlapping and that include the region of V2 spanning from aa168-181, which also contains residues K169 and I181 that sieve analyses identified as sites of vaccine-elicited immune pressure in RV144[316].

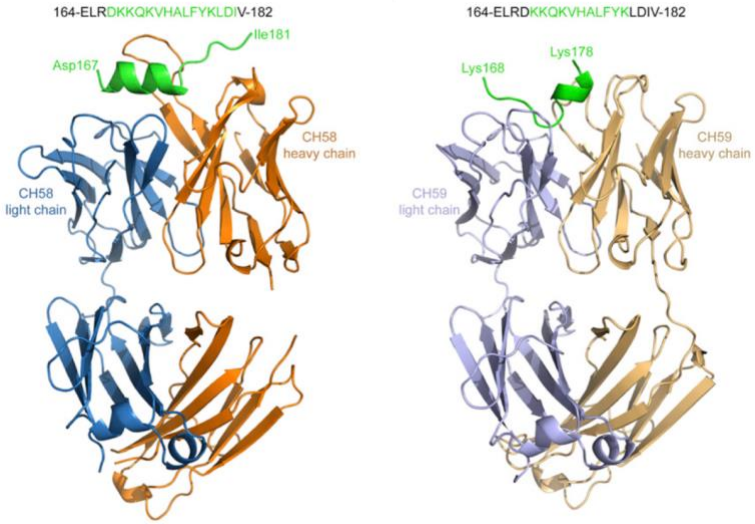

Figure 1. 18: Vaccine-elicited mAbs CH58 and CH59 recognise alternative conformations of V2 peptide. Left: Ribbon representation of the CH58 Fab in complex with a V2 peptide. The sequence of the A244 peptide is shown, with modelled residues in green. Orange: HC; blue: LC. Right: structure of CH59 in complex with peptide, as depicted on the left. Tan: HC; light blue: LC. From reference[359].

More V2-specific mAbs with a preference for helical structures in V2 have been identified: Lertjuthaporn and collaborators recently described Mk16C2, a mAb that was obtained from an immunised rabbit (**Figure 1.19**)[360]. The mAb binds the same structure as CH58, but from a different angle. It is important to note that helix-preferring mAbs are not only elicited by vaccination, but can also be induced by infection. It is the case of CAP228-16H, which was derived from an infected subject and which was found to recognise a V2 helix structure very similar to CH58[361].

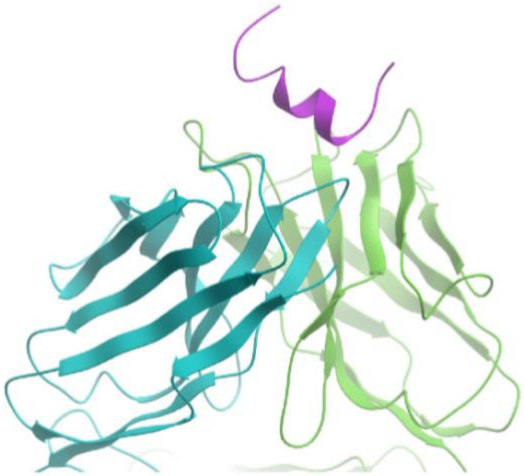

Figure 1. 19: Crystal structure of rabbit mAb Mk16C2 in complex with a V2 peptide. Only the Fv region are shown. Cyan: HC; green: LC; magenta: peptide. From reference[360].

To summarise, mAbs reacting to the region of V2 spanning from amino acids 153 to 194 have been described to recognise two types of epitopes: mAbs like PG9 and 830A recognise a constrained (sheet), and those like CH58 recognise an unconstrained (helical or coiled) structure.

In this thesis, I investigate the immunological mechanisms that mediate protection from SIV infection in rhesus macaques.

In Chapter 2, I address the hypothesis that anti-V2 antibodies might exert a protective mechanism by reducing viral uptake mediated by binding of gp120 to integrin $\alpha4\beta7$. More specifically, I characterised a set of mAbs that I isolated from a rhesus macaque vaccinated in an RV144-like fashion and which resulted in protection from repeated low-dose intrarectal SIVmac251 challenge. The biologic activity of these mAbs was then investigated for binding, neutralisation properties and ability to block $\alpha4\beta7$-to-V2 interaction. These studies were informative in the definition of the humoral responses to SIV vaccination and also the study of viral features.

In Chapter 3, I carried out on rhesus macaques a vaccination approach aimed at increasing the efficacy of RV144 by changing the viral vector used in the prime-boost vaccine protocol. The

outcome of this study provided further insights into the nature of the immune response needed to achieve protection from a primate lentivirus.

Finally, in Chapter 4 an anti-V2 mAb was tested for its ability to provide protection in passive immunisation settings on a group of rhesus macaques then challenged intrarectally with SIVmac251. The results allow for a few considerations to be made on the desirable immune responses that are to be elicited by a protective vaccine.

CHAPTER 2: Isolation and characterisation of monoclonal antibodies targeting the V2 region of gp120 from vaccinated macaques protected against SIVmac251 acquisition

Introduction

The RV144 Thai trial was the only HIV-1 vaccine trial to ever demonstrate protection, although limited to 31.2%, from viral acquisition in a cohort of 16,402 individuals [286]. In the enrolled vaccinees, antibody levels targeting the V2 region of the viral surface glycoprotein gp120 correlated with decreased risk of HIV-1 infection[309]. Similar findings were reported in rhesus macaques (*Macaca mulatta*), where an RV144-modeled vaccination schedule provided 40% protection from SIVmac251 in a group of 27 animals as compared to historical and concurrent controls. In line with the results of RV144, mucosal IgG responses targeting the V2 region of gp120 were associated with delayed viral acquisition[362].

Here we investigate the hypothesis that the molecular mechanism behind this correlation is that anti-V2 antibodies may inhibit the binding of this region to the integrin $\alpha4\beta7$ which, protruding for as many as 22 nm out of the cell surface, may capture and lead free viral particles closer to the cell membrane thus enhancing their likelihood of engaging receptor CD4 and coreceptors CCR5/CXCR4[363].

The structure of V2 has proven elusive to characterise: in complex with the poorly neutralising monoclonal antibodies (mAb) CH58 and CH59, derived from RV144 vaccinees, V2 peptides acquired helical conformations [359]. In contrast, the crystal structure of a V2 scaffold in complex with the mAb PG9 revealed that V2 and V1 form a four-stranded Greek key motif β-sheet domain (V1V2 domain)[355].

The putative site of interaction between $\alpha4\beta7$ and gp120 was identified as the LDI/V motif in HIV (DLV in SIVmac251, hereon referred as “tripeptide”), located in the V2 loop connecting the C and D β strands of the V1V2 domain [231]. However, it is not clear if the tripeptide, necessary for the engagement of $\alpha4\beta7$, interacts directly with the integrin or is necessary to maintain the conformation of the V1V2 domain with points of interaction with $\alpha4\beta7$ located elsewhere in the domain. The notion that V1V2 conformation is necessary for $\alpha4\beta7$ engagement is supported by

the observation that mutations in a region (defined by the authors as "cryptic determinant") located distant from the tripeptide can disrupt binding to $\alpha4\beta7$ [318].

Here, I isolated a set of weakly neutralising anti-V2 mAbs from an RV144-like vaccinated rhesus macaque which resisted multiple rounds of intrarectal SIVmac251 challenge. I then determined binding activity of the mAbs and their ability to inhibit binding of SIV gp120 to human $\alpha4\beta7$ was evaluated. Our findings provided insights into the humoral response to SIV immunisation in rhesus macaques as well as on the structural plasticity of V2.

Materials and Methods

1J08 V1V2 scaffolds

The protein scaffold 1J08, was previously demonstrated to present the SIV Env V1V2 domain in the conformation naturally found on the native V1V2 protomer basing on stable expression, clash score and solvent accessibility, was used to identify V1V2-specific B cell clones and produced as described in [364]. The expression vector pVRC8400 encoding the C-terminal His-tagged, avitagged 1J08-scaffolded SIVmac251-M766r or SIVsmE543 V1V2 sequences (GenScript) was used to transfect 293Freestyle (293F) cells with 293fectin transfection reagent (Life Technologies) following the company's instructions. 6 days post-transfection, cell culture supernatants were harvested and filtered through 0.22 µm filter and supplemented with protease inhibitor tablets (Roche). The constructs were passed through a NiSepharose excel affinity media (GE Healthcare) and further purified with size exclusion chromatography (SEC) on a HiLoad 16/600 200 pg Superdex column (GE Healthcare).

Rhesus macaque P770

P770 is a colony-bred rhesus macaque obtained from Covance Research Products (Alice, TX) previously included in an RV144-like vaccination study (**Figure 2.1**)[362]. Briefly, P770 was immunised at weeks 0, 4, 12 and 24 with intramuscular inoculations of 10^8 plaque-forming units (PFU) of ALVAC (vCP2432) expressing SIV genes gag-pro and gp120TM (Sanofi Pasteur).

A

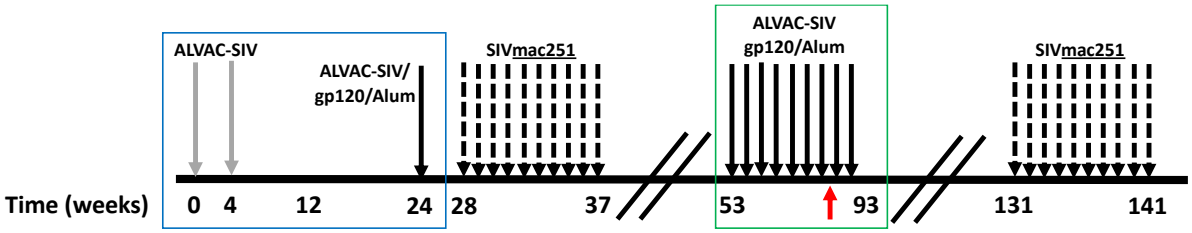

B

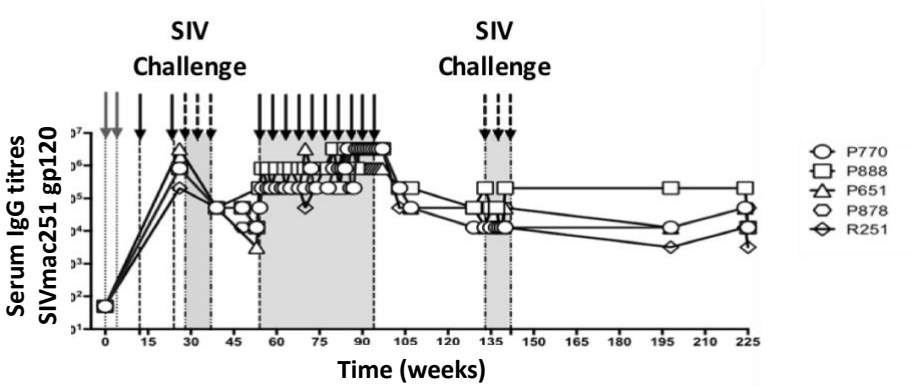

Figure 2. 1 A) Immunisation and virus challenge schedule of macaque P770. P770 underwent an RV144-like vaccination regimen (blue box) based on the administration of two ALVAC-SIV primes and two ALVAC-SIV + monomeric gp120 boosts followed by RLD intrarectal SIVmac251 challenge [3]. Four months after the last viral exposure, P770 was enrolled in a second round of immunization consisting of 9 monthly ALVAC-SIV + monomeric gp120 boosts (hereon referred as *hyperboost* phase, green box). 38 weeks later (approximately 9 months) the animal underwent a second round of RLD SIVmac251 intrarectal challenges and resulted uninfected. Red Arrow: time at which frozen B cells were used for antibody cloning, 2 weeks after the 7th hyperboost. **B)** Anti-SIVmac251 gp120 serum antibody titres of P770 and four other animals P888, P651, P878 and R251 remained high throughout the immunisation, challenge phases. Solid arrows: immunisation; dashed arrows: viral challenge; grey arrows: immunisation prime; Grey boxes: challenge and immunisation phases, as indicated by the arrows.

The sequence of the SIV genes was that of M766r, a mucosally transmitted founder variant of SIVmac251. At weeks 12 and 24, the animal was administered in the thigh opposite to that of vector immunisation a protein boost of 200 µg each of monomeric SIVmac251-M766 gp120-gD and SIVsmE660 gp120-gD CG7V both formulated in alum. At week 28, four weeks after the final immunisation, the animal underwent a challenge phase of 10 low-dose intrarectal 120 $TCID_{50}$ SIVmac251 administrations, and remained uninfected.

At week 53, P770 underwent a second round of 9 immunisations (referred in the text as *hyperimmunisations*) as in weeks 12 and 24, administered every five weeks up to week 93. At

week 131, the animal was challenged as in week 28, with 10 repeated administration of intrarectal 120 $TCID_{50}$ SIVmac251 administrations, and again remained uninfected. Measurable anti-gp120 serum antibody titres were then detected for more than a year after the second challenge round.

Monoclonal antibodies

Single antigen-specific B cells were isolated with the assistance of Richard Nguyen, Vaccine Research Center, NIH, Bethesda, Maryland, USA. The rest of the protocol was carried out by the author with the kind assistance and supervision of Dr. Rosemarie Mason, ImmunoTechnology Section, Vaccine Research Center, NIH, Bethesda, Maryland, USA.

The mAbs ITS01, ITS12.01 (hereafter referred to as "ITS12"), ITS09.01 ("ITS09"), ITS03 and ITS41, isolated from an SIVsmE660-infected rhesus macaque, were kindly provided by Dr. Mario Roederer (ImmunoTechnology Section, Vaccine Research Center, NIAID, NIH) [364]; ITS01 recognises an epitope located in the CD4bs of SIV gp120 and was used as negative control in ELISA binding experiments of mAbs to V2; ITS12 and ITS41 bind epitopes located within the V2 loop. The mAbs NCI05 and NCI09 were isolated from the hyperimmunised, protected rhesus macaque P770 following the methods described[364]. Briefly, frozen P770 PBMCs from week 85 (two weeks after the 7th hyperimmunisation) were thawed and stained to allow the phenotypic identification of CD20+, CD3-, CD4-, CD8-, CD14-, IgG+, IgM- memory B cells. After staining, the cells were washed twice with PBS and resuspended in 200 µl of PBS containing 1J08 SIVmac251-M766 V1V2 conjugated to APC and 1J08 SIVsmE543 V1V2 conjugated to PE and incubated in the dark for 15 minutes at room temperature. The cells were then washed in PBS, analysed and sorted with a modified 3-laser FACSAria cell sorter using the FACSDiva software (BD Biosciences). Antigen (V2)-specific B cells positive for binding to SIVsmE543/V1V2 only or SIVsmE543 and SIVmac251/V1V2 (**Figure 2.2B**) were singularly sorted into well of 96-well plates containing lysis solution. Flow cytometric data was analysed with FlowJo 9.7.5.

Total RNA was reverse transcribed in each well, and rhesus immunoglobulin H, Lκ and Lλ chains variable domain genes amplified by nested PCR. Positive amplification products as analysed on 2% agarose gel (Embi-Tec) were sequenced, and those that were identified as carrying Igγ and IgLκ or IgLλ sequences were re-amplified with sequence-specific primers carrying unique

restriction sites using the first-round nested PCR products as template. Resulting PCR products were run on a 1% agarose gel, purified with QIAGEN Gel Extraction Kit (QIAGEN) and eluted with 25µl of nuclease-free water (Quality Biological). Purified PCR products were then digested and ligated into rhesus Igγ, IgLκ and IgLλ expression vectors designed by Dr. Saunders and kindly provided by Dr. Mascola (VRC, NIAID) containing a multiple cloning site upstream of the rhesus Igγ, Igκ or Igλ constant regions. Full-length IgG were expressed by co-transfecting 293F cells with equal amounts of paired heavy and light chain plasmids then purified using Protein A Sepharose beads (GE Healthcare) according to the manufacturer's instructions.

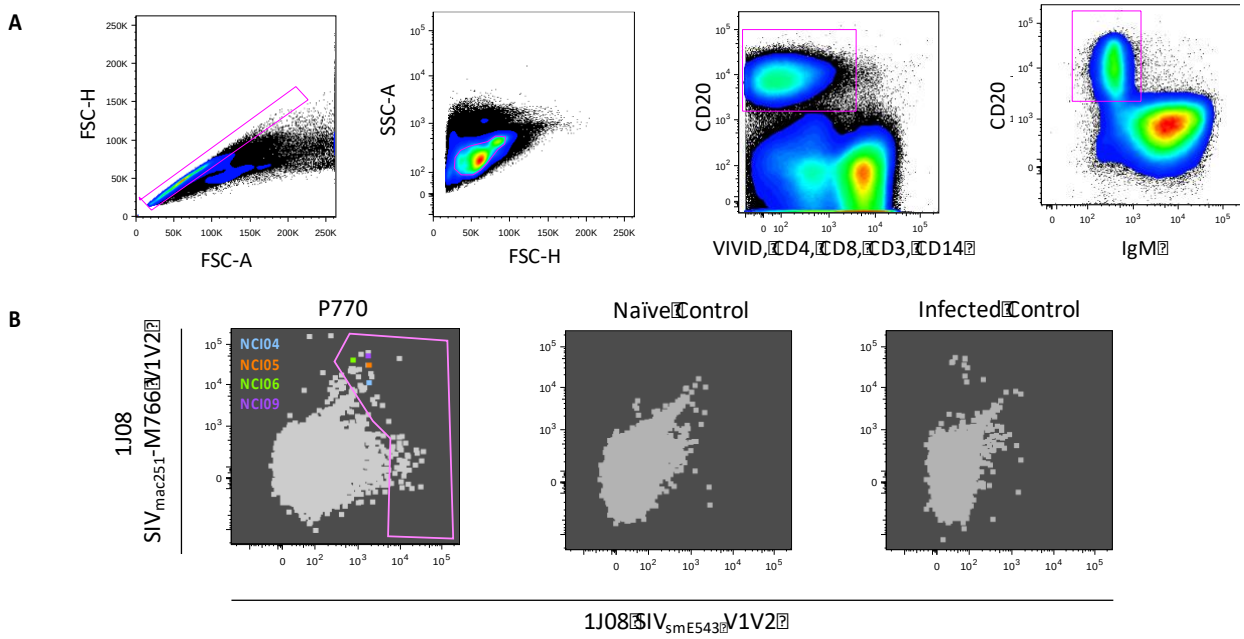

Figure 2. 2: Phenotypic characterisation of memory B cells and localisation of isolated NCI mAbs in antigen-binding dot-plot. **A)** Plots represent the gating strategy, where gating is identified by purple shapes and parent-to-daughter populations flow from left to right. **B)** Binding of the probes 1J08 V1V2 SIVmac251 (Y axis) and SIVsmE543 (X axis) in P770 and one naïve control, one SIVmac251-infected control. The gating strategy for cell sorting is indicated by the purple shape. The sorted events from which the NCI mAbs were cloned are represented in coloured dots.

ELISA peptide mapping of NCI mAbs

ELISA peptide mapping of NCI mAbs was carried out by Irene Kalisz, Advanced Bioscience Laboratories, Frederick, Maryland, USA.

Binding of SIV-specific mAbs to overlapping peptides encompassing the V1V2 region of SIVmac251 gp120 was measured by enzyme-linked immunosorbent assay (ELISA). Plates were coated overnight with 100 µl of peptide at a concentration of 10 µg/ml in $NaHCO_3$, pH 9.6 at 4

˚C, then blocked with 200 µl of PBS Superblock (Thermo Fisher Scientific) for 1 hour at room temperature. After blocking, 100 µl were added to emptied wells, each one containing 10 µg/ml of Ig in ELISA sample diluent (Avioq), and incubated for 1 hour at 37˚C. After washing, 100 µl of goat anti-human IgG conjugated to HRP (KPL) diluted 1:120,000 in sample diluent (Avioq) was added to all wells and incubated for 1 hour at 37 ˚C. After washing, 100 µl of K-Blue Aqueous substrate (Neogen) was added to all wells and incubated for 30 minutes at room temperature. The reaction was stopped by adding 100 µl of 2N H_2SO_4 to all wells, and binding intensity measured at 450 nm.

NCI09 Fab expression, crystallisation and refinement

NCI09 Fab expression, crystallisation and refinement was carried out by Jason Gorman, Structural Biology Section, Vaccine Research Center, NIH, Bethesda, Maryland, USA.

The variable region of the NCI09 heavy chain was synthesized and cloned into a pVRC8400 vector containing an HRV3C cleavage site in the hinge region as previously described [355]. Heavy and light chain plasmids were co-expressed in 1 litre of Expi293F cells. IgG was purified from the supernatant through binding to a protein A Plus Agarose (Pierce) column and eluting with IgG Binding Buffer (Thermo Fisher). Antibodies were buffer-exchanged to PBS and then 10 mg of IgG was cleaved with HRV3C protease. The digested IgG was then passed over a 2 ml protein A Plus column to remove the Fc fragment. The Fab was further purified over a Superdex 200 gel filtration column in buffer containing 5 mM HEPES 7.5, 50 mM NaCl, and 0.02% NaN_3.

To form NCI09-V2 peptide complexes, 5 mg of purified fab at a concentration of 2 mg/ml was incubated at room temperature for 30 minutes with a five-fold molar excess of SIV V2 peptide, synthesized by GenScript, and the complex was then concentrated down to 10 mg/ml using 10,000 MWCO Ultra centrifugal filter units (EMD Millipore). Antibody-peptide complexes were then screened against 576 crystallization conditions using a Mosquito crystallization robot mixing 0.1 µl of protein complex with 0.1 µl of the crystallization screening reservoir. Larger crystals were then grown by the vapor diffusion method in a sitting drop at 20ºC by mixing 1 µl of protein complex with 1 µl of reservoir solution (22% (w/v) PEG 4000, 0.1 M Na Acetate pH 4.6). Crystals were flash frozen in liquid nitrogen supplemented with 20% ethylene glycol as a cryoprotectant.

Data were collected at 1.00Å using the SER-CAT beamline ID-22 of the Advanced Photon Source, Argonne National Laboratory. Diffraction data were processed with HKL2000 (HKL Research). A molecular replacement solution was obtained with Phenix [365] contained one Fab molecule per asymmetric unit in space group $P2_12_12_1$. Model building was carried out using COOT software [366]. The Ramachandran plot determined by Molprobity [367] shows 98.2% of all residues in favoured regions and 100% of all residues in allowed regions for the complex structure.

Binding and competition assays

cV2 binding assays were initially carried out by Kristina Peachman, Antigens and Immunology Section, U.S. Military HIV Research Program, Silver Spring, Maryland, USA, and then replicated by the author.

Binding of SIV-specific mAbs to viral proteins or synthetic peptides was measured by ELISA. Plates were coated overnight at 4˚C with 50µl, 100 ng/well of antigen in PBS, then blocked with 300µl/well of 1% PBS-BSA for 1 hour at 37°C. When cyclic V2 (cV2), a circularised peptide carrying the amino acid sequence of viral V2 was tested, plates were coated at 4˚C overnight with 200 ng/well of streptavidin (Sigma-Aldrich) in bicarbonate buffer, pH 9.6, then incubated with biotinylated cV2 peptide (produced by JPT Peptide Technologies and kindly provided by Dr. Rao, Military HIV Research Program) for 1 h at 37°C and blocked with 0.5% milk in 1× PBS, 0.1% Tween 20, pH 7.4 overnight at 4°C.

Coated, blocked plates were incubated with 40µl/well of serial dilutions of mAbs in 1% PBS-BSA for 1 hour at 37˚C. 40µl/well of a polyclonal preparation of Horseradish peroxidase (HRP)-conjugated goat anti-monkey IgG antibody (Abcam) was then incubated for 1 hour at 37°C. Plates were washed between each step with 0.05% Tween 20 in PBS. Plates were developed using either 3,3′,5,5′- tetramethylbenzidine (TMB) (Thermo Scientific) and read at 450 nm. When testing binding to linear peptides, cyclic V2 or 1J08 V1V2 scaffolds, a ratio of the molecular weights of these constructs to the native glycoprotein monomer was calculated in order to obtain coating with the same approximate number of epitopes/well.

When testing for glycan dependency of antibody binding, SIVmac251/gp120 was deglycosylated with PNGase F (New England BioLabs) according to the manufacturer's indications and coated at 100 ng/well.

Competition assays of anti-V2 mAbs were performed by ELISA as described in [364] and [269]. Briefly, plates were coated with 100 ng/well of purified proteins SIVmac251-M766 gp120 (Advanced BioScience Laboratories, Inc.) or SIVsmE660.CR54 gp140 (kindly provided by Dr. Roederer, VRC)[364] and blocked with 1% PBS/BSA. Serial dilutions of unbiotinylated competitor mAb in 1% PBS-BSA were then added to the wells for 15 minutes prior to addition of biotinylated probe mAbs at a concentration to yield ~50% saturating OD450. After incubation with streptavidin-HRP (KPL) for 1 hr at 37°C, signal was developed through incubation with 3,3',5,5' tetramethylbenzidine (TMB) substrate (Thermo Fisher Scientific) and Optical density (OD) read at 450 nm. Two negative (1%PBS/BSA or serial dilutions of anti-CD4bs ITS01) and one positive (serial dilutions of unbiotinylated probe mAb) control of competition were included in each assay. Percent inhibition was calculated as a subtraction of the signal obtained at the highest concentration of competitor antibody subtracted to the background BSA control, divided by said background control and multiplied by 100.

Viral Neutralisation Assays

Viral neutralisation assays were carried out in collaboration with Rosemarie Mason, Vaccine Research Center, National Institutes of Health, Bethesda, MD, USA.

Viral neutralisation assays were performed by the HIV-pseudotype assay, in which SIV pseudoviruses were produced as previously described[368]. Briefly, a luciferase reporter plasmid containing essential HIV genes was used in combination with a plasmid encoding for SIV gp160 to yield pseudoviruses exposing SIV Env on their surface. Plasmids encoding SIV gp160, clones SIVsmE660.CP3C, SIVsmE660.CR54, SIVmac251.H9 and SIVmac251.30 were kindly provided by David Montefiori. Single-round infection of TZM-bl was detected quantitatively in relative light units (RLU). Virus neutralisation was measured as the 50% inhibitory concentration of mAb necessary to cause a 50% reduction in RLU as compared to virus control wells after subtraction of background RLU.

α4β7 adhesion to SIVmac251-M766 gp120

α4β7 adhesion assays were carried out by Matthew Liu, Laboratory of Immunoregulation, National Institute of Allergy and Infectious Disease, NIH, Bethesda, Maryland, USA.

The binding intensity of SIVmac251-M766 gp120 to α4β7 expressed by the cell line RPMI8866 (a human B lymphoma cell line that constitutively expresses α4β7, purchased from Sigma-Aldrich) in presence or absence of mAbs was assessed following the methods described by Lertjuthaporn and collaborators[360]. Briefly, cell line RPMI8866 was cultured in media containing 1μM of Retinoic Acid (RA) for at least 7 days before start of the adhesion assay, to increase adhesion to V2 peptides. Triplicate wells of 96-well flat-bottom plates (Greiner Bio-One) were coated overnight at 4˚C with 100 μl of 0.5-2.0 μg of deglycosylated SIV gp120 diluted in 50 mM bicarbonate buffer, pH 9.6. The solution from the plates was discarded and then blocked with buffer (25 mM Tris, 2.7 mM potassium Chloride, 150 mM sodium chloride, 0.5% BSA, 4 mM manganese chloride, pH 7.2) for 1 hour at 37˚C. Plates were then washed manually 4 times with blocking buffer, and RPMI8866 cells were pre-incubated in a volume of 50 μl/well for 40 min at 37˚C with sample buffer while using anti-α4 mAb 2B4 or anti-α4β7 inhibitor ELN3 as positive controls of inhibition [327,369]. If competition experiments were being carried out, competitor antibody was added to the well at the indicated concentration and incubated for 30 minutes at 37˚C before this stage. Plates were then incubated with 50 μl/well of $2x10^5$ RPMI8866 cells at 37˚C (5% CO_2) for 1 hour, washed with PBS 5 times. Finally, 100 μl of RPMI-1640 containing 1% FBS, 1% pen/strep/glutamine, 25 mM HEPES with 10 μl/well of AlamarBlue® dye. Fluoresence (excitation 560 nm, emission 590 nm) was detected immediately after dye addition and measured for 8 hours.

Surface plasmon resonance

Surface plasmon resonance assays were carried out by Donald Van Ryk, Laboratory of Immunoregulation, National Institute of Allergy and Infectious Disease, NIH, Bethesda, Maryland, USA.

These experiments were performed using a Biacore 3000 (GE Life Sciences) using CM4 or CM5 sensor chips as in reference[360]. Data were analysed using BIAevaluation 4.1 software (GE Life Sciences). The chip surface was activated by injection of 35 μl of 0.05 M N-hydroxysuccinimide

and 0.2 M N-ethyl-N(dimethylaminopropyl)carbodiimide mixed 1:1 at 5 ≤l/min. NeutrAvidin, SIVmac251-M766 gp120 or SIVsmE660.CR54 were immobilised at concentrations of 5 µg/ml in 10mM NaOAc, PpH4.5 to approximately 750 resonance units (RU). Unreacted sites on each surface were then blocked with 35 µl of 1M Tris-HCl (pH 8.0). Biotinylated cV2 (1µg/ml in 20 mM Tris-HCl, pH 8.0) was bound to NeutrAvidin to a density of approximately 250-300 RU. One surface was kept activated and blocked without ligand to act as a negative control surface for non-specific binding of soluble ligands. Any binding detected was then subtracted from the remaining surfaces. Running buffer was HBS (pH 7.4), 0.01 mM $CaCl_2$, either 1mM $MgCl_2$ or $MnCl_2$, 0.005% Tween-20, 0.05% soluble carboxymethyl-dextran. Binding experiments were then performed at a flow rate of 25 µl/min at 25˚C. After a two-minute injection, the surface was washed for an additional 2 minutes in running buffer to observe dissociation of the bound ligand from the surface. The surfaces were restored with multiple injections of 4.5 $MgCl_2$ at a flow rate of 100 µl/min. Inhibition of anti-V2 loop antibodies by linear V2-loop peptides was carried out by pre-incubating the mAbs with the peptides in running buffer for 2 hours at room temperature prior to passing them over the prepared surfaces as described above. Competition experiments were carried out by pre-incubating tested mAbs with overlapping SIVmac239 15-mers.

Scientist	**Contribution**
Giacomo Gorini	Production of 1J08 probes, isolation of NCI mAbs from memory B cell sorting to purification, ELISA binding and competition assays (including cV2), neutralisation assays, design of ITS41-NCI09 competition on $\alpha4\beta7$ adhesion assay, data analysis, graph editing; first proposed that antibody interference could be a mechanism deployed by SIV to evade the humoral immune response of the host.
Irene Kalisz	NCI mAbs ELISA peptide mapping.
Jason Gorman	NCI09 Fab expression, crystallisation and refinement.
Kristina Peachman	cV2 binding assays.
Rosemarie Mason	Neutralisation assays.
Matthew Liu	$\alpha4\beta7$ adhesion assays.
Donald Van Ryk	Surface plasmon resonance assays.
Richar Nguyen	Memory B cell sorting.

Table 2. 1 List of collaborators and relative contribution to the experiments reported in this chapter.

Results

Isolation of anti-V2 mAbs

A total of 289 memory B cells were identified and sorted using a rhesus memory B cell staining panel. Cells were isolated when resulting positive for binding to the APC-conjugated 1J08 SIVmac251-M766 V1V2 and PE-conjugated 1J08 SIVsmE543 V1V2 or the SIVsmE543 probe alone (**Figure 2.2B**). This number corresponded to the 0.78% of the memory, and the 0.13% of the total B cells in the PBMC sample tested. Nested PCR-amplification of heavy and light V(D)J genes resulted in the amplification of 72 matched pairs, of which 40 were cloned and expressed. Of the expressed clones, two mAbs, namely NCI05 and NCI09 displayed strong antigen recognition in ELISA assays against SIVmac251 and/or SIVsmE543 cV2 and were further tested against whole antigens, with the results summarised in **Table 2.2** and reported in detail in **Figure 2.3**. In addition, two expressed mAbs, namely NCI04 and NCI06, were found to be V1-specific as identified in ELISA assays on a linear SIVmac251 V1 peptide.

	NCI05	NCI09	NCI04	NCI06
SIVsmE543 cV2	++	++	-	-
SIVmac251 cV2	~	++	-	-
SIVsmE543 1J08 V1V2	++	++	-	++
SIVmac251 1J08 V1V2	++	++	++	++
SIVmac239 1J08 V1V2	++	++	+	++
SIVmac251 V2 peptide	-	++	-	-
SIVmac251 V1 peptide	-	-	~	++
Peptide/Epitope	TGLKRDKTKEYNETWYSTD	KFTMTGLKRDKTKEY	PLCITMRCNKSETDRWGLTK	RCNKSETDRWGLTK
SIVmac251 M766 gp120	++	++	++	++
SIVsmE660.CR54 gp140	++	++	-	++

++	OD450≥2
+	1≤OD450<2
~	0.5≤OD450<1
-	OD450<0.5

Table 2. 2: Summary of ELISA binding profiles of anti-V2 (NCI05, NCI09) and anti-V1 (NCI04, NCI06) mAbs. Cloned NCI mAbs were tested against a set of viral antigens with detailed results are reported in **Figure 2.3**. Binding intensity to each antigen as in the legend.

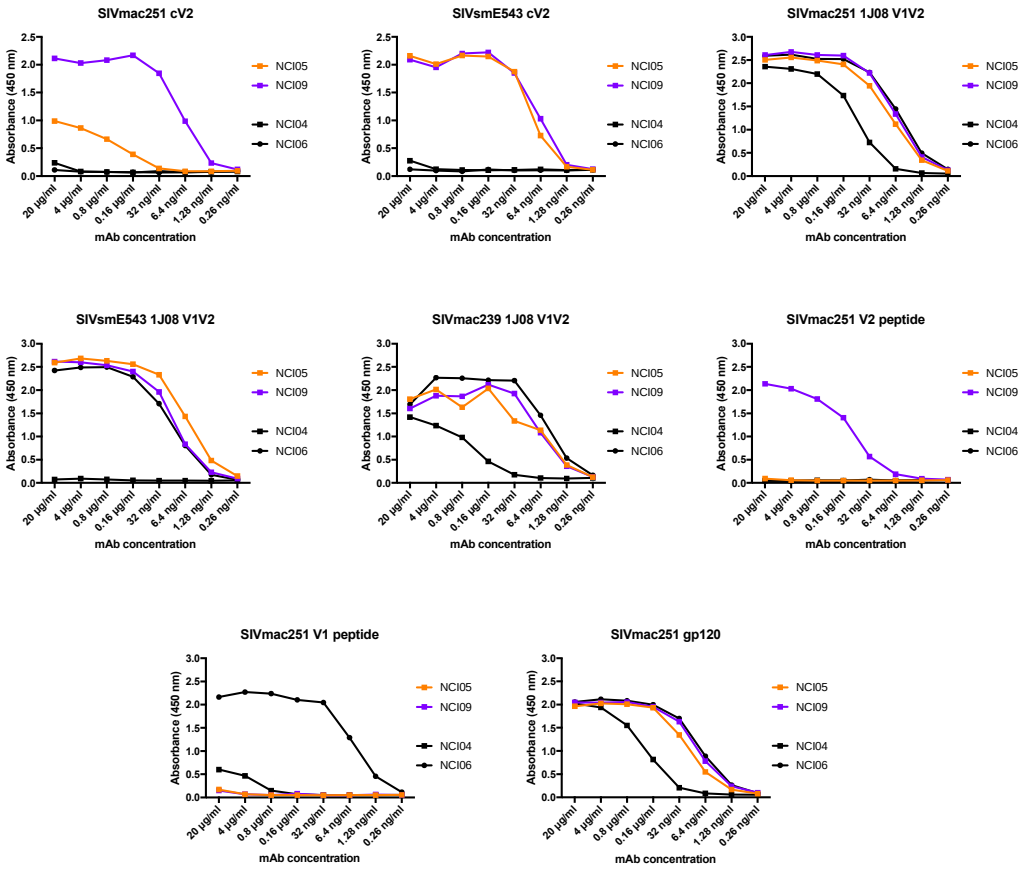

Figure 2. 3: ELISA binding data of NCI mAbs to V1 or V2 antigens. Replicate plates were coated with the antigens reported in the title of each individual graph. Blocked plates were incubated with serial dilution of test mAbs. After incubation with secondary goat anti-monkey*HRP antibody, plates were developed with TMB substrate and absorbance data were acquired at 450 nm.

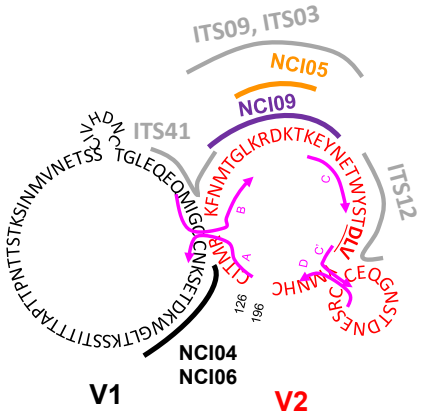

Figure 2. 4: Two-dimensional diagram of the SIVmac251 M766 V1V2 domain with the binding site of the V2-specific mAbs NCI05 and NCI09 and V1-specific mAbs NCI04 and NCI06. Binding sites of ITS mAb tested in this thesis and kindly provided by Dr. Roederer are shown in light grey and described more in detail in reference[364]. Pink arrows represent the location of the putative four beta strands (A-D) building up the Greek key motif previously described in the region[355]. Residues located in the V1 and V2 loops are represented in black and red, respectively. In all the figures, unless stated otherwise, data concerning NCI09 are in purple, NCI05 in orange, NCI04 and NCI06 in black.

ELISA Epitope definition and Neutralisation Assays

To locate the epitope recognised by these antibodies, the NCI mAbs were tested in ELISA against a panel of overlapping 20-mer peptides encompassing the V1, V2 regions of SIVmac251 gp120 consensus sequence. Notably, all of the isolated NCI mAbs were able to bind linear peptide and have their epitope located within V1/V2 with the only exception of NCI05 (**Figure 2.5**). However, none of these mAbs demonstrated strong neutralisation potency against a panel of SIV pseudoparticles (**Figure 2.6** and **Table 2.3**).

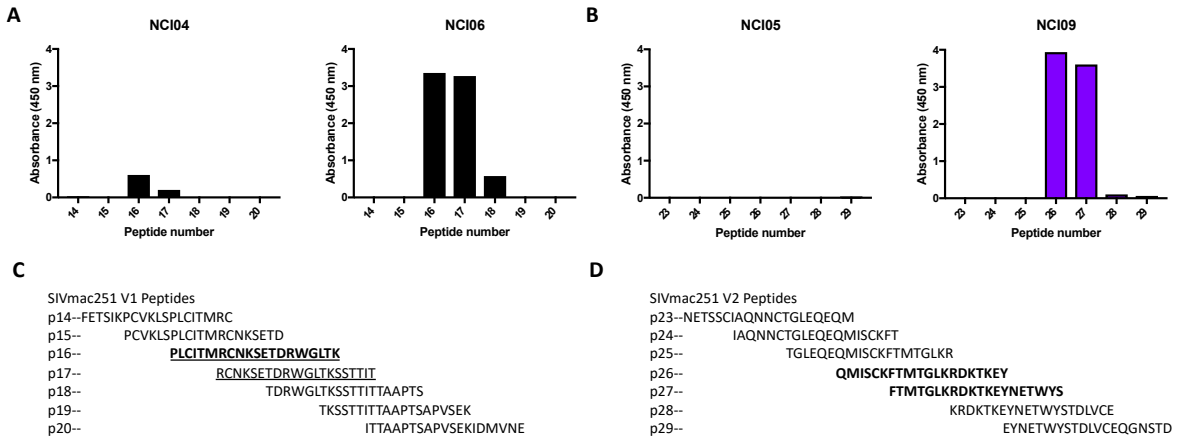

Figure 2. 5: Peptide mapping of NCI mAbs. ELISA binding of **A)** anti-V1 mAbs NCI04 and NCI06 to overlapping 20-mer peptides encompassing the N-terminal region of SIVmac251 gp120 V1 consensus sequence and of **B)** anti-V2 mAbs NCI05 and NCI09 to overlapping 20-mer peptides encompassing the V2 region of SIVmac251 gp120 consensus sequence. Binding is found greatest for NCI09 in the region covered by peptides 26 and 27, while no binding was detected for NCI05. **C)** Sequence of the overlapping 20-mer linear SIVmac251 gp120 peptides encompassing the N-terminal V1 region. Peptides bound with greatest intensity by NCI04 and NCI06 are represented in bold and underlined, respectively. **D)** Sequence of the overlapping 20-mer linear SIVmac251 gp120 peptides encompassing the V2 region. Peptides bound by NCI09 are represented in bold.

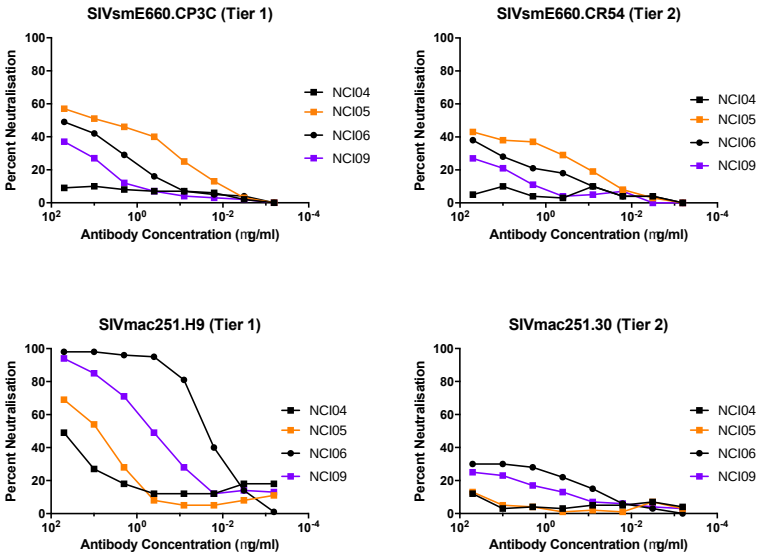

Figure 2. 6: Neutralisation graphs of NCI mAb against a panel of pseudoparticles exposing tier 1 or tier 2 SIV env. Single-round infection of TZM-bl cell line was detected quantitatively in RLU, and percent neutralisation extrapolated as signal reduction in comparison to antibody-free control wells.

	V2-specific		V1-specific	
	NCI05	**NCI09**	**NCI04**	**NCI06**
SIVsmE660.CP3C (Tier 1)	4.449	>50*	>50*	>50*
SIVsmE660.CR54 (Tier 2)	>50*	>50*	>50*	>50*
SIVmac251.H9 (Tier 1)	>50	0.412	>50	0.024
SIVmac251.30 (Tier 2)	>50*	>50*	>50*	>50*

0.01 - 0.099 µg/ml
0.1 - 0.99 µg/ml
1 - 9.99 µg/ml
>50* = curve plateaued below 50%

Table 2. 3: Neutralisation potency (IC50) of NCI mAbs. Cloned V1- or V2- specific mAbs were tested for neutralisation against tier 1 and tier 2 SIVmac251 and SIVsmE660 pseudoviruses. Reported IC50 values were measured as the concentration of mAb necessary to cause a 50% reduction in RLU as compared to antibody-free control wells after subtraction of background RLU. >50: no neutralisation.

Moreover, NCI05 was found to exhibit conformation-, glycan- dependent binding properties against SIVmac251 gp120 (**Figure 2.7**). More in detail, deglycosylation by PNGase treatment of SIVmac251 gp120 was found to completely deplete binding of NCI05 to the antigen (**Figure 2.7A**). While we initially inferred that NCI05 binds to a glycan epitope, this conclusion was proved wrong in tests against SIVsmE543 cV2 (**Figure 2.7B**), where the mAb was found in fact to strongly bind to the deglycosylated cV2 of this viral strain. We therefore concluded that NCI05 recognises a conformational epitope that is represented in the native conformation in cV2 from SIVsmE543 but not from SIVmac251, where glycosylations are also necessary to switch the NCI05 epitope to the correct conformation.

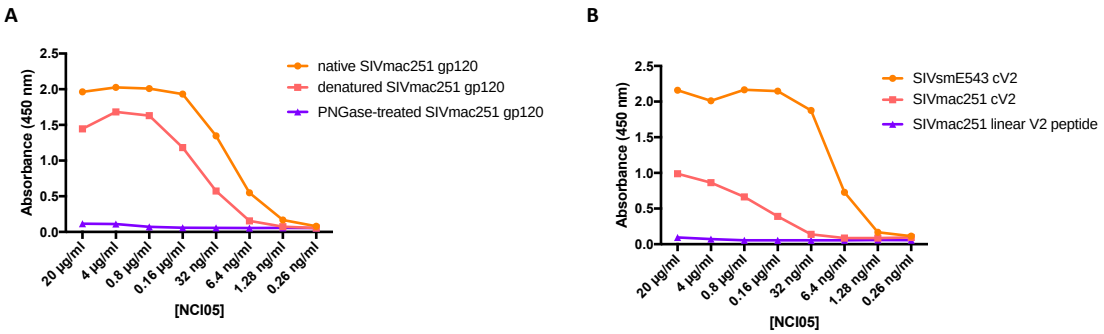

Figure 2. 7: ELISA binding profile of NCI05 to **A)** native, denatured and deglycosylated SIVmac251-M766 gp120 and **B)** linear and cyclic SIVmac V2 peptides. Blocked plates were incubated with serial dilution of test mAbs. After incubation with secondary goat anti-monkey*HRP antibody, plates were developed with TMB substrate and absorbance data were acquired at 450 nm.

Antigen Binding Affinity and Peptide Competition

Association/Dissociation constants (KA/KD, respectively) of NCI05 and NCI09 whole mAbs, as well as ITS41 Fab were calculated by surface plasmon resonance against SIVmac251 gp120, SIVsmE660 gp140 and SIVmac251 cV2 (**Figure 2.8** and **Table 2.4**). The results revealed that, while the two mAbs and the Fab have comparable KA against SIVmac251 gp120, neither ITS41 nor NCI09 were found to bind to SIVsmE660 gp140. This finding was unexpected for NCI09, which we identified as a strong binder of SIVsmE660 gp140 by ELISA. It is however possible that antigen binding to chip surface resulted in masking or alteration of the epitope bound by this mAb. In addition, these results also revealed that NCI05 is actually able to bind to SIVmac251 cV2, but the high KD of this binding results in fast detachment of the mAb from the deglycosylated antigen.

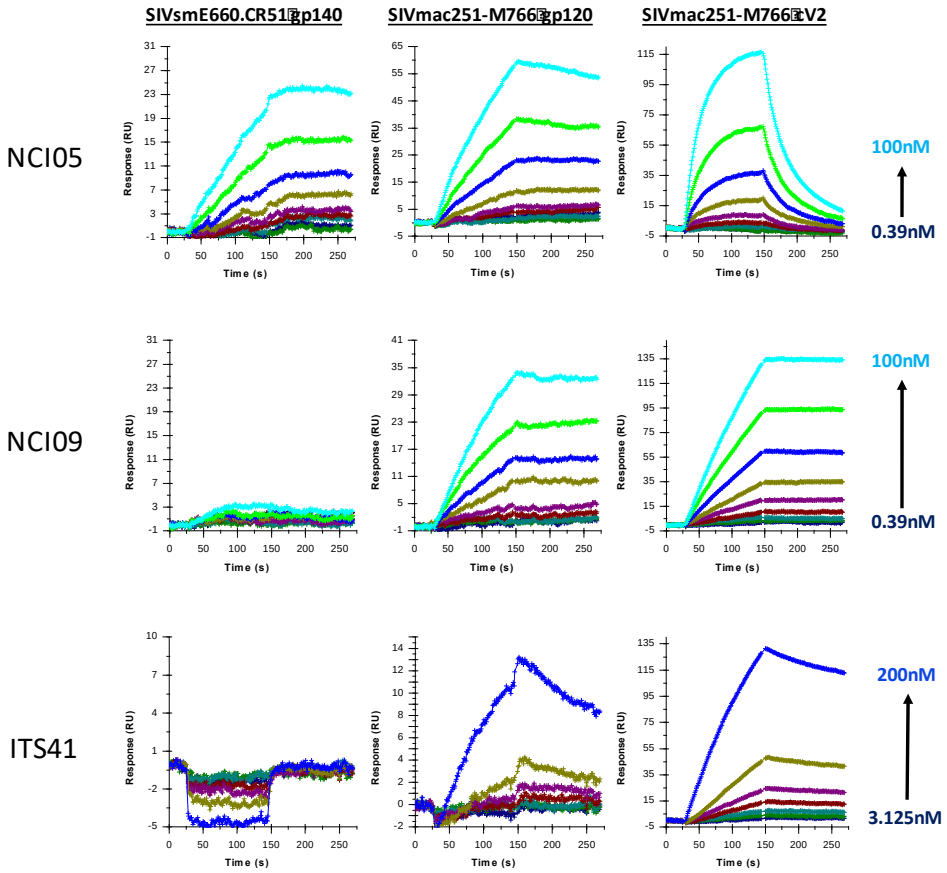

Figure 2. 8: Sensorgram of increasing concentrations of NCI mAbs or ITS41 Fab passed over surface-immobilised SIV antigens. NCI05 (top row), NCI09 (middle row) or ITS41 Fab (bottom row) were passed over SIVsmE660 gp140 antigen (left column), SIVmac251 gp120 (middle column) or SIVmac251 cV2 (right column) for 120 seconds, followed by a 120-second washout/dissociation phase. Mass of bound antibody or Fab expressed as response units (RU). Concentration of mAb or Fab tested is shown on the right of each row.

	ITS41		NCI05		NCI09	
	KA	KD	KA	KD	KA	KD
SIVmac251-M766 gp120	3.90E+04	2.57E-05	1.78E+08	5.60E-09	8.19E+09	1.22E-10
SIVsmE660.CR54 gp140	N/A	N/A	9.60E+10	1.04E-11	N/A	N/A
SIVmac251-M766 cV2	1.06E+08	9.46E-09	5.12E+06	1.97E-07	9.13E+11	1.10E-12

Table 2. 4: Table reporting the KA (1/M) and KD (M) values of ITS41 Fab, NCI05 mAb and NCI09 mAb. Values were calculated by surface plasmon resonance against a panel of three SIV SU antigen as in **Figure 2.8**.

However, these findings allowed for further characterisation of the epitope recognised by the anti-V2 NCI mAbs, and we were able to locate the epitope bound by NCI05 through competition surface plasmon resonance against immobilised SIVmac251-M766 cV2 (Figure **2.9**). The same test was carried out for NCI09 (**Figure 2.10**). Before being exposed to the immobilised antigen, aliquots of anti-V2 NCI mAbs were incubated with 15-mer overlapping peptides encompassing the V2 region of SIVmac239. The results obtained matched those obtained by ELISA on

overlapping peptides on NCI09, and were able to locate the region bound by NCI05 as overlapping that of NCI09.

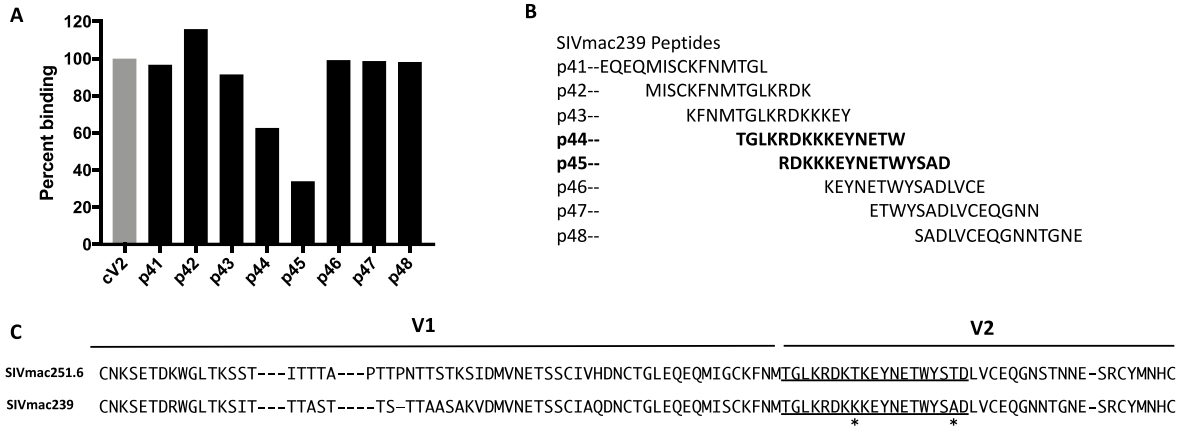

Figure 2. 9: Peptide mapping of mAb NCI05. A) Percentage of binding of mAb NCI05 to a cyclic V2 peptide derived from SIVmac251 M766 (grey column) in presence of competitor overlapping 15 a.a. linear peptides (p41-p48, black columns) derived from SIVmac239 gp120 and encompassing the V2 region. Inhibition is greatest with p45, with partial inhibition mediated by p44. B) Overlapping 15 a.a. linear SIVmac239 gp120 peptides encompassing the V2 region. Bold: peptides that induce the greatest inhibition of NCI05 binding to SIVmac251 cV2. C) Protein sequence alignment of SIVmac251.6 and SIVmac239 V1V2 domain. Stars indicate mutations between the two strains that are located within the putative binding site of NCI05 (underlined).

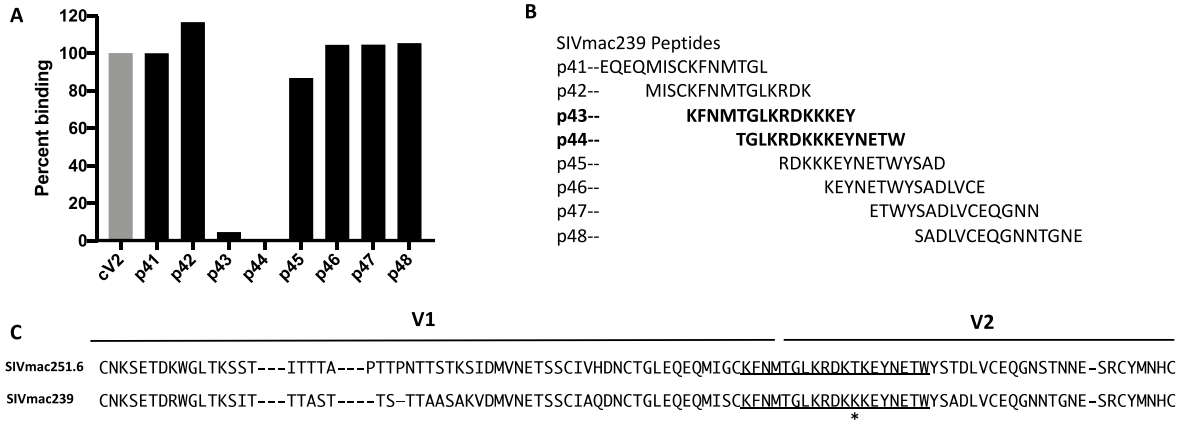

Figure 2. 10: Peptide mapping of mAb NCI09. A) Percentage of binding of mAb NCI09 to a cyclic V2 peptide derived from SIVmac251 M766 (grey column) in presence of competitor overlapping 15 a.a. linear peptides (p41-p48, black columns) derived from SIVmac239 gp120 and encompassing the V2 region. Inhibition is greatest with p43 and p44. B) Overlapping 15 a.a. linear SIVmac239 gp120 peptides encompassing the V2 region. Bold: peptides that induce the greatest inhibition of NCI09 binding to SIVmac251 cV2. C) Protein sequence alignment of SIVmac251.6 and SIVmac239 V1V2 domain. Star indicates the mutation between the two strains that is located within the putative binding site of NCI05 (underlined).

Crystal structure of NCI mAbs in complex with V2 constructs

To characterise more in detail the epitope targeted by NCI09 and NCI05, crystal structures of the Fabs in complex with peptide and scaffolded antigen, respectively, were produced. However, only NCI09 yielded crystals that could produce data of analysis-standard quality. A peptide of sequence N-KFTMTGLKRDKTKEYN-C did not display an organized secondary structure when in complex with NCI09 (**Figure 2.11**). In this peptide, the four N-terminal residues were not ordered in the structure. Almost all of the interactions were found to be limited to the HC, with a clear electrostatic interaction between the base of the CDRH3 and the peptide amino acids Arginine (R9) and Glutamic Acid (E14), as well as main hydrogen bond interactions with a Cysteine located in the CDHR3. Notably, we observed a glycosylation site on the CDRL1 of which the first glycan residues were visible.

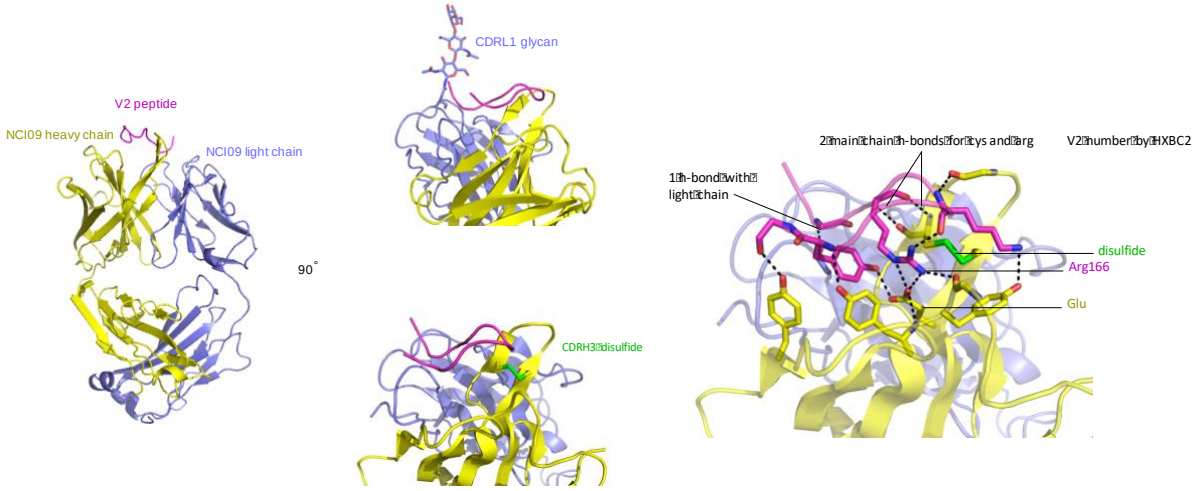

Figure 2. 11: Overall structure of NCI09 in complex with a SIVmac251 linear peptide. The peptide sequence (KFTMTGLKRDKTKEYN) is that of consensus SIVmac251, in complex wit Fab of antibody NCI09. The N-terminal 4 residues were not ordered in the structure. The NCI09 heavy and light chains are displayed as yellow and blue ribbons, respectively. The SIVmac251 peptide is displayed in purple.

ELISA competition assays between pairs of anti-V2 mAbs

Competition of binding experiments were carried out between pairs of anti-V2 mAbs to roughly inter-localise the position of the NCI and ITS epitopes in V2 (summarised in **Table 2.5**). Surprisingly, we found that competition assays were poorly informative as the inhibition of binding against other mAbs was unidirectional most of the time, that is most of the antibodies could inhibit or be inhibited by mAbs on which they exerted no effect. The traditional

A

Competitor mAb \ Probe mAb	ITS41	NCI05	NCI09	ITS09	ITS12
ITS41		*	*	*	NA
NCI05	*		*	*	*
NCI09	*	*		*	
ITS09	*	*	*		
ITS12	NA	*			

B

Competitor mAb \ Probe mAb	ITS41	NCI05	NCI09	ITS09	ITS12
ITS41		86	63	-1	NA
NCI05	6		24	-2	87
NCI09	13	85		-9	-1
ITS09	96	96	95		9
ITS12	NA	36	22	-7	

Table 2. 5: **A**) Matrix recapitulating the pattern of competition between of pairs of anti-V2 mAbs. Red boxes represent inhibition >50%, green boxes inhibition <50%, and stars asymmetric inhibition. Percentages of inhibition are shown in **B**) with colour codes as in **A**). Barred cells represent competition between same mAb tested both as competitor and probe in the same replicate. These combinations were included as positive control, always yielded >50% inhibition and were excluded from this table as irrelevant in the study of the structural dynamics of competition between closely- and far-located epitopes. Percent inhibition was calculated as a subtraction of the signal obtained at the highest concentration of competitor antibody subtracted to the background BSA control, divided by said background control and multiplied by 100. NA: Not Available. Because ITS41 and ITS12 are weak binders of SIVsmE660.CR54 gp140 and SIVmac251-M766 gp120, competition between these two mAbs could not be tested. Antigens tested for each antibody pair are reported in **Table 2.5**; graphs with the results of competition, including those of barred cells, are reported in **Figure 2.13**; Association/dissociation constants of mAbs ITS41, NCI05 and NCI09 against a panel of SIV SU antigens are reported in **Table 2.3**.

symmetric competition that is used to inter-locate overlapping antibody epitopes could not be observed, not even between antibodies NCI05 and NCI09, suggesting that these mAbs hit the same region from different angles. However, amongst the pairs of mAbs tested, we found two that gave particularly interesting results: ITS41, targeting the N-terminal region of V2, would disrupt binding of NCI05 and NCI09 without, however, being negatively affected by their pre-binding to the antigen (**Figure 2.12**). We hypothesise that, when pre-bound to the antigen, ITS41 induces conformational changes within V2 that inhibit binding of NCI09 and NCI05 to the antigen. However, these mAbs do not lead to a disruption of the V2 three-dimensional structure that can inhibit binding of ITS41. These observations point towards immunoglobulin-induced conformational change as a mechanism by which antibodies binding outside of the tripeptide are able to inhibit binding between V2 and $\alpha 4\beta 7$. The antigens tested for each pair of mAbs and relative binding curves are reported in **Table 2.7** and Figure **2.13**, respectively.

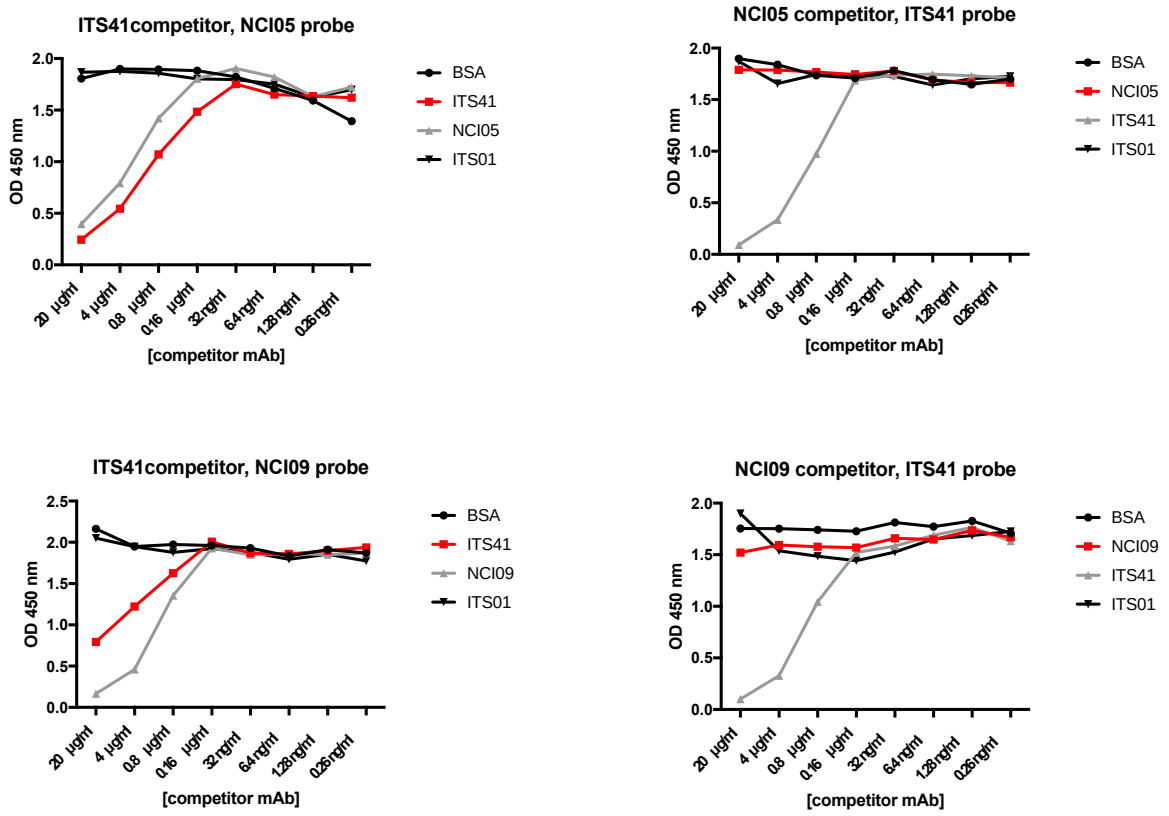

Figure 2. 12: Competition experiments between pairs of anti-V2 mAbs. Each NCI mAb has been tested both as competitor and as probe against ITS41. While ITS41 was able to prevent the binding of both NCI05 and NCI09 when pre-bound to SIVmac251-M766 gp120, the NCI mAbs were unable to affect the binding activity of ITS41. Test curves are represented in red. Negative control curves are represented in black, with ITS01 being a non-relevant anti-CD4 mAb. Positive control curves are in grey.

Competitor mAb \ Probe mAb	ITS41	NCI05	NCI09	ITS09.01	ITS12.01
ITS41					NA
NCI05					
NCI09					
ITS09.01					
ITS12.01	NA				

SIVmac251-M766 gp120

SIVsmE660.CR54 gp140

Table 2. 6: Matrix reporting the antigens tested for each mAb pair. Because ITS41 and ITS12 are weak binders of SIVsmE660.CR54 gp140 and SIVmac251-M766 gp120, competition between these two mAbs could not be tested.

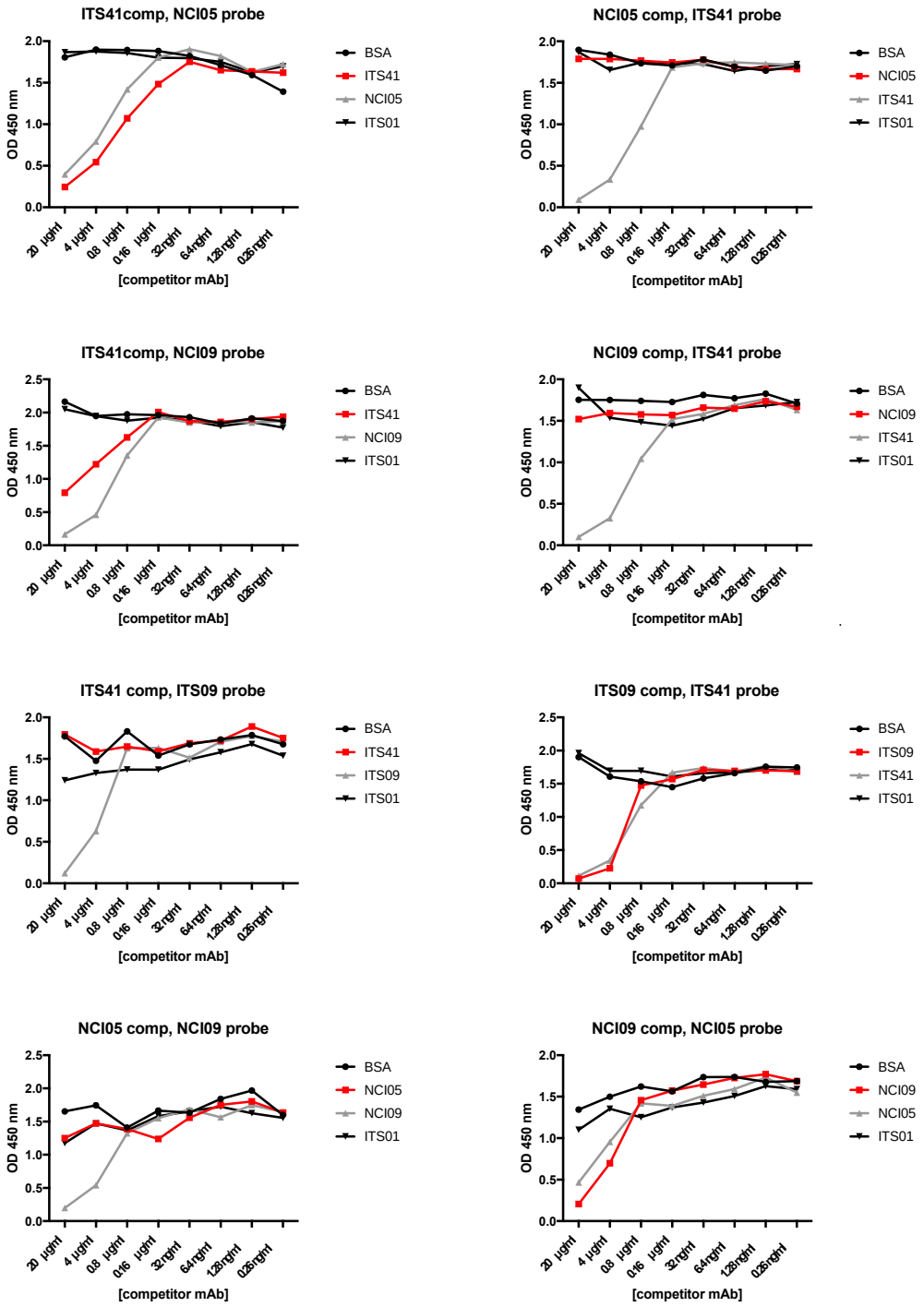

Figure 2. 13: (continues on next page): Graphs of binding competition between mAbs. In each experiment, BSA 1% or serial dilution of anti-CD4 bs ITS01 mAb were used as negative controls of competition (black), while unbiotinylated probe mAb was used as positive control of competition (red). Replicate plates were coated with the antigens reported in **Table 2.6**. Blocked plates were incubated with serial dilution of unbiotinylated competitor mAb at 37˚C for 10 minutes, then fixed concentration of biotinylated probe mAb were added to each well and incubated at 37˚C for 45 minutes. After incubation with streptavidin-HRP, plates were developed with TMB substrate and probe mAb binding data acquired at 450 nm. Comp: unbiotinylated competitor mAb; probe: biotinylated probe mAb, detected with HRP-conjugated Streptavidin.

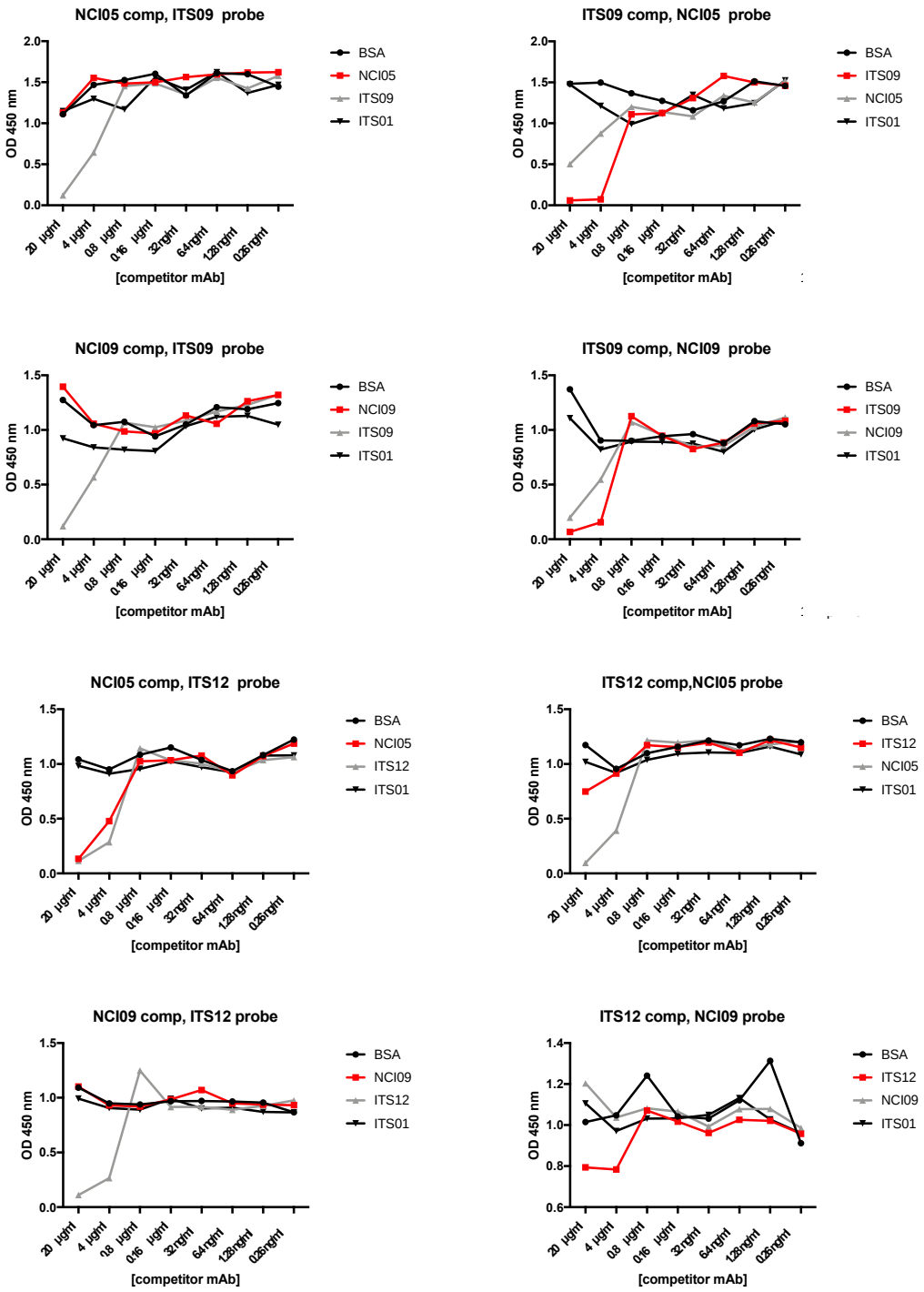

Figure 2.13 (continued from previous page): Graphs of binding competition between mAbs. In each experiment, BSA 1% or serial dilution of anti-CD4 bs ITS01 mAb were used as negative controls of competition (black), while unbiotinylated probe mAb was used as positive control of competition (red). Replicate plates were coated with the antigens reported in **Table 2.6**. Blocked plates were incubated with serial dilution of unbiotinylated competitor mAb at 37˚C for 10 minutes, then fixed concentration of biotinylated probe mAb were added to each well and incubated at 37˚C for 45 minutes. After incubation with streptavidin-HRP, plates were developed with TMB substrate and probe mAb binding data acquired at 450 nm. Comp: unbiotinylated competitor mAb; probe: biotinylated probe mAb, detected with HRP-conjugated Streptavidin.

mAb-mediated Inhibition of SIVgp120 binding to α4β7

The biologic mechanism by which anti-V2 antibodies elicited by vaccination might protect from HIV/SIV acquisition has not yet been explained at the molecular level.

The two V2-specific mAbs NCI05 and NCI09 were tested for their ability to disrupt binding of deglycosylated SIVmac251 gp120 to human α4β7 exposed on the surface of the human B cell line RPMI8866[360]. Interestingly, NCI09 was repeatedly found to exhibit the most potent blocking features of a panel of rhesus anti-V2 mAbs (**Figure 2.14**), while NCI05 was unable to prevent binding between the integrin and the deglycosylated viral antigen (data not shown). However, because NCI05 displays glycan-dependent features against SIVmac251 gp120 (**Figure 2.7**), absence of inhibition of binding to α4β7 is likely due to lack of antibody binding to gp120.

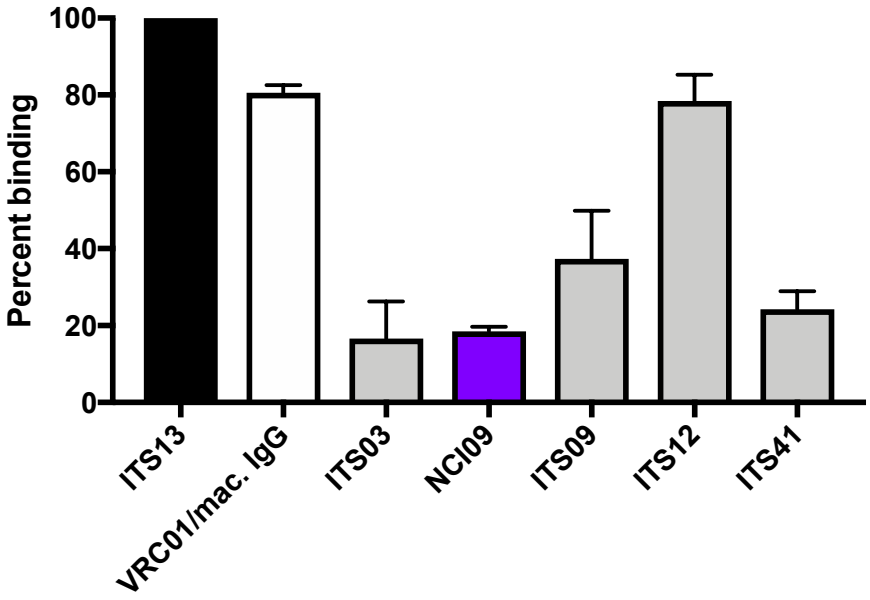

Figure 2. 14: Comparison of the inhibition of binding of SIVmac251-M766 gp120 to human α4β7 mediated by a panel of mAbs. Each mAb was tested at a concentration of 5 µg/ml. VRC01 or polyclonal IgG from naïve macaques (mac. IgG) were used as negative controls. Adapted from reference[360].

We then proceeded to test if the interference that we detected in ELISA binding assay experiments would show repercussion on the inhibition of α4β7 binding to V2 mediated by anti-V2 mAbs. Specifically, we tested if the binding activity of NCI09 would be negatively affected by having SIVmac251 gp120 pre-bound by ITS41 (**Figure 2.15**). However, because ITS41 itself is able to mediate binding inhibition to a maximum of 74% at 1.25 µg/ml (**Figure 2.15A**), we used a working concentration of probe NCI09 to yield 80% inhibition of binding, that is 1.25 µg/ml

(**Figure 2.15B**). Interestingly, we found that high concentrations of competitor ITS41 pre-bound to SIVmac251 gp120 were indeed able to lower the effect of inhibition of binding to α4β7 mediated by NCI09, with the potency of the NCI09-mediated inhibition restored as ITS41 was progressively diluted (**Figure 2.15C**).

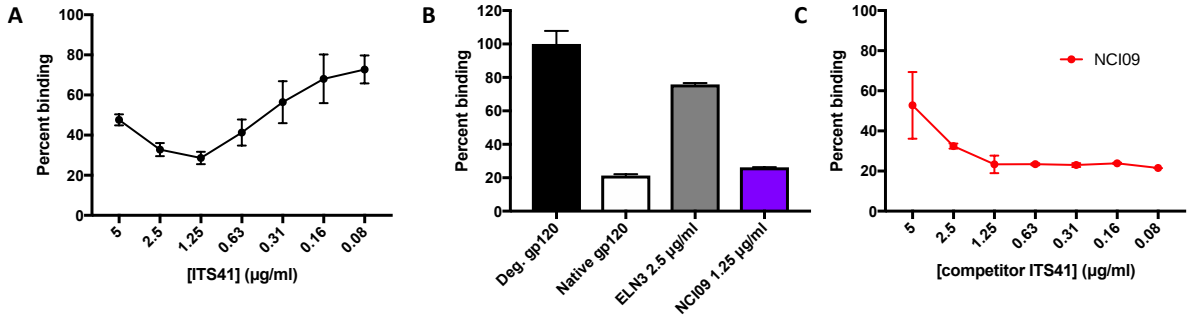

Figure 2. 15: NCI09-mediated inhibition of binding of α4β7 to deglycosylated SIVmac251 gp120 preincubated with serial dilutions of competitor ITS41. **A**) Titration of the ITS41-mediated inhibition of gp120 binding to α4β7 at the concentrations tested in the competition experiment with NCI09. **B**) Binding to human α4β7 of native SIVmac251 M766 gp120 and of deglycosylated SIVmac251 M766 gp120 alone, in presence of inhibitory molecule ELN3 at 2.5 µg/ml or NCI09 at 1.25 µg/ml. NCI09-mediated 81% inhibitory activity is calculated as a ratio of percent binding of native gp120 to α4β7 / percent binding of deglycosylated gp120 to α4β7 in presence of NCI09. **C**) NCI09 inhibition experiment in presence of pre-bound ITS41. When ITS41 is pre-bound to gp120 at high concentrations (left end of the graph) before 81% inhibitory concentration of NCI09 is added (1.25 µg/ml), only the inhibition mediated by ITS41 is detected (53% at 5 µg/ml of competitor). As the concentration of competitor is serially diluted, the inhibitory activity of NCI09 at 1.25 µg/ml is recovered

Discussion

In this study, we isolated and characterized anti-V1V2 mAbs obtained from P770, a vaccinated rhesus macaque protected from SIVmac251 infection. Two mAbs, both weak SIV neutralisers, displayed unique characteristics: (i) NCI05 showed previously undescribed strain-specific conformation-, glycan-dependent epitope specificity; (ii) NCI09, targeting a linear epitope encompassing the B and C strand of the V1V2 motif, was found to be the most potent inhibitor of human α4β7 binding to SIVmac251 gp120 as compared to an array of anti-V2 mAbs isolated from vaccinated, protected and vaccinated, infected animals. Interestingly, the region targeted by NCI09 is located distantly from DLV, the tripeptide considered as the putative binding site to integrin α4β7, thus leading to the conclusion that this mAb, when bound to V1V2, disrupts the conformation of the domain compromising the binding site of α4β7 to the viral envelope.

To better define the effect of NCI09 binding to the conformation of V1V2, we produced the crystal structure of the NCI09 Fab in complex with a V2 peptide. The V2 peptide was revealed

neither as an α-helix nor as a β-sheet, but rather locked into a loop conformation when bound by NCI09. Given that CH58 and CH59 both locked V2 peptides in an alpha-helical conformation were only weak inhibitors of V2 binding to α4β7[339], I postulated that a potent antibody inhibitor of α4β7 binding to V2 would need to maintain limited or extensive regions of the V1V2 devoid of organized secondary structure.

The concept that antibody binding to V2 may disrupt the conformation of the domain thus preventing the engagement of ligands directed to distant binding sites was corroborated by my findings on competition analyses with pairs of mAbs. I observed that mAbs to V2 were able to asymmetrically compete with the binding of antibodies directed against distant epitopes within the domain. The lack of a clear pattern of asymmetric inhibition between these mAbs implies that the conformational changes induced by antibody binding are more dependent on the properties of the antibody binding to the antigen, rather than the area of V2 targeted. However, our results showed that both NCI05 and NCI09, cloned from a protected animal with the latter being a potent inhibitor of α4β7 binding to V2, were unable to bind to V2 pre-bound by mAbs ITS41 isolated from an infected animal. In line with this finding, the potent inhibition of binding between α4β7 and V2 mediated by NCI09 was negatively affected by the presence of ITS41 pre-bound to the antigen. I therefore suggest that the elicitation of ITS41-like antibodies is to be avoided with vaccination, as these might reduce the beneficial effect of antibodies that inhibit binding of α4β7 to gp120 and thus decrease vaccine efficacy.

A viral escape mechanism by which antibodies would negatively affect the binding of antibodies to protective epitopes by binding to distant regions was initially proposed by Dulbecco *et al.* in 1956 on studies on Western Equine Encephalitis virus and poliomyelitis virus [268]. This mechanism, namely antibody interference, has since been investigated for SARS Coronavirus, Influenza Viruses and Hepatitis C Virus [269–272]. Antibody interference has been hypothesized to be exerted by two possible molecular mechanisms: (i) steric hindrance, i.e. the physical covering of the protective epitope by the Fc or Fab regions of the interfering antibody not directly interacting with the antigen or (ii) conformational changes, i.e. the induction of alterations in the three-dimensional structure of the antigen that are propagated to a distant epitope that can thus not be recognized by protective antibodies. While the existence of antibody interference in the HIV-

1 or SIV model has been proposed upon *in vitro* studies involving anti-HIV fusion glycoprotein gp41 mAbs [273], to our knowledge our findings are the first that identify this mechanism on viral envelope gp120.

To conclude, while the elicitation of anti-V2 antibodies with potent inhibition of $\alpha4\beta7$ binding is a desired goal of HIV/SIV vaccination, the structural plasticity of the V1V2 domain might act as a double-edge sword: antibodies targeting regions outside of the putative binding site of $\alpha4\beta7$ may still disrupt V2-mediated virus binding to the human integrin through the induction of conformational changes. However, interfering, non-protective antibodies may also prevent protective antibodies from blocking the engagement of $\alpha4\beta7$.

In summary, these findings may inform structural antigen design for a greater efficacy vaccine against HIV/SIV infection.

CHAPTER 3: ALVAC- but not NYVAC-based vaccination decreases the risk of SIVmac251 acquisition in macaques

Introduction

In addition to vaccine-induced antibody-mediated protection from infection, extensive data support the importance of cell-mediated immune responses in virus clearance or containment once infection has occurred[370–372]. This is in contrast with the results of RV144, where antibodies targeting the viral envelope glycoprotein gp120 have been the only immune correlate of risk of HIV acquisition[373]. However, in RV144 the recombinant canarypox ALVAC-HIV vCP1521 immunogen was administered in combination with the AIDSVAX B/E formulation, which consists in a combination of two monomeric HIV-1 gp120s from Clade B and AE formulated in alum. This composite regimen elicited both antibody- and cellular-mediated immune responses[286,374–376].

The attenuated ALVAC vector was derived by repeated passage of a canarypox virus in chicken embryo fibroblasts. This vector has demonstrated a high level of safety and tolerability in phase I clinical trials in infants [377,378] and in adults [379]. While ALVAC was included in RV144 to elicit cellular-mediated immune responses, only 19.7% of the volunteers enrolled demonstrated $CD8^+$ CTL responses as measured by IFN-γ ELISpot, a result that is consistent with the lack of control of viral replication in vaccinees that became infected[286,380]. Notably, most vaccinees developed Env-specific $CD4^+$ responses [286,380].

However, higher T-cell responses were detected in other studies where another poxviral vector, NYVAC, was tested[381]. NYVAC is a highly immunogenic, human-adapted poxviral vector that has been safely attenuated through the deletion of 18 genes encoding for viral proteins that affect both the virus host range and virulence. This vector has been tested in phase I/IIa clinical studies without demonstrating serious adverse events[381]. A summary of the features of these two poxviral vectors can be found in **Table 3.1**.

Vector	ALVAC	NYVAC
Family	*Poxviridae*	*Poxviridae*
Subfamily	Avipoxvirus	Orthopoxvirus
Origin	Canarypox virus plaque-purified clone	Copenhagen vaccine strain plaque-cloned isolate
Attenuation method	200 passages in chick embryo fibroblasts	Deletion of 18 Open Reading Frames implicated in pathogenicity and virulence

Table 3. 1: Summary of the taxonomic classification and features of poxviral vectors ALVAC and NYVAC, reviewed in detail in reference[382].

Both the poxviral vectors ALVAC and NYVAC have been extensively studied in preclinical settings on rhesus macaques. In this animal model, the efficacy of vaccine candidates is traditionally evaluated on the basis of two parameters: the delay of virus acquisition and the control of viral replication. For brevity, the results of studies of ALVAC or NYVAC immunisation of rhesus macaques against HIV, SIV or chimeric Simian-Human Immunodeficiency Virus (SHIV) are summarised in **Table 3.2**.

Here, we tested the hypothesis that more potent NYVAC-induced responses would improve the efficacy of an RV144 schedule. We tested in parallel the efficacy of recombinant NYVAC-SIV and recombinant ALVAC-SIV boosted with the native SIVmac251 gp120 formulated in alum in two groups of adult female rhesus macaques of Chinese origins. Following immunisation, the vaccinated and control animals were challenged weekly intravaginally with up to 12 repeated low doses of SIVmac251 to model the natural heterosexual exposure of females to HIV.

Although the NYVAC-SIV regimen displayed faster anti-Env antibody kinetics and higher anti-Env T cell responses as compared to the ALVAC-SIV immunisation, contrary to our hypothesis this regimen failed to demonstrate any degree of protection. In contrast, ALVAC-SIV immunisation protected with an estimated vaccine efficacy of 50% at each challenge. However, neither regimen demonstrated long-term control of viral replication.

Notably, while we failed to observe correlation between anti-V2 antibody responses and delayed viral acquisition, we found that higher levels of $\alpha4\beta7$+ plasmablasts associated with delayed SIV acquisition in the ALVAC-SIV group. Similarly, we found that total and classical monocyte lineages positively correlated with protection only in the ALVAC-SIV group, while strong nonclassical monocyte responses correlated with faster SIV acquisition in the ALVAC group. However, none

of these plasmablast, myeloid responses that correlated with delayed or increased SIV acquisition could be associated with vaccine-induced responses.

Prime	Boost	Challenge	Outcome	Ref.
ALVAC-HIV-2	HIV-2/gp120	High-dose HIV-2	Protection	383
ALVAC-SIVgpe + HIV-1/Env	HIV-1/gp120	High-dose SHIV	No protection Control of CD4 T cell loss	306
ALVAC-SIVgpe	SIV/gp120	High-dose SIVmac251	No protection Transient control CD4 cells loss	306
ALVAC-SIVgpe		RLD mac251	10/16 neonatal macaques protected	307
DNA-SIVgpe	SIV/gp120 + ALVAC-SIVgpe	High-dose SIVmac251	No protection	384
		RLD SIVmac251	3/12 macaques protected	
ALVAC-SIVgpe	SIVmac251 gp120 SIVsmE543 gp120 ALVAC-SIVgpe	RLD IR SIVmac251	44% efficacy each challenge	362
NYVAC-HIV-2		IV HIV-2	Protection	385
NYVAC-HIV-2	HIV-2 boost	IV HIV-2	Improved protection	386,387
NYVAC-SIVgpe	IL-2 IL-12	IV, IR SIVmac251	One third of animals protected 6 months after immunisation	388
NYVAC-SIVgpe + DNA-SIV		IR SIVmac251	Protection Lower viremia levels correlate with anti-Gag specific responses	389,390

Table 3. 2: Summary of preclinical studies evaluating poxviral vector-based vaccination regimens in rhesus macaques. Red and blue backgrounds represent ALVAC- and NYVAC-based vaccination regimens, respectively. gpe: Gag-Pol-Env genes expressed by the vector. IV: intravenous; RLD: repeated low-dose; IR: intrarectal; Ref.: reference.

Materials and Methods

Animals, vaccines and SIVmac251 challenge

The vaccination and challenge phases were designed and supervised by Shari Gordon, Animal Models and Retroviral Vaccines Section, National Cancer Institute, NIH, Bethesda, Maryland, USA. All the animals included in this study were female rhesus macaques (*Macaca mulatta*) of Chinese origin, obtained from the Washington National Primate Research Center (Seattle, WA). The care

and use of the animals were in compliance with all relevant institutional (NIH) guidelines. A total of 65 female Rhesus macaques of Chinese origins were randomized in 5 groups (referred in the text as ALVAC-SIV, NYVAC-SIV, ALVAC-control, NYVAC-control or naïve) according to the major histocompatibility status. The animals in the ALVAC- or NYVAC-SIV/groups were immunized at weeks 0, 4, 12 and 24 with intramuscular inoculations at 10^8 PFU either of ALVAC (vCP180) or NYVAC (VP1071) expressing the proteins *env-gag-pol* of the attenuated SIVmac142 clone of SIVmac251. At weeks 12 and 24, the animals from these groups received a bivalent monomeric alum-formulated gp120 protein boost in the opposite deltoid of the vector immunization, containing 200 mg of the native form of SIVmac251/*gp120TM* (Sanofi Pasteur) (referred in the chapter as gp120).

The control groups included 10 animals each, which received either parental ALVAC or NYVAC vectors and alum. 5 naïve control animals were included directly in the challenge phase without receiving previous immunization.

Animals were challenged 4 weeks following the last immunization (week 28), with SIVmac251 at 120 $TCID_{50}$ for each challenge. Animals that tested negative for SIV-RNA in plasma were re-challenged with up to a maximum of 12 weekly administrations.

The animals shared the same site of origin, but given the large number of macaques, the study was split in two parts. Animals from part 1 (n= 24; 8 ALVAC-SIV; 8 NYVAC-SIV; 4 ALVAC-control; 4 NYVAC-control) were housed, immunized and challenged at Washington National Primate Research Center (WaNPRC, Seattle, WA); and animals from part 2 (n= 41; 12 ALVAC-SIV; 12 NYVAC-SIV; 6 ALVAC-control; 6 NYVAC-control; 5 naïve) were housed, immunized and challenged at Advanced Bioscience Laboratories (ABL, Inc., Rockville, MD).

Measurement of viral RNA and DNA

Viral RNA was measured by contractors at the Washington National Primate Research Center, Seattle, Washington, USA and by Ranajit Pal, Advanced Bioscience Laboratories, Frederick, Maryland, USA. Mucosal viral DNA was measured by Hye Chung from Advanced Bioscience Laboratories.

Plasma SIVmac251 RNA levels were quantified by nucleic acid sequence-based amplification, as described in reference [391]. SIV/DNA levels in mucosal biopsies from week 2 post-infection were quantified by real-time qPCR with sensitivity set at ten copies x 10^6 cells, as previously described[392].

IFN-γ ELISpot

IFN-γ ELISpot was carried out by Sampa Santra, Center for Virology and Vaccine Research, Beth Israel Deaconess Medical Center, Harvard Medical School, Boston, Massachusetts, USA.

IFN-γ production by $CD4^+$ T cells or $CD8^+$ T cells was assessed through ELISpot assays, as a reaction toward the optimal CTL epitope peptide p18[393] or a pool of 47, 15 aa-long overlapping HIV-1 IIIB Env gp120 peptides (Centralized Facility for AIDS Reagents, Potters Bar, U.K.). 96-well multiscreen plates (Millipore, Bedford, MA) were coated overnight with 10 µg/ml rat anti-mouse IFN-γ (BD PharMingen, San Diego, CA) in PBS (100 µl/well) then washed with 0.25% Tween 20 endotoxin-free Dulbecco's PBS (Life Technologies, Gaithersburg, MD). The reaction was blocked for 2 hours at 37°C with PBS containing 5% FBS. After washing the plates three times with 0.25% Tween 20 Dulbecco's PBS, they were rinsed with 10% FBS-RPMI 1640, and incubated in triplicate with 5 × 10^5 PBMCs/well in a 100-µl reaction volume with peptide at a concentration of 8 µg/ml. After an 18-hour incubation, Dulbecco's PBS containing 0.25% Tween 20 was used to wash the plates five times, and distilled water once. After a 16-hour incubation with 75 µl/well 5 µg/ml biotinylated rat anti-mouse IFN-γ, the plates were washed six times with Coulter wash (Coulter, Miami, FL), and incubated with a 1/500 dilution of streptavidin-AP (Southern Biotechnology Associates, Birmingham, AL) for 2.5 hours. Later, the plates were washed five times with Coulter wash and once with PBS, then developed with nitro blue tetrazolium/5-bromo-4-chloro-3-indolyl phosphate chromogen (Pierce, Rockford, IL) and stopped by washing with tap water. Last, the plates were air-dried and read using an ELISPOT reader (Hitech Instruments, Edgement, PA).

IgG binding antibody assay

IgG binding antibody assays were measured by contractors at Advanced Bioscience Laboratories, Frederick, Maryland, USA. Quantitation of anti-gp120 mucosal responses was performed by

Georgia Tomaras, Duke Human Vaccine Institute, Duke University School of Medicine, Durham, North Carolina, USA. Anti-cV2 responses were evaluated by Hung and Peachman, Antigens and Immunology Section, U.S. Military HIV Research Program, Silver Spring, Maryland, USA.

The total macaque IgG were measured by macaque IgG ELISA; custom SIV bAb multiplex assay (SIV-BAMA) was used to quantify SIV Env-specific IgG antibodies in serum and mucosal secretions as previously described [316,394,395]. For mucosal samples, specific activity was calculated as a ratio of MFI (in the linear range of the standard curve)/µg/ml total macaque IgG, measured by macaque IgG ELISA to normalise the data to the amount of recovered antibody per sample. Rectal swab samples in solution were spun, filtered and concentrated to approximately half of the starting volume, then examined for blood contamination and measured for semi-quantitative evaluation of haemoglobin. Purified IgG (DBM5) from a SIV-infected macaque (kindly provided by M. Roederer, VRC, NIH) was used as the positive control to extrapolate the concentration of SIV antibody. Levy Jennings Plot was used to track positive controls for each antigen. Specific activity was calculated from the total macaque IgG levels and the SIV specific concentrations. The quantitation of antibodies against native V1V2 epitopes was performed through binding assays against native SIV V1V2 antigens expressed as gp70-fusion proteins related to the CaseA2 antigen used in the RV144 correlate study (provided by A. Pinter). These synthetic proteins contain the glycosylated, disulphide-bonded V1/V2 regions of SIVmac239, SIVmac251 and SIVsmE660 (corresponding to AA 120-204 of HXB2 Env), linked to the residue 263 of the SU (gp70) protein of Friend Murine Leukaemia Virus (Fr-MuLV).

To detect for binding to cV2, ELISA plates were coated overnight with 100 ng/well of streptavidin (Sigma) at 4˚C. Contents were then dumped and 2.8 ng of biotinylated cV2 in bicarbonate buffer were added to each well and incubated for 1h at 37˚C. Serial dilutions of mucosal secretions were then added to each well and incubated for 1h at 37˚C. Plates were finally washed and 40 µl of anti-monkey IgG1 linked to horseradish peroxidase (clone 7H11) diluted 1:5,000 were dispensed to each well and incubated for 1h at 37˚C. After washing, 40µl of ELISA ultra TBM substrate (Thermo Fisher) were added to each well and incubated at room temperature for 10 minutes. 1M sulfuric acid was used to stop the reaction and the results were read at a VICOT-3 (Perkin Elmer) at 450 nm.

IgG linear epitope mapping in serum

Serum IgG ELISA mapping was carried out by Irene Kalisz, Advanced Bioscience Laboratories, Frederick, Maryland, USA.

1:20-diluted sera from the first week after the last immunization were added to ELISA plates coated with overlapping peptides encompassing the entire SIV_{K6W} gp120 amino acid sequence [316]. Linear peptide mapping of serum was done by microarray (PepStar), as previously described [396]. Briefly, JPT Peptide Technologies GmbH (Germany) produced array slides designed by Dr. B. Korber (Los Alamos National Laboratory) by printing onto Epoxy glass slides (PolyAn GmbH, Germany) a library containing overlapping peptides (15-mers overlapping by 12) covering full-length gp160 of SIVmac239 and SIVsmE660. One printing area of each quad-slide contained three identical sub-arrays, each containing the full peptide library. After hybridization to the slides using a Tecan HS4000 Hybridization Workstation, the samples were incubated with DyLight 649-conjugated goat anti-rabbit IgG (Jackson ImmunoResearch, PA). Later, fluorescence intensity was measured with a GenePix 4300 scanner (Molecular Devices) and analyzed with the software GenePix. The background value was subtracted to the binding intensity of the post-immunization serum to each peptide, defined as the median signal of the pre-bleed serum for that peptide plus 3 times the standard error among the 3 sub-arrays on slide. The total IgG concentration measured was used to normalize the values for each peptide as reported above (Unit = signal intensity/µg/ml total IgG).

Plasmablast staining in peripheral blood

Plasmablast staining was carried out by the author in collaboration with Luca Schifanella, Animal Models and Retroviral Vaccines Section, National Cancer Institute, NIH, Bethesda, Maryland, USA.

We measured the frequency of plasmablasts in the peripheral blood of twenty macaques vaccinated with ALVAC-SIV/gp120 and twenty macaques vaccinated with NYVAC-SIV/gp120 before vaccination and at week 25, i.e. 7 days after the last immunization. To stain the cells, the following markers were labelled: CD3 (SP34-2), CD14 (M5E2), CD16 (3G8), CD56 (B159) all in ALEXAFluor700- (BD Biosciences); CD19- PE-Cy5 (J3-119; Beckman Coulter), CD20- Qdot650 (2H7, eBiosciences), CD38- FITC (Clone AT-1, StemCell), CD39-BV421 (MOCP-21, BioLegend), Ki67- PE

(B56, BD Biosciences), and CD183-PE-CF594 (CXCR3; 1C6 BD, Biosciences); Dr. A. A. Ansari kindly provided the anti-α4β7 (Act-1) reagent (cat#11718) through the NIH AIDS (NIAD) Reagent Program, Division of AIDS. Cytofix/Cytoperm (BD Biosciences) which was used to allow intracellular staining. LSR II (BD Biosciences) was used to evaluate acquisition and the resulting data were analyzed with FlowJo (TreeStar). Gating of $^{-}$(CD3^{-}/CD14^{-}/CD16^{-}/ CD56^{-})/ CD20^{+}/CD21^{-}/ Ki67^{+}/ CD38^{+}/CD39^{+} was used to identify plasmablasts [397]. The frequency of the expression of CXCR3 or α4β7 on the plasmablasts was calculated.

NK staining in vaginal mucosa

NK staining was carried out by Namal Liyanage, Animal Models and Retroviral Vaccines Section, National Cancer Institute, NIH, Bethesda, Maryland, USA.

The isolation of mononuclear cells from the tissues was carried out as previously described [398,399]. 2,106 cells were used for the phenotypic characterization, and flow cytometry staining was performed for cell surfaces and intracellular molecules through standard protocols. After stimulation with phorbol myristate acetate (50 ng/mL) and ionomycin (1 μg/mL), NK cell functions were analysed using 3,106 cells. Alternatively, we added 721.221 cells directly to each tube at an effector-target ratio of 5:1. 721.221 is a MHC-devoid, MICA/MICB-negative human cell line. In each tube, we added Anti-CD107a (eBioH4A3) at a concentration of 20 μL/mL, and Golgi PlugTM (Brefeldin A) and Golgi StopTM (Monensin) at 6 μg/mL. Samples were then cultured at 37°C in 5% CO2 for 12h. Negative controls were represented by unstimulated (medium alone) samples. After incubation, cells were washed and stained for surface markers. Then, Cytofix/Cytoperm (BD Biosciences) was used to allow intracellular staining. For the staining, we used the following anti-human fluorochrome-conjugated mAbs, which are described to cross-react with rhesus macaques antigens: V450 anti-IFN-γ (B27), PE-Cy7 anti-CD56 (NCAM 16.2), Alexa Fluor 700 anti-CD3 (SP34-2), Allophycocyanin-Cy7 anti CD3 (SP34-2), PerCP Cy5.5 anti-CCR6, V450 anti-Caspase 3 (C92-605), Alexa Fluor 700 anti- Ki67 (B56) (all from BD Biosciences, San Jose, CA); PE-Cy5 anti- CD107a (eBioH4A3), Alexa 488 anti-IL17 (eBio64DEC17), eFluor 605NC anti-CD20 (2H7), and eFluor 605NC anti-CD8a (RPA-T8) (all from eBioscience, San Diego, CA); PE anti-NKG2A (Z199), ECD anti- CD16 (3G8), PE-Cy5 anti-NKp46 (BAB281)(Beckman Coulter, Fullerton, CA), Fluorescein anti CCR5 (CTC5) (R and D) and allophyco- cyanin anti-NKp44 (P44-8) and

PerCP/Cy5.5 anti-TNF-α (Mab11) (BioLegend, San Diego, CA). Dead cells were excluded through yellow and aqua LIVE/DEAD viability dyes (Invitrogen). At least 500,000 singlet events (PBMCs) or 50,000 CD3 singlet events (mucosal mononuclear cells) were acquired on a LSR II (BD Biosciences). FlowJo Software (TreeStar) was used to analyse the data.

Monocytes staining in blood

Monocyte staining was carried out by Dallas Brown, Animal Models and Retroviral Vaccines Section, National Cancer Institute, NIH, Bethesda, Maryland, USA.

To allow identification of monocytic myeloid cells, PBMCs (5–10 × 10^6 cells) were stained with PE-Cy7 anti-CD20 (2H7; 560735, BD Biosciences), PE-Cy7 anti-CD3 (SP34-2; 563916, BD Biosciences), APC anti-CD14 (M5E2; 561390, BD Biosciences), BV786 anti-NHP-CD45 (D058-1283; 563861, BD Biosciences), HLA-DR-APC-Cy7 (L243; 307618, BioLegend), BV421 anti-CD192 (CCR2) (48607; 564067, BD Biosciences), FITC anti-CD16 (3G8; 555406, BD Biosciences) and PE-CF594 anti-CD184 (CXCR4) (12G5; 562389, BD Biosciences), as well as Aqua LIVE/DEAD kit (L34966, Invitrogen) to dismiss dead cells. $CD45^+Lin^-$ (CD3 and CD20) was considered as a signature of myeloid cell populations. Monocyte populations were further recognised and sub-categorised according to the expression of CD14 and CD16, where: (i) classical monocytes were identified as $Lin^-CD45^+CD14^+CD16^-HLA\text{-}DR^+$, intermediate as $Lin^-CD45^+CD14^+CD16^+HLA\text{-}DR^+$ and non-classical as $Lin^-CD45^+CD14^-CD16^+HLA\text{-}DR^+$. Acquisition was then done on an LSRII (BD Biosciences), and marker expression was examined in real-time using the software FACSDiva (BD Biosciences). Data were analysed more in detail with FlowJo version 10.1 (Treestar, Inc.).

$CD4^+$ T cell staining in blood

T cell staining was carried out by Monica Vaccari, Animal Models and Retroviral Vaccines Section, National Cancer Institute, NIH, Bethesda, Maryland, USA.

Cells were stained as described elsewhere [362]. Briefly, blood $CD4^+$ T cells from part two only, due to limited availability of samples, were analysed from time point week 26. PBMCs were stained with PerCPCy5.5 anti-CD4 (L200; cat. #552838), AlexaFluor 700 anti-CD3 (SP34-2, cat. #557917), and BV650 anti-CCR5 (3A9), PeCy5 anti-CD95 (DX2, #559773; BD Biosciences, San Jose, CA), PE-eFluor 610 anti-CD185 (CXCR5; MU5UBEE, #61-9185-42; eBiocence, FITC anti-Ki67), and CD-38-

PE and APC anti-α4β7, provided by the NIH Nonhuman Primate Reagent Resource (R24 OD010976; NIAID contract HHSN272201300031C). Gating was performed on live $CD3^+CD4^+$ cells and on vaccine induced $Ki67^+$ cells. The CXCR5 was used for circulating Tfh. FACSDiva (BD Biosciences) and FlowJo Software (TreeStar) were used to examine marker expression in real-time and to analyse the final data, respectively.

Statistical analysis

Statistical analyses were carried out or reviewed by David Venzon, National Cancer Institute, NIH, Bethesda, Maryland, USA.

Continuous factors between the two groups were compared through the Mann-Whitney-Wilcoxon test. The Spearman rank correlation was used to perform correlation analyses, with the calculation of exact permutation p values. The LogRank test of the discrete-time proportional hazards model allowed the definition of the number of the challenges before acquisition of infection. The changes in plasmablasts levels from pre- to post-vaccination were evaluated through the Wilcoxon signed rank test. The Kruskal-Wallis test was used for multiple comparisons where specified in figure legends.

Scientist	Contribution
Giacomo Gorini	Study management from second part onward, sample processing, distribution of samples to collaborators, data analysis, graph editing, coordination of collaborations, plasmablasts staining and data collection.
Shari Gordon	Study design and management up to first part included, sample processing, distribution of samples to collaborators.
Washington National Primate Research Center (Contractors)	Measurement of viral RNA blood levels.
Ranajit Pal	Measurement of viral RNA blood levels.
Hye Chung	Measurement of viral DNA mucosal levels.
Sampa Santra	IFN-γ ELISpot.
Advanced Bioscience Laboratories (Contractors)	IgG binding antibody assays.
Georgia Tomaras	Quantitation of anti-gp120 mucosal responses.
Irene Kalisz	Serum IgG ELISA mapping.
Luca Schifanella	Plasmablast staining, collection and elaboration of plasmablast-related data.
Namal Liyanage	NK cell staining, collection and elaboration of NK cell-related data.
Dallas Brown	Monocyte staining, collection and elaboration of monocyte-related data.
Monica Vaccari	T cell staining, collection and elaboration of T cell-related data.
David Venzon	Validation of statistical analyses.

Table 3. 3: List of collaborators that directly contributed to the experiments summarised in this chapter.

Results

ALVAC- but not NYVAC-based vaccination reduced the risk of SIVmac251 acquisition

Our study was not powered to compare the relative efficacy of the ALVAC- or NYVAC-based vaccines to each other but rather to compare each platform to the control groups. Forty female rhesus macaques characterized for their major histocompatibility complex (MHC)-I alleles, age and weight were equally distributed into two vaccination groups (**Table 3.4**). The animals were immunized at week 0 and 4 with either ALVAC-SIV or NYVAC-SIV and boosted at week 12 and 24 with the corresponding viral vector and the monomeric SIVmac251 gp120 formulated in alum

(**Figure 3.1**). In addition, 25 macaques were used as control groups: two groups of 10 macaques each were immunised with sham viral vectors and adjuvant only, while 5 animals were left naïve. The challenge was performed weekly for up to 12 intravaginal low doses of the same stock of SIVmac251, starting at 4 weeks following the last immunization.

Group	Facility		Total
	Part 1	Part 2	
ALVAC-SIV/gp120	7*	11*	18
NYVAC-SIV/gp120	8	12	20
ALVAC-control	4	6	10
NYVAC-control	3*	6	9
Naïve	/	5	5
Total	22	40	**62**

Table 3. 4: Distribution of the animals into the vaccination groups. Of the 65 rhesus macaques that were sorted into the groups, 62 underwent the challenge phase. *Groups in which macaques were sacrificed before challenge for unrelated causes.

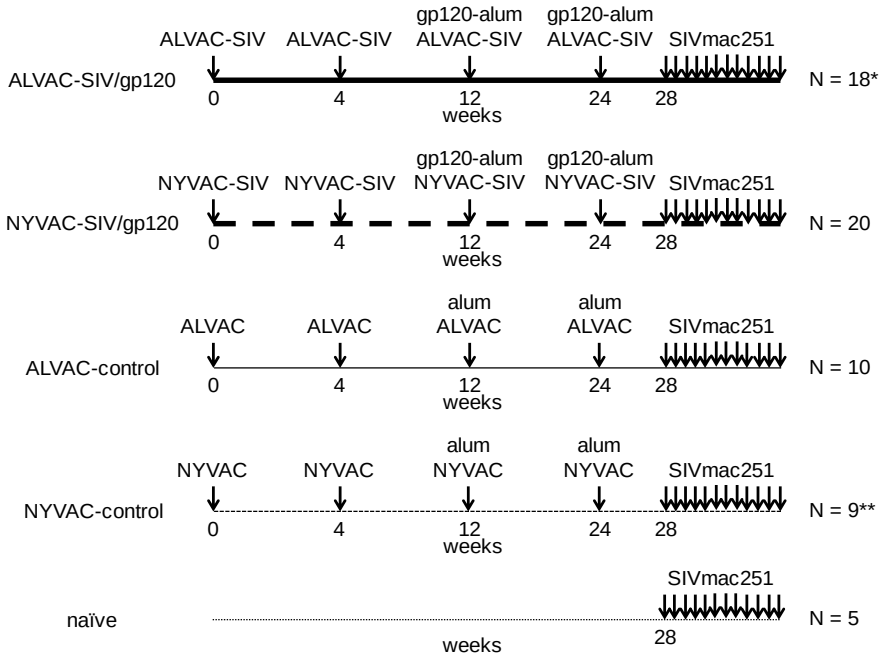

Figure 3. 1: Study design. Animals were immunized with either ALVAC (vCP180) or NYVAC (VP1071) inducing the expression of *gag-pro-env* of the attenuated SIVmac142 clone of SIVmac251 and boosted with the native form of SIVmac251/gp120TM (referred in the text as gp120) adjuvanted in alum (200 mg). *of the 20 animals that were included in the ALVAC-group, 2 died before the challenge phase for vaccine-unrelated reasons. ** of the 10 animals that were included in the NYVAC mock group, 1 died before the challenge phase for unrelated reasons.

Because of the large number of animals included (n=65), the study was divided in two parts and carried out in different facilities at different times (Washington University Primate Research Center for Part 1, and Advanced Bioscience Laboratories, Inc. for Part 2, **Table 3.4**). It was planned prior to study initiation that in case no difference in the rate of SIVmac251 acquisition was observed in the sham and naive controls, the data from the animals in all control groups could be pooled and compared with the vaccinated groups. As the infection rates in the naïve and sham NYVAC and ALVAC control groups did not differ significantly (**Figure 3.2**), the infection rates of the animals in the ALVAC-SIV group were compared to the infection rates of the control groups (ALVAC-control, NYVAC-control and naïve from both parts of the study), with an estimated vaccine efficacy of 50% at each challenge (Log-rank test: p=0.0471; **Figure 3.3A**). In contrast, NYVAC-SIV vaccination failed to protect animals (Log-rank test: p=0.2062; **Figure 3.3B**).

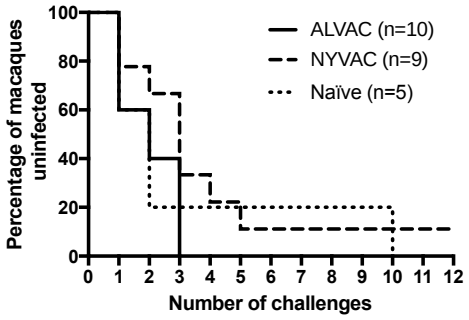

Figure 3. 2: Acquisition of SIVmac251 in the control groups from each part of the study. Naïve animals were present only in the second part. The null hypothesis of equal survival distributions in the five control groups is not rejected by the Log Rank test, allowing for the combination of the animals into one control group.

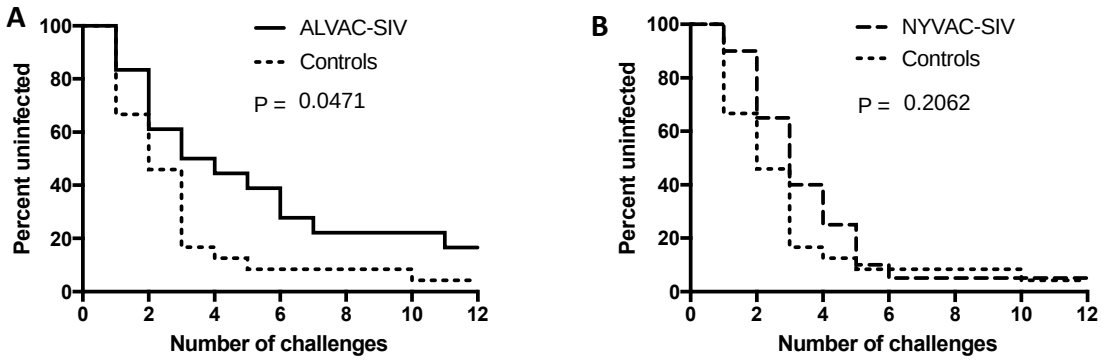

Figure 3. 3: Acquisition curves of SIVmac251 administered intravaginally in the **A**) ALVAC-vaccinated and **B**) NYVAC-vaccinated groups, as compared to the pooled control groups. P values calculated with LogRank test.

The animals that became infected in both vaccine groups did not differ from the controls in the level of plasma virus (**Figure 3.4A**) except for the NYVAC-SIV group at two weeks from infection (P = 0.0035; **Figure 3.4B**). However, this containment of plasma viral levels was lost thereafter (**Figure 3.4C**).

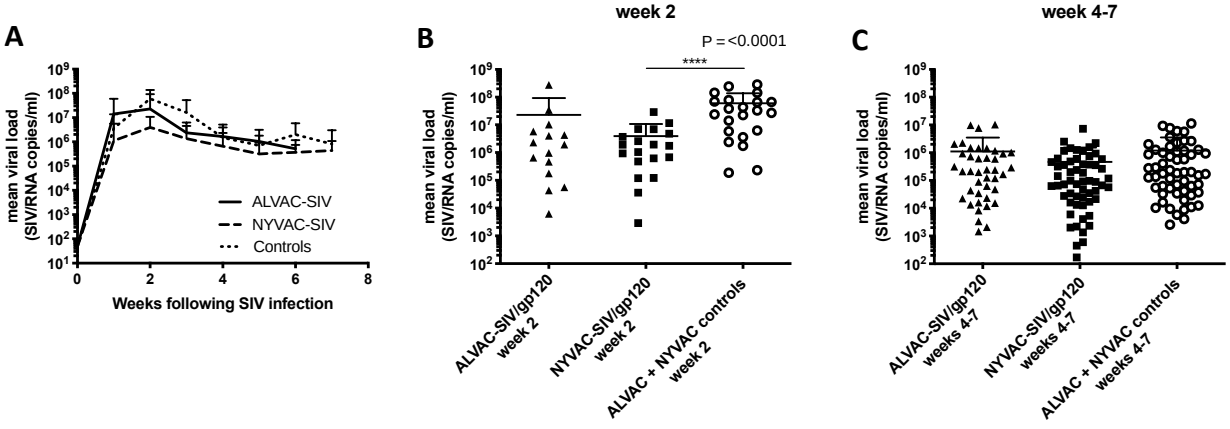

Figure 3. 4: Mean SIV viral loads of infected macaques. **A**) Logarithmic mean + s.d. of SIV/RNA levels in the plasma of the infected animals in the three animal groups (ALVAC-SIV, NYVAC-SIV and pooled controls). (**B, C**) Logarithmic mean ± s.d. of SIV/RNA levels in the plasma of infected animals in the **B**) acute and **C**) chronic phase of infection. Data in **B** and **C** analysed Mann-Whitney test. Only the P value of significant differences is shown.

To determine whether vaccination affected virus levels in mucosal tissues we quantified the SIV DNA levels in the vaginal and rectal biopsies of the infected animals at 2 weeks post-infection, but we observed no significant differences in the ALVAC-SIV- or NYVAC-SIV-vaccinated animals and the control group (**Figure 3.5A**, **B**).

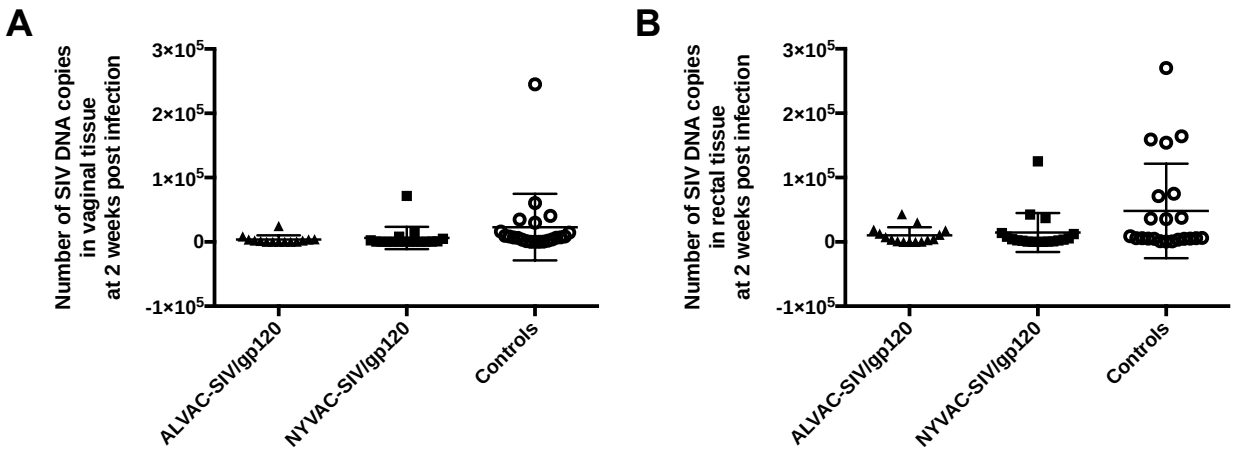

Figure 3. 5: SIV/DNA copy numbers in the **A**) vaginal and **B**) rectal mucosa of the infected animals amongst the vaccinated and control groups at week 2 post infection (horizontal lines: median ± s.d.). Mann-Whitney test revealed no statistically significant differences between control and treated groups.

Adaptive responses induced by the ALVAC- and NYVAC-SIV vaccines that correlates with SIVmac251 acquisition

Vaccine-induced $CD4^+$ lymphoproliferation was among the strongest vaccine-induced responses detected in the patients enrolled in the RV144 trial, and the intensity of $CD4^+$T-cell responses was a secondary correlate of vaccine protection [382]. The NYVAC-SIV vaccine regimen induced higher responses to Env and Gag as measured by IFN-γ ELISpot (**Figure 3.6A** and **6B**), but following the last immunization only the Env-specific response was significantly higher in the NYVAC–SIV than the ALVAC-SIV group (P = 0.012, **Figure 3.6C**).

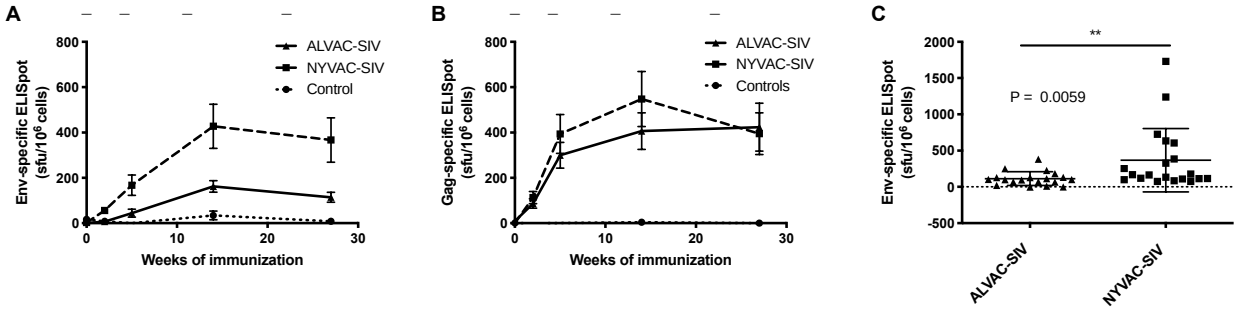

Figure 3. 6: Vaccine-induced T cell responses as measured by IFN-γ ELISpot. (**A**, **B**) IFN-γ-secreting cells (mean ± SEM) measured by ELISpot in response to SIV **A**) Env or **B**) Gag. Arrows represent immunization time points. **C**) Dot plot of the Env-specific ELISpot responses at week 27 (3 weeks after the last immunisation)(mean ± s.d.). Statistical analysis on data in **C** was performed with Mann-Whitney test.

In regard to the vaccine-induced humoral immune responses, the kinetic of antibody production against SIVmac251 gp120 was faster in the NYVAC-SIV group and before the administration of gp120/alum serum titres above 10^3, but by the end of the immunisation regimens, gp120-binding antibody titres in the two groups reached equivalent levels (**Figure 3.7**).

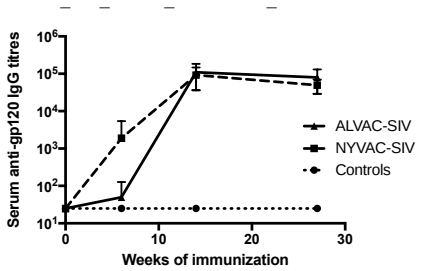

Figure 3. 7: Vaccine-induced serum IgG responses. Logarithmic mean + s.d. of SIVmac251 gp120-specific IgG titres in the two vaccination and one control groups. Arrows represent immunisation time points.

Both vaccination approaches induced similar patterns of recognition of gp120-overlapping linear peptides, including the V1 and V2 regions (**Figure 3.8**).

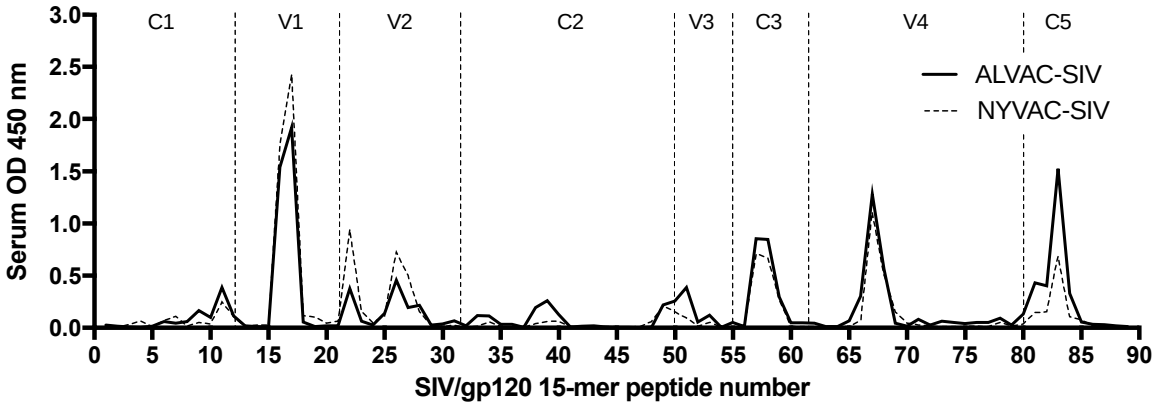

Figure 3. 8: Average serum IgG binding at week 25 to 89 overlapping peptides that span gp120 in the two vaccination groups. 1:20 diluted sera from the first week after the last immunisation were added to ELISA plates coated with 15-mer overlapping peptides encompassing the entire SIV_{K6W} SU amino acid sequence. Samples were incubated with secondary antibody and absorbance at 450 nm was measured, with subtraction of background value, defined as the median signal of the pre-immunisation serum for that peptide plus three times the standard error. Total IgG sample concentration was used to normalise the values for each peptide.

Similarly, the IgG responses to the envelope gp130 SIVmac251 and the gp70 V1V2 scaffold of SIVmac251 in the vaginal secretions also did not differ significantly in the two groups (**Figure 3.9A** and **B**). Surprisingly, mucosal antibody binding data to cV2 revealed almost absent antigen recognition in the ALVAC-SIV group and baseline recognition in the NYVAC-SIV as compared to the control group (**Figure 3.10**).

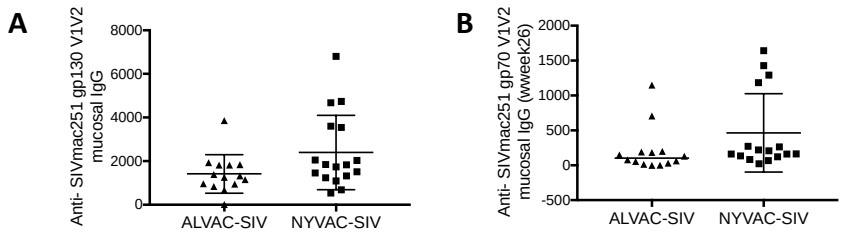

Figure 3. 9: Vaginal mucosa antibody recognition (mean ± s.d.) of V1/V2 as presented on **A**) gp130 and **B**) gp70 fusion proteins. Mann-Whitney test revealed no statistically significant differences between control and treated groups.

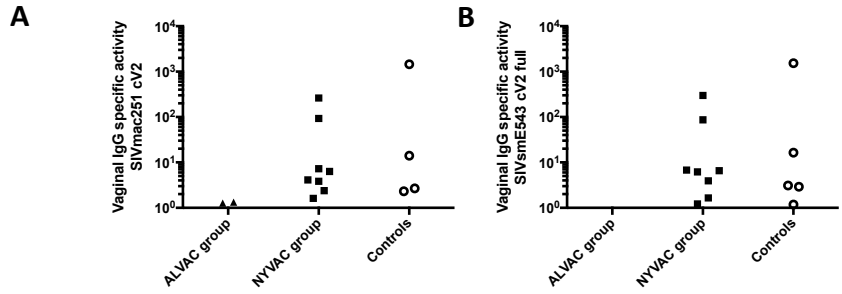

Figure 3. 10: Vaginal mucosa antibody recognition of **A**) SIVmac251 cV2 and **B**) SIVsmE543 cV2. Extremely low binding activity prevented informative comparison of the study groups.

Plasmablast migration affects vaccine efficacy

We studied how the vaccine regimens altered the frequency of PBs in blood at one week after the last immunization and found that neither NYVAC- nor ALVAC-SIV vaccination increased the percentage of total circulating blood PBs after immunisation. However, the different frequency (delta) between the total post- and pre-vaccination PB levels positively correlated with the mucosal IgG levels specific for SIV/gp120-V1V2 scaffolds in the ALVAC-SIV (P = 0.0272, **Figure 3.11C**) and the NYVAC-SIV (P = 0.0296, **Figure 3.11D**) groups.

To determine the PBs homing marker following immunisation, the expression of two homing markers, i.e. α4β7 and CXCR3A, was investigated on the surface of PBs. α4β7 is an integrin that mediates lymphocytes migration to the mucosal sites through binding to MAdCAM-1, expressed on the inner surface of the mucosal venules [400]. The chemokine receptor CXCR3 binds the chemokines CXCL9 and 10 generally released at the site of inflammation, where CXCR3A-expressing cells are recruited [401]. Interestingly, we found a decrease in the percentage of $\alpha4\beta7^+$ PBs (P = 0.0106, **Figure 3.12A**) and a rise in the levels of $CXCR3^+$PBs (P = 0.0324, **Figure 3.12B**) in the blood of NYVAC-SIV animals in the post-vaccination (week 25) as compared to the pre-vaccination time point. In contrast, no significant changes in the frequency of these PB

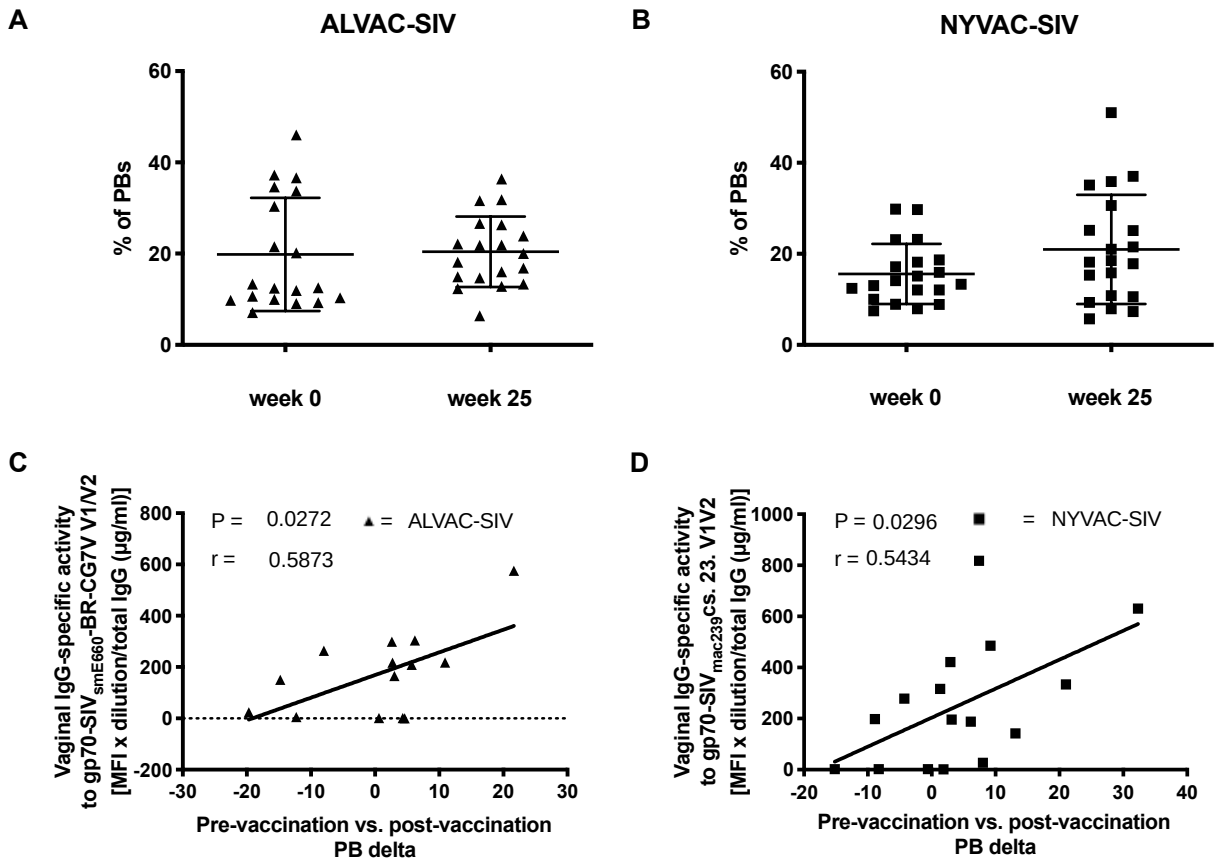

Figure 3. 11: Vaccine-induced plasmablast responses. Comparison (Mann-Whitney test) of the vaccine-induced variations in frequency of total peripheral PBs before vaccination (week 0) and post-vaccination (week 25) revealed no significant difference in the **A**) ALVAC-SIV and **B**) NYVAC-SIV groups. Bars represent mean ± s.d. Pearson correlation of the differential between PBs post- and pre-vaccination to vaginal mucosa **C**) anti-SIVsmE660-V1/V2 IgGs in the ALVAC-vaccinated group and **D**) anti-SIVmac239-V1/V2 in the NYVAC-vaccinated group.

populations were observed in the ALVAC-SIV vaccinated macaques (**Figure 3.12C** and **D**) and interestingly, the difference between the frequency of the $\alpha4\beta7^{+}$ PBs pre- and post- vaccination was associated with delayed acquisition in the ALVAC-SIV but not the NYVAC-SIV group as compared to the acquisition curve of the control animals (**Figure 3.13A** and **B**).

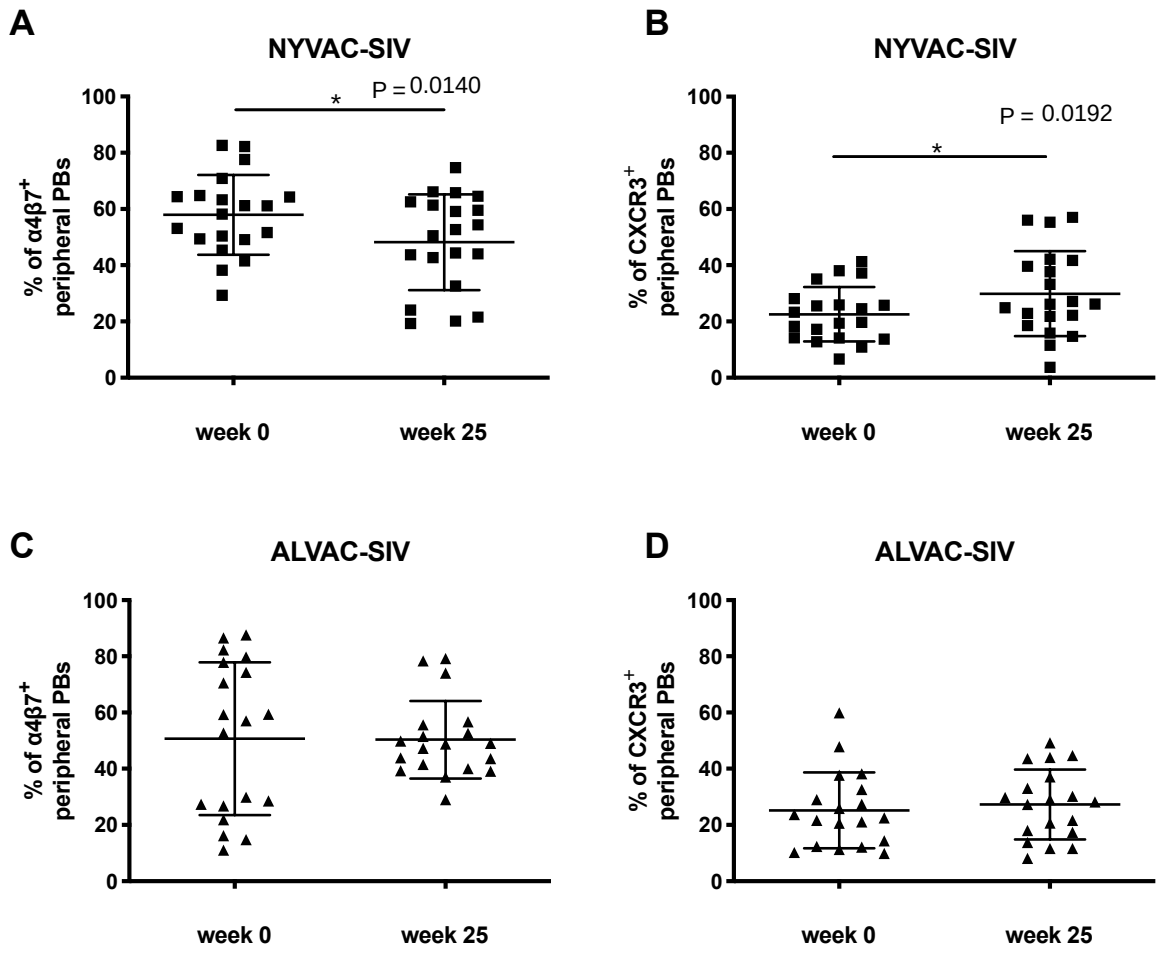

Figure 3. 12: Comparison (Mann-Whitney test) of the vaccine-induced variations in frequency of α4β7⁺ (**A** and **C**) and CXCR3⁺ (**B** and **D**) peripheral PBs before vaccination (week 0) and post-vaccination (week 25) of the two vaccinated groups. Bars represent mean ± s.d. P value reported only for significant differences.

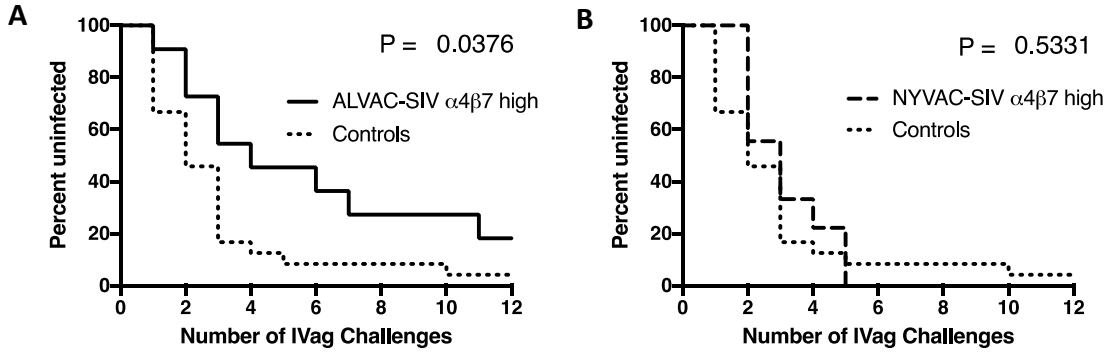

Figure 3. 13: Acquisition curves of macaques with higher post-pre α4β7⁺ PB differential in the **A**) ALVAC-SIV and the **B**) NYVAC-SIV group as compared to the control group. P values were calculated with the LogRank test.

Innate responses induced by ALVAC-SIV and NYVAC-SIV correlate with SIVmac251 acquisition

The cells of the myeloid lineage play a key role in antigen presentation and the generation of adaptive $CD4^+$, $CD8^+$ T and B cell responses [402]. Once believed to be a homogeneous population, since the 1980s several subpopulations of monocytes were identified, each one with distinct functions[403,404]: (i) classical $CD14^+CD16^-$ monocytes are phagocytic cells that also mediate inflammation; (ii) intermediate $CD14^+CD16^+$ monocytes are a transitional population involved in the production of anti-inflammatory and pro-inflammatory cytokines and $CD4^+$ T cell proliferation (iii) non-classical $CD14^-CD16^+$ monocytes are mainly involved in tissue repair and removal of debris from the vasculature.

We found that the two vaccine regimens did not significantly change the overall blood frequency of total classical, intermediate, or nonclassical $CD16^+$ monocyte subsets (**Figure 3.14**).

Through microarray data, we have previously shown[89] that ALVAC-based prime/boost strategies activate the inflammasome pathways within classical monocytes which in turn associates with protection from rectal exposures to SIVmac251 in rhesus macaques. Indeed, in the ALVAC-SIV group, the frequency of total monocytes (**Figure 3.15A**) and of the classical monocyte subset (**Figure 3.15B**) significantly correlated with protection against vaginal challenges with the same virus stock in Chinese macaques (P = 0.0277, r = 0.7038 and P = 0.0208, r = 0.7285, respectively). On the contrary, the levels of non-classical monocytes were correlated with risk of SIV acquisition (p = 0.0313, R = –0.6915) (**Figure 3.15C**).

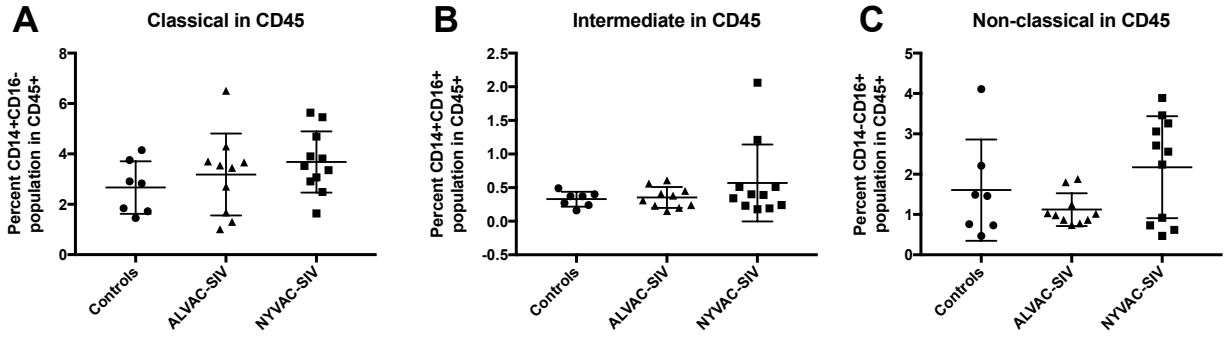

Figure 3. 14: Frequency of monocyte subpopulations at week 25 in the total population of leukocytes (as identified by positivity to CD45 staining, the leukocyte common antigen). Frequencies of **A**) classical, **B**) intermediate and **C**) non-classical monocytes are shown. Bars represent mean ± s.d. Due to limited availability of samples, only data from part 2 of the study were collected. The Kruskal-Wallis test revealed no statistically significant differences among the groups.

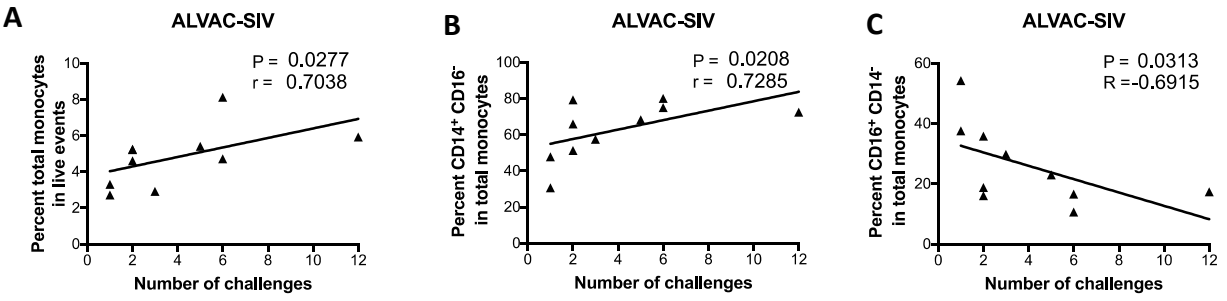

Figure 3. 15: Pearson correlation of myeloid cells subsets with SIVmac251 acquisition in the ALVAC-SIV group. Correlation with **A**) the total percentage of monocytes, **B**) of $CD14^{+}$ $CD16^{-}$ classical monocytes and **C**) $CD14^{-}CD16^{+}$ non-classical monocytes to the time of virus acquisition. Because of limited sample availability, only data from part 2 of the study were collected.

Overall, the intermediate $CD14^{+}CD16^{+}$ monocytes correlated directly with the percentage of cytotoxic NK cells in the vaginal mucosa in the ALVAC-SIV group (**Figure 3.16A**), although the levels of the $CCR2^{+}CD14^{++}CD16^{+}$ intermediate monocyte subsets were significantly higher in the NYVAC-SIV immunised animals (**Figure 3.16B**), with CCR2 being a chemokine receptor marker of macrophage activation which mediates the infiltration of the monocyte to the site of inflammation [405].

Finally, myeloid-derived suppressor cells (MDSCs) were found to correlate with faster virus acquisition in the ALVAC-SIV group if positive for CXCR4 (**Figure 3.17**). MDSCs are a population of cells generated in a large array of pathologic conditions such as infection and cancer, with the ability to suppress T cell function, and are considered to be a pathologic state of activation of monocytes and immature neutrophils [406].

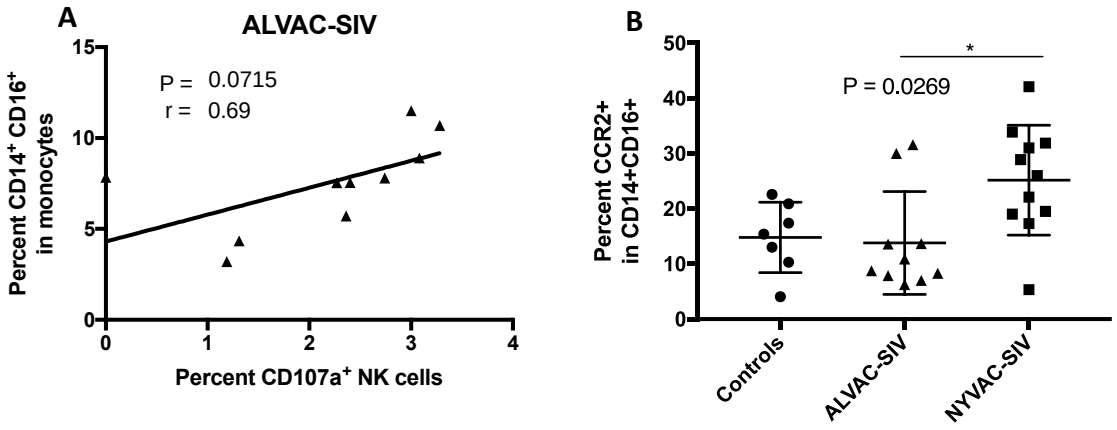

Figure 3. 16: Interplay of the innate immunity as revealed. **A**) Pearson correlation of intermediate monocytes with NK response in the ALVAC-SIV group and **B**) prevalence in the vaccination groups of $CCR2^+$ intermediate monocytes. Bars in **B** represent mean ± s.d., with statistical significance revealed by one-way non-parametric ANOVA test. Due to limited availability of samples, only data from part 2 of the study were collected.

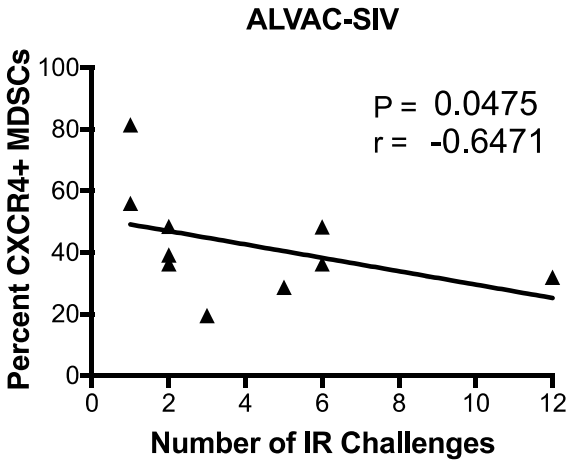

Figure 3. 17: $CXCR4^+$ MDSCs Pearson correlation with time of acquisition in the ALVAC-SIV group. Due to limited availability of samples, only data from part 2 of the study are reported.

We next investigated whether the two vaccine regimens differed in their ability to harness NK cells. In prior studies, we found that the ALVAC-SIV regimen induced the production of IL-17 by $NKp44^+$ cells in the rectal mucosa that correlated with delayed virus acquisition[362]. This type of cells is responsible for promoting epithelial integrity and mucosal homeostasis[362]. Additionally, substituting the ALVAC-SIV priming with DNA resulted in changes in classical monocytes and MDC frequency that affected the SIV specific $CD4^+$ T cells and, consequently, vaccine efficacy.

NK cells are considered to be the first-line of defence against viral infections [407] because of their ability to exert cytotoxic activity toward virus-infected cells without the need of MHC-mediated

activation. Neither vaccination regimen induced variations in the overall prevalence of NK cells ($CD45^+$, $CD3^-$, $CD20^-$, $CD14^-$, $NKG2A^+$) in vaginal mucosa (**Figure 3.18A**) and, surprisingly, we found no detectable levels of $NKp44^+$ cells in this compartment (data not shown). Although one week after the last immunization the frequency of $NKG2A^+$ NK cells with cytotoxic profiles ($CD107a^+$) increased significantly in the ALVAC-SIV compared to the NYVAC-SIV and the control groups (**Figure 3.18B**), the frequency of the $NKG2A^+CD107^+$ cells did not correlate with SIVmac251 acquisition (data not shown).

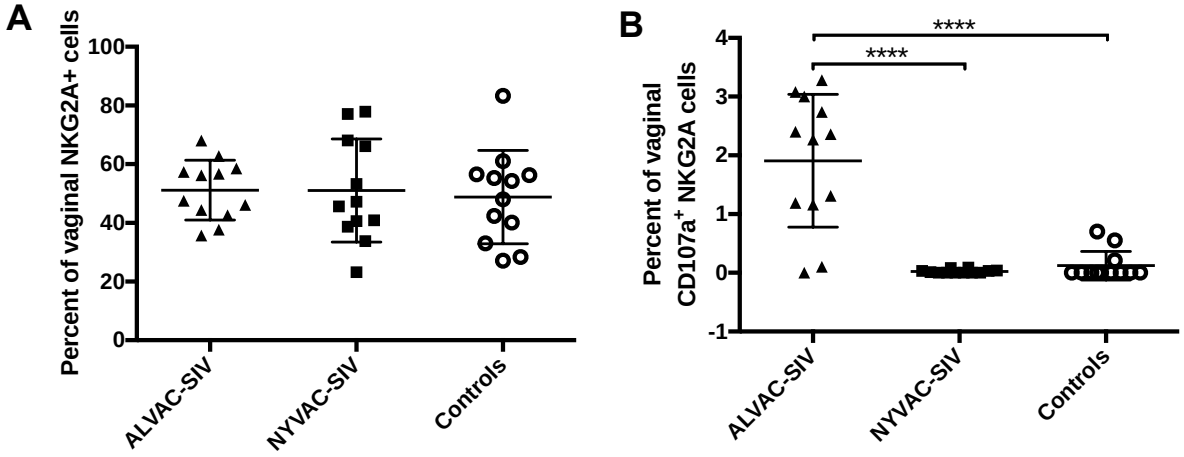

Figure 3. 18: Relative frequency of NK cells (defined as $CD45^+$, $CD3^-$, $CD20^-$, $CD14^-$) **A**) $NKG2A^+$ and **B**) $NKG2A^+$ $CD107^+$cells at week 13 of the animals included in the ALVAC-SIV, NYVAC-SIV and control groups from part 2 of the study (horizontal lines: mean ± s.d). Due to limited availability of samples, only data from part 2 of the study were collected. P values between vaccinated and control groups in **B** were below 0.0001 by Mann-Whitney t test.

Blood $CD4^+$ T cell responses

NYVAC-vaccinated animals were found to have a significantly higher percentage of activated ($CD38^+$) (**Figure 3.19A**) and gut homing ($\alpha4\beta7^+$) $CD4^+$ T cells (**Figure 3.19B**) than ALVAC-vaccinated animals in the blood at week 26 ($p = 0.029$ and $p= 0.0010$ by the Mann-Whitney test, respectively). The levels of $CD4^+$ T cells expressing the HIV/SIV co-receptor CCR5, and of peripheral Tfh ($CXCR5^+$) did not differ (data not shown).

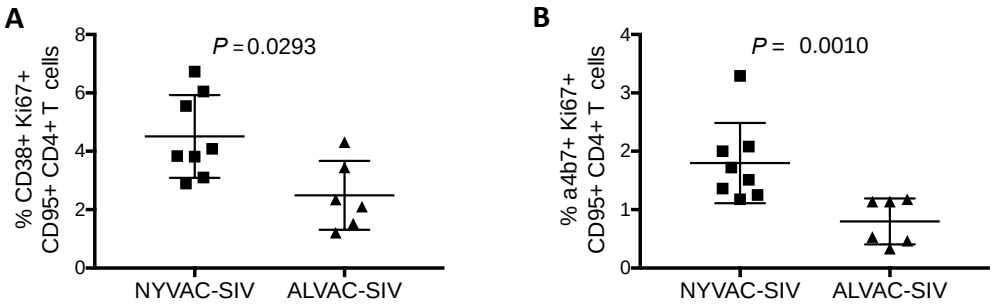

Figure 3. 19: Vaccine-induced CD4⁺ T cell subsets. **A**) Percentage of activated vaccine-induced Ki67⁺ CD38⁺ CD4⁺ T and **B**) gut-homing $\alpha 4\beta 7^+$ CD4⁺ T cells. Due to limited availability of samples, only data from part 2 of the study were collected; data from samples with detectable results are reported in figure. P values were calculated with the Mann-Whitney test.

Interestingly, the two vaccine strategies induced different subsets of CD4⁺ T cells, measured by the subset CXCR3 and CCR6 marker discriminators in the blood at week 26 (**Figure 3.20**). The ALVAC-SIV vaccinated macaques had significantly higher T_H1-type CD4⁺ T cells (CXCR3⁺ CCR6⁻, p = 0.006), (**Figure 3.20A**) and significantly lower T_H 2-type cells (CXCR3⁻ CCR6⁻, p = 0.009) (**Figure 3.20B**) than the NYVAC-SIV animals. Picture 3.20 B: edit legend to Th2

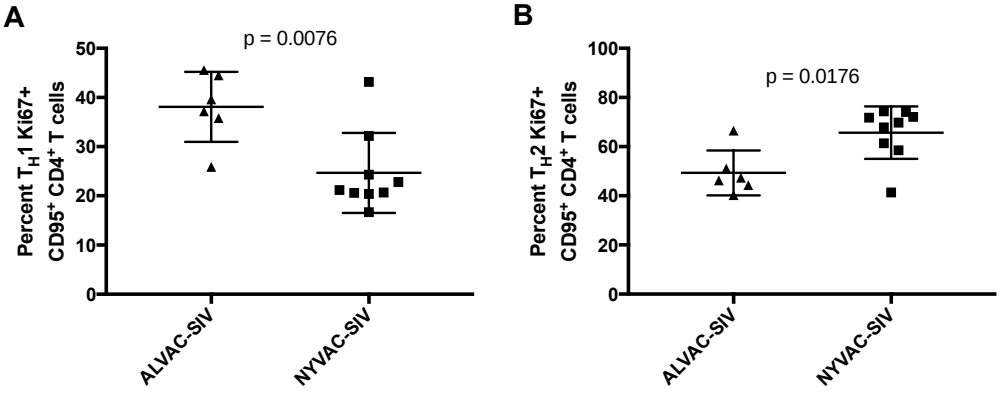

Figure 3. 20: Vaccine-induced CD4⁺ T_H cell subsets at week 26. **A**) Percentage of vaccine-induced T_H1 and **B**) T_H2 cells. Due to limited availability of samples, only data from part 2 of the study were collected; data from samples with detectable results are reported in figure. P values were calculated with the Mann-Whitney test.

Importantly, the frequency of ALVAC-induced T_H1 was found to be associated with the number of challenges to infection (**Figure 3.21A**) and with the levels of classical monocytes at week 25 (**Figure 3.21B**), suggesting a role for T cell-monocyte crosstalk in protection from SIV acquisition. No differences were found in the percentage of other subsets (T_H17 and Tfh cells), and no correlations were observed in the NYVAC group (data not shown).

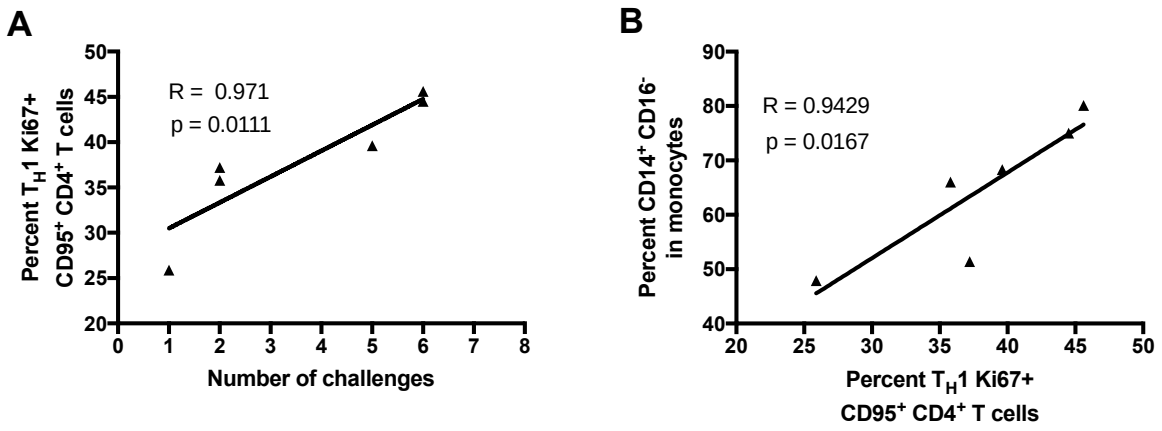

Figure 3. 21: Vaccine-induced $CD4^+$ T cell subsets in protection and monocyte cross talk. **A**) Direct significant associations between the levels of ALVAC- induced T_H1 cells at week 26 and the number of challenges to infection and **B**) to classical monocytes at week 25 in blood. Due to limited sample availability, only data from part 2 of the study were collected; data from samples with detectable results are reported in figure. Statistical analysis performed by Spearman correlation test.

Discussion

The RV144 phase III trial tested the efficacy on 16,402 patients of a vaccine regimen based on the administration of the canarypox vector ALVAC driving the expression of HIV-1 antigens in combination with the protein boost AIDSVAX, containing the HIV-1 surface glycoprotein gp120 formulated in the alum adjuvant. The significant but limited protection induced by this vaccine was nevertheless indicative in allowing the identification of possible mediators of protection.

In this study, we tested in the rigorous SIVmac251 animal model a second poxvirus vector, the vaccinia–derivative NYVAC, previously proved to be highly immunogenic in preclinical and clinical studies, in an attempt to increase vaccine efficacy[382]. The NYVAC-SIV vaccine regimen was modelled on RV144 and run in parallel with the ALVAC-SIV vaccine. In both vaccines, the immunogens expressed by the two vectors were identical as were the protein boosts.

The animals underwent repeated low dose intravaginal challenge to mimic the heterosexual transmission of HIV in female patients, and the study was powered to compare the vaccination groups to control groups of animals, immunised with one of the empty vectors and adjuvant only or not immunized. Contrary to our expectations, the higher immunogenicity of NYVAC described in previous clinical and preclinical studies by other groups[382,389,408,409], and hereby confirmed by the data on Env-specific IFN-γ ELISpot after immunisation, failed to translate into an increase in

vaccine efficacy. In contrast, only the ALVAC-based vaccination resulted in a significant estimated vaccine efficacy of 50%.

In the infected animals, both vaccination regimens failed to demonstrate long-term control of viral load in the peripheral blood, or of SIV/DNA levels in the rectal or vaginal mucosa.

Similarly to the human trial, our results provide clues to the possible mechanisms that mediate protection from viral acquisition, indicating that the quality over the quantity of the immune responses may be key in providing protection from SIV acquisition in the macaque model.

Although NYVAC-SIV proved generally more immunogenic, an association between higher $\alpha4\beta7$+ PBs responses and delayed viral acquisition was observed only in the ALVAC-SIV group, although no differences were observed in terms of total circulating $\alpha4\beta7^+$ PBs between the NYVAC-SIV and the ALVAC-SIV group post-vaccination. This indicates that, besides $\alpha4\beta7^+$ PBs *per se*, a milieu of background immune responses elicited by the ALVAC-SIV but not the NYVAC-SIV vaccination might be necessary to favour protection.

This hypothesis is further corroborated by the observation that although no significant difference was identified between the levels of monocyte subsets in the ALVAC-SIV and NYVAC-SIV group, delayed viral acquisition was found to correlate with the classical subset of monocytes only in the ALVAC-SIV group. The subset of classical $CD14^+CD16^-$ monocytes is constituted by cells that mediate inflammation and exert phagocytic activity, and it is therefore possible that one of these two mechanisms might be the mediator of protection from viral acquisition. Since our collaborating group at the NIH has shown that ALVAC-based vaccination strategies activate the inflammasome pathways within this subset of cells which in turn associates with protection from rectal SIV exposures in rhesus macaques[89], it is possible that it is a general inflammation state elicited by the classical monocyte subset to be mediating protection. Another possibility is that classical monocytes might be mediating protection through ADCP, a mechanism by which immune complexes or antibody-opsonised infected cells activate the FcγR on the surface of monocytes thus triggering phagocytosis and boosting the antiviral activity of non-neutralising or neutralising antibodies[85]. The results of ongoing microarray analyses will elucidate the extent to which these two monocyte-related functions, inflammation or phagocytosis, contribute to the delay of viral acquisition observed in the ALVAC-SIV group.

In contrast to the observations in the classical subset, non-classical monocyte and MDSC levels correlated negatively in this group. Because the quantity of monocytes that correlated with protection was not vaccine-induced, we hypothesise that the gene expression and the overall activity of these cell types was altered by the vaccine to ultimately mediate protection. Again, this hypothesis is in line with previous observations from our collaborating group at the NIH, classical monocytes function rather than titres associated with protection from mucosal exposure to SIVmac251 in groups of rhesus macaques[89].

A crosstalk between NK cells and monocytes that causes mutual amplification between the two cell types and results in recruitment of inflammatory cells to the sites of inflammation has been described before[410]. In the ALVAC-SIV group, intermediate monocytes correlated positively with the levels of cytotoxic NK cells in the vaginal mucosa, which were observed to be significantly increased in the ALVAC-SIV group, but not in the NYVAC-SIV group. The observation that intermediate monocytes might be mediating an increase of cytotoxic NK cells in the mucosa, without a total difference of intermediate monocytes between the two vaccination groups corroborates the hypothesis that the two vaccines have differently affected the functionality of myeloid subsets.

Although the levels of mucosal cytotoxic NK cells did not correlate with delayed acquisition in the ALVAC-SIV group, the fact that we found a positive correlation between the total number of monocytes and the classical subset and acquisition in the ALVAC-SIV group, still supports that innate immunity might be a key mediator of protection upon vaccination. Importantly, the role of innate immunity in providing protection from viral infection has also been identified following HIV vaccination studies: D.J.M. Lewis and collaborators observed that vaginal immunisation with an HIVgp140 vaccine linked to the 70kDa heat shock protein downregulated HIV coreceptor CCR5 and increased the expression of the HIV resistance factor apolipoprotein B mRNA-editing, enzyme-catalytic, polypeptide-like 3G (APOBEC3G) in women, effects which correlated with HIV suppression *ex vivo*[411].

While the results of the ongoing gene expression analyses are necessary to further define what immune mechanisms it is necessary to elicit to protect from mucosal SIV acquisition in rhesus macaques, the data hereby presented sustain two conclusions: (i) the quality over the quantity of the immune responses is key in providing protection from SIV acquisition in rhesus macaques. Therefore, it is not to be expected that more immunogenic approaches will result in increased protection; (ii) contrary to the traditional mechanisms of vaccine-induced protection, where the induction of a protective adaptive humoral immune response is desired to provide protection from viral acquisition, more and more data of this and other animal studies on SIV as well as HIV vaccines reiterate the role of the innate immune response in providing protection, although the precise effector mechanisms remain to be elucidated.

These data provide insights into mechanisms associated with HIV vaccine protection, and alternative strategies to refine and improve protocols for higher efficacy.

CHAPTER 4: Passive administration of a mAb with strong inhibitory activity of α4β7 to V2 interaction fails to protect rhesus macaques from SIVmac251 intrarectal challenge

Introduction

While the induction of potent neutralising antibodies has been the end goal of most HIV vaccine researchers, to date no vaccination approach tested in animals or humans has induced bnAbs: the protection, albeit limited, in RV144 was achieved in the absence of detectable bnAbs [286,309]. In contrast, non-neutralising humoral immune responses targeting the V2 region of gp120 have been found to be a correlate of protection from HIV and SIV both in the human RV144 trial and macaque studies, respectively [309,362,412,413].

Non-neutralising anti-HIV/SIV antibody immunity is increasingly associated to Fc-related antibody functions, also considering that in RV144 a correlation was found with ADCC and high levels of anti-V2 serum IgGs if anti-gp120 IgA titres were low [309,414,415]. Yet, no studies report that antibody effector functions alone are able to prevent HIV/SIV infection in the absence of neutralisation [245]. In neonatal macaques, non-neutralising polyclonal preparations that displayed strong ADCC did not protect animals from oral SIVmac251 challenge[416]. Similarly, no protection was detected with the passive administration of non-neutralising antibodies highly enriched for ADCC activity and derived from HIV-infected individuals[417]. Therefore, despite a statistical association with reduced risk of infection by anti-V2 IgGs in RV144 vaccinees and animal models that displayed post-infection viral control, the antiviral activity exerted by the Fc region alone has not proven to be sufficient to prevent infection [245]. Similarly, enhancing Fcγ receptor binding efficiency of bnmAb b12 did not provide protection from SHIV challenge in macaques [418].

Although these studies evaluated the possibility that ADCC might act alone or in combination with viral neutralisation as a mediator of protection from viral acquisition, no passive transfer studies have been performed to evaluate if the humoral non-neutralising anti-V2 response could delay viral acquisition. To date, the only anti-V2 mAb tested in passive transfer macaque studies is the broadly neutralising PG9, which targets the anti-V1V2 glycopeptides and was able to afford protection in 4 out of 6 macaques [419].

We hypothesise that the non-neutralising anti-V2 response might be a mediator of protection by preventing interaction of viral envelope gp120 with human $\alpha4\beta7$. The pivotal role of this integrin in HIV infection has been demonstrated by the studies of Byrareddy *et al.* on infected macaques treated with ART in combination with the anti-$\alpha4\beta7$ mAb vedolizumab[337]. When treatment was withdrawn, the animals maintained low to undetectable viral loads and normal $CD4^+$ T cell counts in plasma and GI tract for more than nine months[337]. Notably, the authors identified a skew of the antibody response towards the V2 domain among the correlates of viral control, while neutralisation and ADCC failed to demonstrate correlation.

While the mechanisms by which vedolizumab infusion contributed to prolonged viral load control are yet to be defined in detail, some propose that this mAb might target $\alpha4\beta7$ incorporated in the viral envelope of the virions during the budding process, and thus prevent the virus from targeting the intestinal tissue [420]. However, it is possible that viral control might be due to the disruption of the interaction between $\alpha4\beta7$ and V2, either directly by $\alpha4\beta7$-bound vedolizumab or indirectly through the treatment-induced boost of anti-V2 humoral responses.

The present study was designed to evaluate whether passive infusion of the non-neutralising anti-V2 mAbs NCI09 and NCI05 isolated from the vaccinated, protected rhesus macaque P770 and described in **chapter 2** are able to provide protection from mucosal SIVmac251 RLD challenge in groups of rhesus macaques. A further group was included to test for the protection efficacy of the weakly SIVmac251-neutraliser anti-V2 mAb ITS09, which was isolated from an infected animal [364]. While NCI05 did not display any activity of inhibition between human $\alpha4\beta7$ and deglycosylated SIVmac251 gp120, both NCI09 and ITS09 proved to significantly disrupt this interaction, with NCI09 being the greatest inhibitor amongst the mAbs tested in the binding assay [360].

Because of the high doses of mAb administered per animal (50 mg/kg) require a total of approximately 5 mg of mAb to be prepared before an animal group can undergo immunisation, only the control and ITS09 group have been tested to date, while sufficient quantities of NCI09 and NCI05 mAbs should be ready for infusion before the end of 2018.

Materials and Methods

Monoclonal Antibodies

Current-Good Manufactory Practice (cGMP) ITS09.01 (ITS09) was produced by Drs. Elizabeth Scheideman, Abasha Williams, Stephanie Golub, Daniel Ragheb, Nga Tran, Lena Wang, Vaccine Production Program, VRC, NIAID, NIH, Gaithersburg, MD, USA.

An expression vector encoding the heavy chain and light chain genes of ITS09-LS along with a *dhfr* selection marker was transfected into CHO-DG44 cells by electroporation using the Amaxa™ 4D Nucleofector™ (Lonza). Transfected cells were cultivated in an Infors Multitron shaker set to 37°C, 5% CO_2, and 80% relative humidity with a shaking speed of 130 rpm (orbital throw of 1 inch) in CDM4CHO medium with 6 mM L-glutamine. Forty-eight hours after transfection, methotrexate (MTX) was added to the culture to a final concentration of 100 nM. Viable cell density and viability for the culture was assessed every three to four days using the Cedex HiRes. Once a week, the cells were centrifuged at 100 x g for 10 minutes and resuspended in fresh CDM4CHO medium with 6 mM L-glutamine and 100 nM MTX. When the viability of the pools recovered to ≥ 80%, the medium was replaced with ActiCHO P medium containing 6 mM L-glutamine and 100 nM MTX.

ITS09-LS production was carried out in two 50L single-use bioreactors (SUB). The pool was expanded in a 50L WAVE bioreactor in 12L ActiCHO P with 6mM L-glutamine for three days with ViCell and NOVA BioProfile FLEX measurements taken daily. The cells were then seeded into a 50L SUB in 40L ActiCHO P with 6 mM L-glutamine. The cells were maintained in the SUB for 14 days with ViCell and NOVA BioProfile FLEX measurements taken daily. Samples were also taken for protein A HPLC titre analysis starting on day 6. Starting on day 3, 1.5% Feed A and 0.15% Feed B were added daily and reduced as needed based on glucose and lactate utilization rates. Additional glucose supplementation was provided when levels dropped below 1 g/L as measured on the NOVA meter to maintain residual glucose at 1 g/L.

Following clarification of the harvest with Clarisolve® and Millistak+® depth filters and subsequent filtration, the mAb was purified by Protein A capture and endotoxin removal was performed by a salt-tolerant interaction chromatography (STIC) anion exchange step. The final product was concentrated to greater than 10 mg/mL and buffer exchanged into 1X PBS prior to sterile filtration.

Animals, vaccines and SIVmac251 challenge

The staff at the National Cancer Institute Animal Facility directly handled the animal models in respect of all the relevant guidelines of our institute.

The animals of this study were male colony-bred rhesus macaques (*Macaca mulatta*) of Indian origins obtained from the Eunice Kennedy Shriver National Institute of Child Health and Human Development (Rockville, Maryland, USA). Animals were housed and treated in respect of all the relevant guidelines of our institute (NIH) in the NCI Animal Facility. A total of 60 macaques were randomised in groups of 8 animals according to their major histocompatibility alleles. The animals underwent passive immunoprophylaxis through a total of three subcutaneous administrations of the anti-V2 mAb ITS09.01 at a dose of 50 mg/kg every three weeks (**Figure 4.1**). Control group animals received an equal volume of PBS through the same route with the same frequency.

Animals were challenged weekly for a total of nine times, starting from five days after the first mAb administration, with intrarectal SIVmac251 at 120 $TCID_{50}$.

Immunisation was discontinued for animals that tested positive for SIV-RNA and their blood viral loads were tested weekly until symptom development.

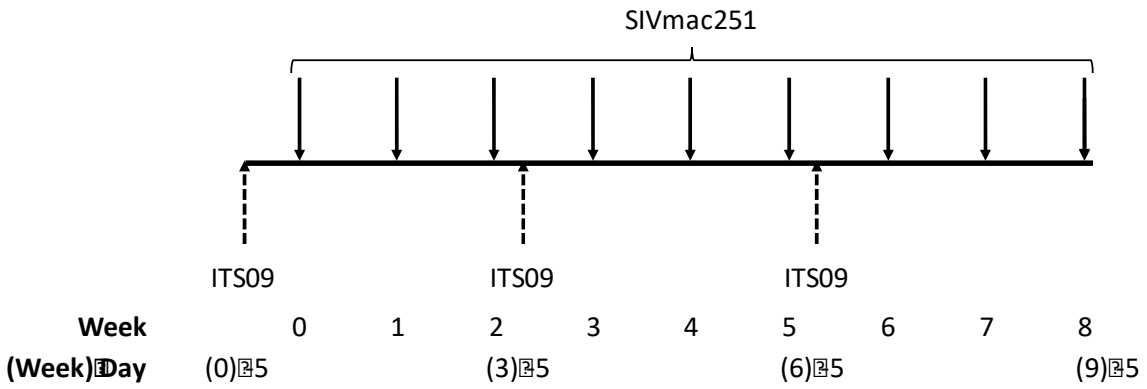

Figure 4. 1: Study design. Animals underwent a total of three subcutaneous passive immunisations with mAb ITS09 (dashed arrows) every three weeks throughout the repeated low dose challenge phase, which consisted of a total of nine weekly intrarectal SIVmac251 administrations (solid arrows). Control animals were administered PBS instead of ITS09.

Measurement of viral RNA and DNA

Viral RNA levels were investigated by Ranajit Pal, Advanced Bioscience Laboratories, Frederick, Maryland, USA. Data was co-analysed by Isabela S. de Castro, Animal Models and Retroviral Vaccines Section, NCI, NIH, Bethesda, MD, USA.

Plasma SIVmac251 RNA levels were evaluated by nucleic acid sequence-based amplification, as described in **chapter 3** and in reference [391].

Serum ITS09 titration

Serum ITS09 reactivity to V2 was evaluated by ELISA. Samples from three PBS-treated control animals were used for reference. ELISA plates were coated overnight at room temperature with 100 ng per well of 1J08 scaffold SIVsmE660.CR54, kindly provided by Dr. Mario Roederer (VRC) and described in **chapter 2** and in reference [364]. The contents were then dumped and 1% PBS-BSA was added to the well to block. 40 µl of serial 1:4 dilutions of monkey plasma starting from 1:100 were dispensed in each well and incubated for 1 h at 37 °C. Each plate also included a 1:5 serial dilution of purified mAb ITS09, starting from 20 µg ml^{-1}. Plates were washed using a plate washer and 40 µl of 1:5,000-diluted anti-monkey IgG1 + horseradish peroxidase (clone 7H11) were dispensed in each well and incubated for 1 h at 37 °C. After washing and incubation with streptavidin-HRP (KPL) for 1 hr at 37°C, signal was developed through incubation with 3,3',5,5'

TMB substrate (Thermo Fisher Scientific) and Optical density (OD) read at 450 nm. Plasma dilutions in the linear range of the curve were compared to the binding curve of the ITS09 standard to interpolate ITS09 plasma concentration values.

Statistical analysis

The LogRank test of the discete-time proportional hazards model was used to identify the number of the challenges before acquisition of infection. Viral loads were compared through the Mann-Whitney Wilcoxon test.

Scientist	**Contribution**
Giacomo Gorini	Study design, virus and mAb dilution and aliquot preparation for animal use, sample processing, supervision of animal immunisation and challenge, anti-V2 plasma IgG titration, data processing, graph editing.
Staff of Vaccine Production Program	cGMP production of ITS09.01.
Ranajit Pal	Titration of viral RNA.
Isabela S. de Castro	Processing of part of the data of viral RNA levels.
National Cancer Institute Animal Facility	Staff responsible for animal handling and treatment.

Table 4. 1: List of collaborators that directly contributed to the experiments summarised in this chapter.

Results

ITS09 failed to reduce the risk of SIVmac251 acquisition

This study was designed to compare the efficacy of each mAb to the control group. To date, only the results of the group treated with the mAb ITS09, derived from an SIVsmE660-infected macaque [364], are available. Surprisingly, despite the potent inhibition of $\alpha4\beta7$ and V2 interaction that this mAb displayed in vitro [360], subcutaneous infusion of ITS09 failed to significantly protect from viral acquisition as compared to the PBS-treated group (Log-rank test: p=0.8725; **Figure 4.2**).

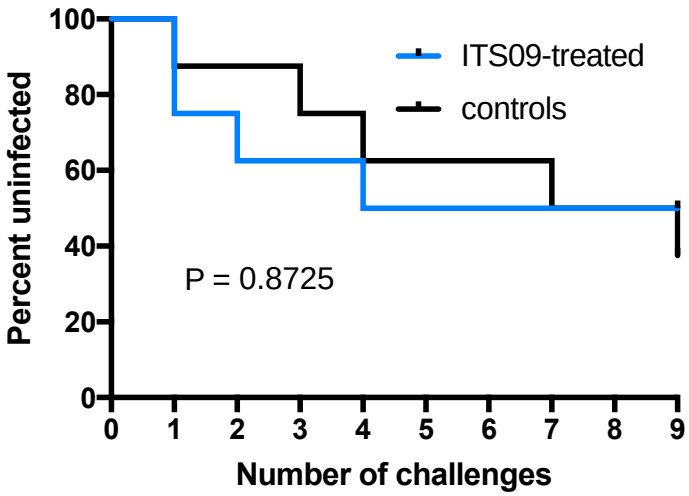

Figure 4. 2: Acquisition curves of SIVmac251 administered intrarectally in the ITS09-treated group, as compared to the PBS-treated control group. Statistical analysis: LogRank test.

ITS09 increased viral loads in the chronic phase

The animals that did contract infection did not display significant control of viremia as compared to the control groups (**Figure 4.3**). On the contrary, ITS09-treated animals displayed significantly higher plasma viral loads in the chronic phase as compared to the control group ($p < 0.0001$, **Figure 4.3D**). However, these results are difficult to interpret because of the lack of a suitable control group of animals treated with an irrelevant mAb, that is a mAb that does not bind to SIV antigen. To allow better understanding of future results, a group of animals receiving irrelevant antibody has been included in the study.

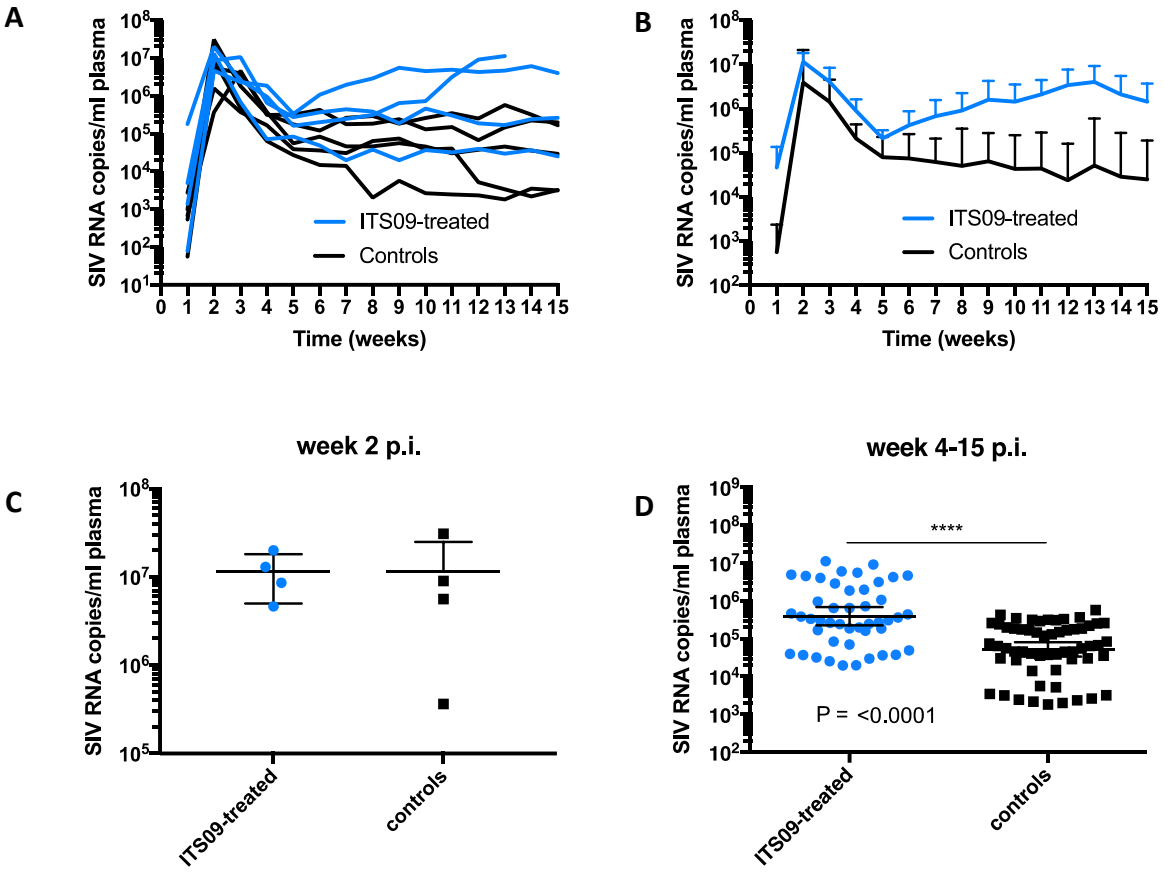

Figure 4. 3: Viral loads of infected macaques at 1-15 weeks post-infection (p.i.). **A**) SIV/RNA levels in the plasma of each separate infected animal in the ITS09-treated and control (blue and black, respectively) group. **B**) Logarithmic mean ± s.d. of SIV/RNA levels in the plasma of infected animals, pooled by group, after infection. **C**) Logarithmic mean ± s.d. of SIV/RNA levels in the plasma of infected animals in the acute phase of infection. The Mann-whitney test reveals not significant difference between the two groups at this stage of infection. **D**). Values from weeks 4 to 15 p.i. were pooled to compare viral loads throughout the chronic phase of infection, with significant difference between groups revealed by the Mann-Whitney test. Lack of an animal group receiving control antibody hinders the correct interpretation of the increased viremia in animals treated with ITS09.

ITS09 reached stable blood titres after the second mAb administration

ITS09 plasma levels were monitored as anti-V1V2 IgG plasma reactivity throughout the immunisation, challenge phase (**Figure 4.4**). After the first mAb administration, ITS09 levels reached between 1,500 and 2,000 µg/ml in the treated animals, while remaining negative in the controls. While mAb titres were found to drop in the following weeks, the second and third administration recovered and maintained steady blood mAb levels for the duration of the challenge phase. In the infected animals, the anti-V1V2 plasma reactivity was confirmed to decrease upon treatment interruption.

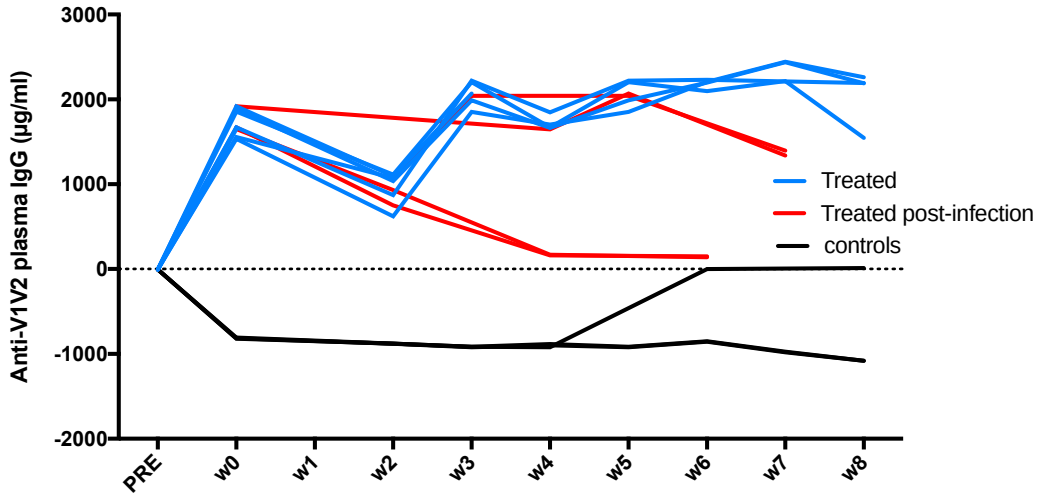

Figure 4. 4: ITS09 levels measured as anti-V1V2 activity in the plasma of control (black), treated uninfected (blue) and treated post-infection (red) animals. Plasma binding activity was detected by ELISA against fixed SIVsmE660.CR54 1J08-V1V2 antigen, and ITS09 concentration in samples interpolated against a control curve of known concentrations of ITS09.

Discussion

The $\alpha 4\beta 7$ integrin has been demonstrated to bind to the V2 domain of both HIV-1 and SIV envelope glycoprotein gp120[231,360], with this interaction likely enhancing virus transmission.

While administration of anti-$\alpha 4\beta 7$ antibodies has resulted in inhibition of SIV in the macaque challenge model[327], the potential of antibodies targeting V2 to result in a similar effect has not yet been demonstrated.

While the molecular details of the interaction between $\alpha 4\beta 7$ and gp120 remain controversial, studies have demonstrated that glycosylation is a key modulator of the V1V2 conformation and binding to the integrin, with partially glycosylated, but not fully glycosylated envelope proteins as preferred substrates for $\alpha 4\beta 7$ binding[363]. In addition, it has been observed that monomers, not functional trimers are strong binders of $\alpha 4\beta 7$[363]. It seems therefore that the V2 domain of poorly glycosylated monomeric gp120 allows binding of the virion to $\alpha 4\beta 7$, with this integrin bringing the virion closer to the target cell surface, where functional Env trimers proceed to engage coreceptors and CD4 to initiate the entry process[363]. Thus, while the gp120 monomers present on the surface of the virion have often been referred in literature as “defective” Env products, it seems that these forms have a precise function and have been positively selected by their binding ability to $\alpha 4\beta 7$.

This study was designed to determine if non-neutralising anti-V2 antibodies elicited by ALVAC-SIV vaccination can be mediators of protection when passively administered to naïve rhesus macaques, possibly by hindering the interaction between $\alpha4\beta7$ and the poorly glycosylated, monomeric Env proteins present on the surface of the virions.

Although the results of the passive immunoprophylaxis with the two mAbs NCI05 and NCI09 isolated from the immunised, protected macaque P770 have not yet been produced, some observations can nonetheless be made on the negative outcome of the passive administration of ITS09. First of all, the fact that ITS09 showed detectable inhibition of $\alpha4\beta7$ binding to V2 (**Figure 2.11**) and yet failed to protect suggests that the disruption of gp120 binding to the integrin is not alone a predictor of the efficacy of a treatment in preventing mucosal SIV infection. Secondly, the presence in the bloodstream of ITS09 not only failed to contain, but also seemed to increase plasma viral loads of the treated animals in the chronic phase of infection. While it would be tempting to conclude that ITS09 directly mediated an increment in SIV virulence, the lack of a control group treated with an irrelevant mAb results in difficult interpretation of this finding. For this reason, a further control group scheduled to be receiving equal doses of an irrelevant mAb will be included in the study.

While the results with ITS09 are sufficient to make these observations, complementing the study with the NCI05 and NCI09 immunisation groups will certainly prove more insights into the role of the anti-V2 humoral response in protection, regardless of the outcome.

In case of protection with NCI05 and/or NCI09, one might hypothesise that the positive outcome is due to the source of the mAbs, that is a vaccinated, protected macaque. However, protection could only suggest that the NCI mAbs display biological features with which ITS09 is not endowed, without demonstrating that NCI-like antibodies might not be elicited during infection. It would, however, be finally confirmed beyond statistical correlation that the elicitation of antibodies that bind to V2 is a mechanism by which ALVAC-SIV vaccination provides protection from HIV/SIV. This could possibly be due to the prevention of binding of gp120 to $\alpha4\beta7$ in the mucosal site, or possibly through different mAb(s)-induced biologic activities that would need further

investigation.

Considering however that passive infusion of ITS09 did not prove protective despite detectable inhibition of binding of $\alpha4\beta7$ to viral V2 *in vitro*, it is a concrete possibility that the NCI mAbs will not prove protective either. A negative outcome would thus corroborate the hypothesis that the inflammatory milieu produced by the ALVAC prime elicits innate immune responses necessary to trigger vaccine protection.

CHAPTER 5: Conclusions

Nine years after the outcome of the RV144 clinical trial, the exact immunological mechanisms that mediated partial protection from HIV-1 infection remain to be elucidated.

While antibody responses to vaccines have traditionally been associated with protection in many immunisation approaches approved for clinical practice, RV144 proved atypical when virus neutralisation was not identified as a mechanism of protection. However, the humoral immune response still proved to be important in preventing HIV-1 acquisition when vaccine-induced serum IgG levels targeting the V2 loop of gp120 were found to correlate with protection[309].

The key role played by the non-neutralising humoral immune response in protection from immunodeficiency virus infection was also confirmed by an RV144-like regimen which yielded similar protection rates in rhesus macaques vaccinated against SIV, while also eliciting anti-V2 IgGs which correlated with delayed acquisition[362].

The findings reported in my thesis offer further insight into the immunological mechanisms of protection by providing information on three main themes: (i) the anti-V2 humoral response in the animal model; (ii) the role of the innate immunity elicited by vaccination in mediating protection and (iii) a potential new mechanism of escape from the humoral immune response of the host.

Blocking of the $\alpha 4\beta 7$ to V2 interaction

Of the anti-V2 mAbs isolated from macaque P770, NCI09 demonstrated the most potent inhibition of binding between human $\alpha 4\beta 7$ and SIV gp120 in the human B lymphoma cell assay RPMI8866. That blocking this interaction could be the mechanism underlying protection from viral acquisition observed first in RV144 and later in macaques studies has been hypothesised by many, but not yet proven experimentally.

This hypothesis has been formulated following three main observations: (i) data of both clinical and preclinical studies found correlations between the levels of anti-V2 antibody responses and delayed viral acquisition [309,362]; (ii) *in vitro* experiments showed that V2 binds to the integrin $\alpha 4\beta 7$

and this interaction can be blocked by anti V2-mAbs[231,360] and (iii) treatment with the anti-$\alpha4\beta7$ mAb vedolizumab both protected macaques from viral acquisition and suppressed the viral load in infected animals for several weeks after ART+mAb discontinuation[327,337].

However, while extensive data with the mAb vedolizumab proved that targeting $\alpha4\beta7$ can be a strategy of viral prevention and control, no direct proof has been provided that targeting V2 with the humoral immune response may lead to protection. Passive infusion of anti-V2 mAbs in the macaque model would be key in validating this potentially protective mechanism.

In the setting of passive immunoprophylaxis in the RLD challenge model of rhesus macaque, ITS09 was unable to prevent viral acquisition despite a detectable inhibitory activity of $\alpha4\beta7$-V2 interaction. Conversely, this mAb was found to increase viremia levels throughout the chronic phase of infection in the animals that acquired the virus, although this observation needs to be further investigated.

From the two contrasting results that we obtained with ITS09 (the first one consisting in detectable inhibition of binding between gp120 and $\alpha4\beta7$, the second one being apparent increase of the chronic viremia in the vivo model), it could be hypothesised that more than simple blocking of $\alpha4\beta7$ and V2 interaction alone is needed to impede viral entry and replication in target cells.

The lack of a suitable cell line to study how the interaction between gp120 and the integrin affects viral replication rates hinders the study of what exact mechanisms are at play. While TZM-bl cells expressing CD4 and viral entry coreceptors CXCR4 and CCR5 have traditionally been the gold-standard system to study viral entry and replication and antibody-mediated viral neutralisation, this cell line lacks detectable levels of activated $\alpha4\beta7$ on the cell membrane (personal communication by James Arthos, NIAID). The implementation of an $\alpha4\beta7^{+}$ cell system to study viral neutralisation and anti-V2 antibody-mediated inhibition of viral entry is becoming a pressing need in the field.

Innate immune response

In Chapter 3, the ALVAC/NYVAC comparison study generated two main conclusions: (i) greater immunogenicity of the vaccine vector component did not directly lead to higher protection from viral acquisition, and (ii) the innate response, particularly through the monocyte subsets, plays a key role in preventing mucosal transmission of SIV in rhesus macaques following vaccination.

As for the higher activation of the adaptive immune response not being a correlate of protection, it could be that the increased NYVAC-SIV-induced T cell activation as observed by IFN-γ ELISpot led to a metabolic activation of target cells thus favouring SIV replication. The key role of the innate response in providing protection from viral acquisition has already been described both in HIV[411] and SIV[89] vaccination. Notably, the SIV study pointed to the protective effect being mediated in part by the monocyte subsets, although it is not clear whether protection might be mediated by a pro-inflammatory activity of this subset or by FcR-, antibody-dependent functions such as ADCP. Microarray data will likely provide insights into the mechanism by which this cell subset might mediate protection. However, the ALVAC-NYVAC study corroborated the hypothesis that an effective HIV/SIV vaccine would require not only the induction of a memory humoral immune response towards V2, but also an optimal stimulation of innate immune responses.

While ITS09 passive treatment has failed to provide protection in macaques, no data is yet available on NCI05 and NCI09 (which are currently under production for passive transfer studies). It is a possibility that these mAbs will similarly fail to protect without having the ALVAC-induced background of innate responses that I and others described to play a role in providing immunity. A further arm has recently been added to the passive transfer study, where these mAbs will be administered together with an ALVAC-SIV prime without a gp120 boost. The hypothesis is that the ALVAC prime will elicit a complementary innate immune response to provide protection. A gp120 boost has not been included in the study for two main reasons: (i) to evaluate the exclusive role of anti-V2 NCI mAbs in preventing infection in the absence of vaccine-induced anti-gp120 polyclonal responses and (ii) to exclude the possibility that vaccine-induced antibodies might interfere with mAb binding to the challenge virus

Antibody interference

The main goal of the studies reported in this thesis was to lead to further mechanistic insight into the protective immune response generated by vaccination regimens against HIV/SIV. In doing so, I have provided additional knowledge on intrinsic SIV properties, which may be confirmed to exist in HIV as well. I observed that SIV has evolved a structural plasticity within the V1V2 domain that prevents gp120 from binding to too many ligands at the same time. I described this property as directed mAb-to-mAb (antibody interference), while previous studies[318] have shown a mAb-to-$\alpha 4\beta 7$ interfering activity (ligand interference). While the former might be detrimental in vaccine protection, allowing the virus to escape some of the humoral response by preventing binding of too many immunoglobulins at a time, the latter is a desirable goal of vaccination.

The identification of antibody interference, where non-protective antibodies disrupt the binding of potentially protective antibodies targeting distant epitopes, has important implications in the design of novel immunogens. This escape mechanism is to be avoided either by designing immunogens that are depleted of areas where interfering, non-protective antibodies are more likely to bind or, alternatively, that stimulate high-affinity antibodies targeting regions associated with protection. The binding of lower-affinity interfering antibodies would then be less disruptive of the high-affinity protective immunity, shifting the equilibrium of target-bound immunoglobulins towards protection. At the same time, I hypothesise that it is essential to maximise immunoglobulin access to key antigenic sites that, when bound, lead to an alteration of the V2 structure sufficient to prevent binding of $\alpha 4\beta 7$ to the putative binding site on gp120.

Final remarks

I would like to conclude this thesis by reproposing, in an edited version, a few considerations that I had the pleasure and honour to have published as a guest blogger on the website of the United States Agency for International Development (USAID) on HIV Vaccine Awarness Day, 2017, in a joint article written with and upon invitation of my friend and mentor Dr. Margaret McCluskey, Senior Technical Advisor for HIV Vaccines in the Office of HIV/AIDS, Bureau for Global Health, USAID[421]*.*

It has been more than 35 years since the discovery of the HIV virus in 1983 and the only vaccine that ever demonstrated protection in a phase III clinical trial showed a 31.2% efficacy rate. Despite extensive efforts, the mechanisms behind the immunity afforded in some of the vaccinated individuals still have not yet been clearly elucidated. While it was announced soon after the discovery of HIV-1 that a vaccine would be following within two years, the scientific community has encountered a number of insurmountable obstacles. The genomic integration of HIV into key cells of the immune system, the high mutation rates and a cunning ability of this pathogen to take advantage of the pathways needed to activate the immune system itself have proven to be tough scientific challenges that have pushed the goal of a vaccine back much farther than originally predicted. More than twenty years ago, on 18 May 1997, President Clinton said:

"*We are grateful that new and effective anti-HIV strategies are available and bringing longer and better lives to those who are infected, but we dare not be complacent. HIV is capable of mutating and becoming resistant to therapies and could well become even more dangerous. Only a truly effective, preventive HIV vaccine can limit and eventually eliminate the threat of AIDS*."

Twenty years from the announcement of that 18 May, now marked as HIV Vaccine Awareness Day, one wonders how close we are to the discovery of this final major Public Health tool to finally end the HIV/AIDS epidemic. This day has the goal of not only praising scientists for their efforts, but also the participation of many clinical volunteers.

At the 2017 Keystone HIV vaccine scientific conference that I attended, I had the pleasure to have dinner with a small group of senior scientists who have been working on HIV vaccines for many years. I soon found myself involved in a discussion over the difficulties that still lay ahead of the scientific community in this effort.

To my surprise, this conversation revealed a shared frustration. While on the one hand I understood their sentiment, I still believe that the development of an effective vaccine is an achievable goal. Our field continues to attract talented young investigators, which are continuously joining forces with more senior scientists. As one of the young scientists who joined this international effort, I feel that its future success lies in novel ideas, rather than old ones that have yet to show some strong signs of efficacy. I am a firm believer that a successful, cost-effective and accessible vaccine will be developed as long as the research on the HIV field goes hand-in-hand with the invention and evolution of new technologies, and continued investment to test new ideas and concepts.

I have no doubts that, as technologies progress, following generations of scientists will be up to the task to deliver a final, highly effective HIV vaccine.

BIBLIOGRAPHY

1. WHO | Immunization coverage. *WHO* (2018).
2. Services, U. S. D. of H. and H. Vaccines.gov - Vaccine Types.
3. Vaccines: Vac-Gen/Additives in Vaccines Fact Sheet. Available at: https://www.cdc.gov/vaccines/vac-gen/additives.htm. (Accessed: 4th April 2018)
4. Vaccine Types | NIH: National Institute of Allergy and Infectious Diseases. Available at: https://www.niaid.nih.gov/research/vaccine-types. (Accessed: 4th April 2018)
5. Deering, R. P., Kommareddy, S., Ulmer, J. B., Brito, L. A. & Geall, A. J. Nucleic acid vaccines: prospects for non-viral delivery of mRNA vaccines. *Expert Opin. Drug Deliv.* **11**, 885–899 (2014).
6. Atsdr. Agency for Toxic Substances and Disease Registry. (2008).
7. Kool, M., Fierens, K., Lambrecht, B. N. & Nl, K. Alum adjuvant: some of the tricks of the oldest adjuvant. doi:10.1099/jmm.0.038943-0
8. Baylor, N. W., Egan, W. & Richman, P. Aluminum salts in vaccines--US perspective. *Vaccine* **20 Suppl 3**, S18-23 (2002).
9. Shirodkar, S., Hutchinson, R. L., Perry, D. L., White, J. L. & Hem, S. L. Aluminum compounds used as adjuvants in vaccines. *Pharm. Res.* **7**, 1282–8 (1990).
10. Ghimire, T. R. The mechanisms of action of vaccines containing aluminum adjuvants: an in vitro vs in vivo paradigm. *Springerplus* **4**, 181 (2015).
11. Glenny, A. T., Buttle, G. A. H. & Stevens, M. F. Rate of disappearance of diphtheria toxoid injected into rabbits and guinea - pigs: Toxoid precipitated with alum. *J. Pathol. Bacteriol.* **34**, 267–275 (1931).
12. Lindblad, E. B. Aluminium compounds for use in vaccines. *Immunol. Cell Biol.* **82**, 497–505 (2004).

13. Lindblad, E. B. Aluminium adjuvants--in retrospect and prospect. *Vaccine* **22**, 3658–68 (2004).

14. WHITE, R. G., COONS, A. H. & CONNOLLY, J. M. Studies on antibody production. III. The alum granuloma. *J. Exp. Med.* **102**, 73–82 (1955).

15. Qin, H. *et al.* Vaccine site inflammation potentiates idiotype DNA vaccine-induced therapeutic T cell-, and not B cell-, dependent antilymphoma immunity. *Blood* **114**, 4142–9 (2009).

16. Matzinger, P. Tolerance, Danger, and the Extended Family. *Annu. Rev. Immunol.* **12**, 991–1045 (1994).

17. Gherardi, R. K. *et al.* Macrophagic myofasciitis lesions assess long-term persistence of vaccine-derived aluminium hydroxide in muscle. *Brain* **124**, 1821–31 (2001).

18. Kool, M. *et al.* Cutting edge: alum adjuvant stimulates inflammatory dendritic cells through activation of the NALP3 inflammasome. *J. Immunol.* **181**, 3755–9 (2008).

19. Wang, Y., Rahman, D. & Lehner, T. A comparative study of stress-mediated immunological functions with the adjuvanticity of alum. *J. Biol. Chem.* **287**, 17152–60 (2012).

20. Marichal, T. *et al.* DNA released from dying host cells mediates aluminum adjuvant activity. *Nat. Med.* **17**, 996–1002 (2011).

21. McKee, A. S. *et al.* Host DNA released in response to aluminum adjuvant enhances MHC class II-mediated antigen presentation and prolongs CD4 T-cell interactions with dendritic cells. *Proc. Natl. Acad. Sci. U. S. A.* **110**, E1122-31 (2013).

22. Casadevall, A. The methodology for determining the efficacy of antibody-mediated immunity. *J. Immunol. Methods* **291**, 1–10 (2004).

23. Claire-Anne Siegrist. Vaccine Immunology.

24. Kurosaki, T., Kometani, K. & Ise, W. Memory B cells. *Nat. Rev. Immunol.* **15**, 149–159 (2015).

25. Abbas, A. K., Lichtman, A. H. & Pillai, S. *Cellular and molecular immunology*. (2014).

26. Gnann, J. W. & Whitley, R. J. Clinical practice. Herpes zoster. *N. Engl. J. Med.* **347**, 340–6 (2002).

27. Geginat, J. *et al.* Plasticity of Human CD4 T Cell Subsets. *Front. Immunol.* **5**, 630 (2014).

28. Crotty, S. A brief history of T cell help to B cells. *Nat. Rev. Immunol.* **15**, 185–9 (2015).

29. Lin, Y., Slight, S. R. & Khader, S. A. Th17 cytokines and vaccine-induced immunity. *Semin. Immunopathol.* **32**, 79–90 (2010).

30. Kumar, P., Chen, K. & Kolls, J. K. Th17 cell based vaccines in mucosal immunity. *Curr. Opin. Immunol.* **25**, 373–80 (2013).

31. Sakaguchi, S., Miyara, M., Costantino, C. M. & Hafler, D. A. FOXP3+ regulatory T cells in the human immune system. *Nat. Rev. Immunol.* **10**, 490–500 (2010).

32. Wu, L. & KewalRamani, V. N. Dendritic-cell interactions with HIV: infection and viral dissemination. *Nat. Rev. Immunol.* **6**, 859–68 (2006).

33. Bixler, S. L. & Mattapallil, J. J. Loss and dysregulation of Th17 cells during HIV infection. *Clin. Dev. Immunol.* **2013**, 852418 (2013).

34. Luteijn Ã, R. *et al.* Early viral replication in lymph nodes provides HIV with a means by which to escape NK-cell-mediated control. doi:10.1002/eji.201040886

35. Trotter, C. L. *et al.* Optimising the use of conjugate vaccines to prevent disease caused by Haemophilus influenzae type b, Neisseria meningitidis and Streptococcus pneumoniae. *Vaccine* **26**, 4434–4445 (2008).

36. Clark, E. A. & Ledbetter, J. A. Activation of human B cells mediated through two distinct cell surface differentiation antigens, Bp35 and Bp50. *Proc. Natl. Acad. Sci. U. S. A.* **83**, 4494–8 (1986).

37. Victora, G. D. & Nussenzweig, M. C. Germinal Centers. *Annu. Rev. Immunol.* **30**, 429–457 (2012).

38. Crotty, S. Follicular helper CD4 T cells (TFH). *Annu. Rev. Immunol.* **29**, 621–63 (2011).

39. Crotty, S. T follicular helper cell differentiation, function, and roles in disease. *Immunity* **41**, 529–42 (2014).

40. Victora, G. D. & Mesin, L. Clonal and cellular dynamics in germinal centers. *Curr. Opin. Immunol.* **28**, 90–6 (2014).

41. De Silva, N. S. & Klein, U. Dynamics of B cells in germinal centres. *Nat. Rev. Immunol.* **15**, 137–48 (2015).

42. Crotty, S., Johnston, R. J. & Schoenberger, S. P. Effectors and memories: Bcl-6 and Blimp-1 in T and B lymphocyte differentiation. *Nat. Immunol.* **11**, 114–120 (2010).

43. Nojima, T. *et al.* In-vitro derived germinal centre B cells differentially generate memory B or plasma cells in vivo. *Nat. Commun.* **2**, 465 (2011).

44. Avery, D. T. *et al.* B cell-intrinsic signaling through IL-21 receptor and STAT3 is required for establishing long-lived antibody responses in humans. *J. Exp. Med.* **207**, 155–71 (2010).

45. Suto, A. *et al.* Interleukin 21 prevents antigen-induced IgE production by inhibiting germ line C(epsilon) transcription of IL-4-stimulated B cells. *Blood* **100**, 4565–73 (2002).

46. Crotty, S., Kersh, E. N., Cannons, J., Schwartzberg, P. L. & Ahmed, R. SAP is required for generating long-term humoral immunity. *Nature* **421**, 282–7 (2003).

47. McAdam, A. J. *et al.* ICOS is critical for CD40-mediated antibody class switching. *Nature* **409**, 102–5 (2001).

48. Tafuri, A. *et al.* ICOS is essential for effective T-helper-cell responses. *Nature* **409**, 105–9 (2001).

49. Dong, C., Temann, U. A. & Flavell, R. A. Cutting edge: critical role of inducible costimulator in germinal center reactions. *J. Immunol.* **166**, 3659–62 (2001).

50. Kroenke, M. A. *et al.* Bcl6 and Maf cooperate to instruct human follicular helper CD4 T cell differentiation. *J. Immunol.* **188**, 3734–44 (2012).

51. Rasheed, A.-U., Rahn, H.-P., Sallusto, F., Lipp, M. & Müller, G. Follicular B helper T cell activity is confined to CXCR5(hi)ICOS(hi) CD4 T cells and is independent of CD57 expression.

Eur. J. Immunol. **36**, 1892–903 (2006).

52. Harwood, N. E. & Batista, F. D. New Insights into the Early Molecular Events Underlying B Cell Activation. *Immunity* **28**, 609–619 (2008).

53. Hwang, J. K., Alt, F. W., Yeap, L.-S., Alt*, F. W. & Hwang*, J. K. *Related Mechanisms of Antibody Somatic Hypermutation and Class Switch Recombination*. **3**, (American Society of Microbiology, 2015).

54. Cobb, R. M., Oestreich, K. J., Osipovich, O. A. & Oltz, E. M. Accessibility Control of V(D)J Recombination. in *Advances in immunology* **91**, 45–109 (2006).

55. Schatz, D. G. & Swanson, P. C. V(D)J Recombination: Mechanisms of Initiation. *Annu. Rev. Genet.* **45**, 167–202 (2011).

56. Deriano, L. & Roth, D. B. Modernizing the Nonhomologous End-Joining Repertoire: Alternative and Classical NHEJ Share the Stage. *Annu. Rev. Genet.* **47**, 433–455 (2013).

57. Alt, F. W., Zhang, Y., Meng, F.-L., Guo, C. & Schwer, B. Mechanisms of Programmed DNA Lesions and Genomic Instability in the Immune System. *Cell* **152**, 417–429 (2013).

58. Alt, F. W. & Baltimore, D. Joining of immunoglobulin heavy chain gene segments: implications from a chromosome with evidence of three D-JH fusions. *Proc. Natl. Acad. Sci. U. S. A.* **79**, 4118–22 (1982).

59. Davis, M. M. & Bjorkman, P. J. T-cell antigen receptor genes and T-cell recognition. *Nature* **334**, 395–402 (1988).

60. Di Noia, J. M. & Neuberger, M. S. Molecular mechanisms of antibody somatic hypermutation. *Annu. Rev. Biochem.* **76**, 1–22 (2007).

61. Stewart, A. K. & Schwartz, R. S. Immunoglobulin V regions and the B cell. *Blood* **83**, 1717–30 (1994).

62. Roy, A. L., Sen, R. & Roeder, R. G. Enhancer-promoter communication and transcriptional regulation of Igh. *Trends Immunol.* **32**, 532–9 (2011).

63. Muramatsu, M., Nagaoka, H., Shinkura, R., Begum, N. A. & Honjo, T. Discovery of

activation-induced cytidine deaminase, the engraver of antibody memory. *Adv. Immunol.* **94**, 1–36 (2007).

64. Chen, K. & Cerutti, A. New insights into the enigma of immunoglobulin D. *Immunol. Rev.* **237**, 160–79 (2010).

65. Alt, F. W. *et al.* Ordered rearrangement of immunoglobulin heavy chain variable region segments. *EMBO J.* **3**, 1209–19 (1984).

66. Mostoslavsky, R., Alt, F. W. & Rajewsky, K. The Lingering Enigma of the Allelic Exclusion Mechanism. *Cell* **118**, 539–544 (2004).

67. Chaudhuri, J. *et al.* Evolution of the immunoglobulin heavy chain class switch recombination mechanism. *Adv. Immunol.* **94**, 157–214 (2007).

68. Fagarasan, S., Kawamoto, S., Kanagawa, O. & Suzuki, K. Adaptive immune regulation in the gut: T cell-dependent and T cell-independent IgA synthesis. *Annu. Rev. Immunol.* **28**, 243–73 (2010).

69. Stavnezer, J., Guikema, J. E. J. & Schrader, C. E. Mechanism and regulation of class switch recombination. *Annu. Rev. Immunol.* **26**, 261–92 (2008).

70. Muramatsu, M. *et al.* Class switch recombination and hypermutation require activation-induced cytidine deaminase (AID), a potential RNA editing enzyme. *Cell* **102**, 553–63 (2000).

71. Revy, P. *et al.* Activation-induced cytidine deaminase (AID) deficiency causes the autosomal recessive form of the Hyper-IgM syndrome (HIGM2). *Cell* **102**, 565–75 (2000).

72. Wilson, P. C. *et al.* Somatic hypermutation introduces insertions and deletions into immunoglobulin V genes. *J. Exp. Med.* **187**, 59–70 (1998).

73. Goossens, T., Klein, U. & Küppers, R. Frequent occurrence of deletions and duplications during somatic hypermutation: implications for oncogene translocations and heavy chain disease. *Proc. Natl. Acad. Sci. U. S. A.* **95**, 2463–8 (1998).

74. Rada, C. *et al.* Immunoglobulin isotype switching is inhibited and somatic hypermutation

perturbed in UNG-deficient mice. *Curr. Biol.* **12**, 1748–55 (2002).

75. Maul, R. W. & Gearhart, P. J. AID and somatic hypermutation. *Adv. Immunol.* **105**, 159–91 (2010).

76. Peled, J. U. *et al.* The biochemistry of somatic hypermutation. *Annu. Rev. Immunol.* **26**, 481–511 (2008).

77. Matthews, A. J., Zheng, S., DiMenna, L. J. & Chaudhuri, J. Regulation of immunoglobulin class-switch recombination: choreography of noncoding transcription, targeted DNA deamination, and long-range DNA repair. *Adv. Immunol.* **122**, 1–57 (2014).

78. Janeway, Travers, W. et al. Immunobiology: the immune system in health and disease. (2001). Available at: https://www.ncbi.nlm.nih.gov/books/NBK10757/?term=immunobiology the immune system in health and diseasee. (Accessed: 15th September 2018)

79. Ramesh, A. *et al.* Structure and Diversity of the Rhesus Macaque Immunoglobulin Loci through Multiple De Novo Genome Assemblies. *Front. Immunol.* **8**, 1407 (2017).

80. Lefranc, M.-P. *et al.* IMGT, the international ImMunoGeneTics information system(R). *Nucleic Acids Res.* **33**, D593–D597 (2004).

81. Forthal, D., Hope, T. J. & Alter, G. New paradigms for functional HIV-specific nonneutralizing antibodies. *Curr. Opin. HIV AIDS* **8**, 393–401 (2013).

82. Forthal, D. N. Functions of Antibodies. in *Antibodies for Infectious Diseases* **2**, 25–48 (American Society of Microbiology, 2014).

83. Nimmerjahn, F. & Ravetch, J. V. FcγRs in health and disease. *Curr. Top. Microbiol. Immunol.* **350**, 105–25 (2011).

84. Powell, M. S. & Hogarth, P. M. Fc Receptors. in *Multichain Immune Recognition Receptor Signaling* **640**, 22–34 (Springer New York, 2008).

85. Mayr, L. M., Su, B. & Moog, C. Non-Neutralizing Antibodies Directed against HIV and Their Functions. *Front. Immunol.* **8**, 1590 (2017).

86. Hidajat, R. *et al.* Correlation of vaccine-elicited systemic and mucosal nonneutralizing antibody activities with reduced acute viremia following intrarectal simian immunodeficiency virus SIVmac251 challenge of rhesus macaques. *J. Virol.* **83**, 791–801 (2009).

87. Gómez-Román, V. R. *et al.* Vaccine-elicited antibodies mediate antibody-dependent cellular cytotoxicity correlated with significantly reduced acute viremia in rhesus macaques challenged with SIVmac251. *J. Immunol.* **174**, 2185–9 (2005).

88. Alpert, M. D. *et al.* ADCC develops over time during persistent infection with live-attenuated SIV and is associated with complete protection against SIV(mac)251 challenge. *PLoS Pathog.* **8**, e1002890 (2012).

89. Vaccari, M. *et al.* HIV vaccine candidate activation of hypoxia and the inflammasome in CD14+ monocytes is associated with a decreased risk of SIVmac251 acquisition. *Nat. Med.* **24**, 847–856 (2018).

90. Kamen, L. A., Kho, E., Ordonia, B., Langsdorf, C. & Chung, S. A method for determining antibody-dependent cellular phagocytosis. *J. Immunol.* **198**, (2017).

91. Xiao, P. *et al.* Multiple vaccine-elicited nonneutralizing antienvelope antibody activities contribute to protective efficacy by reducing both acute and chronic viremia following simian/human immunodeficiency virus SHIV89.6P challenge in rhesus macaques. *J. Virol.* **84**, 7161–73 (2010).

92. Florese, R. H. *et al.* Contribution of nonneutralizing vaccine-elicited antibody activities to improved protective efficacy in rhesus macaques immunized with Tat/Env compared with multigenic vaccines. *J. Immunol.* **182**, 3718–27 (2009).

93. Takai, T. Roles of Fc receptors in autoimmunity. *Nat. Rev. Immunol.* **2**, 580–92 (2002).

94. Klasse, P. J. Modeling how many envelope glycoprotein trimers per virion participate in human immunodeficiency virus infectivity and its neutralization by antibody. *Virology* **369**, 245–62 (2007).

95. Campbell, S. M., Crowe, S. M. & Mak, J. Lipid rafts and HIV-1: from viral entry to assembly of progeny virions. *J. Clin. Virol.* **22**, 217–27 (2001).

96. Sörman, A., Zhang, L., Ding, Z. & Heyman, B. How antibodies use complement to regulate antibody responses. *Mol. Immunol.* **61**, 79–88 (2014).

97. Botto, M. *et al.* Complement in human diseases: Lessons from complement deficiencies. *Mol. Immunol.* **46**, 2774–83 (2009).

98. Carroll, M. C. & Isenman, D. E. Regulation of humoral immunity by complement. *Immunity* **37**, 199–207 (2012).

99. Rutemark, C. *et al.* Requirement for complement in antibody responses is not explained by the classic pathway activator IgM. *Proc. Natl. Acad. Sci. U. S. A.* **108**, E934-42 (2011).

100. Tegla, C. A. *et al.* Membrane attack by complement: the assembly and biology of terminal complement complexes. *Immunol. Res.* **51**, 45–60 (2011).

101. Sonnen, A. F.-P. & Henneke, P. Structural Biology of the Membrane Attack Complex. in *Sub-cellular biochemistry* **80**, 83–116 (2014).

102. Morgan, B. P. The membrane attack complex as an inflammatory trigger. *Immunobiology* **221**, 747–751 (2016).

103. MacLennan, I. C. M. Germinal Centers. *Annu. Rev. Immunol.* **12**, 117–139 (1994).

104. Jacob, J., Kelsoe, G., Rajewsky, K. & Weiss, U. Intraclonal generation of antibody mutants in germinal centres. *Nature* **354**, 389–392 (1991).

105. Berek, C., Berger, A. & Apel, M. Maturation of the immune response in germinal centers. *Cell* **67**, 1121–9 (1991).

106. Blink, E. J. *et al.* Early appearance of germinal center-derived memory B cells and plasma cells in blood after primary immunization. *J. Exp. Med.* **201**, 545–54 (2005).

107. Batista, F. D. & Harwood, N. E. The who, how and where of antigen presentation to B cells. *Nat. Rev. Immunol.* **9**, 15–27 (2009).

108. Okada, T. *et al.* Antigen-engaged B cells undergo chemotaxis toward the T zone and form motile conjugates with helper T cells. *PLoS Biol.* **3**, e150 (2005).

109. Qi, H., Cannons, J. L., Klauschen, F., Schwartzberg, P. L. & Germain, R. N. SAP-controlled T-B cell interactions underlie germinal centre formation. *Nature* **455**, 764–9 (2008).

110. Kerfoot, S. M. *et al.* Germinal center B cell and T follicular helper cell development initiates in the interfollicular zone. *Immunity* **34**, 947–60 (2011).

111. Kitano, M. *et al.* Bcl6 protein expression shapes pre-germinal center B cell dynamics and follicular helper T cell heterogeneity. *Immunity* **34**, 961–72 (2011).

112. Choi, Y. S. *et al.* ICOS receptor instructs T follicular helper cell versus effector cell differentiation via induction of the transcriptional repressor Bcl6. *Immunity* **34**, 932–46 (2011).

113. Baumjohann, D., Okada, T. & Ansel, K. M. Cutting Edge: Distinct waves of BCL6 expression during T follicular helper cell development. *J. Immunol.* **187**, 2089–92 (2011).

114. Masciarelli, S. & Sitia, R. Building and operating an antibody factory: Redox control during B to plasma cell terminal differentiation. *Biochim. Biophys. Acta - Mol. Cell Res.* **1783**, 578–588 (2008).

115. Allen, C. D. C. *et al.* Germinal center dark and light zone organization is mediated by CXCR4 and CXCR5. *Nat. Immunol.* **5**, 943–52 (2004).

116. Bannard, O. *et al.* Germinal center centroblasts transition to a centrocyte phenotype according to a timed program and depend on the dark zone for effective selection. *Immunity* **39**, 912–24 (2013).

117. Victora, G. D. *et al.* Identification of human germinal center light and dark zone cells and their relationship to human B-cell lymphomas. *Blood* **120**, 2240–8 (2012).

118. Victora, G. D. *et al.* Germinal center dynamics revealed by multiphoton microscopy with a photoactivatable fluorescent reporter. *Cell* **143**, 592–605 (2010).

119. Shulman, Z. *et al.* Dynamic signaling by T follicular helper cells during germinal center B

cell selection. *Science* **345**, 1058–62 (2014).

120. Khalil, A. M., Cambier, J. C. & Shlomchik, M. J. B cell receptor signal transduction in the GC is short-circuited by high phosphatase activity. *Science* **336**, 1178–81 (2012).

121. Gitlin, A. D., Shulman, Z. & Nussenzweig, M. C. Clonal selection in the germinal centre by regulated proliferation and hypermutation. *Nature* **509**, 637–640 (2014).

122. Zhang, Y. *et al.* Germinal center B cells govern their own fate via antibody feedback. *J. Exp. Med.* **210**, 457–64 (2013).

123. Shulman, Z. *et al.* T follicular helper cell dynamics in germinal centers. *Science* **341**, 673–7 (2013).

124. Schwickert, T. A., Alabyev, B., Manser, T. & Nussenzweig, M. C. Germinal center reutilization by newly activated B cells. *J. Exp. Med.* **206**, 2907–14 (2009).

125. Ahmed, R. & Gray, D. Immunological memory and protective immunity: understanding their relation. *Science* **272**, 54–60 (1996).

126. Anderson, S. M., Tomayko, M. M., Ahuja, A., Haberman, A. M. & Shlomchik, M. J. New markers for murine memory B cells that define mutated and unmutated subsets. *J. Exp. Med.* **204**, 2103–2114 (2007).

127. Kaji, T. *et al.* Distinct cellular pathways select germline-encoded and somatically mutated antibodies into immunological memory. *J. Exp. Med.* **209**, 2079–97 (2012).

128. Klein, U., Küppers, R. & Rajewsky, K. Evidence for a large compartment of IgM-expressing memory B cells in humans. *Blood* **89**, 1288–98 (1997).

129. Dogan, I. *et al.* Multiple layers of B cell memory with different effector functions. *Nat. Immunol.* **10**, 1292–1299 (2009).

130. Pape, K. A., Taylor, J. J., Maul, R. W., Gearhart, P. J. & Jenkins, M. K. Different B cell populations mediate early and late memory during an endogenous immune response. *Science* **331**, 1203–7 (2011).

131. Takemori, T., Kaji, T., Takahashi, Y., Shimoda, M. & Rajewsky, K. Generation of memory

B cells inside and outside germinal centers. *Eur. J. Immunol.* **44**, 1258–64 (2014).

132. Alugupalli, K. R. *et al.* B1b Lymphocytes Confer T Cell-Independent Long-Lasting Immunity. *Immunity* **21**, 379–390 (2004).

133. Obukhanych, T. V. & Nussenzweig, M. C. T-independent type II immune responses generate memory B cells. *J. Exp. Med.* **203**, 305–310 (2006).

134. Yang, Y. *et al.* Antigen-specific memory in B-1a and its relationship to natural immunity. *Proc. Natl. Acad. Sci.* **109**, 5388–5393 (2012).

135. Montecino-Rodriguez, E. & Dorshkind, K. B-1 B Cell Development in the Fetus and Adult. *Immunity* **36**, 13–21 (2012).

136. Haas, K. M., Poe, J. C., Steeber, D. A. & Tedder, T. F. B-1a and B-1b cells exhibit distinct developmental requirements and have unique functional roles in innate and adaptive immunity to S. pneumoniae. *Immunity* **23**, 7–18 (2005).

137. Tarlinton, D. & Good-Jacobson, K. Diversity among memory B cells: origin, consequences, and utility. *Science* **341**, 1205–11 (2013).

138. Berek, C. The development of B cells and the B-cell repertoire in the microenvironment of the germinal center. *Immunol. Rev.* **126**, 5–19 (1992).

139. Gould, H. J. & Sutton, B. J. IgE in allergy and asthma today. *Nat. Rev. Immunol.* **8**, 205–17 (2008).

140. Xiong, H., Dolpady, J., Wabl, M., Curotto de Lafaille, M. A. & Lafaille, J. J. Sequential class switching is required for the generation of high affinity IgE antibodies. *J. Exp. Med.* **209**, 353–64 (2012).

141. Luckey, C. J. *et al.* Memory T and memory B cells share a transcriptional program of self-renewal with long-term hematopoietic stem cells. *Proc. Natl. Acad. Sci. U. S. A.* **103**, 3304–9 (2006).

142. Barrington, R. A., Pozdnyakova, O., Zafari, M. R., Benjamin, C. D. & Carroll, M. C. B lymphocyte memory: role of stromal cell complement and FcgammaRIIB receptors. *J. Exp.*

Med. **196**, 1189–99 (2002).

143. Hikida, M. *et al.* PLC-γ2 is essential for formation and maintenance of memory B cells. *J. Exp. Med.* **206**, 681–689 (2009).

144. Maruyama, M., Lam, K. P. & Rajewsky, K. Memory B-cell persistence is independent of persisting immunizing antigen. *Nature* **407**, 636–42 (2000).

145. Yu, X. *et al.* Neutralizing antibodies derived from the B cells of 1918 influenza pandemic survivors. *Nature* **455**, 532–6 (2008).

146. Kometani, K. *et al.* Repression of the transcription factor Bach2 contributes to predisposition of IgG1 memory B cells toward plasma cell differentiation. *Immunity* **39**, 136–47 (2013).

147. Martin, S. W. & Goodnow, C. C. Burst-enhancing role of the IgG membrane tail as a molecular determinant of memory. *Nat. Immunol.* **3**, 182–8 (2002).

148. Hebeis, B. J. *et al.* Activation of virus-specific memory B cells in the absence of T cell help. *J. Exp. Med.* **199**, 593–602 (2004).

149. Aiba, Y. *et al.* Preferential localization of IgG memory B cells adjacent to contracted germinal centers. *Proc. Natl. Acad. Sci. U. S. A.* **107**, 12192–7 (2010).

150. Schaerli, P. *et al.* CXC chemokine receptor 5 expression defines follicular homing T cells with B cell helper function. *J. Exp. Med.* **192**, 1553–62 (2000).

151. Kim, C. H. *et al.* Subspecialization of CXCR5+ T cells: B helper activity is focused in a germinal center-localized subset of CXCR5+ T cells. *J. Exp. Med.* **193**, 1373–81 (2001).

152. MacLeod, M. K. L. *et al.* Memory CD4 T cells that express CXCR5 provide accelerated help to B cells. *J. Immunol.* **186**, 2889–96 (2011).

153. Weber, J. P., Fuhrmann, F. & Hutloff, A. T-follicular helper cells survive as long-term memory cells. *Eur. J. Immunol.* **42**, 1981–1988 (2012).

154. Hale, J. S. *et al.* Distinct Memory CD4+ T Cells with Commitment to T Follicular Helper- and T Helper 1-Cell Lineages Are Generated after Acute Viral Infection. *Immunity* **38**, 805–817

(2013).

155. Ise, W. *et al.* Memory B cells contribute to rapid Bcl6 expression by memory follicular helper T cells. *Proc. Natl. Acad. Sci. U. S. A.* **111**, 11792–7 (2014).

156. Shimoda, M., Li, T., Pihkala, J. P. S. & Koni, P. A. Role of MHC class II on memory B cells in post-germinal center B cell homeostasis and memory response. *J. Immunol.* **176**, 2122–33 (2006).

157. Heesters, B. A. *et al.* Endocytosis and recycling of immune complexes by follicular dendritic cells enhances B cell antigen binding and activation. *Immunity* **38**, 1164–75 (2013).

158. Weill, J.-C., Le Gallou, S., Hao, Y. & Reynaud, C.-A. Multiple players in mouse B cell memory. *Curr. Opin. Immunol.* **25**, 334–8 (2013).

159. Kardava, L. *et al.* Attenuation of HIV-associated human B cell exhaustion by siRNA downregulation of inhibitory receptors. *J. Clin. Invest.* **121**, 2614–24 (2011).

160. Centers for Disease Control (CDC). Kaposi's sarcoma and Pneumocystis pneumonia among homosexual men--New York City and California. *MMWR. Morb. Mortal. Wkly. Rep.* **30**, 305–8 (1981).

161. Greene, W. C. A history of AIDS: looking back to see ahead. *Eur. J. Immunol.* **37 Suppl 1**, S94-102 (2007).

162. Barré-Sinoussi, F. *et al.* Isolation of a T-lymphotropic retrovirus from a patient at risk for acquired immune deficiency syndrome (AIDS). (1983).

163. Gallo, R. C. *et al.* Frequent detection and isolation of cytopathic retroviruses (HTLV-III) from patients with AIDS and at risk for AIDS. *Science (80-.).* **224**, 500–503 (1984).

164. Popovic, M., Sarngadharan, M. G., Read, E. & Gallo, R. C. Detection, isolation, and continuous production of cytopathic retroviruses (HTLV-III) from patients with AIDS and pre-AIDS. *Science* **224**, 497–500 (1984).

165. Hladik, F. & McElrath, M. J. Setting the stage: host invasion by HIV. **8**, (2008).

166. Cohen, M. S., Shaw, G. M., McMichael, A. J. & Haynes, B. F. Acute HIV-1 Infection. *N. Engl.*

J. Med. **364**, 1943–1954 (2011).

167. UNAIDS. WHO | Global AIDS Update | UNAIDS. *WHO* (2016).

168. Clavel, F. *et al.* Isolation of a new human retrovirus from West African patients with AIDS. *Science* **233**, 343–6 (1986).

169. Chakrabarti, L. *et al.* Sequence of simian immunodeficiency virus from macaque and its relationship to other human and simian retroviruses. *Nature* **328**, (1987).

170. Guyader, M. *et al.* Genome organization and transactivation of the human immunodeficiency virus type 2. *Nature* **326**, 662–9 (1987).

171. Sharp, P. M. & Hahn, B. H. Origins of HIV and the AIDS Pandemic. *Cold Spring Harb. Perspect. Med.* **1**, a006841–a006841 (2011).

172. Huet, T., Cheynier, R., Meyerhans, A., Roelants, G. & Wain-Hobson, S. Genetic organization of a chimpanzee lentivirus related to HIV-1. *Nature* **345**, 356–9 (1990).

173. Hirsch, V. M., Olmsted, R. A., Murphey-Corb, M., Purcell, R. H. & Johnson, P. R. An African primate lentivirus (SIVsmclosely related to HIV-2. *Nature* **339**, 389–392 (1989).

174. Apetrei, C. *et al.* Molecular Epidemiology of Simian Immunodeficiency Virus SIVsm in U.S. Primate Centers Unravels the Origin of SIVmac and SIVstm. *J. Virol.* **79**, 8991–9005 (2005).

175. Apetrei, C. *et al.* Kuru experiments triggered the emergence of pathogenic SIVmac. *AIDS* **20**, 317–21 (2006).

176. Hahn, B. H., Shaw, G. M., De Cock, K. M. & Sharp, P. M. AIDS as a zoonosis: scientific and public health implications. *Science* **287**, 607–14 (2000).

177. Fabre, P.-. H., Rodrigues, A. & Douzery, E. J. P. Patterns of macroevolution among Primates inferred from a supermatrix of mitochondrial and nuclear DNA. *Mol. Phylogenet. Evol.* **53**, 808–825 (2009).

178. Takehisa, J. *et al.* Origin and Biology of Simian Immunodeficiency Virus in Wild-Living Western Gorillas. *J. Virol.* **83**, 1635–1648 (2009).

179. Heeney, J. L., Dalgleish, A. G. & Weiss, R. A. Origins of HIV and the Evolution of Resistance to AIDS. *Science (80-.).* **313**, 462–466 (2006).

180. Heeney, J. L. AIDS: a disease of impaired Th-cell renewal? *Immunol. Today* **16**, 515–20 (1995).

181. Rutjens, E. *et al.* Lentivirus infections and mechanisms of disease resistance in chimpanzees. *Front. Biosci.* **8**, d1134-45 (2003).

182. Gougeon, M. L. *et al.* Lack of chronic immune activation in HIV-infected chimpanzees correlates with the resistance of T cells to Fas/Apo-1 (CD95)-induced apoptosis and preservation of a T helper 1 phenotype. *J. Immunol.* **158**, 2964–76 (1997).

183. Copeland, K. F. & Heeney, J. L. T helper cell activation and human retroviral pathogenesis. *Microbiol. Rev.* **60**, 722–42 (1996).

184. Balla-Jhagjhoorsingh, S. S. *et al.* Conserved CTL epitopes shared between HIV-infected human long-term survivors and chimpanzees. *J. Immunol.* **162**, 2308–14 (1999).

185. de Groot, N. G. *et al.* Evidence for an ancient selective sweep in the MHC class I gene repertoire of chimpanzees. *Proc. Natl. Acad. Sci. U. S. A.* **99**, 11748–53 (2002).

186. Kiepiela, P. *et al.* Dominant influence of HLA-B in mediating the potential co-evolution of HIV and HLA. *Nature* **432**, 769–75 (2004).

187. ten Haaft, P. *et al.* Differences in early virus loads with different phenotypic variants of HIV-1 and SIV(cpz) in chimpanzees. *AIDS* **15**, 2085–92 (2001).

188. De Leys, R. *et al.* Isolation and partial characterization of an unusual human immunodeficiency retrovirus from two persons of west-central African origin. *J. Virol.* **64**, 1207–16 (1990).

189. Gürtler, L. G. *et al.* A new subtype of human immunodeficiency virus type 1 (MVP-5180) from Cameroon. *J. Virol.* **68**, 1581–5 (1994).

190. Mauclère, P. *et al.* Serological and virological characterization of HIV-1 group O infection in Cameroon. *AIDS* **11**, 445–53 (1997).

191. Peeters, M. *et al.* Geographical distribution of HIV-1 group O viruses in Africa. *AIDS* **11**, 493–8 (1997).

192. Simon, F. *et al.* Identification of a new human immunodeficiency virus type 1 distinct from group M and group O. *Nat. Med.* **4**, 1032–7 (1998).

193. Vallari, A. *et al.* Four new HIV-1 group N isolates from Cameroon: Prevalence continues to be low. *AIDS Res. Hum. Retroviruses* **26**, 109–15 (2010).

194. Plantier, J.-C. *et al.* A new human immunodeficiency virus derived from gorillas. *Nat. Med.* **15**, 871–2 (2009).

195. Peeters, M. *et al.* Risk to Human Health from a Plethora of Simian Immunodeficiency Viruses in Primate Bushmeat. *Emerg. Infect. Dis.* **8**, 451–457 (2002).

196. Korber, B. *et al.* Timing the ancestor of the HIV-1 pandemic strains. *Science* **288**, 1789–96 (2000).

197. Lemey, P. *et al.* The Molecular Population Genetics of HIV-1 Group O. *Genetics* **167**, 1059–1068 (2004).

198. Worobey, M. *et al.* Origin of AIDS: contaminated polio vaccine theory refuted. *Nature* **428**, 820 (2004).

199. Li, W. H., Tanimura, M. & Sharp, P. M. Rates and dates of divergence between AIDS virus nucleotide sequences. *Mol. Biol. Evol.* **5**, 313–30 (1988).

200. Lemey, P., Rambaut, A. & Pybus, O. G. HIV evolutionary dynamics within and among hosts. *AIDS Rev.* **8**, 125–40

201. Ho, D. D. *et al.* Rapid turnover of plasma virions and CD4 lymphocytes in HIV-1 infection. *Nature* **373**, 123–126 (1995).

202. Wei, X. *et al.* Viral dynamics in human immunodeficiency virus type 1 infection. *Nature* **373**, 117–122 (1995).

203. Vidal, N. *et al.* Unprecedented degree of human immunodeficiency virus type 1 (HIV-1) group M genetic diversity in the Democratic Republic of Congo suggests that the HIV-1

pandemic originated in Central Africa. *J. Virol.* **74**, 10498–507 (2000).

204. Taylor, B. S. & Hammer, S. M. The Challenge of HIV-1 Subtype Diversity. *N. Engl. J. Med.* **359**, 1965–1966 (2008).

205. Gilbert, M. T. P. *et al.* The emergence of HIV/AIDS in the Americas and beyond. *Proc. Natl. Acad. Sci. U. S. A.* **104**, 18566–70 (2007).

206. Atlas - Map - Hiv-1 Global Distribution - 2003 IAVI Report. Available at: https://www.pbs.org/wgbh/pages/frontline/aids/atlas/clade.html. (Accessed: 27th February 2019)

207. WHO. HIV/AIDS: Global situation and trends. *WHO* (2017).

208. Atta, M. G., De Seigneux, S. & Lucas, G. M. Clinical Pharmacology in HIV Therapy. *Clin. J. Am. Soc. Nephrol.* CJN.02240218 (2018). doi:10.2215/CJN.02240218

209. Günthard, H. F. *et al.* Antiretroviral Drugs for Treatment and Prevention of HIV Infection in Adults: 2016 Recommendations of the International Antiviral Society-USA Panel. *JAMA* **316**, 191–210 (2016).

210. Starting antiretroviral treatment for HIV | AVERT. Available at: https://www.avert.org/living-with-hiv/starting-treatment. (Accessed: 27th February 2019)

211. Antiretroviral Therapy Cohort Collaboration. Life expectancy of individuals on combination antiretroviral therapy in high-income countries: a collaborative analysis of 14 cohort studies. *Lancet* **372**, 293–299 (2008).

212. Katz, I. T. & Maughan-Brown, B. Improved life expectancy of people living with HIV: who is left behind? *lancet. HIV* **4**, e324–e326 (2017).

213. Cohen, M. S. *et al.* Prevention of HIV-1 infection with early antiretroviral therapy. *N. Engl. J. Med.* **365**, 493–505 (2011).

214. TEMPRANO ANRS 12136 Study Group *et al.* A Trial of Early Antiretrovirals and Isoniazid Preventive Therapy in Africa. *N. Engl. J. Med.* **373**, 808–22 (2015).

215. INSIGHT START Study Group *et al.* Initiation of Antiretroviral Therapy in Early Asymptomatic HIV Infection. *N. Engl. J. Med.* **373**, 795–807 (2015).

216. Haberer, J. E. *et al.* Real-Time Adherence Monitoring for HIV Antiretroviral Therapy. *AIDS Behav.* **14**, 1340–1346 (2010).

217. UNAIDS and Médecins Sans Frontières 2015. Community-Based Antiretroviral Therapy Delivery. (2015).

218. Mills, E. J. *et al.* Life expectancy of persons receiving combination antiretroviral therapy in low-income countries: a cohort analysis from Uganda. *Ann. Intern. Med.* **155**, 209–16 (2011).

219. Losina, E. *et al.* Racial and sex disparities in life expectancy losses among HIV-infected persons in the united states: impact of risk behavior, late initiation, and early discontinuation of antiretroviral therapy. *Clin. Infect. Dis.* **49**, 1570–8 (2009).

220. Samji, H. *et al.* Closing the gap: increases in life expectancy among treated HIV-positive individuals in the United States and Canada. *PLoS One* **8**, e81355 (2013).

221. Guaraldi, G., Prakash, M., Moecklinghoff, C. & Stellbrink, H.-J. Morbidity in older HIV-infected patients: impact of long-term antiretroviral use. *AIDS Rev.* **16**, 75–89

222. Guaraldi, G., Silva, A. R. & Stentarelli, C. Multimorbidity and functional status assessment. *Curr. Opin. HIV AIDS* **9**, 386–397 (2014).

223. Nasi, M., Pinti, M., Mussini, C. & Cossarizza, A. Persistent inflammation in HIV infection: established concepts, new perspectives. *Immunol. Lett.* **161**, 184–8 (2014).

224. Nasi, M. *et al.* Ageing and inflammation in patients with HIV infection. *Clin. Exp. Immunol.* **187**, 44–52 (2017).

225. Deeks, S. G. HIV infection, inflammation, immunosenescence, and aging. *Annu. Rev. Med.* **62**, 141–55 (2011).

226. Franceschi, C. Inflammaging as a major characteristic of old people: can it be prevented or cured? *Nutr. Rev.* **65**, S173-6 (2007).

227. Minciullo, P. L. *et al.* Inflammaging and Anti-Inflammaging: The Role of Cytokines in Extreme Longevity. *Arch. Immunol. Ther. Exp. (Warsz).* **64**, 111–126 (2016).

228. Justice, A. C. HIV and aging: time for a new paradigm. *Curr. HIV/AIDS Rep.* **7**, 69–76 (2010).

229. Sattentau, Q. Envelope Glycoprotein Trimers as HIV-1 Vaccine Immunogens. *Vaccines* **1**, 497–512 (2013).

230. Kwong, P. D. *et al.* Structure of an HIV gp120 envelope glycoprotein in complex with the CD4 receptor and a neutralizing human antibody. *Nature* **393**, 648–659 (1998).

231. Arthos, J. *et al.* HIV-1 envelope protein binds to and signals through integrin alpha4beta7, the gut mucosal homing receptor for peripheral T cells. **9**, (2008).

232. Kwong, P. D. *et al.* HIV-1 evades antibody-mediated neutralization through conformational masking of receptor-binding sites. *Nature* **420**, 678–82 (2002).

233. Wilen, C. B., Tilton, J. C. & Doms, R. W. HIV: Cell Binding and Entry. *Cold Spring Harb. Perspect. Med.* **2**, a006866–a006866 (2012).

234. Blumenthal, R., Durell, S. & Viard, M. HIV Entry and Envelope Glycoprotein-mediated Fusion. *J. Biol. Chem.* **287**, 40841–40849 (2012).

235. Klasse, P. J. Neutralization of Virus Infectivity by Antibodies: Old Problems in New Perspectives. *Adv. Biol.* **2014**, 1–24 (2014).

236. Mascola, J. R. & Haynes, B. F. HIV-1 neutralizing antibodies: understanding nature's pathways. *Immunol. Rev.* **254**, 225–44 (2013).

237. Robbins, J. B., Schneerson, R. & Szu, S. C. Perspective: hypothesis: serum IgG antibody is sufficient to confer protection against infectious diseases by inactivating the inoculum. *J. Infect. Dis.* **171**, 1387–98 (1995).

238. Plotkin, S. A. Vaccines: correlates of vaccine-induced immunity. *Clin. Infect. Dis.* **47**, 401–9 (2008).

239. Amanna, I. J., Messaoudi, I. & Slifka, M. K. Protective immunity following vaccination: how is it defined? *Hum. Vaccin.* **4**, 316–9

240. Shibata, R. *et al.* Neutralizing antibody directed against the HIV-1 envelope glycoprotein can completely block HIV-1/SIV chimeric virus infections of macaque monkeys. *Nat. Med.* **5**, 204–10 (1999).

241. Montefiori, D. C. & Mascola, J. R. Neutralizing antibodies against HIV-1: can we elicit them with vaccines and how much do we need? *Curr. Opin. HIV AIDS* **4**, 347–51 (2009).

242. Mascola, J. R. *et al.* Protection of macaques against vaginal transmission of a pathogenic HIV-1/SIV chimeric virus by passive infusion of neutralizing antibodies. *Nat. Med.* **6**, 207–10 (2000).

243. Stamatatos, L., Morris, L., Burton, D. R. & Mascola, J. R. Neutralizing antibodies generated during natural HIV-1 infection: good news for an HIV-1 vaccine? *Nat. Med.* **15**, 866–870 (2009).

244. Liao, H.-X. *et al.* Co-evolution of a broadly neutralizing HIV-1 antibody and founder virus. *Nature* **496**, 469–476 (2013).

245. Pegu, A., Hessell, A. J., Mascola, J. R. & Haigwood, N. L. Use of broadly neutralizing antibodies for HIV-1 prevention. *Immunol. Rev.* **275**, 296–312 (2017).

246. Mascola, J. R. *et al.* Protection of Macaques against pathogenic simian/human immunodeficiency virus 89.6PD by passive transfer of neutralizing antibodies. *J. Virol.* **73**, 4009–18 (1999).

247. Parren, P. W. *et al.* Antibody protects macaques against vaginal challenge with a pathogenic R5 simian/human immunodeficiency virus at serum levels giving complete neutralization in vitro. *J. Virol.* **75**, 8340–7 (2001).

248. Hessell, A. J. *et al.* Fc receptor but not complement binding is important in antibody protection against HIV. *Nature* **449**, 101–4 (2007).

249. McCoy, L. E. The expanding array of HIV broadly neutralizing antibodies. *Retrovirology* **15**, 70 (2018).

250. Pantophlet, R. & Burton, D. R. GP120: target for neutralizing HIV-1 antibodies. *Annu. Rev.*

Immunol. **24**, 739–69 (2006).

251. Craigie, R. & Bushman, F. D. HIV DNA Integration. *Cold Spring Harb. Perspect. Med.* **2**, a006890–a006890 (2012).

252. Hu, W.-S. & Hughes, S. H. HIV-1 Reverse Transcription. *Cold Spring Harb. Perspect. Med.* **2**, a006882–a006882 (2012).

253. Hughes, S. H. & Coffin, J. M. What Integration Sites Tell Us about HIV Persistence. *Cell Host Microbe* **19**, 588–98 (2016).

254. Siliciano, R. F. & Greene, W. C. HIV Latency. *Cold Spring Harb. Perspect. Med.* **1**, a007096–a007096 (2011).

255. Cao, J. *et al.* Replication and neutralization of human immunodeficiency virus type 1 lacking the V1 and V2 variable loops of the gp120 envelope glycoprotein. *J. Virol.* **71**, 9808–12 (1997).

256. Shioda, T., Levy, J. A. & Cheng-Mayer, C. Small amino acid changes in the V3 hypervariable region of gp120 can affect the T-cell-line and macrophage tropism of human immunodeficiency virus type 1. *Proc. Natl. Acad. Sci. U. S. A.* **89**, 9434–8 (1992).

257. Labrosse, B., Treboute, C., Brelot, A. & Alizon, M. Cooperation of the V1/V2 and V3 domains of human immunodeficiency virus type 1 gp120 for interaction with the CXCR4 receptor. *J. Virol.* **75**, 5457–64 (2001).

258. Trkola, A. *et al.* CD4-dependent, antibody-sensitive interactions between HIV-1 and its co-receptor CCR-5. *Nature* **384**, 184–7 (1996).

259. Hill, C. M. *et al.* The Amino Terminus of Human CCR5 Is Required for Its Function as a Receptor for Diverse Human and Simian Immunodeficiency Virus Envelope Glycoproteins. *Virology* **248**, 357–371 (1998).

260. Sharon, M. *et al.* Alternative conformations of HIV-1 V3 loops mimic beta hairpins in chemokines, suggesting a mechanism for coreceptor selectivity. *Structure* **11**, 225–36 (2003).

261. Cardozo, T. *et al.* Structural Basis for Coreceptor Selectivity by The HIV Type 1 V3 Loop. *AIDS Res. Hum. Retroviruses* **23**, 415–426 (2007).

262. Gaschen, B. *et al.* Diversity considerations in HIV-1 vaccine selection. *Science* **296**, 2354–60 (2002).

263. Wei, X. *et al.* Antibody neutralization and escape by HIV-1. *Nature* **422**, 307–312 (2003).

264. Sagar, M., Wu, X., Lee, S. & Overbaugh, J. Human immunodeficiency virus type 1 V1-V2 envelope loop sequences expand and add glycosylation sites over the course of infection, and these modifications affect antibody neutralization sensitivity. *J. Virol.* **80**, 9586–98 (2006).

265. Derdeyn, C. A. *et al.* Envelope-constrained neutralization-sensitive HIV-1 after heterosexual transmission. *Science* **303**, 2019–22 (2004).

266. Ly, A. & Stamatatos, L. V2 loop glycosylation of the human immunodeficiency virus type 1 SF162 envelope facilitates interaction of this protein with CD4 and CCR5 receptors and protects the virus from neutralization by anti-V3 loop and anti-CD4 binding site antibodies. *J. Virol.* **74**, 6769–76 (2000).

267. Wyatt, R. *et al.* The antigenic structure of the HIV gp120 envelope glycoprotein. *Nature* **393**, 705–711 (1998).

268. DULBECCO, R., VOGT, M. & STRICKLAND, A. G. A study of the basic aspects of neutralization of two animal viruses, western equine encephalitis virus and poliomyelitis virus. *Virology* **2**, 162–205 (1956).

269. Sautto, G. *et al.* Anti-hepatitis C virus E2 (HCV/E2) glycoprotein monoclonal antibodies and neutralization interference. **96**, (2012).

270. To, K. K. W. *et al.* High titer and avidity of nonneutralizing antibodies against influenza vaccine antigen are associated with severe influenza. *Clin. Vaccine Immunol.* **19**, 1012–8 (2012).

271. Zhong, L. *et al.* Antibody-mediated synergy and interference in the neutralization of SARS-

CoV at an epitope cluster on the spike protein. *Biochem. Biophys. Res. Commun.* **390**, 1056–60 (2009).

272. Tripp, R. A. *et al.* Monoclonal antibodies to SARS-associated coronavirus (SARS-CoV): identification of neutralizing and antibodies reactive to S, N, M and E viral proteins. *J. Virol. Methods* **128**, 21–8 (2005).

273. Verrier, F., Nádas, A., Gorny, M. K. & Zolla-Pazner, S. Additive effects characterize the interaction of antibodies involved in neutralization of the primary dualtropic human immunodeficiency virus type 1 isolate 89.6. *J. Virol.* **75**, 9177–86 (2001).

274. Picker, L. J., Hansen, S. G. & Lifson, J. D. New paradigms for HIV/AIDS vaccine development. *Annu. Rev. Med.* **63**, 95–111 (2012).

275. Barouch, D. H. *et al.* Vaccine protection against acquisition of neutralization-resistant SIV challenges in rhesus monkeys. *Nature* **482**, 89–93 (2012).

276. Day, T. A. & Kublin, J. G. Lessons learned from HIV vaccine clinical efficacy trials. *Curr. HIV Res.* **11**, 441–9 (2013).

277. Flynn, N. M. *et al.* Placebo-controlled phase 3 trial of a recombinant glycoprotein 120 vaccine to prevent HIV-1 infection. *J. Infect. Dis.* **191**, 654–65 (2005).

278. Pitisuttithum, P. *et al.* Randomized, double-blind, placebo-controlled efficacy trial of a bivalent recombinant glycoprotein 120 HIV-1 vaccine among injection drug users in Bangkok, Thailand. *J. Infect. Dis.* **194**, 1661–71 (2006).

279. Gilbert, P. B. *et al.* Correlation between immunologic responses to a recombinant glycoprotein 120 vaccine and incidence of HIV-1 infection in a phase 3 HIV-1 preventive vaccine trial. *J. Infect. Dis.* **191**, 666–77 (2005).

280. Hessell, A. J. *et al.* Broadly neutralizing monoclonal antibodies 2F5 and 4E10 directed against the human immunodeficiency virus type 1 gp41 membrane-proximal external region protect against mucosal challenge by simian-human immunodeficiency virus SHIVBa-L. *J. Virol.* **84**, 1302–13 (2010).

281. Gilbert, P. *et al.* Magnitude and breadth of a nonprotective neutralizing antibody response in an efficacy trial of a candidate HIV-1 gp120 vaccine. *J. Infect. Dis.* **202**, 595–605 (2010).

282. Buchbinder, S. P. *et al.* Efficacy assessment of a cell-mediated immunity HIV-1 vaccine (the Step Study): a double-blind, randomised, placebo-controlled, test-of-concept trial. *Lancet (London, England)* **372**, 1881–1893 (2008).

283. Gray, G. E. *et al.* Safety and efficacy of the HVTN 503/Phambili Study of a clade-B-based HIV-1 vaccine in South Africa: a double-blind, randomised, placebo-controlled test-of-concept phase 2b study. *Lancet Infect. Dis.* **11**, 507–515 (2011).

284. Rolland, M. *et al.* Genetic impact of vaccination on breakthrough HIV-1 sequences from the STEP trial. *Nat. Med.* **17**, 366–71 (2011).

285. Kublin, J. G. *et al.* HIV Vaccine Trials Network: activities and achievements of the first decade and beyond. *Clin. Investig. (Lond).* **2**, 245–254 (2012).

286. Rerks-Ngarm, S. *et al.* Vaccination with ALVAC and AIDSVAX to Prevent HIV-1 Infection in Thailand. *N. Engl. J. Med.* **361**, 2209–2220 (2009).

287. Vaccari, M., Poonam, P. & Franchini, G. Phase III HIV vaccine trial in Thailand: a step toward a protective vaccine for HIV. *Expert Rev. Vaccines* **9**, 997–1005 (2010).

288. NIAID. 08 Report on the global AIDS epidemic. (2008).

289. Phanuphak, P., Locharernkul, C., Panmuong, W. & Wilde, H. A report of three cases of AIDS in Thailand. *Asian Pacific J. allergy Immunol.* **3**, 195–9 (1985).

290. Markowitz, L. E. *et al.* Feasibility of a preventive HIV-1 vaccine cohort among persons attending sexually transmitted disease clinics in Thailand. *J. Acquir. Immune Defic. Syndr. Hum. Retrovirol.* **20**, 488–94 (1999).

291. Kitayaporn, D. *et al.* Infection with HIV-1 subtypes B and E in injecting drug users screened for enrollment into a prospective cohort in Bangkok, Thailand. *J. Acquir. Immune Defic. Syndr. Hum. Retrovirol.* **19**, 289–95 (1998).

292. Xiridou, M. *et al.* The spread of HIV-1 subtypes B and CRF01_AE among injecting drug users

in Bangkok, Thailand. *J. Acquir. Immune Defic. Syndr.* **45**, 468–75 (2007).

293. Klein, M. AIDS and HIV vaccines. *Vaccine* **17 Suppl 2**, S65-70 (1999).

294. Paoletti, E., Tartaglia, J. & Taylor, J. Safe and effective poxvirus vectors--NYVAC and ALVAC. *Dev. Biol. Stand.* **82**, 65–9 (1994).

295. Paoletti, E., Taylor, J., Meignier, B., Meric, C. & Tartaglia, J. Highly attenuated poxvirus vectors: NYVAC, ALVAC and TROVAC. *Dev. Biol. Stand.* **84**, 159–63 (1995).

296. Baxby, D. & Paoletti, E. Potential use of non-replicating vectors as recombinant vaccines. *Vaccine* **10**, 8–9 (1992).

297. Plotkin, S. A. *et al.* The safety and use of canarypox vectored vaccines. *Dev. Biol. Stand.* **84**, 165–70 (1995).

298. FRANCHINI, G., BENSON, J., GALLO, R., PAOLETTI, E. & TARTAGLIA, J. Attenuated Poxvirus Vectors as Carriers in Vaccines against Human T Cell Leukemia-Lymphoma Virus Type I. *AIDS Res. Hum. Retroviruses* **12**, 407–408 (1996).

299. Taylor, J. *et al.* Biological and immunogenic properties of a canarypox-rabies recombinant, ALVAC-RG (vCP65) in non-avian species. *Vaccine* **13**, 539–49 (1995).

300. Egan, M. A. *et al.* Induction of human immunodeficiency virus type 1 (HIV-1)-specific cytolytic T lymphocyte responses in seronegative adults by a nonreplicating, host-range-restricted canarypox vector (ALVAC) carrying the HIV-1MN env gene. *J. Infect. Dis.* **171**, 1623–7 (1995).

301. Clements-Mann, M. L. *et al.* Immune responses to human immunodeficiency virus (HIV) type 1 induced by canarypox expressing HIV-1MN gp120, HIV-1SF2 recombinant gp120, or both vaccines in seronegative adults. NIAID AIDS Vaccine Evaluation Group. *J. Infect. Dis.* **177**, 1230–46 (1998).

302. Belshe, R. B. *et al.* Induction of immune responses to HIV-1 by canarypox virus (ALVAC) HIV-1 and gp120 SF-2 recombinant vaccines in uninfected volunteers. NIAID AIDS Vaccine Evaluation Group. *AIDS* **12**, 2407–15 (1998).

303. Wills, J. W. & Craven, R. C. Form, function, and use of retroviral gag proteins. *AIDS* **5**, 639–54 (1991).

304. Haffar, O. *et al.* Human immunodeficiency virus-like, nonreplicating, gag-env particles assemble in a recombinant vaccinia virus expression system. *J. Virol.* **64**, 2653–9 (1990).

305. Rerks-Ngarm, S. *et al.* Randomized, Double-Blind Evaluation of Late Boost Strategies for HIV-Uninfected Vaccine Recipients in the RV144 HIV Vaccine Efficacy Trial. *J. Infect. Dis.* **215**, 1255–1263 (2017).

306. Pal, R. *et al.* ALVAC-SIV-gag-pol-env-based vaccination and macaque major histocompatibility complex class I (A*01) delay simian immunodeficiency virus SIVmac-induced immunodeficiency. *J. Virol.* **76**, 292–302 (2002).

307. Van Rompay, K. K. A. *et al.* Attenuated poxvirus-based simian immunodeficiency virus (SIV) vaccines given in infancy partially protect infant and juvenile macaques against repeated oral challenge with virulent SIV. *J. Acquir. Immune Defic. Syndr.* **38**, 124–34 (2005).

308. Kim, J. H., Excler, J.-L. & Michael, N. L. Lessons from the RV144 Thai phase III HIV-1 vaccine trial and the search for correlates of protection. *Annu. Rev. Med.* **66**, 423–37 (2015).

309. Haynes, B. F. *et al.* Immune-Correlates Analysis of an HIV-1 Vaccine Efficacy Trial. *N. Engl. J. Med.* **366**, 1275–1286 (2012).

310. Pinter, A., Honnen, W. J., Kayman, S. C., Trochev, O. & Wu, Z. Potent neutralization of primary HIV-1 isolates by antibodies directed against epitopes present in the V1/V2 domain of HIV-1 gp120. *Vaccine* **16**, 1803–11 (1998).

311. Montefiori, D. C. *et al.* Magnitude and breadth of the neutralizing antibody response in the RV144 and Vax003 HIV-1 vaccine efficacy trials. *J. Infect. Dis.* **206**, 431–41 (2012).

312. Gottardo, R. *et al.* Plasma IgG to linear epitopes in the V2 and V3 regions of HIV-1 gp120 correlate with a reduced risk of infection in the RV144 vaccine efficacy trial. *PLoS One* **8**, e75665 (2013).

313. Alam, S. M. *et al.* Antigenicity and Immunogenicity of RV144 Vaccine AIDSVAX Clade E

Envelope Immunogen Is Enhanced by a gp120 N-Terminal Deletion. *J. Virol.* **87**, 1554–1568 (2013).

314. Berman, P. W. *et al.* Genetic and immunologic characterization of viruses infecting MN-rgp120-vaccinated volunteers. *J. Infect. Dis.* **176**, 384–97 (1997).

315. Gilbert, P. B., Wu, C. & Jobes, D. V. Genome scanning tests for comparing amino acid sequences between groups. *Biometrics* **64**, 198–207 (2008).

316. Rolland, M. *et al.* Increased HIV-1 vaccine efficacy against viruses with genetic signatures in Env V2. *Nature* **490**, 417–20 (2012).

317. Nakamura, G. R., Fonseca, D. P. A. J., O'Rourke, S. M., Vollrath, A. L. & Berman, P. W. Monoclonal antibodies to the V2 domain of MN-rgp120: fine mapping of epitopes and inhibition of α4β7 binding. *PLoS One* **7**, e39045 (2012).

318. Tassaneetrithep, B. *et al.* Cryptic determinant of α4β7 binding in the V2 loop of HIV-1 gp120. *PLoS One* **9**, e108446 (2014).

319. Nelson, J. A. *et al.* Human immunodeficiency virus detected in bowel epithelium from patients with gastrointestinal symptoms. *Lancet (London, England)* **1**, 259–62 (1988).

320. Brenchley, J. M. & Douek, D. C. HIV infection and the gastrointestinal immune system. *Mucosal Immunol.* **1**, 23–30 (2008).

321. Brenchley, J. M. & Douek, D. C. The mucosal barrier and immune activation in HIV pathogenesis. *Curr. Opin. HIV AIDS* **3**, 356–61 (2008).

322. Mehandru, S. *et al.* Lack of mucosal immune reconstitution during prolonged treatment of acute and early HIV-1 infection. *PLoS Med.* **3**, e484 (2006).

323. Arthos, J. *et al.* The Role of Integrin α4β7 in HIV Pathogenesis and Treatment. *Curr. HIV/AIDS Rep.* **15**, 127–135 (2018).

324. Szabo, M. C., Butcher, E. C. & McEvoy, L. M. Specialization of mucosal follicular dendritic cells revealed by mucosal addressin-cell adhesion molecule-1 display. *J. Immunol.* **158**, 5584–8 (1997).

325. Luster, A. D., Alon, R. & von Andrian, U. H. Immune cell migration in inflammation: present and future therapeutic targets. *Nat. Immunol.* **6**, 1182–90 (2005).

326. Hussein, H. A. M. *et al.* Beyond RGD: virus interactions with integrins. *Arch. Virol.* **160**, 2669–81 (2015).

327. Byrareddy, S. N. *et al.* Targeting α4β7 integrin reduces mucosal transmission of simian immunodeficiency virus and protects gut-associated lymphoid tissue from infection. *Nat. Med.* **20**, 1397–400 (2014).

328. Graham, K. L. *et al.* Rotaviruses interact with alpha4beta7 and alpha4beta1 integrins by binding the same integrin domains as natural ligands. *J. Gen. Virol.* **86**, 3397–408 (2005).

329. López, S. & Arias, C. F. Multistep entry of rotavirus into cells: a Versaillesque dance. *Trends Microbiol.* **12**, 271–8 (2004).

330. Cicala, C., Arthos, J. & Fauci, A. S. HIV-1 envelope, integrins and co-receptor use in mucosal transmission of HIV. *J. Transl. Med.* **9**, S2 (2011).

331. Sivro, A. *et al.* Integrin α4β7 expression on peripheral blood CD4+ T cells predicts HIV acquisition and disease progression outcomes. *Sci. Transl. Med.* **10**, eaam6354 (2018).

332. Martinelli, E. *et al.* HSV-2 Infection of Dendritic Cells Amplifies a Highly Susceptible HIV-1 Cell Target. *PLoS Pathog.* **7**, e1002109 (2011).

333. Shannon, B. *et al.* Impact of asymptomatic herpes simplex virus type 2 infection on mucosal homing and immune cell subsets in the blood and female genital tract. *J. Immunol.* **192**, 5074–82 (2014).

334. Ansari, A. A. *et al.* Blocking of α4β7 gut-homing integrin during acute infection leads to decreased plasma and gastrointestinal tissue viral loads in simian immunodeficiency virus-infected rhesus macaques. *J. Immunol.* **186**, 1044–59 (2011).

335. Santangelo, P. J. *et al.* Early treatment of SIV+ macaques with an α4β7 mAb alters virus distribution and preserves CD4+ T cells in later stages of infection. *Mucosal Immunol.* **11**, 932–946 (2018).

336. McKinnon, L. R. *et al.* Characterization of a human cervical CD4+ T cell subset coexpressing multiple markers of HIV susceptibility. *J. Immunol.* **187**, 6032–42 (2011).

337. Byrareddy, S. N. *et al.* Sustained virologic control in SIV+ macaques after antiretroviral and α4β7 antibody therapy. *Science* **354**, 197–202 (2016).

338. Mudd, J. C. & Brenchley, J. M. ILC You Later: Early and Irreparable Loss of Innate Lymphocytes in HIV Infection. *Immunity* **44**, 216–8 (2016).

339. Peachman, K. K. *et al.* Identification of New Regions in HIV-1 gp120 Variable 2 and 3 Loops that Bind to α4β7 Integrin Receptor. **10**, e0143895 (2015).

340. Cicala, C. *et al.* The integrin 4 7 forms a complex with cell-surface CD4 and defines a T-cell subset that is highly susceptible to infection by HIV-1. *Proc. Natl. Acad. Sci.* **106**, 20877–20882 (2009).

341. Parrish, N. F. *et al.* Transmitted/founder and chronic subtype C HIV-1 use CD4 and CCR5 receptors with equal efficiency and are not inhibited by blocking the integrin α4β7. *PLoS Pathog.* **8**, e1002686 (2012).

342. Richardson, S. I. *et al.* South African HIV-1 subtype C transmitted variants with a specific V2 motif show higher dependence on α4β7 for replication. *Retrovirology* **12**, 54 (2015).

343. Schweighoffer, T. *et al.* Selective expression of integrin alpha 4 beta 7 on a subset of human CD4+ memory T cells with Hallmarks of gut-trophism. *J. Immunol.* **151**, 717–29 (1993).

344. Takada, Y., Elices, M. J., Crouse, C. & Hemler, M. E. The primary structure of the alpha 4 subunit of VLA-4: homology to other integrins and a possible cell-cell adhesion function. *EMBO J.* **8**, 1361–8 (1989).

345. Yuan, Q. A., Jiang, W. M., Krissansen, G. W. & Watson, J. D. Cloning and sequence analysis of a novel beta 2-related integrin transcript from T lymphocytes: homology of integrin cysteine-rich repeats to domain III of laminin B chains. *Int. Immunol.* **3**, 1373–4 (1991).

346. Yu, Y. *et al.* Structural specializations of α(4)β(7), an integrin that mediates rolling adhesion. *J. Cell Biol.* **196**, 131–46 (2012).

347. Springer, T. A. Traffic signals for lymphocyte recirculation and leukocyte emigration: the multistep paradigm. *Cell* **76**, 301–14 (1994).

348. Hamann, A., Andrew, D. P., Jablonski-Westrich, D., Holzmann, B. & Butcher, E. C. Role of alpha 4-integrins in lymphocyte homing to mucosal tissues in vivo. *J. Immunol.* **152**, 3282–93 (1994).

349. Chen, J. *et al.* The relative influence of metal ion binding sites in the I-like domain and the interface with the hybrid domain on rolling and firm adhesion by integrin alpha4beta7. *J. Biol. Chem.* **279**, 55556–61 (2004).

350. Nawaz, F. *et al.* The genotype of early-transmitting HIV gp120s promotes α (4) β(7)-reactivity, revealing α (4) β(7) +/CD4+ T cells as key targets in mucosal transmission. *PLoS Pathog.* **7**, e1001301 (2011).

351. Liu, J., Bartesaghi, A., Borgnia, M. J., Sapiro, G. & Subramaniam, S. Molecular architecture of native HIV-1 gp120 trimers. *Nature* **455**, 109–13 (2008).

352. Julien, J.-P. *et al.* Crystal structure of a soluble cleaved HIV-1 envelope trimer. *Science* **342**, 1477–83 (2013).

353. Pancera, M. *et al.* Structure and immune recognition of trimeric pre-fusion HIV-1 Env. *Nature* **514**, 455–461 (2014).

354. Pan, R., Gorny, M. K., Zolla-Pazner, S. & Kong, X.-P. The V1V2 Region of HIV-1 gp120 Forms a Five-Stranded Beta Barrel. *J. Virol.* **89**, 8003–10 (2015).

355. McLellan, J. S. *et al.* Structure of HIV-1 gp120 V1/V2 domain with broadly neutralizing antibody PG9. *Nature* **480**, 336–343 (2011).

356. Gorman, J. *et al.* Structures of HIV-1 Env V1V2 with broadly neutralizing antibodies reveal commonalities that enable vaccine design. *Nat. Struct. Mol. Biol.* **23**, 81–90 (2016).

357. Cale, E. M. *et al.* Virus-like Particles Identify an HIV V1V2 Apex-Binding Neutralizing Antibody that Lacks a Protruding Loop. *Immunity* **46**, 777–791.e10 (2017).

358. Aiyegbo, M. S. *et al.* Peptide Targeted by Human Antibodies Associated with HIV Vaccine-

Associated Protection Assumes a Dynamic α-Helical Structure. *PLoS One* **12**, e0170530 (2017).

359. Liao, H.-X. *et al.* Vaccine induction of antibodies against a structurally heterogeneous site of immune pressure within HIV-1 envelope protein variable regions 1 and 2. *Immunity* **38**, (2013).

360. Lertjuthaporn, S. *et al.* Select gp120 V2 domain specific antibodies derived from HIV and SIV infection and vaccination inhibit gp120 binding to α4β7. *PLoS Pathog.* **14**, e1007278 (2018).

361. Abstracts of the HIV Research for Prevention Meeting, HIVR4P, 17-20 October, 2016, Chicago, USA. *AIDS Res. Hum. Retroviruses* **32**, 1–409 (2016).

362. Vaccari, M. *et al.* Adjuvant-dependent innate and adaptive immune signatures of risk of SIVmac251 acquisition. *Nat. Med.* **22**, 762–770 (2016).

363. Chand, S. *et al.* Glycosylation and oligomeric state of envelope protein might influence HIV-1 virion capture by α4β7 integrin. *Virology* **508**, 199–212 (2017).

364. Mason, R. D. *et al.* Targeted Isolation of Antibodies Directed against Major Sites of SIV Env Vulnerability. *PLOS Pathog.* **12**, e1005537 (2016).

365. www.phenix-online.org. Available at: http://www.phenix-online.org/. (Accessed: 31st July 2018)

366. https://www2.mrc-lmb.cam.ac.uk/personal/pemsley/coot/. Available at: https://www2.mrc-lmb.cam.ac.uk/personal/pemsley/coot/. (Accessed: 31st July 2018)

367. http://molprobity.biochem.duke.edu. Available at: http://molprobity.biochem.duke.edu/. (Accessed: 31st July 2018)

368. Li, M. *et al.* Human Immunodeficiency Virus Type 1 env Clones from Acute and Early Subtype B Infections for Standardized Assessments of Vaccine-Elicited Neutralizing Antibodies. *J. Virol.* **79**, 10108–10125 (2005).

369. Arrode-Brusés, G. *et al.* A Small Molecule, Which Competes with MAdCAM-1, Activates

Integrin α4β7 and Fails to Prevent Mucosal Transmission of SHIV-SF162P3. *PLoS Pathog.* **12**, e1005720 (2016).

370. Koup, R. A. *et al.* Temporal association of cellular immune responses with the initial control of viremia in primary human immunodeficiency virus type 1 syndrome. *J Virol* **68**, 4650–4655 (1994).

371. Jin, X. *et al.* Dramatic rise in plasma viremia after CD8(+) T cell depletion in simian immunodeficiency virus-infected macaques. *J Exp Med* **189**, 991–998 (1999).

372. Schmitz, J. E. *et al.* Control of viremia in simian immunodeficiency virus infection by CD8+ lymphocytes. *Science (80-.).* **283**, 857–860 (1999).

373. Karasavvas, N. *et al.* The Thai Phase III HIV Type 1 Vaccine Trial (RV144) Regimen Induces Antibodies That Target Conserved Regions Within the V2 Loop of gp120. *AIDS Res. Hum. Retroviruses* **28**, 1444–1457 (2012).

374. Johnson, J. A., Barouch, D. H. & Baden, L. R. Nonreplicating vectors in HIV vaccines. *Curr Opin HIV AIDS* **8**, 412–420 (2013).

375. Khowsroy, K. *et al.* Expectation of volunteers towards the vaccine efficacy of the prime-boost HIV vaccine phase III trial during unblinding. *AIDS Res Hum Retroviruses* **30**, 1041–1045 (2014).

376. Franchini, G., Gurunathan, S., Baglyos, L., Plotkin, S. & Tartaglia, J. Poxvirus-based vaccine candidates for HIV: two decades of experience with special emphasis on canarypox vectors. *Expert Rev. Vaccines* **3**, S75-88 (2004).

377. McFarland, E. J. *et al.* Human immunodeficiency virus type 1 (HIV-1) gp120-specific antibodies in neonates receiving an HIV-1 recombinant gp120 vaccine. *J Infect Dis* **184**, 1331–1335 (2001).

378. Kintu, K. *et al.* Feasibility and safety of ALVAC-HIV vCP1521 vaccine in HIV-exposed infants in Uganda: results from the first HIV vaccine trial in infants in Africa. *J Acquir Immune Defic Syndr* **63**, 1–8 (2013).

379. Russell, N. D. *et al.* Phase 2 study of an HIV-1 canarypox vaccine (vCP1452) alone and in combination with rgp120: negative results fail to trigger a phase 3 correlates trial. *J Acquir Immune Defic Syndr* **44**, 203–212 (2007).

380. Pitisuttithum, P. *et al.* Randomized, Double-Blind, Placebo-Controlled Efficacy Trial of a Bivalent Recombinant Glycoprotein 120 HIV-1 Vaccine among Injection Drug Users in Bangkok, Thailand. *J. Infect. Dis.* **194**, 1661–1671 (2006).

381. Ockenhouse, C. F. *et al.* Phase I/IIa safety, immunogenicity, and efficacy trial of NYVAC-Pf7, a pox-vectored, multiantigen, multistage vaccine candidate for Plasmodium falciparum malaria. *J. Infect. Dis.* **177**, 1664–73 (1998).

382. Gomez, C. E., Perdiguero, B., Garcia-Arriaza, J. & Esteban, M. Poxvirus vectors as HIV/AIDS vaccines in humans. *Hum Vaccin Immunother* **8**, 1192–1207 (2012).

383. Franchini, G. *et al.* Highly attenuated HIV type 2 recombinant poxviruses, but not HIV-2 recombinant Salmonella vaccines, induce long-lasting protection in rhesus macaques. *AIDS Res Hum Retroviruses* **11**, 909–920 (1995).

384. Vaccari, M. *et al.* Protection afforded by an HIV vaccine candidate in macaques depends on the dose of SIVmac251 at challenge exposure. *J Virol* **87**, 3538–3548 (2013).

385. Patterson, L. J. *et al.* Cross-protection in NYVAC-HIV-1-immunized/HIV-2-challenged but not in NYVAC-HIV-2-immunized/SHIV-challenged rhesus macaques. *AIDS* **14**, 2445–2455 (2000).

386. Abimiku, A. G. *et al.* HIV-1 recombinant poxvirus vaccine induces cross-protection against HIV-2 challenge in rhesus macaques. *Nat Med* **1**, 321–329 (1995).

387. Walther-Jallow, L. *et al.* Cross-protection against mucosal simian immunodeficiency virus (SIVsm) challenge in human immunodeficiency virus type 2-vaccinated cynomolgus monkeys. *J Gen Virol* **82**, 1601–1612 (2001).

388. Benson, J. *et al.* Recombinant vaccine-induced protection against the highly pathogenic simian immunodeficiency virus SIV(mac251): dependence on route of challenge exposure.

J Virol **72**, 4170–4182 (1998).

389. Hel, Z. *et al.* Containment of simian immunodeficiency virus infection in vaccinated macaques: correlation with the magnitude of virus-specific pre- and postchallenge CD4+ and CD8+ T cell responses. *J Immunol* **169**, 4778–4787 (2002).

390. Hel, Z. *et al.* Potentiation of simian immunodeficiency virus (SIV)-specific CD4(+) and CD8(+) T cell responses by a DNA-SIV and NYVAC-SIV prime/boost regimen. *J Immunol* **167**, 7180–7191 (2001).

391. Romano, J. W., Williams, K. G., Shurtliff, R. N., Ginocchio, C. & Kaplan, M. NASBA technology: isothermal RNA amplification in qualitative and quantitative diagnostics. *Immunol. Invest.* **26**, 15–28

392. Lee, E. M. *et al.* Molecular methods for evaluation of virological status of nonhuman primates challenged with simian immunodeficiency or simian-human immunodeficiency viruses. *J. Virol. Methods* **163**, 287–294 (2010).

393. Takahashi, H. *et al.* Induction of broadly cross-reactive cytotoxic T cells recognizing an HIV-1 envelope determinant. *Science (80-.).* **255**, 333–336 (1992).

394. Jefferis, R. Isotype and glycoform selection for antibody therapeutics. *Arch Biochem Biophys* **526**, 159–166 (2012).

395. Tomaras, G. D. *et al.* Vaccine-induced plasma IgA specific for the C1 region of the HIV-1 envelope blocks binding and effector function of IgG. *Proc Natl Acad Sci U S A* **110**, 9019–9024 (2013).

396. Yates, N. L. *et al.* Vaccine-induced Env V1-V2 IgG3 correlates with lower HIV-1 infection risk and declines soon after vaccination. *Sci Transl Med* **6**, 228ra39 (2014).

397. Sharp, F. A. *et al.* Uptake of particulate vaccine adjuvants by dendritic cells activates the NALP3 inflammasome. *Proc Natl Acad Sci U S A* **106**, 870–875 (2009).

398. Reeves, R. K. *et al.* Gut inflammation and indoleamine deoxygenase inhibit IL-17 production and promote cytotoxic potential in NKp44+ mucosal NK cells during SIV

infection. *Blood* **118**, 3321–3330 (2011).

399. Vargas-Inchaustegui, D. A., Demberg, T. & Robert-Guroff, M. A CD8alpha(-) subpopulation of macaque circulatory natural killer cells can mediate both antibody-dependent and antibody-independent cytotoxic activities. *Immunology* **134**, 326–340 (2011).

400. Berlin, C. *et al.* Alpha 4 beta 7 integrin mediates lymphocyte binding to the mucosal vascular addressin MAdCAM-1. *Cell* **74**, 185–195 (1993).

401. Kunkel, E. J. & Butcher, E. C. Plasma-cell homing. *Nat Rev Immunol* **3**, 822–829 (2003).

402. Shi, C. & Pamer, E. G. Monocyte recruitment during infection and inflammation. *Nat. Rev. Immunol.* **11**, 762–774 (2011).

403. Idzkowska, E. *et al.* The Role of Different Monocyte Subsets in the Pathogenesis of Atherosclerosis and Acute Coronary Syndromes. *Scand. J. Immunol.* **82**, 163–173 (2015).

404. França, C. N. *et al.* Monocyte subtypes and the CCR2 chemokine receptor in cardiovascular disease. *Clin. Sci. (Lond).* **131**, 1215–1224 (2017).

405. Behfar, S., Hassanshahi, G., Nazari, A. & Khorramdelazad, H. A brief look at the role of monocyte chemoattractant protein-1 (CCL2) in the pathophysiology of psoriasis. *Cytokine* **110**, 226–231 (2018).

406. Veglia, F., Perego, M. & Gabrilovich, D. Myeloid-derived suppressor cells coming of age. *Nat. Immunol.* **19**, 108–119 (2018).

407. Lugli, E., Marcenaro, E. & Mavilio, D. NK Cell Subset Redistribution during the Course of Viral Infections. *Front Immunol* **5**, 390 (2014).

408. Bart, P. A. *et al.* EV01: a phase I trial in healthy HIV negative volunteers to evaluate a clade C HIV vaccine, NYVAC-C undertaken by the EuroVacc Consortium. *Vaccine* **26**, 3153–3161 (2008).

409. McCormack, S. *et al.* EV02: a Phase I trial to compare the safety and immunogenicity of HIV DNA-C prime-NYVAC-C boost to NYVAC-C alone. *Vaccine* **26**, 3162–3174 (2008).

410. Knorr, M., Münzel, T. & Wenzel, P. Interplay of NK cells and monocytes in vascular

inflammation and myocardial infarction. *Front. Physiol.* **5**, 295 (2014).

411. Lewis, D. J. M. *et al.* Effect of vaginal immunization with HIVgp140 and HSP70 on HIV-1 replication and innate and T cell adaptive immunity in women. *J. Virol.* **88**, 11648–57 (2014).

412. Zolla-Pazner, S. *et al.* Analysis of V2 antibody responses induced in vaccinees in the ALVAC/AIDSVAX HIV-1 vaccine efficacy trial. *PLoS One* **8**, e53629 (2013).

413. Zolla-Pazner, S. *et al.* Vaccine-induced IgG antibodies to V1V2 regions of multiple HIV-1 subtypes correlate with decreased risk of HIV-1 infection. *PLoS One* **9**, e87572 (2014).

414. Pollara, J. *et al.* HIV-1 vaccine-induced C1 and V2 Env-specific antibodies synergize for increased antiviral activities. *J. Virol.* **88**, 7715–26 (2014).

415. Bonsignori, M. *et al.* Antibody-dependent cellular cytotoxicity-mediating antibodies from an HIV-1 vaccine efficacy trial target multiple epitopes and preferentially use the VH1 gene family. *J. Virol.* **86**, 11521–32 (2012).

416. Florese, R. H. *et al.* Evaluation of passively transferred, nonneutralizing antibody-dependent cellular cytotoxicity-mediating IgG in protection of neonatal rhesus macaques against oral SIVmac251 challenge. *J. Immunol.* **177**, 4028–36 (2006).

417. Dugast, A.-S. *et al.* Lack of protection following passive transfer of polyclonal highly functional low-dose non-neutralizing antibodies. *PLoS One* **9**, e97229 (2014).

418. Moldt, B. *et al.* A nonfucosylated variant of the anti-HIV-1 monoclonal antibody b12 has enhanced FcγRIIIa-mediated antiviral activity in vitro but does not improve protection against mucosal SHIV challenge in macaques. *J. Virol.* **86**, 6189–96 (2012).

419. Pegu, A. *et al.* Neutralizing antibodies to HIV-1 envelope protect more effectively in vivo than those to the CD4 receptor. *Sci. Transl. Med.* **6**, 243ra88-243ra88 (2014).

420. Guzzo, C. *et al.* Virion incorporation of integrin α4β7 facilitates HIV-1 infection and intestinal homing. *Sci. Immunol.* **2**, (2017).

421. McCluskey, M. & Gorini, G. HIV Vaccine Awareness Day: Renewed Hope and Determination

| U.S. Agency for International Development. (2017). Available at: https://www.usaid.gov/what-we-do/global-health/hiv-and-aids/information-center/hiv-and-aids-research-corner/hiv-vaccine-awareness-day-2017. (Accessed: 16th September 2018)